ROLE OF THE PROLIFERATION-RELATED MOLECULES IN THE PATHOGENESIS OF ALZHEIMER'S DISEASE

By

SHARON CHRISTINE YATES

A thesis submitted to the University of Birmingham for the degree of Master of Philosophy

Clinical and Experimental Medicine

The Medical School

University of Birmingham

April 2012

ABSTRACT

The cell cycle theory of Alzheimer's Disease (AD) states that neurodegeneration is secondary to aberrant cell cycle activity in neurons. Previous studies suggest that this may be partly attributed to alterations in the mTOR pathway, which promotes cell growth and division, and partly to genetic variants on genes responsible for cell cycle control.

In this study we perform a systematic analysis of the rapamycin-regulated genes that are differentially regulated in brain affected by AD compared to control. These genes may serve as novel therapeutic targets or biomarkers of AD. Secondly, we investigate the association of a cancer-associated variant of $p21^{cip1}$, and a variant of $p57^{kip2}$, with AD. These cyclin dependent kinase inhibitors are crucial cell cycle regulatory components that function downstream of mTOR. We confirm the association of the $p21^{cip1}$ SNPs with AD, and inform on the mechanisms by which they cause loss of function. We also show a weak association between variant $p57^{kip2}$ and AD. Furthermore, we demonstrate that $p57^{kip2}$ is differentially imprinted in the frontal and occipital lobe; and suggest that AD may be associated with change in the imprinting status of $p57^{kip2}$ in the brain.

ACKNOWLEDGEMENTS

I would like to express my gratitude to Zsuzsanna Nagy for her help and support during the course of this MPhil. Without her encouragement it is doubtful I would have started.

Secondly, I would like to thank Roy Bicknell, my second supervisor, for his expert advice.

I am grateful to Cytox Ltd for financing this study; and to the Oxford Project to Investigate Memory and Aging for providing the necessary resources. Without the contribution of the many patients, carers and staff involved, this study would not have been possible.

I would also like to thank my co-workers- Erzsebet Rabai, Amen Zafar, Sheila Nagy, Sarah Durant, and Ghaniah Hassan-Smith- for technical help, encouragement, and friendship during the many months of hard work. The experience was made more enjoyable by your presence.

And finally, I am grateful to my husband, Tom Yates, for marrying me at the start of this MPhil, and supporting me throughout; and my family and friends for hours of trying to understand its subject matter.

TABLE OF CONTENTS

LIST OF FIGURES

LIST OF TABLES

ABBREVIATIONS

AD	Alzheimer's disease
ANOVA	Analysis of variance
ApoE	Apolipoprotein E
APP	Amyloid precursor protein
APP-C	Amyloid precursor protein C-terminal
BSA	Bovine serum albumin
CAMCOG	The Cambridge Cognitive Examination
CAMDEX	Cambridge examination for mental disorders of the elderly
CDK	Cyclin dependent kinase
CDKI	Cyclin dependent kinase inhibitor
cDNA	Complementary DNA
CNS	Central nervous system
CRH	Corticotrophin releasing hormone
CTCF	Transcriptional regulator: 11 zinc finger protein
CV	Coefficient of variance
DNA	Deoxyribonucleic acid
dNTP	Deoxyribonucleotide triphosphate
DZIP3	DAZ interacting protein 3, zinc finger
EIF4E	Eukaryotic translation initiation factor 4E
ELISA	Enzyme linked immunosorbant assay
FAM	Carboxyfluorescein

FDR	False discovery rate
G^0	Resting phase of the cell cycle
G1	Gap phase 1 of the cell cycle
G2	Gap phase 2 of the cell cycle
GABBR2	Gamma-aminobutyric acid B receptor
GAP-43	Growth associated protein- 43
ICR	Imprinting control region
IPA	IPA Ingenuity programme
KvDMR1	Imprinting control region that regulates $p57^{kip2}$ imprinting
M	Mitosis phase of the cell cycle
MANOVA	Multi-analysis of variance
MAPK1	Mitogen activated protein kinase 1
MCI	Mild cognitive impairment
mTOR	Mammalian target of rapamycin
NFT	Neurofibrillary tangle
OPTIMA	Oxford Project to Investigate Memory and Aging
PAPA domain	Proline/alanine rich domain
PBS	Phosphate buffered saline
PCNA	Proliferating cell nuclear antigen
PCR	Polymerase chain reaction
PHF	Paired helical filaments
Q-PCR	Real time polymerase chain reaction
RBM38	RNA-binding motif protein 38

RCF or g	Relative centrifugal force
RIPA	Radioimmunoprecipitation assay buffer
RNA	Ribonucleic acid
RPM	Rotations per minute
RPM13	Gene coding for 60S ribosomal protein L13
RT	Room temperature
S	DNA synthesis phase of the cell cycle
SAM	Statistical Analysis of Microarray
SEMA4C	Semaphorin 4C
SERPINE 1	Serpin peptidase inhibitor 1
SNP	Single nucleotide polymorphism
SR	Sulforhodamine (emits red fluorescence)
TGF-beta	Transforming growth factor beta
TSSC3	Tumour suppressing subtransferable candidate 3
UTR	Untranslated region
18S	Ribosomal RNA

1. INTRODUCTION

Late-onset Alzheimer's disease (AD) is a progressive neurodegenerative disorder that affects primarily the limbic and cortical brain regions responsible for memory, learning and emotion (for review see[1]). Risk factors include increasing age, poor diet, high homocysteine, low educational level and head trauma. There is a strong genetic component to AD, as indicated by studies suggesting a heritability of 60-80%[2, 3]. However, few associated genes are currently established. The reality of today's ageing population is adding to the financial and social burden of AD, with an estimated 15% of the population above the age of 65 affected: this figure increasing to ~50% of the population over the age of 85[4].

1.1. PATHOLOGICAL HALLMARKS OF AD

The pathological hallmarks of AD are the extracellular beta-amyloid plaques and intracellular neurofibrillary tangles (NFT) that accumulate in the brain, accompanied by extensive neuronal cell death[5]. Beta-amyloid is a 39 to 43 amino acid cleavage product of the amyloid precursor protein (APP)[1]. The function of APP is poorly understood, although it has been implicated in neuronal and synaptic function[6, 7]. In healthy brain it is processed by secretases to produce various soluble cleavage products. However, pathological processing by beta- and gamma-secretases results in the production of insoluble beta-amyloid that accumulates in the brain in AD. Interestingly, whilst extracellular beta-amyloid plaques are one of the hallmarks of AD, plaques may also accumulate in the brain of subjects with no

symptoms of AD, although generally at low levels. Studies show that there is a relatively poor correlation between the number of plaques and severity of AD[8].

NFT are composed of paired helical filaments (PHF) of hyperphosphorylated tau, and accumulate inside neurons in AD. Tau is an intracellular scaffolding protein that stabilises microtubules in neurons[9]. The microtubule structure is dependent on the phosphorylation status of tau: with sequential phosphorylation and dephosphorylation driving the structural changes required for activities such as axonal transport and neurite outgrowth. In AD, tau is pathologically hyperphosphorylated, resulting in the formation of the PHF that aggregate to form insoluble intracellular NFTs[10].

1.2. DIAGNOSIS

Currently, there is no definitive diagnostic test for AD. Diagnosis is based on clinical examination, and can be confirmed at post-mortem by the presence of AD-related brain pathology[11]. The Cambridge Cognitive Examination (CAMCOG) is a standardised cognitive performance test that is used to estimate severity of dementia, and forms part of the Cambridge Examination for Mental Disorders of the Elderly[12, 13]. On post-mortem, the Consortium to Establish a Registry for Alzheimer's disease (CERAD) Neuropathology Assessment[14] is a standardised system for diagnosing AD, and relies on the presence and location of senile plaques (beta-amyloid deposits associated with diseased neurites) in the brain, and the age of the patient at death.

The Braak staging system[15] is used to estimate the severity and progression of AD. It relies on the fact that tau pathology has a characteristic distribution in AD; and that the spread and density of NFTs correlates well with disease severity[16, 17]. The accumulation of tau pathology in the entorhinal cortex is defined as preclinical AD (entorhinal stage); tau pathology in the entorhinal and limbic regions is defined as mild AD (limbic stage); whereas additional spread to the neocortical areas is defined as advanced AD (neocortical stage).

1.3. TREATMENT AND BIOMARKERS OF DISEASE

AD is currently incurable: with the majority of treatments focused on the management of symptoms[1]. Despite the identification of numerous risk factors, very little can be done to prevent or improve the course of the disease, highlighting the need for more research. The absence of a reliable diagnostic test is hugely problematic to research, as preclinical and mild AD sufferers cannot be reliably identified, making early targeted clinical drug trials impossible. The search is on to identify biomarkers of AD that could be used to diagnose pre-clinical AD and monitor AD progression[18]. An ideal biomarker would be a reliable predictor of disease, and easily measurable (for example, from blood).

1.4. AD PATHOGENESIS

The reasons neurons degenerate in AD are not fully understood. Numerous theories exist; mainly focusing on the hallmarks of AD. The amyloid cascade hypothesis suggests that neurodegeneration is secondary to beta-amyloid deposition[19], based on the finding that

aggregates of beta-amyloid accumulate in the brain in AD, often in close proximity to areas of neurodegeneration[20]. Furthermore, mutations of APP and the presenilin genes (involved in APP processing) that result in rapid accumulation of beta-amyloid in the brain are associated with early-onset AD[20]. Similarly, the tau hypothesis states that neurodegeneration is secondary to NFT accumulation in neurons, based on the finding that spread of tau pathology is closely related to disease severity[15].

Whether the hallmarks are a cause or consequence of AD remains controversial. Neither the amyloid nor tau hypotheses[10, 19] satisfactorily explain the accumulation of the other hallmark. Whilst they may partially explain the progressive character of the disease (for example, beta-amyloid peptides have been found to be neurotoxic in the presence of tau pathology[21]), there is no explanation for how or why AD initiates.

Studies show that the heritability of late-onset AD is 60-80%[2, 3], indicating that there is a strong genetic component to AD. However, despite extensive research, few associated genes are currently known. The Apolipoprotein E (ApoE) gene is the main established risk factor for late-onset AD[22, 23], with the ApoE ε4 allele significantly associated with increased risk and earlier age of onset[24]. The ApoE ε3 allele has no effect on AD risk, whereas the ApoE ε2 allele may be protective. The mechanism by which the ApoE ε4 allele is detrimental to brain function remain unclear, although the ApoE gene is known to be involved in lipid transport during synaptic remodelling and mitochondrial metabolism in the central nervous system[25].

Oxidative stress has also been implicated in AD pathogenesis[11, 26-28]; as has neuronal cell cycle activity. The cell cycle hypothesis of AD postulates that neurodegeneration in AD is secondary to aberrant neuronal cell cycle activity[29, 30].

1.5. ROLE OF THE CELL CYCLE IN AD

1.5.1 The cell cycle

The cell cycle is a sequence of four defined phases, namely: first gap phase (G1), DNA synthesis phase (S), second gap phase (G2) and mitosis phase (M). The entry into the cell cycle is driven by signalling from various growth factors, cytokines and other mitogenic factors, resulting in the expression of Cyclin D, an activator of cyclin dependent kinase-4 (CDK4) and CDK6. The kinase activity of CDK4/6 is required for progression through the G1 phase. At each phase of the cell cycle, progression is driven by the activity of a specific cyclin/CDK complex: with progression through the G1/S, S/G2 and G2/M checkpoints requiring the activity of cyclin E/CDK2, cyclin A/CDK2 and cyclin A or B/CDK1 respectively (Figure 1).

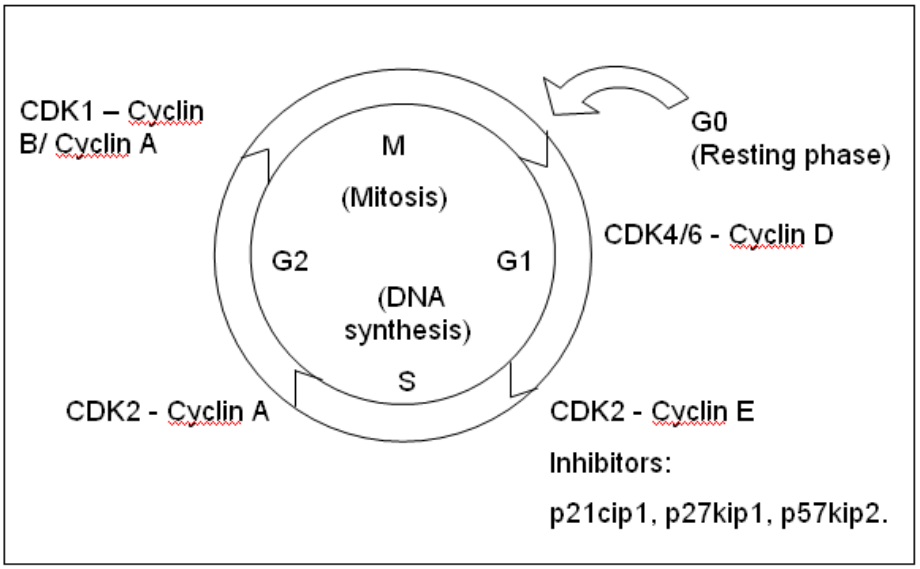

Figure 1 **Overview of cyclin/CDK interactions required for progression through G1, S, G2 and M phase of the cell cycle.**

Cell cycle activity is tightly regulated: with the cyclin dependent kinase inhibitors (CDKI) largely responsible for the checkpoints that regulate progression, by directly inhibiting the activity of cyclin/CDK complexes. They are turned on in response to intra- and extra-cellular signals to prevent cell division. The CDKI: $p21^{cip1}$ inhibits CDK2 activation by cyclin A and cyclin E, and inhibits various other cyclin/CDK complexes to some extent[31]. Its expression is regulated on a transcriptional level by the p53 tumour suppressor pathway: with DNA damage triggering up-regulation. The activity of CDK2 is necessary for cell cycle progression through the G1/S and S/G2 checkpoints, so $p21^{cip1}$ is an inhibitor at several cell cycle stages[32]. $P21^{cip1}$ is also involved in regulating apoptosis, and directly inhibits DNA replication by interacting with proliferating cell nuclear antigen (PCNA) (reviewed in[31]).

Similarly, the CDKI: $p57^{kip2}$ inhibits CDK2 activation by cyclin A and E; and CDK4/6 activation by cyclin D, thereby inhibiting cell cycle progression at several cell cycle phases. It has a number of additional functions, including involvement in the regulation of apoptosis and cytoskeleton dynamics[33]. It is the only member of the cip/kip family of CDKI found to be essential during development: with knock-out mice suffering severe developmental abnormalities and premature death. $p57^{kip2}$ is also the only cip/kip family member that is imprinted: with the maternal allele preferentially expressed (reviewed in[33]).

1.6. CELL CYCLE REGULATORY FAILURE IN AD

Whilst neurons were historically thought to be terminally differentiated, there is now considerable evidence to indicate that this is not the case and that neurons can in fact re-enter the cell cycle[34, 35]. Whether re-entry is part of the lifespan of a healthy neuron, or restricted to diseased neuronal states, remains unclear. It is possible that the re-entry into the early G1 phase may be a necessary step for synaptic plasticity and brain remodelling, as suggested by Arendt[36-38]. However, healthy neurons are not thought to pass the G1/S checkpoint, but instead return to resting phase when remodelling is complete.

The association of AD with neuronal cell cycle activity prompted the cell cycle theory of AD that states that neurodegeneration is secondary to aberrant neuronal cell cycle re-entry and subsequent G1/S checkpoint failure[29, 30]. Neurons do not possess the machinery necessary for successful division or apoptosis, so are forced into a prolonged period of inappropriate activity, culminating in cell death. This is supported by the observation that levels of various

growth and mitogenic factors are raised in the brain of patients with mild AD[39-43]. Furthermore, AD neurons express proteins involved in the cell cycle (e.g. cell cycle markers): including proteins involved beyond G1 phase[44-52]. In addition, a number of studies demonstrate that a small proportion of neurons in AD brain (up to 10%) have replicated their DNA[53, 54]. It appears that cell cycle regulation may be defective in AD. For example, cell cycle regulators are expressed at high levels in AD brain, but may be inappropriately located in the cytoplasm rather than in the nucleus [45, 48, 52]. The nature of cell death in AD is also not fully understood[55], although the slow course of the disease suggests that cells do not die simply by apoptosis.

The cell cycle hypothesis goes further than the other theories in providing a link between the pathological hallmarks of AD. The entry and progression of a cell through the cell cycle is driven by the activity of numerous kinases. The microtubule associated protein: tau is one of the proteins involved in the re-organisation of the cytoskeleton during the cell cycle, and is also tightly regulated by phosphorylation[10]. The aberrant re-entry into the cell cycle and inappropriate progression beyond the G1/S checkpoint may lead to inappropriate kinase activity, inappropriate phosphorylation of tau, and ultimately NFT formation[10]. Cell cycle kinases are also involved in the processing of APP, potentially leadings to beta-amyloid deposition[43]. Interestingly, beta-amyloid is a mitogen in vitro, which may contribute to the self-perpetuating nature of the disease[56, 57]. Assuming Arendt's theory[36-38] is correct, the cell cycle hypothesis also fits with the overall picture of AD, as pathology characteristically spreads from more to less plastic areas of the brain[15].

There is considerable evidence to suggest that the cell cycle regulatory failure that takes place in neurons in AD also occurs in other cell types of these patients[58-63]. For example, there is an association between AD and some cancers[64-66]: with Burke and co-workers[67] demonstrating that AD patients have a higher risk of developing certain cancers than controls. Furthermore, there is evidence to suggest that lymphocytes from AD patients respond inappropriately to mitogenic stimuli compared to lymphocytes from controls[11, 61, 68, 69]. In particular, the mammalian target of rapamycin (mTOR) signalling pathway that promotes cell growth, division and differentiation seems to be altered. A study found altered expression of mTOR pathway component in lymphocytes from AD patients compared to controls[70]. Furthermore, two studies have shown that peripheral lymphocytes from AD and mild cognitive impairment (MCI) patients have a reduced response to rapamycin: a potent upstream inhibitor of mTOR, compared to lymphocytes from controls[71, 72].

1.7. MTOR PATHWAY

mTOR is a highly conserved serine-threonine kinase that is essential to the co-ordination of intra and extra-cellular signals concerning cell growth, division and differentiation. It is found in two complexes within the cell: mTOR complex (mTORC) 1 and mTORC2[73] that act upstream of the hugely complex mTOR pathway (Figure 2).

The mTOR complexes are turned on in response to various upstream signals that promote cell division (for example, growth factors and hypoxia). mTORC1 activates two translation initiation factors (4E-BP1 and p70S6K) that are needed for the synthesis of proteins required

for cell cycle initiation and progression[73]; whereas mTOR2 activates kinases involved in actin re-organisation: an integral part of the cell cycle. Both complexes are part of an excitatory pathway that promotes proliferation; whereas their inactivation (by rapamycin) should actively inhibit proliferation.

The fact that lymphocytes from AD patients have a reduced response to rapamycin (a potent cell cycle inhibitor) implies that the mTOR signalling pathway is inappropriately regulated in AD. It is possible that the mTOR pathway components that are responsible for the cell cycle regulatory failure in lymphocytes may also be responsible for the cell cycle regulatory failure in neurons in AD. The identification of these components is of vital importance as they may serve as novel drug targets for the treatment of AD, or may represent novel diagnostic biomarkers.

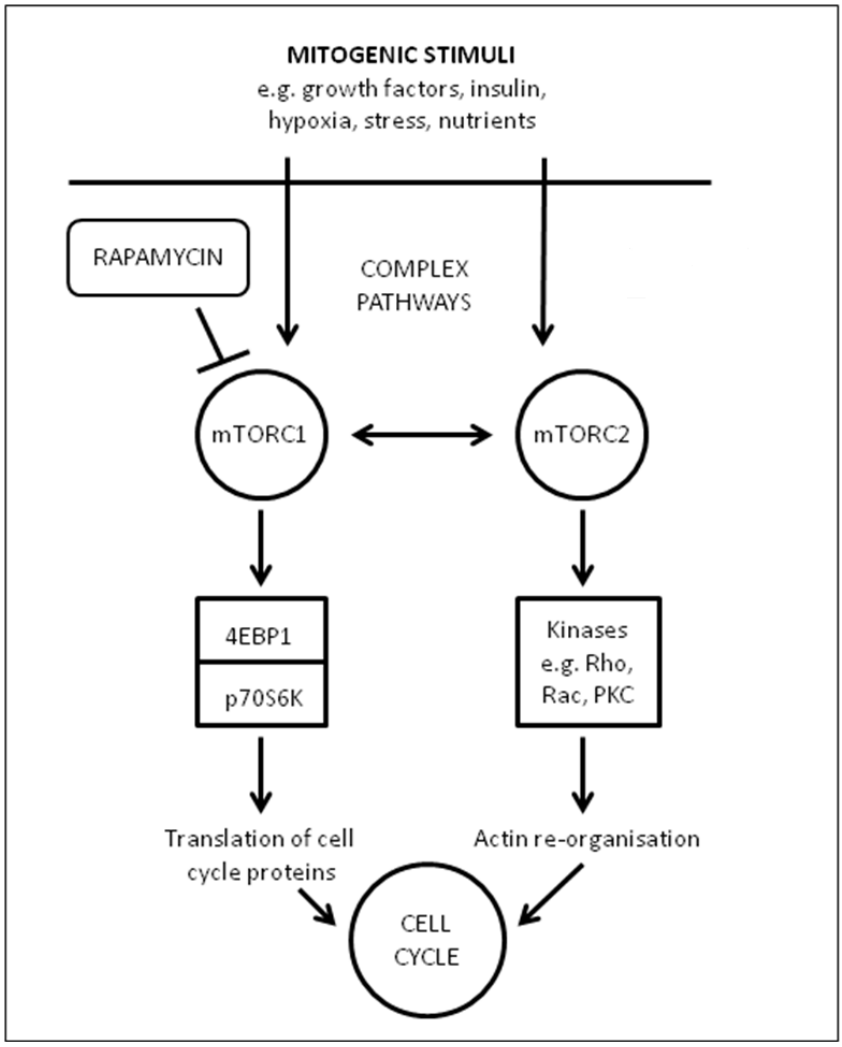

Figure 2 **Simplified version of the mTOR signalling pathway. The pathway responds to various upstream mitogenic signals, transmits the signals downstream, and culminates in the co-ordinated translation of various proteins requires for cell cycle activity.**

1.8. CYCLIN DEPENDENT KINASE INHIBITORS (CDKI)

The G1/S checkpoint is controlled by the cip/kip family of CDKIs, namely: $p21^{cip1}$ (CDKN1A), $p27^{kip1}$ (CDKN1B) and $p57^{kip2}$ (CDKN1C). It is possible that genetic variants of the CDKIs, that have reduced expression or function, may contribute to the loss of G1/S checkpoint control that is postulated to be a cause of neurodegeneration in AD[29, 30, 74]. Interestingly, a common genetic variant of $p21^{cip1}$ that is associated with an increased risk of cancer[75-79] was also found to be associated with an increased risk and earlier age of onset of AD[74]. The association with cancer implies that the variant has reduced function and/or expression: thereby limiting its ability to inhibit cyclin/CDK complexes, contributing to the loss of cell cycle control. Furthermore, genetic linkage studies have identified variants of the 6p21 loci, on which the $p21^{cip1}$ gene is located, as associated with an increased risk of AD[80, 80-83]. This may indicate an association of the $p21^{cip1}$ gene with AD.

The $p21^{cip1}$ variant has two polymorphisms: a cytosine to adenine change (SNP A) that induces a serine to alanine substitution at codon 31 of $p21^{cip175-79}$, and a cytosine to thymine change (SNP B) in its 3-prime untranslated region (UTR)[76, 77] (Figure 4 and 5). It appears that the SNPs are only associated with cancer and AD when found together [76, 77]. SNP A triggers an amino acid change in the CDK inhibitory region of the $p21^{cip1}$ protein, potentially altering its CDK binding capacity[74]. SNP B is located within the 3'-UTR of $p21^{cip1}$: a site involved in $p21^{cip1}$ mRNA binding to various non-coding RNAs and proteins that regulate mRNA stability[84]. This implies that SNP B may alter mRNA stability, potentially altering expression at the protein level.

The study[74] also identified a SNP on $p57^{kip2}$ that may be associated with an earlier age of onset of AD (Figure 3). The SNP leads to an amino acid change within the central proline/alanine rich domain of $p57^{kip2}$. Currently, the SNP is not known to be associated with cancer. The analysis of the SNP is complicated by the finding that $p57^{kip2}$ is paternally imprinted in humans: with extent of imprinting tissue-dependent. Its imprinting status in the brain is currently unknown[85].

Imprinting refers to the preferential expression of a gene of one parent of origin over another, and is regulated by various epigenetic mechanisms: for example, DNA methylation, histone modification and chromosome re-organisation. The $p57^{kip2}$ gene is located within a cluster of imprinted genes on 11p15.5: their imprinting controlled by a common imprinting control region (ICR) located within another gene member of the cluster. Beckwich-Wiederman syndrome, an overgrowth/cancer syndrome, is associated with inappropriate imprinting and expression of the imprinted genes within the 11p15.5 imprinted cluster[33]. It is possible that inefficient imprinting of $p57^{kip2}$ in the brain may alter $p57^{kip2}$ expression, potentially contributing to the loss of cell cycle control that is postulated to be a cause of neurodegeneration in AD. However, as very little is known about the imprinting status of $p57^{kip2}$ in the human brain, research regarding normal imprinting status is necessary before conclusions can be drawn on imprinting status and disease.

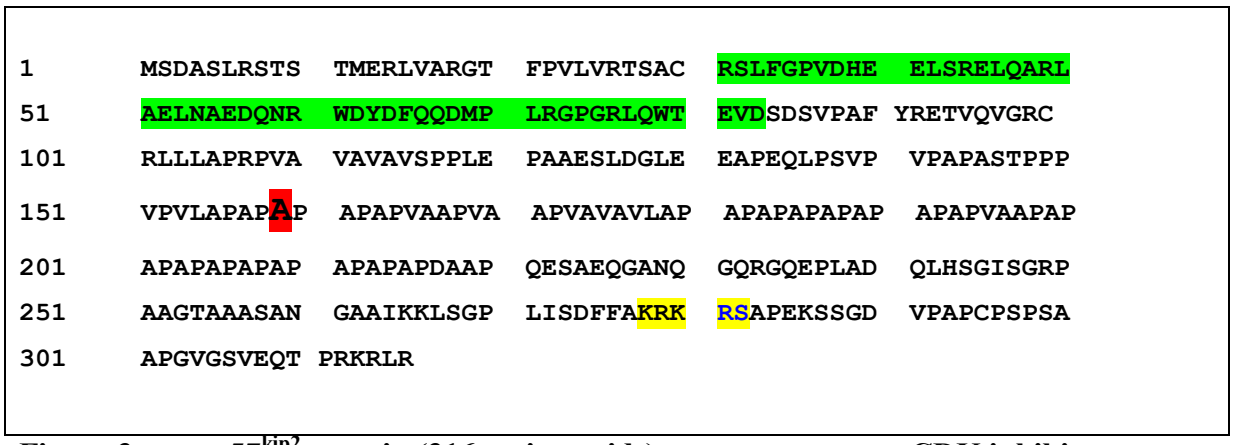

Figure 3 **p57^{kip2} protein (316 amino acids): green represents CDK inhibitory domain; red represents codon 159 (altered by SNP); yellow represents the nuclear localisation signal.**

```
1081    GTGTGGCTCC TTCCCATCGC TGTCACAGGC GGTTATGAAA TTCACCCCCT TTCCTGGACA
1141    CTCAGACCTG AATTCTTTTT CATTTGAGAA GTAAACAGAT GGCACTTTGA AGGGGCCTCA
1201    CCGAGTGGGG GCATCATCAA AAACTTTGGA GTCCCCTCAC CTCCTCTAAG GTTGGGCAGG
1261    GTGACCCTGA AGTGAGCACA GCCTAGGGCT GAGCTGGGGA CCTGGTACCC TCCTGGCTCT
1321    TGATACCCCC CTCTGTCTTG TGAAGGCAGG GGGAAGGTGG GGTCCTGGAG CAGACCACCC
1381    CGCCTGCCCT CATGGCCCCT CTGACCTGCA CTGGGGAGCC CGTCTCAGTG TTGAGCCTTT
1441    TCCCTCTTTG GCTCCCCTGT ACCTTTTGAG GAGCCCCAGC TACCCTTCTT CTCCAGCTGG
1501    GCTCTGCAAT TCCCCTCTGC TGCTGTCCCT CCCCCTTGTC CTTTCCCTTC AGTACCCTCT
1561    CAGCTCCAGG TGGCTCTGAG GTGCCTGTCC CACCCCCACC CCCAGCTCAA TGGACTGGAA
1621    GGGGAAGGGA CACACAAGAA GAAGGGCACC CTAGTTCTAC CTCAGGCAGC TCAAGCAGCG
1681    ACCGCCCCCT CCTCTAGCTG TGGGGGTGAG GGTCCCATGT GGTGGCACAG GCCCCCTTGA
1741    GTGGGGTTAT CTCTGTGTTA GGGGTATATG ATGGGGGAGT AGATCTTTCT AGGAGGGAGA
1801    CACTGGCCCC TCAAATCGTC CAGCGACCTT CCTCATCCAC CCCATCCCTC CCCAGTTCAT
1861    TGCACTTTGA TTAGCAGCGG AACAAGGAGT CAGACATTTT AAGATGGTGG CAGTAGAGGC
1921    TATGGACAGG GCATGCCACG TGGGCTCATA TGGGGCTGGG AGTAGTTGTC TTTCCTGGCA
1981    CTAACGTTGA GCCCCTGGAG GCACTGAAGT GCTTAGTGTA CTTGGAGTAT TGGGGTCTGA
2041    CCCCAAACAC CTTCCAGCTC CTGTAACATA CTGGCCTGGA CTGTTTTCTC TCGGCTCCCC
2101    ATGTGTCCTG GTTCCCGTTT CTCCACCTAG ACTGTAAACC TCTCGAGGGC AGGGACCACA
2161    CCCTGTACTG TTCTGTGTCT TTCACAGCTC CTCCCACAAT GCTGAATATA CAGCAGGTGC
2221    TCAATAAATG ATTCTTAGTG ACTTTAAAAA AAAAAAAAAA AAAAA
```

Figure 4 **p21[cip1] mRNA (2265 nucleotides): yellow represents translated region; red represents location of SNP A; blue represents location of SNP B.**

```
1     MSEPAGDVRQ  NPCGSKACRR  LFGPVDSEQL  SRDCDALMAG  CIQEARERWN
51    FDFVTETPLE  GDFAWERVRG  LGLPKLYLPT  GPRRGRDELG  GGRRPGTSPA
101   LLQGTAEEDH  VDLSLSCTLV  PRSGEQAEGS  PGGPGDSQGR  KRRQTSMTGK
151   DRRRGGKILR  EAAC
```

Figure 5 **p21[cip1] protein (164 amino acids): green represents the CDK inhibitory domain; red represents codon 31 (altered by SNP A); yellow represents the nuclear localisation signal.**

1.9. AIMS

The aims of the study were three fold. Firstly, to identify the rapamycin-regulated genes that are differentially expressed in brain from AD patients compared to control. These genes may play a causal role in the pathogenesis of AD, and may serve as novel drug targets or biomarkers of disease. Genes were identified with a gene expression microarray: a sensitive tool that allows rapid screening of a large number of genes for differential expression in a group-of-interest compared to control. A whole human genome microarray was used to identify genes that were rapamycin-regulated in lymphocytes by comparing expression in lymphocytes treated with rapamycin to expression in untreated lymphocytes. A custom microarray was then created to include the identified rapamycin-response elements, plus established rapamycin-regulated genes, to allow screening for differential expression in AD brain compared to control.

A second aim was to elucidate the effects of the $p21^{cip1}$ SNPs on the risk of AD, the age of onset of AD, and the accumulation of AD-related pathology in the brain. This was achieved by genotyping a cohort of AD patients for the $p21^{cip1}$ SNPs, and quantifying various markers of AD-related pathology in the brain by enzyme linked immunosorbant assay (ELISA). The effects of the $p21^{cip1}$ SNPs on the function and stability of $p21^{cip1}$ were determined by transient transfection of a vector containing the wild type or variant $p21^{cip1}$ into a rapidly dividing cell line. $p21^{cip1}$ mRNA stability was determined by Q-PCR; $p21^{cip1}$ expression determined by Acumen analysis after immunolabelling; and effects of the different versions of $p21^{cip1}$ on cell cycle activity determined by Acumen cytometry.

A third aim was to investigate the imprinting status of $p57^{kip2}$ in the brain, and the association of the imprinting status with AD. Furthermore, we investigated the association of the $p57^{kip2}$ SNP with AD, and the effects of the SNP on $p57^{kip2}$ expression. Elderly control and AD patients were genotyped for the $p57^{kip2}$ SNP, and various markers of AD-related pathology in the brain quantified by ELISA. Individuals that were heterozygous for the $p57^{kip2}$ SNP were informative in terms of imprinting status. They were additionally genotyped from cDNA to establish whether there was preferential expression of one allele over another. $p57^{kip2}$ mRNA stability and $p57^{kip2}$ expression were determined by Q-PCR and ELISA respectively.

2. MATERIALS AND METHODS

2.1. PATIENTS AND BIOMATERIALS

Human brain tissue collected by the Oxford Project to Investigate Memory and Aging (OPTIMA) was made available through the Thomas Willis brain bank. In total, samples from 252 brains were available from a mix of elderly controls and patients suffering from preclinical, mild and severe AD at the time of death (as determined by Braak staging). The number of cases included in the study was based on availability, not statistical power calculations, as the outcome, and hence number of patients in each group-of-interest, was unknown. The tissue was snap frozen at the time of autopsy: and available from the lateral temporal lobe (severely affected by AD pathology), frontal lobe (affected by AD pathology) and occipital lobe (largely unaffected by AD pathology). A wealth of clinical information was available for each subject, including: Braak stage (severity of AD); additional pathology; age of onset and age at death; personal and family history of cancer; plasma homocysteine level, and the results of annual clinical tests including test of cognitive performance (CAMCOG).

2.2. DNA, RNA AND PROTEIN EXTRACTION

RNA, DNA and protein were isolated from lateral temporal, frontal and occipital lobe tissue of each subject by TRI-reagent extraction. Appendix 1 (Table 52) identifies the chemical manufacturers relating to this protocol. 100mg of frozen tissue was homogenised in 1ml

TRI-reagent, incubated at room temperature (RT) for 5 minutes, and supplemented with 100µl 1-bromo-3-chloropropane. Following 15 sec of vigorous mixing, the solution was incubated for 2 min and centifuged at 12,000 rotational centrifugal force (g) for 15 minutes at 4ºC to separate the RNA, DNA and protein layers.

The aqueous RNA layer was supplemented with 500µl isopropanol and mixed gently by inversion. After a five minute incubation, the solution was centrifuged at 12,000g for 8 minutes at 4ºC. The pellet was washed in 1ml 75% ethanol, centrifuged at 7,500g for 5 minutes at 4ºC, and ethanol wash removed. The pellet was air-dried for 30 minutes and rehydrated in 100µl nuclease free water by incubation at 55ºC for 15 minutes, prior to storage at -80ºC.

RNA was converted to cDNA by reverse transcription. 10µg of RNA in a 50µl volume was added to 50µl of reverse transcriptase master mix (composed of 10µl 10 x reverse transcriptase buffer; 4 µl dNTP mix (100mM); 10µl random primers; 5µl MultiScribe Reverse Transcriptase (50U/µl); and 21µl nuclease free water), and incubated at 25ºC for 10 minutes; 37ºC for 120 minutes; and 85ºC for 5 seconds in a Thermal cycler. The cDNA was precipitated with isopropanol with pH correction (100µl cDNA supplemented with 20µl of 3M sodium citrate at pH 5 and 400 µl isopropanol), centrifuged at high speed for 10 minutes, and the resulting pellet washed in ice cold ethanol. Following high speed centrifugation and supernatant removal, the pellet was air dried overnight, rehydrated in 100µl nuclease free water and stored at 4ºC.

The remaining TRI-reagent layers were supplemented with 300µl ethanol, centrifuged at 12,000g for 5 minutes at 4ºC, and supernatant transferred to a clean tube for subsequent protein extraction (see below). The DNA pellet was washed three times, 1 hour per wash, in 0.1M sodium citrate in 10% ethanol, with centrifugation at 12,000g for 5 minutes between each wash. Following a 30 minute wash in 75% ethanol, the pellet was centrifuged at 2,000g for 5 minutes, supernatant removed, and the pellet air dried overnight. The pellet was dissolved in nuclease free water for 24 hours, centrifuged at 16,000g for 10 minutes, and supernatant transferred to a clean tube to separate DNA from the insoluble material. The DNA was stored at 4ºC.

The protein was precipitated by 15 minute incubation with 3 times its volume of acetone prior to centrifugation at 12,000g for 10 min at 4ºC. The protein pellet was subjected to three 10 minute washes in 0.3M guanidine hydrochloride in 95% ethanol and 2.5% glycerol, and subsequently dissolved in radio-immunoprecipitation (RIPA) buffer (composition: 0.1M sodium chloride, 0.01M Tris hydrochloride, 1:500 EDTA, 400µg/ml phenylmethanesulfonylfluoride, 2µg/ml aprotinin and 1% sodium dodecyl sulphate). The protein was stored at -20ºC.

2.3. GENE EXPRESSION MICROARRAY

Two-colour microarray based gene expression analysis (Agilent Technologies) was used to identify genes that were differentially expressed in lymphocytes treated with rapamycin compared to lymphocytes that were left untreated (Agilent Whole Human Genome Microarray: 4x44K). The identified differentially expressed genes were rapamycin-regulated, and were screened in one-colour custom microarray based gene expression analysis (Agilent Technologies) for differential expression in brain affected by AD compared to control. Appendix 1 (Table 53) outlines the chemical manufacturers relating to gene expression microarray.

2.3.1 Two-colour microarray based gene expression analysis

Lymphocyte cell culture and rapamycin treatment, in preparation for two-colour microarray based gene expression analysis, were carried out by Zsuzsanna Nagy, and are described in appendix 4. RNA was extracted from the lymphocyte pellets by TRI-reagent method (as described in 2.2). To ensure that there was no DNA contamination, the RNA was treated with DNase prior to microarray analysis, by standard Qiagen protocol as described in appendix 2. The RNA quality was determined by RNA nano-chip analysis on the Agilent 2100 Bioanalyser, also by standard protocol[86]. The RNA quality ranged from 8-10 RNA Integrity number[87] (RIN): indicative of good quality RNA[88] suitable for gene expression microarray.

2.3.1.1. Conversion of RNA to cDNA

200ng of RNA was converted to cDNA with the low-input quick amplification labelling kit. Spike Mix A and B were prepared separately. For each, the spike mix was thawed and vortexed; incubated at 37ºC for 5 minutes; and diluted in the provided dilution buffer (see Table 1 for dilution protocol). 2µl of diluted spike mix A and spike mix B were added to 200ng of RNA in a 1.5µl volume from the rapamycin-treated and untreated lymphocytes respectively. The T7 promoter primer was prepared as shown in Table 2, and 1.8µl added per 3.5µl sample. The samples were incubated at 65ºC for 10 minutes, and placed on ice for 5 minutes. The cDNA master mix was set up immediately prior to use as shown in Table 3. 4.7µl of the cDNA master mix was added per sample; and samples incubated at 40ºC for 2 hours; 70ºC for 15 minutes; and placed on ice for 5 minutes.

Table 1 Preparation of Spike Mix A and Spike Mix B

Starting amount of RNA		**Serial dilutions**			
Total RNA (ng)	**Concentration (ng/µl)**	**First**	**Second**	**Third**	**Spike mix volume per labelling (µl)**
200	133.3	1:20	1:40	1:16	2

Table 2 Dilution of T7 promoter primer

Component (Agilent)	**Volume (µl) per reaction**
T7 promoter primer	0.8
Nuclease free water	1
Total volume	**1.8**

Table 3 cDNA master mix

Components (Agilent)	**Volume (µl) per reaction**
5x first strand buffer (pre-warmed at 80°C for 4 minutes prior to use)	2
0.1M DTT	1
10mM dNTP mix	0.5
AffinityScript RNase Block mix	1.2
Total volume	**4.7**

2.3.1.2. Conversion of cDNA to labelled cRNA

The low-input quick amplification labelling kit was used to convert the cDNA to labelled cRNA. The transcription master mix was set up immediately prior to use as shown in Table 4. Spike Mix A samples were added to transcription master mix prepared with Cyanine 3-CTP (green); whereas Spike Mix B samples were added to transcription master mix prepared with Cyanine 5-CTP (red). 6µl of the transcription master mix was added per 10µl cDNA sample; and incubated at 40ºC for 2 hours.

Table 4 Composition of transcription master mix

Component (Agilent)	**Volume (µl) per reaction**
Nuclease free water	0.75
5 x transcription buffer	3.2
0.1 M DTT	0.6
NTP mix	1
T7 RNA polymerase Blend (store on ice until use)	0.21
Cyanine 3-CTP or Cyanine 5-CTP	0.24
Total volume	6

2.3.1.3. cRNA purification and quantification

The cRNA was purified by standard RNeasy mini column protocol (Qiagen) as described in appendix 2. The cRNA was quantified with a nanodrop spectrophotometer on the Microarray setting. The yield and specific activity of the cRNA samples were calculated as follows:

Yield = Concentration of cRNA x remaining cRNA volume / 1000

Specific activity = Concentration of Cy3 or Cy5/ Concentration of cRNA x 1000

The specific activity and yield of all the samples were greater than 6 and 825ng respectively, indicating suitability for hybridisation.

2.3.1.4. Hybridisation

825ng of labelled cRNA was added to various fragmentation components as described in Table 5, incubated at 60ºC for 30 minutes, and cooled on ice for 1 minute. 55µl of GEx Hybridisation buffer HI-RPM was subsequently added to stop fragmentation. The samples were mixed, centrifuged at 13,000 rotations per minute (RPM) for 1 minute, and placed on ice in preparation for microarray assembly. The microarray of choice was the 4x44K Agilent Whole Human Genome Microarray. A clean gasket slide was placed into the chamber base, 100µl of sample dispensed per well, and array placed onto the gasket slide to facilitate hybridisation. The gasket and microarray slides were clamped together and incubated at 65ºC for 17 hours.

Table 5 Components of Fragmentation mix

Components (Agilent)	**Volume/ Mass (for 4x44K microarray)**
Cy3-labelled cRNA	825ng
Cy5-labelled cRNA	825ng
10 x blocking agent	11 µl
Nuclease free water	Bring total volume to 52.8 µl
25 x fragmentation buffer	2.2 µl
Total volume	**55 µl**

Following hybridisation, the microarrays were washed in various wash solutions as described in Table 6. To summarise, the microarrays were removed from the hybridisation assembly and carefully separated from the gasket slide whilst fully submersed in wash buffer 1. Slides were washed for 1 minute, transferred to wash buffer 2 at 37ºC for 1 minute, and

washed in acetonitrile for 10 seconds. The final wash was in stabilisation and drying solution for 30 seconds. The slides were air-dried and stored in a dark slide box in a nitrogen rich environment prior to scanning on the Agilent C Scanner. The AgilentHD_GX_2color programme was used, and settings amended as shown in Table 7.

Table 6 Microarray wash protocol

Dish	**Wash buffer (Agilent)**	**Temp**	**Time**
1	GE Wash buffer 1	Room temperature (RT)	
2	GE Wash buffer 1	RT (with stir bar)	1 min
3	GE Wash buffer 2	37ºC (with stir bar)	1 min
4	Acetonitrile	RT (with stir bar)	10 sec
5	Stabilisation and drying solution (Agilent)	RT (with stir bar)	30 sec

Table 7 Microarray scanner settings for two-colour microarray based gene expression analysis (Agilent)

	4x44K HD microarray format
Dye Channel	Red and Green
Scan region	Scan area (61 x 21.6mm)
Scan resolution (µM)	5
Tiff	20 bit

2.3.1.5. Data analysis: microarray

The feature extraction programme was used to collate the Microarray layout with the output of the scanner. The output was normalised to various housekeeping genes present on the microarray, and results processed to provide a list of genes that were differentially expressed in rapamycin-treated lymphocytes compared to untreated lymphocytes. Estimates of the false discovery rate (FDR) were provided for each gene. For the purpose of our study, genes with a FDR up to 10% were accepted as differentially expressed[89].

2.3.2 One-colour custom microarray based gene expression analysis (Agilent)

8x 15K Custom Microarrays (Agilent Technologies: able to accommodate up to 15,000 genes) were designed to include various housekeeping genes (719 genes), internal controls (3141 genes), and genes that were differentially expressed in AD brain relative to control brain based on a published dataset[90, 91] (3718 genes). The remaining 7422 spaces were filled with known rapamycin-regulated genes (based on an IPA Ingenuity search: see appendix 6, Table 58) and the genes that were identified as rapamycin-regulated in lymphocytes based on the two-colour microarray based gene expression analysis (see appendix 6, Table 56 and Table 57).

Of the 252 subjects for whom tissue was available through the Thomas Willis brain bank, 32 subjects were selected for one-colour custom microarray based gene expression analysis. They included control subjects and patients with mild and advanced AD. The exclusion

criteria were as follows: vascular disease; Parkinson's disease; ApoE ε2/ε2, ApoE ε2/ε3 and ApoE ε4/ε4 genotypes (not enough patients for meaningful statistical analysis); and high plasma homocysteine level (> 35 μM).

2.3.2.1. Sample preparation

RNA was extracted from the frontal lobe of each subject by TRI-reagent protocol as described in 2.2. The RNA was treated with DNase as described in appendix 2. The suitability of the RNA for microarray based gene expression analysis was determined by Agilent RNA nano-chip analysis. RIN values ranged from 2-3 indicating relatively poor quality RNA. However, this was unavoidable, as the source brain tissue had significant post-mortem time prior to freezing, resulting in inevitable degradation.

2.3.2.2. Conversion of RNA to labelled cRNA

200ng of RNA was converted to cDNA, and subsequently to labelled cRNA, with the low-input quick amplification labelling kit. The spike mix was incubated at 37ºC for 5 minutes, and diluted in the provided dilution buffer (Agilent Techologies) as shown in Table 8. 2μl of the diluted spike mix was added to the RNA (200ng) in a 1.5μl volume. The next part of the labelling protocol was identical to that described in section 2.3.1.1 and 2.3.1.2. Note that cyanine 3-CTP was used to label all samples. The labelled and amplified cRNA samples were purified by standard Qiagen RNeasy mini column protocol, and quality assessed and quantified as described in section 2.3.1.3.

Table 8 Preparation of Spike Mix

Starting amount of RNA		**Serial dilutions**				
Total RNA (ng)	**Concentration (ng/µl)**	**First**	**Second**	**Third**	**Fourth**	**Spike mix volume per labelling (µl)**
200	133.3	1:20	1:25	1:10		2

2.3.2.3. Hybridisation

600ng of labelled cRNA was added to various fragmentation components (Table 9), incubated at 60ºC for 30 minutes, and cooled on ice for 1 min. 25µl of GEx Hybridisation buffer HI-RPM was added to stop fragmentation. The sample was gently mixed, centrifuged at 13,000 rpm for 1 min, and placed on ice in preparation for hybridisation. The microarray was assembled and incubated overnight as described in section 2.3.1.4, with two alterations: the Custom 8x15K Microarray was used and 40µl of sample was added per 15K array. After 17 hour hybridisation, the microarrays were washed as described in section 2.3.1.4, and scanned on the Agilent C Scanner on programme AgilentHD_GX_1color, with the settings amended as shown in Table 10.

Table 9 Components of Fragmentation mix

Components (Agilent)	**Volume/ Mass (for 8x15K microarray)**
Cy3-labelled cRNA	600 ng
10 x blocking agent	5 µl
Nuclease free water	Bring total volume to 24 µl
25 x fragmentation buffer	1 µl
Total volume	25 µl

Table 10 Microarray scanner settings for one-colour microarray based gene expression analysis (Agilent)

	8x15K HD microarray format
Dye Channel	Green
Scan region	Scan area (61 x 21.6mm)
Scan resolution (µM)	5
Tiff	20 bit

2.3.2.4. Data analysis: microarray

The feature extraction programme was used to collate the Custom Microarray layout with the output of the scanner. The results from individual patients were grouped based on subject diagnosis, disease severity (as defined by Braak stage) and ApoE genotype. For the purposes of this study, the groups-of-interest were as follows (see Table 11):

Table 11 Microarray: subject groups

Patient diagnosis	**ApoE genotype**	**Number of patients**
Control (entorhinal stage)	ApoE ε3/ε3	5
Mild AD (limbic stage)	ApoE ε3/ε3	5
Advanced AD (neocortical stage)	ApoE ε3/ε3	4
Advanced AD (neocortical stage)	ApoE ε3/ε4	18

Statistical Analysis of Microarray (SAM)[92] was used to carry out unpaired, two-sample T tests for each gene in a group-of-interest compared to control. SAM identifies genes that are differentially expressed at RNA level in the group-of-interest compared to control group; the direction of expression; fold change; and an estimate of the false discovery rate (FDR). For the purpose of our study, we selected an estimated FDR of 10% as acceptable for identifying differentially expressed genes[89]. SAM was carried out with 1000 permutations, and the output processed to remove duplicates. The output was analysed with the IPA Ingenuity software (www.ingenuity.com).

2.4. Q-PCR VALIDATION OF MICROARRAY RESULTS

Real-time PCR (Q-PCR) measures the expression of a gene-of-interest relative to a housekeeping gene such as beta-actin, thereby allowing relative quantification of the gene-of-interest. Validation was carried out on cDNA obtained from the same subjects and brain regions used for the microarray study (see Table 6). The genes-of-interest were selected as they were shown to be either significantly up- or down- regulated in advanced AD (neocortical stage) compared to control in the microarray study.

The Universal probe library design centre (Roche Diagnostic Website) was used to design Q-PCR systems (Table 12); and primers and probes ordered from Sigma Genosys and Roche respectively. For the composition of each 20µl Q-PCR mix see Table 13. Two negative controls (water) and a cDNA standard curve (five serial dilutions starting with neat cDNA) were included per Q-PCR run. The samples were denatured at 96^{o}C for 15 minutes and amplified by 40 cycles of 96^{o}C for 15 seconds, optimal annealing temperature (Table 12) for 30 seconds and 72^{o}C for 30 seconds. FAM output was read in the annealing phase.

Table 12 Q-PCR: Probe, primer sequences, and annealing temperature corresponding to each gene-of-interest

Gene	Roche Probe	Forward primer	Backward primer	Optimal annealing temp (ºC)
Beta actin	**24**	5'-TCAGCTGTGG GGTCCTGT-3'	5'-GAAGGGGACA GGCAGTGAG-3'	62
EIF4E (Variant 1/ 2)	**35**	5'-GATGGCGAC TGTCGAACC-3'	5'-TGGGTTAGCAA CCTCCTGAT-3'	60
EIF4E (Variant 3)	**35**	5'-GTGTAGCGCA CACTTTCTGG-3'	5'-TGGGTTAGCA ACCTCCTGAT-3'	60
MAPK1 (Variant 1/ 2)	**62**	5'-CCGTGACCT CAAGCCTTC-3'	5'-GCCAGGCCA AAGTCACAG-3'	58
GABBR2	**3**	5'-GCGAAGGAC AGTGGAGAAGT-3'	5'-GAGAGGGCG GATGGAGATA-3'	62
SEMA4C	**14**	5'-TTGTGCCGC GTAAGACAGT-3'	5'-CAGCGTCA GTGTCAGGAAGT-3'	60
DZIP3	**39**	5'-TGCCCAAGAT CTGATACAAGG-3'	5'-CTCCAACAC ACCACCGTACA-3'	60
SERPINE1	**80**	5'-CTCCTGGTTC TGCCCAAGT-3'	5'-CAGGTTCT CTAGGGGCTTCC-3'	58

Table 13 Q-PCR reaction for validation of microarray

Composition of Q-PCR reaction	**Manufacturer**
0.5µl Universal probe (10µM)	Roche
10µl Absolute Q-PCR mix (Compositition: 0.625 Units ThermoPrime Taq DNA polymerase, 75mM Tris HCl (pH 8.8 at 25ºC), 20mM $(NH_4)_2SO_4$, 1.5mM $MgCl_2$, 0.01% (v/v) tween 20, 0.2mM each of dATP, dCTP, dGTP, dTTP).	ThermoScientific
0.5µl forward primer (20µM)	Sigma Genosys
0.5µl backward primer (20µM)	Sigma Genosys
6.5µl nuclease free water	Qiagen
2µl cDNA (neat, 1:4 and 1:16)	Prepared as in section 2.2

2.4.1 Data analysis: Q-PCR

Each of the cDNA standard curve serial dilutions were assigned an arbitrary copy number (1:1 = 10,000; 1:2 = 5,000; 1:4 = 2500; 1:8 = 1250; 1:16 = 625). The Rotor gene-6 programme automatically identifies the optimal threshold and determines the copy number of the gene-of-interest relative to the standard curve for each sample. The Q-PCR was considered fully optimised when the calculated standard curve copy number varied less than 10% from the assigned copy number. The values obtained for each gene were normalised to the corresponding beta-actin values to allow quantitative comparison of samples.

2.5. $P21^{CIP1}$ AND $P57^{KIP2}$ GENOTYPING

Of the 252 brains made available for the study, those with rare additional pathologies were excluded from the analysis (for example: motor neurone disease, Huntington's disease and frontal lobe dementia). Brains from AD patients with common additional pathologies (Parkinson's disease, vascular disease and Lewy bodies) were included in the study to boost patient numbers. The subjects were genotyped for SNP A and SNP B on $p21^{cip1}$ and for the $p57^{kip2}$ SNP (refer to section 1.8).

2.5.1 $p21^{cip1}$ genotyping: SNP A

$p21^{cip1}$ was genotyped for SNP A by standard PCR/ restriction digest protocol. PCR was set up as described in Table 14, and amplified on a thermal cycler with an initial denaturation step of 95°C for 5 minutes, followed by 40 cycles of 95°C for 60 seconds, 65°C for 60 seconds and 72°C for 60 seconds. 17µl of the PCR product was digested with 1µl BsmA1 (5000U/ml) and 2µl of NEbuffer 3 (both New England Biolabs) at 55°C for 18 hours.

Restriction digest products were separated on a 3% Metaphor agarose (Lonza) and 0.5% Multipurpose agarose (Roche) gel prepared with 1x Tris-borate-EDTA (TBE) buffer (Invitrogen), and supplemented with Sybr safe to a final concentration of 1:10,000 (Sybr safe). The gel was run at 150 volts for 3 hours in 0.5x TBE buffer. Gels were viewed and photographed in an Uvitec ultraviolet light box and results interpreted as shown (Figure 6).

Table 14 Composition of PCR mix ($p21^{cip1}$ genotyping: SNP A)

Composition of PCR reaction	**Volume (µl)**	**Concentration**	**Manufacturer**
DNA	2	25ng/µl	See section 2.2
Forward primer (5'-CGGGATCCGGCGCCATGTC AGAACCGGC-3')	0.1	100µM	Sigma Genosys
Backward primer (5'-CCAGACAGGTCAGCCCTTGG-3')	0.1	100µM	Sigma Genosys
Nuclease free water	5.3		Qiagen
Polyethylene glycol	2.5	40% w/w	Sigma
Reddymix PCR master mix (Composition: 0.625 units ThermoPrime Taq DNA polymerase, 75mM Tris-HCl (pH 8.8 at 25ºC), 20mM $(NH^4)^2SO^4$, 1.5M MgCl, 0.01% (v/v) Tween 20, 0.2mM each of dATP, dCTP, dGTP and dTTP).	10	2 x	Thermoscientific

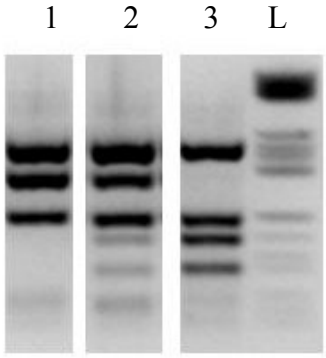

Figure 6 $p21^{cip1}$ SNP A: restriction digest banding pattern: 1 = wild type for SNP A on $p21^{cip1}$; 2 = heterozygous for SNP A on $p21^{cip1}$; 3 = homozygous for SNP A on $p21^{cip1}$; L = ladder (molecular weight marker V, Roche).

2.5.2 $p21^{cip1}$ genotyping: SNP B

$p21^{cip1}$ was genotyped for SNP B by standard PCR/ restriction digest protocol. PCR was set up as described in Table 15, and amplified on a thermal cycler with an initial denaturation step of 95°C for 5 minutes, followed by 40 cycles of 95°C for 30 seconds, 56°C for 30 seconds and 72°C for 30 seconds. 17µl of PCR product was digested with 1.25µl Pst1 (20,000U/ml), 2.5µl NE buffer 3, 4µl nuclease free water and 0.25µl bovine serum albumin (all New England Biolabs) at 37ºC for 18 hours. The restriction digest products were separated on a 2% Multipurpose agarose (Roche) gel prepared with 1 x TBE buffer and 1:10,000 Sybr safe. The gel was run in 0.5 x TBE buffer at 150 volts for 3 hours. The results were interpreted as shown (Figure 7).

Table 15 Composition of PCR mix ($p21^{cip1}$ genotyping: SNP B)

Composition of PCR reaction	**Volume (µl)**	**Concentration**	**Manufacturer**
DNA	2	25ng/µl	See section 2.2
Forward primer 5'-CCCAGGGAAGGGTGTCCTG-3'	0.11	100µM	Sigma Genosys
Backward primer 5'-GGGCGGCCAGGGTATGTAC-3'	0.11	100µM	Sigma Genosys
Nuclease free water	7.68		Qiagen
Gelatin	1.1	2%	Sigma
Reddymix PCR master mix (composition outlined in Table 14)	11	2 x	Thermoscientific

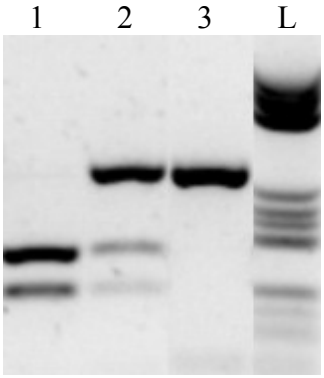

Figure 7 $p21^{cip1}$ SNP B: restriction digest banding pattern: 1 = wild type for SNP B on $p21^{cip1}$; 2 = heterozygous for SNP B on $p21^{cip1}$; 3 = homozygous for SNP B on $p21^{cip1}$; L= ladder (molecular weight marker V, Roche).

2.5.3 $p57^{kip2}$ genotyping

$p57^{kip2}$ was genotyped by standard PCR/ restriction digest protocol (see section 1.8 for SNP description). PCR was set up as described in Table 16, and amplified on a thermal cycler on the following programme: 95ºC for 5 minutes; 35 cycles of 95ºC for 30 seconds, 60ºC for 1 minute and 72ºC for 30 seconds. 17µl PCR product was digested with 1µl AvaII (10,000 units/ml) and 2µl NE buffer 4 (both New England biolabs) at 37ºC for 18 hours. The restriction digest products were resolved on a gel composed of 3% Metaphor agarose (Lonza), 0.5% Multipurpose agarose (Roche), 1x TBE buffer and 1:10,000 Sybr Safe by running at 150 volts for 3 hours. The gels were interpreted as shown in Figure 8.

Table 16 Composition of PCR mix ($p57^{kip2}$ genotyping)

Composition of PCR reaction	**Volume (µl)**	**Concentration**	**Manufacturer**
DNA or cDNA	2	25ng/µl	See section 2.2
5´-CCGGAGCAGCTGCCTAGTG-3´	0.075	100µM	Sigma Genosys
Backward primer 5´-AATCCCCGAGTGCAGCTG-3´	0.075	100µM	Sigma Genosys
Nuclease free water	6.05		Qiagen
DMSO	2.05		Sigma
Reddymix PCR master mix (composition outlined in Table 14)	10.25	2 x	Thermoscientific

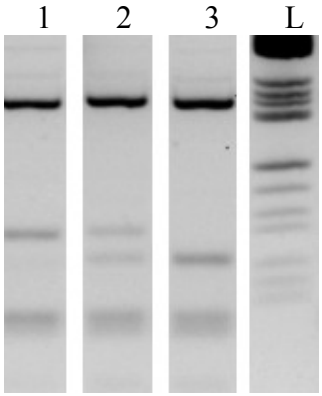

Figure 8 **Restriction digest banding pattern for $p57^{kip2}$ SNP: 1 = wild type for SNP on $p57^{kip2}$; 2 = heterozygous for SNP on $p57^{kip2}$; 3 = homozygous for SNP on $p57^{kip2}$; L = molecular weight marker V, Roche).**

2.5.4 $p57^{kip2}$ imprinting status

The patients that were heterozygous for the $p57^{kip2}$ SNP were informative in terms of imprinting status. They were genotyped from frontal and occipital lobe cDNA and results analysed with the National Institute of Health (NIH) imaging software: Image J. We measured the mean intensity of the wild type and variant bands (72 and 54 base pair bands respectively) of the DNA and cDNA results, and calculated the ratio of intensity of the wild type band to variant band for each as shown below:

$$\text{Ratio} = \frac{\text{wild type band intensity}}{\text{variant band intensity}}$$

For heterozygous samples, the ratios calculated from DNA represent equal wild type and variant content. cDNA samples with a ratio greater than the DNA ratio were interpreted as having greater $p57^{kip2}$ wild type expression than $p57^{kip2}$ variant expression; whereas samples with a ratio below the DNA ratio were interpreted as having more $p57^{kip2}$ variant expression than $p57^{kip2}$ wild type expression. For more detailed description of analysis refer to appendix 3.

2.6. ELISA: QUANTIFICATION OF AD-RELATED PATHOLOGY

Enzyme linked immunosorbant assay (ELISA) is a technique that allows relative quantification of a protein-of-interest. Amen Zafar (research technician) quantified the proteins described in Table 17 in the temporal, frontal and occipital lobe of each subject prior to the start of this MPhil. As part of this MPhil, $p21^{cip1}$, $p57^{kip2}$ and beta-actin were quantified in the temporal, frontal and occipital lobe of each subject. All data analysis and interpretation were carried out as part of this study.

Table 17 AD-related pathology markers

Marker	**Description**
Beta-amyloid	39-43 amino acid cleavage product of APP that accumulates in the brain of AD patients. One of the hallmarks of AD.
Amyloid precursor protein-C terminal (APP-C)	Beta-amyloid is contained within the C-terminal of APP-C, so APP-C presence is indicative of abnormal APP-C processing.
Phospho-tau (AT8)	Hyperphoshorylated (Ser 202/Thr 205) version of tau found in neurofibrillary tangles[93]: one of the hallmarks of AD. The antibody detects hyperphosphorylated tau both prior to incorporation into tangles and within tangles.
PHF tangles (DC11)	Antibody recognises a conformational epitope of the neurofibrillary tangle that is highly AD specific[94]. DC11 is therefore a measure of tangles only.
Synaptophysin	38kDa glycoprotein located on neuronal synapses that can be used as a marker of synaptic density[95].
Growth associated protein 43 (GAP-43)	Neuron specific protein expressed on axonal growth cones during synaptic remodelling (synaptic remodelling marker)[96].
Neuronal nuclei (NeuN)	A neuron specific protein: a measure of neuronal density[97].

2.6.1 Method: ELISA

A protein sample with a high quantity of the protein-of-interest was selected for each standard curve. The standard curve samples and samples-of-interest were included on each plate in triplicates. 100µl of protein (diluted in 0.1M Carbonate Buffer, pH 9.6 to concentration shown in Table 18) was loaded per well and incubated overnight at 4ºC. Following liquid aspiration, the wells were incubated with 200µl phosphate buffered saline (PBS) (Sigma) with 1% Bovine Serum Albumin (BSA) (Sigma) for 2 hours. The samples were incubated with 100µl of primary antibody (Table 18) diluted in PBS with 1% BSA and 0.1% tween-20. Following the overnight incubation at 4ºC, the wells were washed with PBS with 0.1% tween-20, and incubated with 100µl secondary antibody (Table 18) at room temperature for 2 hours. The wells were washed and incubated with 100µl of Streptavidin-horseradish peroxidate (1:200, R&D Systems) for 2 hours at RT. The reaction was visualised with o-phenylenediamine dihydrochloride (Sigma fast OPD), and reaction stopped with 25µl of 4M H_2SO_4 when colour was appropriately developed. The absorbance was read at 490nm with a plate reader.

Table 18 ELISA

Protein	**Protein loading concentration (µm/ml)**	**Primary antibody**	**Secondary antibody**
Beta-amyloid	2	Mouse monoclonal to amyloid-β (1:5000, Dako)	Polyclonal Rabbit anti-mouse Immunoglobulin biotinylated (1:2000, Dako)
AT8	2.5	Mouse monoclonal to AT8	Polyclonal Rabbit anti-mouse Immunoglobulin biotinylated

Protein	**Protein loading concentration (µm/ml)**	**Primary antibody**	**Secondary antibody**
		(1:1000, Innogenetics)	(1:2000, Dako)
DC11	4	Mouse monoclonal Alzheimer's disease tau, DCII (1:500, Sigma)	Polyclonal Rabbit anti-mouse Immunoglobulin biotinylated (1:2000, Dako)
GAP-43	2	Rabbit polyclonal to growth associated protein, GAP43 (1:1000, Chemicon)	Polyclonal Swine anti-rabbit Immunoglobulin biotinylated (1:2000, Dako)
APP-C	4	Rabbit monoclonal to APP-C-terminal (1:1000, Sigma)	Polyclonal Swine anti-rabbit Immunoglobulin biotinylated (1:2000, Dako)
Synapto-physin	2	Mouse monoclonal to synaptophysin (1:1000, Dako)	Polyclonal Rabbit anti-mouse Immunoglobulin biotinylated (1:2000, Dako)
NeuN	2.5	Mouse monoclonal to neuronal nuclei (NeuN) (1:1000, Chemicon)	Polyclonal Rabbit anti-mouse Immunoglobulin biotinylated (1:2000, Dako)
$P57^{kip2}$	4	Mouse monoclonal to $p57^{kip2}$ (1:500, BD)	Polyclonal Rabbit anti-mouse Immunoglobulin biotinylated (1:2000, Dako)
Beta-actin	4	Mouse monoclonal to beta-actin (1:2000, ABcam)	Polyclonal Rabbit anti-mouse Immunoglobulin biotinylated (1:1000, Dako)
$P21^{cip1}$	4	Rabbit polyclonal to $p21^{cip1}$ (1:500, ABcam)	Polyclonal Rabbit anti-mouse Immunoglobulin biotinylated (1:2000, Dako)

2.6.2 Data analysis: ELISA

The calibration curve, obtained from the serial dilution of the standard curve sample, was used to estimate concentration of the protein-of-interest in the samples based on their optical density readings. The ELISA results were normalised for protein content.

2.7. SNP DEPENDENT Q-PCR

The Amplifluor SNPs genotyping system for assay development (Millipore) is a Q-PCR based technique that allows quantification of two alleles of a gene-of-interest in a sample at RNA level[98]. The kit is most commonly used for genotyping DNA, but can be used to determine ratio of mRNA corresponding to two gene variants in cDNA. The kit was used to determine the ratio of wild type $p21^{cip1}$ mRNA relative to variant $p21^{cip1}$ mRNA in the brain of patients that were heterozygous for both SNP A and B on $p21^{cip1}$. Of the 252 AD patients available for the study, all individuals that were heterozygous for SNP A and B were included in the analysis (28 subjects).

The Amplifluor AssayArchitect Software available through the Millipore website allowed the design of $p21^{cip1}$ allele specific primers (specific for SNP A). The sequences are given in Table 20. Note that green represents the sequence corresponding to the Amplifluor SNP FAM primer, whereas red represents the sequence corresponding to the Amplifluor SNP SR primer. Q-PCR was set up as described in Table 19 and subjected to an initial denaturation

step of 96ºC for 5 minutes, followed by 50 cycles of 96°C for 30 seconds, 55°C for 30 seconds, and 72°C for 30 seconds. The FAM and SR fluorescent signals were acquired in the annealing and elongation step.

Table 19 Composition of SNP dependent Q-PCR mix ($p21^{cip1}$: SNP A)

Q-PCR mix composition	Volume	Concentration	Manufacturer
cDNA	4	(unknown concentration: prepared as described in section 2.2	
Nuclease free water	9.2		Qiagen
dNTP mix	1.6	2.5mM per dNTP	Millipore kit
Amplifluor SNP FAM primer	1.0	5µM	Millipore kit
Amplifluor SNP SR Primer	1.0	5µM	Millipore kit
Reaction buffer S	2.0	10x	Millipore kit
SNP specific primer mix (Composed of 0.5µM wild type allele-specific forward primer, 0.5µM variant-specific forward primer and 7.5µM common reverse primer	1.0	20x	Sigma Genosys
Taq DNA polymerase	0.2	5 U/ml	Promega

Table 20 Primer sequences for SNP dependent Q-PCR

Primer	Sequence
$P21^{cip1}$ allele 1 (wild type) forward primer	5'**GAAGGTGACCAAGTTCATGCT**ATTAGCGCATCAC AGTCGCGG -3'
$P21^{cip1}$ allele 2 (variant) forward primer	5'- **GAAGGTCGGAGTCAACGGATT**AGCGCATCACAGT CGCGT-3'
$P21^{cip1}$ common reverse primer	5'-CTCTTCGGCCCAGTGGA -3'

2.7.1 Data analysis: SNP dependent Q-PCR

A calibration curve was constructed by assigning each of the DNA standard curve serial dilutions with an arbitrary copy number (1:1 = 10,000; 1:2 = 5,000; 1:4 = 2500; 1:8 = 1250; 1:16 = 625). The calibration curve was used to estimate the relative copy number of the wild type mRNA to variant mRNA in each sample, and ratio of wild type allele to variant allele calculated.

2.8. P21^{CIP1} AND P57^{KIP2} Q-PCR

The relative amount of p21^{cip} and p57^{kip2} mRNA in the temporal, frontal and occipital lobe of the 252 individuals in our cohort was determined by Q-PCR and normalised to beta-actin content. The Q-PCR systems (p21^{cip1}, p57^{kip2} and beta-actin) were developed using the primer design programme available on the Roche Diagnostic website in combination with the Universal probe library (Roche). The primers were designed to amplify irrespective of p21^{cip1} and p57^{kip2} genotype.

Q-PCR was set up as described in Table 21, and amplified on the Rotor Gene-6 Q-PCR machine with a initial denaturation step of 95ºC for 15 minutes, followed by 50 cycles of 96ºC for 15 seconds, optimal annealing temperature for 30 seconds, and 72ºC for 30 seconds. See Table 22 for the probe, primers, and optimal annealing temperature that correspond to each gene. The results were analysed as described in section 2.4: with p21^{cip1} and p57^{kip2} values normalised to the corresponding beta-actin values, to allow sample to sample comparisons.

Table 21 Composition of Q-PCR mix

Q-PCR mix composition	Volume	Concentration	Manufacturer
cDNA	2	Neat	(prepared as in section 2.2)
Nuclease free water	6.5		Qiagen
Forward primer	0.5	100 µM	Sigma Genosys
Backward primer	0.5	100 µM	Sigma Genosys
Universal probe	0.5	10 µM	Roche
Absolute Q-PCR mix	10	Neat	Thermoscientific

Table 22 Primer sequences for Q-PCR

Gene	Roche Probe	Forward primer (Sigma Genosys)	Backward primer (Sigma Genosys)	Optimised annealing temp (^{o}C)
Beta-actin	**24**	5'-TCAGCTGTGGGGTCC TGT-3'	5'-GAAGGGGACAGG CAGTGAG-3'	62
$p21^{cip1}$	**12**	5'-TGGGTGGTACCCTC TGGA-3'	5'TGAATTTCATA ACCGCCTGTG-3'	58
$p57^{kip2}$	**18**	5'-AACCGCTGGGATT ACGACT-3'	5'-TCCACTTCGGTC CACTGC-3'	58

2.9. CELL CULTURE AND TRANSFECTION

The effect of the $p21^{cip1}$ SNPs on the function and expression of $p21^{cip1}$ was investigated by transient transfection of wild type $p21^{cip1}$ or variant $p21^{cip1}$ (with SNP A and B) into the rapidly dividing Flp-In-T-Rex-293 (human embryonic kidney) cell line. The cell cycle activity of the cells was determined by Acumen Cytometry after propidium iodide staining; the expression of $p21^{cip1}$ mRNA determined by Q-PCR; and $p21^{cip1}$ protein expression determined by Acumen analysis after immunolabelling with $p21^{cip1}$ and beta-actin antibody. The transient transfection was carried out by Erzsebet Rabai (Research Associate) and the immunolabelling and propidium iodide staining carried out by Sheila Nagy (Research Technician). The procotols are described in appendix 5. The Q-PCR and data analysis were carried out as part of this MPhil.

2.9.1 $p21^{cip1}$ Q-PCR

RNA was extracted from pellets of cells transfected with wild type, variant, or no $p21^{cip1}$; and RNA converted to cDNA as described in 2.2. The $p21^{cip1}$ and beta-actin mRNA content was determined by Q-PCR as described in 2.8. The $p21^{cip1}$ content was normalised to beta-actin content to allow sample to sample comparisons.

2.9.2 Data analysis

The Acumen Explorer Cytometer scans cell cultures in situ and combines image analysis with the measurement of fluorescence: thereby allowing quantification of fluorescence within a defined area of the image. The propidium iodide stained cultures provided measurements of DNA content and cell size, and were analysed by standard flow Cytometry method[99] to determine cell cycle phase of the individual cells in the sample. The immunolabelled cell cultures provided measurements of $p21^{cip1}$ and beta-actin protein content per cell and per cell nucleus.

2.10. STATISTICAL ANALYSIS

A description of the data analysis methods relating to each technique can be found in the methods section. All statistical analysis was carried out with the MedCalc statistical package unless specified. The distribution of all data sets was investigated prior to statistical analysis to allow selection of the most appropriate test. For data that was normally distributed, one-way ANOVA, multi-factorial ANOVA, regression or multiple-regression was used as appropriate. Logarithmic transformation was carried out if suitable. The non-parametric test: Kruskall Wallis was used for data that did not follow a normal distribution. The chosen statistical test for each analysis can be found in the accompanying figure legend.

The accumulation of AD-related pathology in the brain is highly dependent on the severity of AD. Therefore, the analysis of the effect of the $p21^{cip1}$ and $p57^{kip2}$ genotype on the

accumulation of AD-related pathology had to take into account the severity of AD of the individual. Two-way ANOVA was used to analyse parametric data (entering genotype and severity of AD as independent variables), whereas the Kruskal-Wallis test was used to analyse non-parametric data (analysing data in subgroups defined by severity of AD, and entering genotype as the independent variable). Note that subjects with rare additional pathologies were excluded from the analysis (for example: motor neurone disease, Huntington's disease and frontal lobe dementia), whereas subjects with common pathologies in addition to AD (Parkison's disease, vascular disease, Lewy bodies and tumours) were included in the analysis to boost patient numbers.

For the purpose of the $p21^{cip1}$ study, individuals that were heterozygous or homozygous for SNPs A and B on $p21^{cip1}$ were classed as having the $p21^{cip1}$ variant, whereas individuals that were wild type for $p21^{cip1}$, or had only one of the SNPs were classed as being wild type for $p21^{cip1}$. Analysis of the effect of the $p21^{cip1}$ genotype on AD-related pathology was impeded by the small number of cases in the $p21^{cip1}$ variant subgroups defined by the severity of AD. Z-scores were calculated for each variable, taking into account the severity of AD (Braak staging), to eliminate the need for subgroups. The z-score is a measure of the deviation of a variable from the group mean. Patients were sorted into three groups depending on the severity of AD (entorhinal, limbic and neocortical), and group means calculated for each variable. For each variable, the individual patient measurements were compared to the relevant mean, to eliminate the severity of AD from the analysis.

3. RESULTS

3.1. ALTERED RAPAMYCIN RESPONSE ELEMENTS IN THE BRAIN OF ALZHEIMER'S DISEASE PATIENTS

Two previous studies[71, 72] have shown that lymphocytes from AD patients have a reduced response to rapamycin compared to lymphocytes from control subjects. As rapamycin is an upstream inhibitor of the mTOR pathway, a pathway that promotes cell cycle activity, these studies suggest that lymphocytes from AD patients have a deficiency downstream of mTOR that impedes appropriate cell cycle control. The fact that the cell cycle regulatory failure is not restricted to lymphocytes in AD[58, 59, 63, 100], and that the deficit is present in lymphocytes obtained from advanced AD patients and MCI sufferers[71], implies that the failure is systemic.

The cell cycle theory of AD postulates that neurodegeneration is secondary to inappropriate cell cycle re-entry of neurons with subsequent progression beyond the G1/S checkpoint[30]. We hypothesise that the defective components of the mTOR pathway that are responsible for the loss of cell cycle control in AD lymphocytes are also responsible for the loss of appropriate cell cycle control in AD neurons. Despite extensive research, ApoE ε4 is the only established genetic risk factor for AD. This suggests that the cause of the regulatory failure in AD may differ from patient to patient: with different mTOR pathway components involved in each case.

To identify these components, rapamycin-regulated genes were revealed by two-colour microarray based gene expression analysis (comparison between rapamycin-treated lymphocytes and untreated lymphocytes from subjects with appropriate rapamycin-response, identified by flow cytometry). The identified rapamycin-regulated genes were screened for differential expression in the frontal lobe of brain affected by AD compared to frontal lobe unaffected by AD using a custom-made gene expression microarray. The identified genes act downstream of mTOR, and are differentially regulated in brain affected by AD, suggesting that they may have a role in the development of the disease. They may severe as new therapeutic targets for AD or novel diagnostic biomarkers. The genes were further analysed with the IPA Ingenuity software to identify associated networks and pathways. As the list contained both positive and negative pathway regulators, it was decided that the up- and down- regulated genes should be analysed together to give the best overview of networks and pathways involved.

3.1.1 Rapamycin-regulated genes

The two-colour gene expression microarray identified 1138 genes that were rapamycin-regulated in lymphocytes. 1043 of the genes were up-regulated in response to rapamycin treatment and 95 genes downregulated in response to rapamycin. The full list of rapamycin-regulated genes in lymphocytes can be found in appendix 6 (Table 56 and Table 57).

Genes that are functionally controlled by rapamycin in human brain are not necessarily functionally controlled by rapamycin in lymphocytes. Therefore, genes that were known to

be rapamycin-regulated (identified with IPA Ingenuity), which were not identified as rapamycin-regulated in lymphocytes, were added to the list for screening for differential expression in AD brain compared to control (34 additional genes: appendix 6, Table 58).

3.1.2 Altered rapamycin-response elements as a result of mild AD

The rapamycin-regulated genes were analysed with SAM (see 2.3.2.4) for altered expression in the frontal lobe of mild (limbic) AD patients with the ApoE ε3/ε3 genotype relative to frontal lobe of control subjects with the ApoE ε3/ε3 genotype. Only ApoE ε3/ε3 patients were included in the analysis to eliminate the effect of the ApoE genotype from the analysis[22].

Of the 1172 rapamycin-regulated genes, SAM analysis identified 18 that were differentially expressed (Appendix 7, Table 59) in brain affected by mild AD relative to control (all up-regulated). Genes for enzymes, growth factors, ion channels, receptors and transporters were marked as possible therapeutic targets; whereas genes for cytokines and proteins located in the extracellular space were marked as possible biomarkers of AD. Of the 18 genes: 9 were identified as possible drug targets, and 6 identified as possible biomarkers of disease (Appendix 7, Table 59). The IPA software identified existing drugs to two of the differentially expressed gene (Appendix 7, Table 59).

3.1.2.1. Associated pathways, networks and functions

The list of 18 differentially expressed genes included transcriptional regulators (HDAC5, POU4F2, RUNX1T1); genes involved in nucleic acid metabolism (ENTPD8); genes involved in post-translational modification of proteins (FN3K, TGM4, ADAMTS2, PRODH2**)**; the neuronal guidance molecule SEMA4C; genes involved in cytoskeletal re-organisation (ADAMTS2) and inflammatory pathways (CCL2, IL6, FCGBP).

The differentially expressed genes were further analysed with IPA to identify associated molecular and cellular functions (Table 23), known diseases and disorders (Table 24), and physiological systems (Table 25). The differentially expressed transcripts were significantly enriched for involved in cellular development, cellular growth and proliferation, cellular movement, cell cycle, and antigen presentation (Table 23). IPA also identified networks associated with the differentially expressed genes: with 9 of the genes shown to be part of a network involved in connective tissue disorders, inflammatory disease, and skeletal and muscular disorders. The network was given a highly significant score of 22: based on the right-tailed Fisher's exact test, a score of 22 indicates that there was a $1x10^{-22}$ chance of the network being randomly identified. The only pathways significantly associated with the differentially expressed genes were the inflammatory pathways (data not shown).

Table 23 Molecular and cellular functions significantly associated with the genes identified to be differentially expressed as a result of mild AD only

Molecular and cellular functions	p-value	Number of genes
Cellular Development	<0.05	5
Cellular Growth and Proliferation	<0.05	8
Cellular Movement	<0.05	3
Cell Cycle	<0.05	2
Antigen Presentation	<0.05	2

Table 24 Diseases and disorders significantly associated with the genes identified to be differentially expressed as a result of mild AD only

Diseases and disorders	p-value	Number of genes
Connective Tissue Disorders	<0.05	3
Inflammatory Disease	<0.05	5
Skeletal and Muscular Disorders	<0.05	3
Infectious Disease	<0.05	2
Hematological Disease	<0.05	4

Table 25 Physiological systems significantly associated with the genes identified to be differentially expressed as a result of mild AD only

Physiological system development and function	p-value	Number of genes
Lymphoid tissue structure and development	<0.001- 0.0213	3
Nervous system development and function	<0.001- 0.0323	5
Skeletal muscle system development and function	<0.001- 0.0279	4
Connective tissue development and function	<0.001- 0.0290	2
Hematological system development and function	<0.001- 0.0301	4

3.1.3 Altered rapamycin-response elements as a result of advanced AD

To identify rapamycin-regulated genes whose transcription are altered as a consequence of advanced AD only, gene transcripts in the frontal lobe of advanced AD patients (neocortical stage) with ApoE ε3/ε3 genotype were compared to gene transcripts in the frontal lobe of elderly controls with ApoE ε3/ε3 genotype. Inclusion of only ApoE ε3/ε3 subjects in this analysis eliminated the effect of ApoE [22]. Of the 1172 rapamycin-regulated genes, SAM analysis identified 203 that were differentially transcribed in brain affected by advanced AD compared to control (see Appendix 8, Table 60 for full list).

To identify rapamycin-regulated genes whose transcription are altered as a result of advanced AD (neocortical stage) in subjects carrying the ApoE ε4 allele, gene transcripts in the frontal lobe of advanced AD patients with ApoE ε3/ε4 genotype were compared to gene transcripts in control subjects with ApoE ε3/ε3 genotype. Of the 1172 rapamycin-regulated genes, SAM analysis identified 168 that were differentially transcribed as a result of advanced AD and the ApoE ε4 allele (See Appendix 9, Table 68).

The rapamycin-regulated genes whose transcription were altered in brain of advanced AD patients with the ApoE ε3/ε3 genotype (203 genes) were compared to the rapamycin-regulated genes whose transcription were altered in brain of advanced AD patients with the ApoE ε3/ε4 genotype (168 genes). As we only had a small number of subjects in each group, the rapamycin-regulated genes that were differentially transcribed as a consequence of advanced AD only, and advanced AD in combination with the ApoE ε4 allele (i.e. the

overlapping genes), were likely to represent the most accurate picture of altered rapamycin-regulated genes as a result of advanced AD (i.e. the overlapping genes). The analysis identified 104 such genes (62% overlap) (Appendix 10, Table 76).

Genes for enzymes, growth factors, ion channels, receptors and transporters were marked as possible drug targets; whereas genes for cytokines and proteins located in the extracellular space were marked as possible biomarkers of disease. Of the 104 differentially expressed genes, 43 were identified as possible drug targets, and 19 identified as possible biomarkers of disease (Appendix 10, Table 76). The IPA software identified existing drugs to 5 of the possible drug targets (Appendix 10, Table 77).

3.1.3.1. Associated pathways, networks and functions

The 104 genes that were differentially transcribed as a result of advanced AD, irrespective of ApoE genotype, represent 8.9% (104/1172) of the total number of rapamycin-regulated genes; and includes transcriptional regulators, genes involved in post-translational modification, genes involved in nucleic acid metabolism, growth factors, various receptors and channels, inflammatory genes, genes involved in cytoskeleton reorganisation; tumour suppressors, and cell signalling genes.

The list was analysed with IPA to identify molecular and cellular functions (Table 26), diseases and disorders (Table 27) and physiological systems (Table 28) that were significantly associated with the differentially expressed genes. The genes were enriched for

involved in cellular development, cellular movement, protein synthesis, cell morphology and cellular growth and proliferation. IPA also identified a number of networks (Table 29) and pathways (Table 30) that were significantly associated with the differentially expressed genes. Note that the score (x) in Table 29 is based on the right-tailed Fisher's exact test and represents a $1x10^{x}$ chance of the network having been randomly identified.

Table 26 Molecular and cellular functions significantly associated with the genes identified to be differentially expressed as a result of advanced AD

Molecular and cellular functions	**p-value**	**Number of Genes**
Cellular development	<0.05	12
Cellular movement	<0.05	14
Protein synthesis	<0.05	5
Cell morphology	<0.05	13
Cellular growth and proliferation	<0.05	14

Table 27 Diseases and disorders significantly associated with the genes identified to be differentially expressed as a result of advanced AD

Diseases and disorders	**p-value**	**Number of genes**
Cardiovascular disease	<0.05	30
Genetic disorders	<0.05	59
Cancer	<0.05	31
Renal and urological disorders	<0.05	9
Infectious disease	<0.05	16

Table 28 Physiological systems significantly associated with the genes identified to be differentially expressed as a result of advanced AD

Physiological system development and function	**p-value**	**Number of Genes**
Skeletal and muscular system development and function	<0.05	9
Tissue development	<0.05	13
Hematological system development and function	<0.05	13
Immune cell trafficking	<0.05	8
Nervous system development and function	<0.05	13

Table 29 Top networks associated with the genes identified to be differentially expressed as a result of advanced AD

Network	**Score**	**Focus Molecules**	**Top Functions**
1	33	17	Cellular growth and proliferation, cancer
2	22	13	Connective tissue development, skeletal and muscular system development and function, Tissue morphology
3	19	11	Cellular function and maintenance, cell-to-cell signalling and interaction, Nervous system development and function
4	15	9	Decreased levels of albumin, gene expression, post-translational modifications
5	13	9	Cellular development, genetic disorders, metabolic disease

Table 30 Top pathways associated with the genes identified as differentially expressed as a result of advanced AD

Canonical pathway	**p-value**
mTOR Signaling	<0.001
Corticotropin Releasing Hormone Signaling	<0.001
Insulin Receptor Signaling	<0.001
IL-17 Signaling	<0.001
TGF-β Signaling	<0.05

Note that identical analyses to the one shown above were carried out for the differentially regulated genes in subjects with advanced AD, who were ApoE ε3 carriers only; and in subjects with advanced AD, who were ApoE ε4 carriers (see appendix 8 and 9 respectively).

3.1.4 Altered rapamycin-response elements as a result of the ApoE ε4 allele

Rapamycin-regulated transcripts that were differentially expressed in advanced AD (neocortical stage, ApoE ε3/ε4) compared to control (ApoE ε3/ε3), but not differentially expressed in advanced AD (neocortical stage: ApoE ε3/ε3) compared to control (ApoE ε3/ε3), were differentially expressed as a result of the ApoE ε4 allele only. The analysis identified 64 such genes (Appendix 11, Table 78).

3.1.4.1. Associated pathways, networks and functions

The 64 genes represent 5.4% (64/1172) of the total number of genes regulated by mTOR. Their altered expression can be attributed to the ApoE ε4 allele only. They included genes involved in energy metabolism (mitochondrial activity), fatty acid metabolism, synaptic activity, cell motility (adhesion and cytoskeleton structure), and cell signalling (receptors, channels and signalling molecules). Analysis with IPA identified associated molecular and cellular functions (Table 31), diseases and disorders (Table 32), and physiological systems (Table 33). The differentially expressed transcripts were significantly enriched for genes involved in cell death, cellular development, cellular growth and proliferation, drug metabolism and lipid metabolism.

IPA identified a number of networks associated with the differentially expressed genes (Table 34). The score is based on the right-tailed Fisher's exact test and represents a $1x10^{-score}$ chance of the network having been randomly identified. The genes were strongly associated with all the networks shown.

Table 31 Molecular and cellular functions significantly associated with the genes identified to be differentially expressed as a result of the ApoE ε4 allele

Molecular and cellular functions	**p-value**	**Number of Genes**
Cell death	<0.05	4
Cellular development	<0.05	7
Cellular growth and proliferation	<0.05	7
Drug metabolism	<0.05	2
Lipid metabolism	<0.05	2

Table 32 Diseases and disorders significantly associated with the genes identified to be differentially expressed as a result of the ApoE ε4 allele

Diseases and disorders	**p-value**	**Number of genes**
Neurological disease	<0.05	25
Psychological disease	<0.05	16
Skeletal and muscular disorders	<0.05	23
Genetic disorders	<0.05	34
Reproductive system disease	<0.05	12

Table 33 Physiological systems significantly associated with the genes identified to be differentially expressed as a result of the ApoE ε4 allele

Physiological system development and function	**p-value**	**Number of Genes**
Cardiovascular system development and function	<0.05	6
Hair and skin development and function	<0.05	4
Nervous system development and function	<0.05	4
Organismal function	<0.05	1
Renal and urological system development and function	<0.05	1

Table 34 Networks significantly associated with the genes identified to be differentially expressed as a result of the ApoE ε4 allele

Network	**Score**	**No. of focus Molecules**	**Top Functions**
1	26	13	Cardiovascular System Development and Function, Cell Death, Organismal Functions
2	22	11	Infection Mechanism, Cellular Compromise, Lipid Metabolism
3	22	11	Cell Signaling, Molecular Transport, Vitamin and Mineral Metabolism

3.1.5 Altered rapamycin-response elements in AD irrespective of severity of AD

The rapamycin-regulated genes whose transcription were altered as a result of advanced AD (refer to section 3.1.3) were compared to the rapamycin-regulated genes whose transcription were altered as a result of mild stage AD (refer to section 3.1.2). This analysis was carried out to identify rapamycin-regulated genes that were differentially expressed in the frontal lobe in both early and later phases of the disease.

Of the 18 differentially expressed transcripts in early stage AD (limbic stage), 15 (83%) overlapped with the differentially expressed transcripts in advanced AD (neocortical stage) (104 genes) (Appendix 11, Table 79). These genes are potential therapeutic and biomarker targets, irrespective of disease severity. Of the 15 differentially expressed genes, 8 were identified as possible therapeutic targets, and 3 identified as possible biomarkers of disease (Appendix 11, Table 79). No existing drugs target the genes identified as possible drug targets.

Three of the genes were differentially transcribed in mild AD, but not advanced AD; whereas 89 of the genes were differentially transcribed in advanced AD, but not in mild AD. These genes could potentially be used as biomarkers of disease progression (Appendix 11, Table 80). Fourteen of the genes met the requirements for a potential biomarker (Appendix 11, Table 80).

3.1.6 Microarray validation

The IPA Ingenuity knowledge database contains information about established gene associations with disease that have been manually derived from peer-reviewed journals and other high quality sources. Only verified gene/disease associations are included in this database (associations based on genetics and expression).

IPA Ingenuity identified 954 genes known to be involved in AD. These genes were compared to the rapamycin-regulated genes that were shown to be altered in AD brain compared to control. Two of the 18 (11%) altered mTOR genes in mild AD (limbic stage, ApoE ε3/ε3), and 13 of the 104 (12.5%) altered mTOR genes in advanced AD (neocortical stage), were established to be associated with AD based on the IPA Ingenuity database. To summarise, we have looked at approximately 2% (1172/ 40000) of the whole human genome (only genes downstream of the mTOR signalling pathway), and found that approximately 12% of the identified AD associated mTOR genes, are already established to be associated with AD based on the IPA Ingenuity knowledge base.

3.1.7 Q-PCR validation of microarray

Microarray analysis showed that eukaryotic translation initiation factor 4E (EIF4E), mitogen activated protein kinase 1 (MAPK1), gamma-aminobutyric acid B receptor 2 (GABBR2) and DAZ interacting protein 3 (DZIP3) were significantly down-regulated in advanced AD compared to control, whereas semaphorin 4C (SEMA4C) and serpin peptidase inhibitor, clade E, member 1 (SERPINE 1) were significantly up-regulated in advanced AD compared to control (Figure 9). Q-PCR was used to measure the expression of the listed genes in the frontal lobe of the AD patients and controls that were examined with gene expression microarray (all ApoE ε3/ε3). The beta-actin content of the samples was also measured by Q-PCR, to allow normalisation of the data.

For all 6 genes, Q-PCR demonstrated differential expression in the same direction as the microarray, although results failed to reach statistical significance for all of the genes (Figure 10).

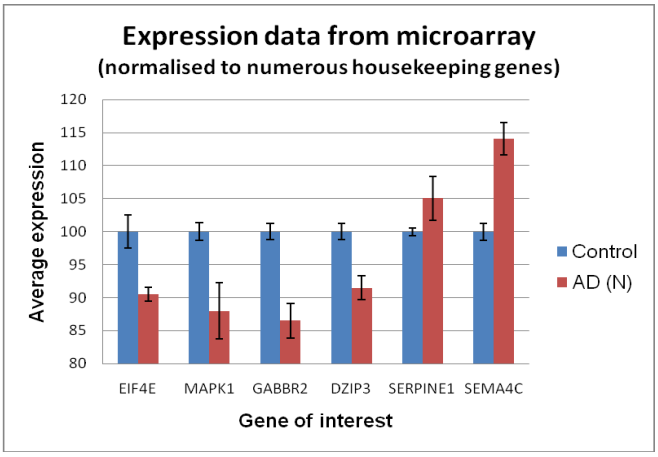

Figure 9 **Gene expression in control and advanced AD brain as determined by microarray (x-axis = gene-of-interest; y-axis = expression normalised to beta-actin, and expressed as a percentage of the control value (%); top of bar represents mean; error bars represent standard error of the mean; blue represents control subject; red represents advanced AD subject).**

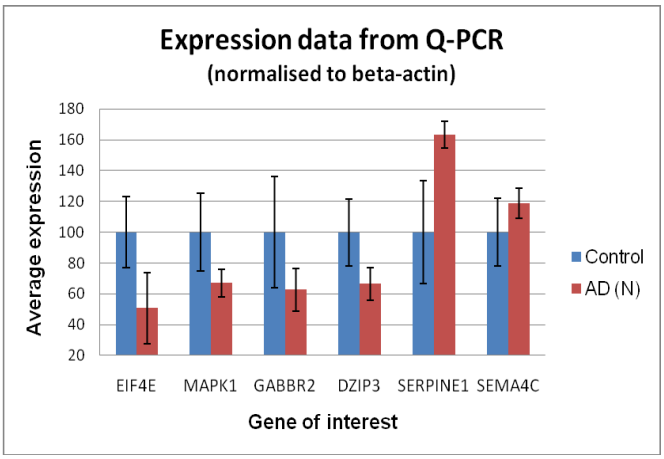

Figure 10 **Gene expression in control and advanced AD brain as determined by Q-PCR (x-axis = Gene-of-interest; y-axis = expression normalised to beta-actin, and expressed as a percentage of the control value (%); top of bar represents mean; error bars represent standard error of the mean; blue represents control subject; red represents advanced AD subject).**

3.2. THE EFFECT OF THE P21^{CIP1} SNPS ON P21^{CIP1} EXPRESSION AND FUNCTION, AND ASSOCIATION WITH AD-RELATED PATHOLOGY

The cell cycle theory of AD postulates that neurons degenerate as a consequence of aberrant cell cycle re-entry and progression beyond the G1/S checkpoint[30]. P21^{cip1} is a member of the cip/kip family of CDKIs that inhibit the activity of the cyclin/CDK complexes that drive entry into the cell cycle and progression from one phase to the next. P21^{cip1} specifically inhibits cyclin/CDK2 complexes, which are required for progression through the G1/S and S/G2 checkpoints. It is possible that the inappropriate progression beyond the G1/S checkpoint, which is postulated to be a cause of neurodegeneration in AD, is a consequence of altered expression or activity of the p21^{cip1} protein in some individuals.

Several genetic linkage studies suggest that genetic variants of p21^{cip1} may be associated with AD[80, 82, 83, 101]. Furthermore, a previous study[74] found that a genetic variant of p21^{cip1} that is known to be cancer associated[77] is also associated with AD. The genetic variant contained a cytosine to adenine substitution on an exonic region (SNP A), and a cytosine to thymine substitution on the 3'- untranslated region (SNP B). The literature suggests that the SNPs are only associated with cancer and AD when found together[74, 76, 77]. An aim of the study was to determine the effect of the p21^{cip1} SNPs on the age of onset of AD, cognitive performance, and the accumulation of AD-related pathology in the brain. We also investigated the effect of the p21^{cip1} SNPs on the stability of the p21^{cip1} mRNA, and on the expression and function of the p21^{cip1} protein.

Subjects that were heterozygous or homozygous for both SNP A and B were identified as having the variant version of $p21^{cipl}$; whereas individuals that were wild type for SNP A and B (or had only one of the SNPs) were identified as having the wild type version of $p21^{cip1}$.

3.2.1 Frequency of the $p21^{cip1}$ variant

Post-mortem brain tissue sections, from 209 AD sufferers, were available for the study. Of the 209 subjects, one was homozygous for SNP A and B, 24 were heterozygous for SNP A and B, and 184 were wild type for SNP A and B or heterozygous or homozygous for one of the SNPs only (Table 35). Overall, 12% of the cohort was either heterozygous or homozygous for the $p21^{cip1}$ SNPs (A and B). The distribution of the $p21^{cip1}$ variant in the population followed the Hardy-Weinberg equilibrium[102].

Table 35 Frequency of the $p21^{cip1}$ variant in the cohort

$p21^{cip1}$ genotype	**Number of patients**	**Relative frequency %**
Wild type	184	88.0
Heterozygous	24	11.5
Homozygous	1	0.5
TOTAL	209	

The frequency of the $p21^{cip1}$ variant in subjects in different stages of AD is summarised in Table 36 (note that only 193 of the 209 subjects had information regarding Braak staging). Of the pre-clinical (entorhinal stage), mild (limbic stage) and advanced (neocortical stage) AD sufferers: 9.3%, 10.7% and 15.7% respectively had at least one copy of the $p21^{cip1}$

variant. There was a trend (not statistically significant) for patients with advanced AD to have a higher frequency of variant $p21^{cip1}$ than patients earlier stages of AD (see odds ratios in Table 36, and Figure 11).

Table 36 Frequency of the $p21^{cip1}$ variant in subjects in different stages of AD

DIAGNOSIS	Number of patients that are wild type for $p21^{cip1}$	Number of patients that have variant $p21^{cip1}$	Relative frequency (%)	Odds ratio
Pre-clinical	49	5	9.3	
Mild AD	50	6	10.7	1.18
Advanced AD	70	13	15.7	1.82

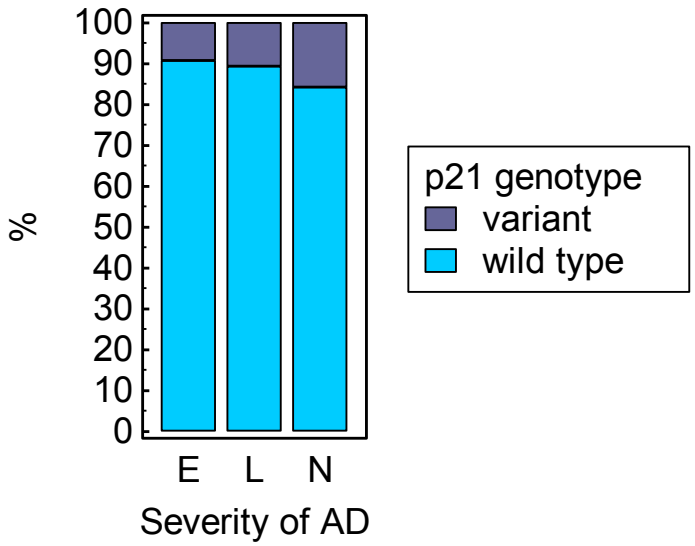

Figure 11 Distribution of variant $p21^{cip1}$ in subjects in different stages of AD (x-axis: E = entorhinal stage, L = limbic stage, N = neocortical stage; y-axis = percentage of total; legend: purple = $p21^{cip1}$ variant; blue = $p21^{cip1}$ wild type).

3.2.2 Distribution of additional pathology by AD severity and $p21^{cip1}$ genotype

The AD cohort included subjects with Parkinson's disease, vascular disease, Lewy bodies and tumours in addition to AD. It was not possible to exclude subjects with additional pathology from the analysis, as removal of these subjects would have reduced the number of patients in the $p21^{cip1}$ variant group to an extent where meaningful statistical analysis would not have been possible. Patients with less common additional pathologies were excluded from the analysis.

The analysis of the frequency of additional pathology by disease severity showed that a significantly greater proportion of subjects in the early stages of AD had additional pathology compared to subjects with advanced AD ($p=0.009$) (Figure 12). There was no significant difference in the distribution of additional pathology by $p21^{cip1}$ genotype (Figure 13), irrespective of disease severity (data not shown).

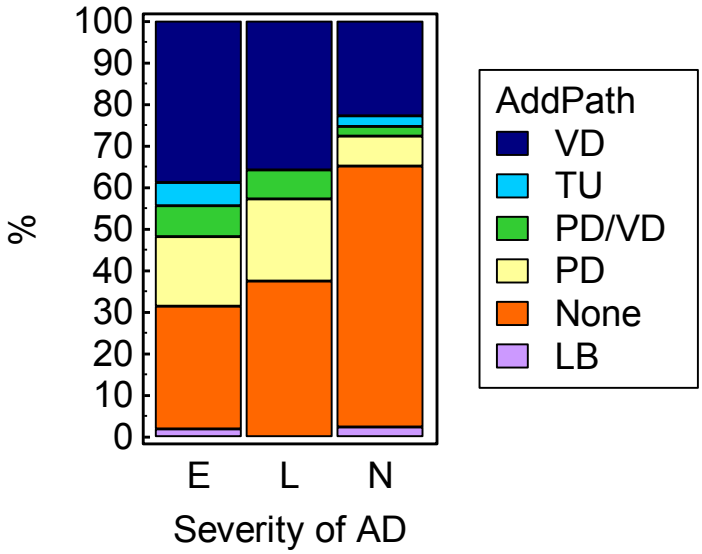

Figure 12 **Frequency of additional pathology in subjects in different stages of AD (x-axis: severity of AD as defined by Braak: E= entorhinal stage, L = limbic stage, N = neocortical stage; y-axis = percentage of total; key: VD= vascular dementia, TU= tumours, PD= Parkinson's disease, LB= Lewy body dementia, none= no additional pathology).**

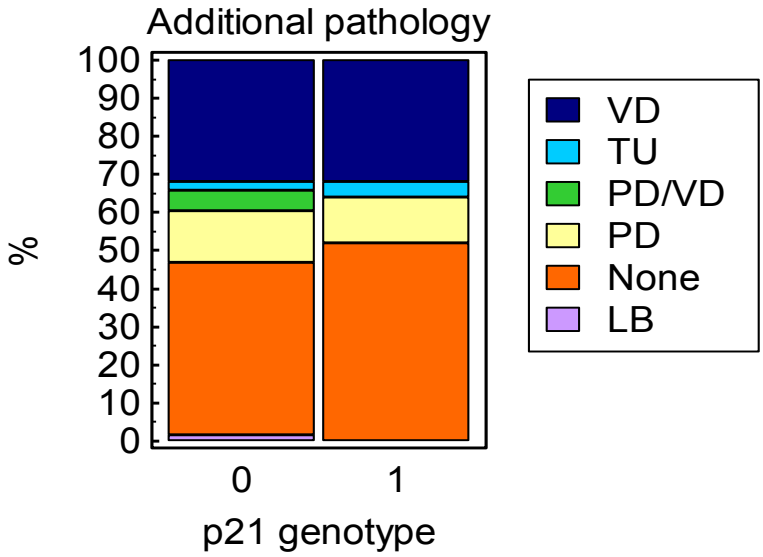

Figure 13 **Frequency of additional pathology in subjects with different p21 genotype (x-axis: $p21^{cip1}$ genotype, 0 = wild type, 1 = variant; y-axis = percentage of total; legend: VD= Vascular dementia, TU= tumours, PD= Parkinson's disease, LB= Lewy body dementia, none= no additional pathology).**

3.2.3 Distribution of ApoE genotypes by AD severity and $p21^{cip1}$ genotype

The ApoE ε4 allele is an established risk factor for late-onset AD[22]. There is a significant difference in the distribution of ApoE genotypes in patients in different stages of AD: a significantly greater percentage of advanced AD patients had the ApoE ε4/ε4 and ApoE ε4/ε3 genotypes compared to patients in earlier stages of AD ($p<0.001$) (Figure 14). However, there was no significant difference in the distribution of ApoE genotypes between the $p21^{cip1}$ wild type and $p21^{cip1}$ variant groups (Figure 15), irrespective of the severity of AD (data not shown).

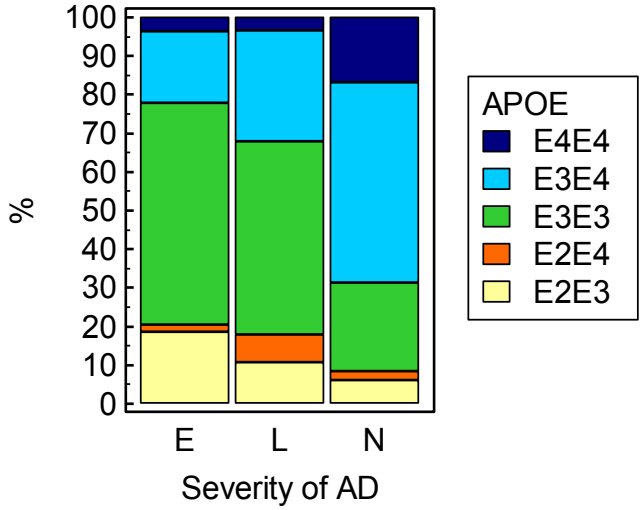

Figure 14 **The distribution of ApoE genotypes by severity of AD (x-axis = disease severity as defined by Braak: E = entorhinal stage, L = limbic stage, N = neocortical stage; y-axis = percentage of total; legend refers to ApoE genotype).**

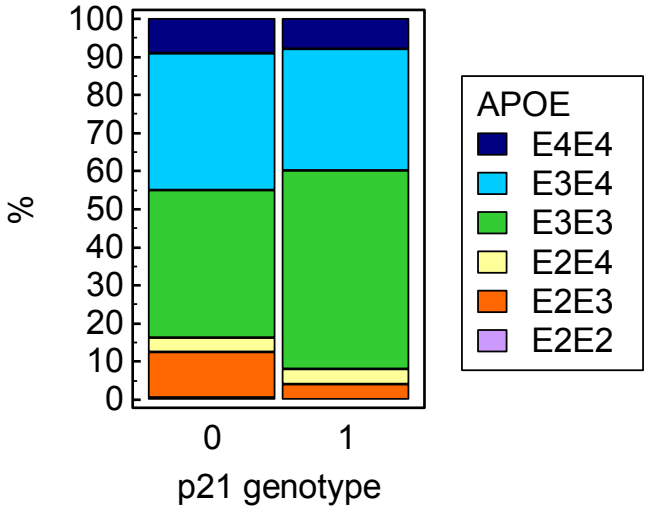

Figure 15 **The distribution of ApoE genotypes in groups defined by the $p21^{cip1}$ genotype (x-axis = p21 genotype, 0 = wild type, 1 = variant; y-axis = percentage of total; key: ApoE genotype).**

3.2.4 Distribution of the ApoE ε4 allele by AD severity and p21^{cip1} genotype

A significantly greater percentage of subjects with advanced AD were ApoE ε4 carriers than subjects with pre-clinical or mild AD ($p<0.001$) (Figure 16). There was no difference in the frequency of the ApoE ε4 allele in the p21^{cip1} wild type group compared to p21^{cip1} variant group (Figure 17), irrespective of disease severity (data not shown).

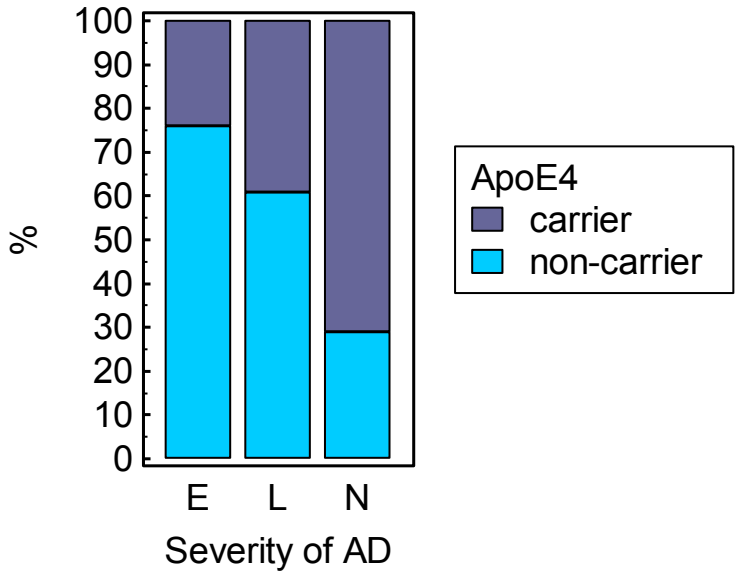

Figure 16 **The distribution of the ApoE ε4 allele by the severity of AD (x-axis = severity of AD as defined by Braak: E = entorhinal stage, L = limbic stage, N = neocortical stage; y-axis = percentage of total; key: purple = carrier of the ApoE ε4 allele, light blue = non-carrier of the ApoE ε4 allele).**

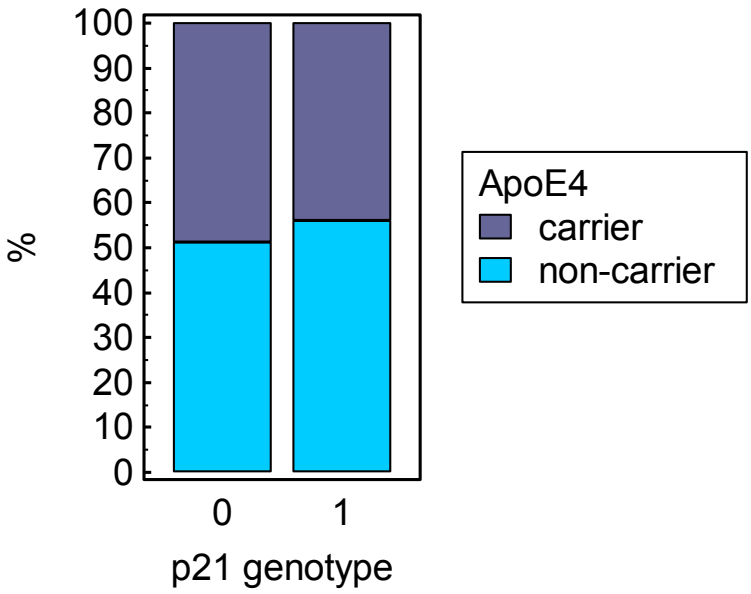

Figure 17 The distribution of the ApoE ε4 allele in groups defined by p21^{cip1} genotype (x-axis = p21 genotype: 0 = wild type, 1 = variant; y-axis = percentage of total; purple = carrier of the ApoE ε4 allele, light blue = non-carrier of the ApoE ε4 allele).

3.2.5 The effect of the p21^{cip1} genotype on the age of onset, age at death, and the duration of AD

The severity of AD at the time of death is dependent, at least partially, on the age of onset of AD and the age of the patient at death. To elucidate the effect of the p21^{cip1} genotype on the age of onset of AD, age at death and disease duration, we first examined the association of these outcomes with disease severity.

3.2.5.1. The effect of the severity of AD on the age of onset of AD

The mean age of onset of AD of subjects with mild (limbic stage) and advanced (neocortical stage) AD at the time of death are outlined in Table 37 and Figure 18. Subjects with entorhinal stage AD had no age of AD onset, as these individuals were in a pre-clinical stage at the time of death.

Advanced AD (neocortical stage) sufferers had a mean age of onset of 69 years. This was significantly lower ($p<0.001$) than the mean age of onset of subjects with mild AD (limbic stage) (77 years) (Figure 18).

Table 37 Mean age of onset of AD of subjects in different stages of AD

Diagnosis (Braak staging of AD)	**Number of patients**	**Mean age of AD onset (years)**
Entorhinal stage		N/A
Limbic stage	40	77
Neocortical stage	76	69

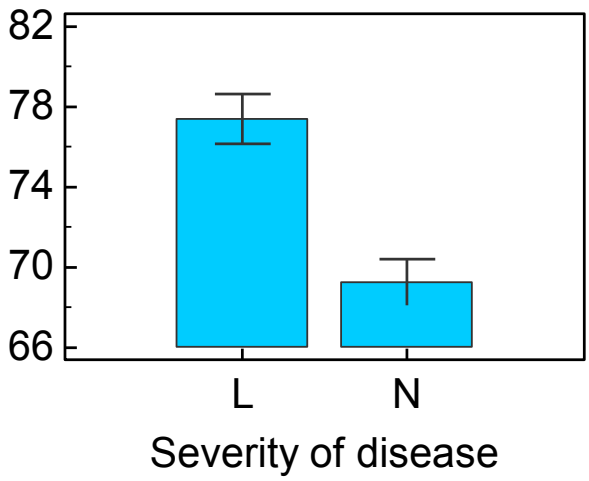

Figure 18 **Mean age of onset of AD of subjects in different stages of AD (x-axis = severity of disease: L = limbic stage, N = neocortical stage; y-axis = age of onset of AD in years; top of bars represents mean; error bars represent standard error of the mean) (one-way ANOVA).**

3.2.5.2. The effect of the severity of AD on the age at death

The mean age at death of subjects with pre-clinical (entorhinal stage), mild (limbic stage) and advanced (neocortical stage) AD at the time of death are outlined in Table 38 and Figure 19.

Table 38 **Mean age of death of subjects in different stages of AD**

Diagnosis (Braak staging of AD)	Number of patients	Mean age at death (years)
Entorhinal stage	49	80
Limbic stage	50	84
Neocortical stage	70	77

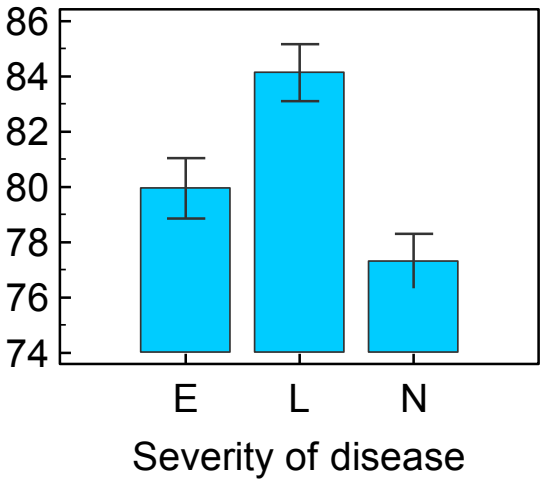

Figure 19 **Mean age at death of subjects in different stages of AD (x-axis = severity of disease: E = entorhinal stage, L = limbic stage, N = neocortical stage; y-axis = age at death in years; top of bars represent mean; error bars represent standard error of the mean) (one-way ANOVA).**

Advanced AD sufferers (neocortical stage) had a mean age at death of 77, which was significantly lower ($p<0.001$) than the mean age at death of mild AD sufferers (limbic stage) at 84. The mean age at death of subjects with preclinical AD (entorhinal stage) was between the mean age at death of mild and advanced AD suffers at 80.

3.2.5.3. The effect of the severity of AD on the disease duration

The mean disease duration of subjects with mild AD (limbic stage) was significantly lower than the mean disease duration of subjects with advanced AD (neocortical stage) (Table 39 and Figure 20) (p=0.012).

Table 39 Disease duration of subjects in different stages of AD

Diagnosis (Braak staging of AD)	Mean Disease duration (years)
Limbic stage	6
Neocortical stage	7.7

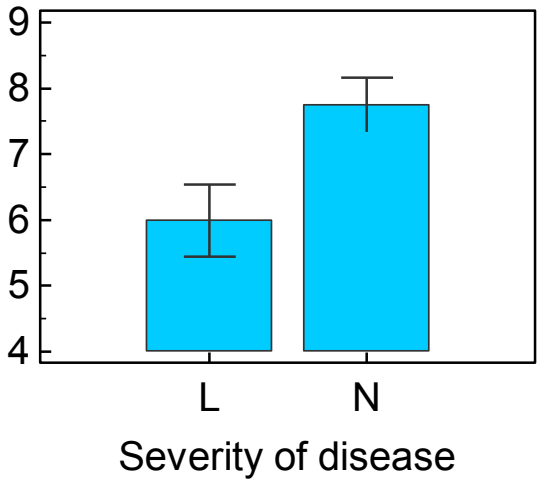

Figure 20 Mean age of disease duration of subjects in different stages of AD (x-axis = severity of disease: L = limbic stage, N = neocortical stage; y-axis = duration of disease in years; top of bars represent mean; error bars represent standard error of the mean) (one-way ANOVA).

3.2.5.4. The effect of the p21^{cip1} genotype on the age of onset, age at death and the duration of AD

The p21^{cip1} genotype had no effect on the age of AD onset of subjects with preclinical (entorhinal) or mild (limbic stage) AD at the time of death (data not shown). In subjects with advanced AD, the age of onset of AD was significantly lower in subjects with the variant p21^{cip1} compared to subjects with wild type p21^{cip1} (p=0.016) (Figure 21).

The p21^{cip1} genotype had no effect on the age at death, or the duration of AD, irrespective of AD severity (data not shown).

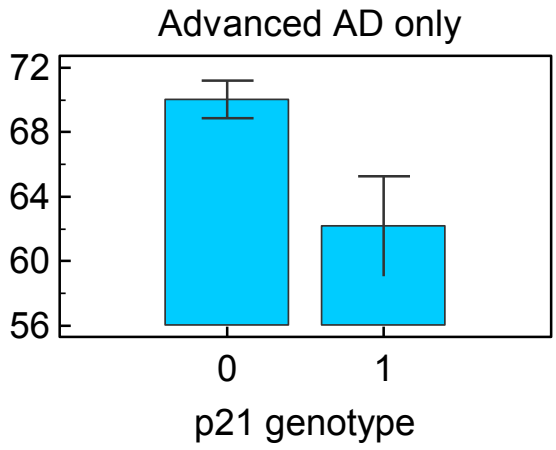

Figure 21 **The effect of the p21 genotype on the mean age of onset of AD in subjects with advanced AD only (x-axis = p21^{cip1} genotype: 0 = wild type, 1 = variant; y-axis = age of onset in years; top of bars represent mean; error bars represent standard error of the mean) (one-way ANOVA).**

3.2.6 The effect of the $p21^{cip1}$ genotype on the accumulation of AD-related pathology

To elucidate the effect of the $p21^{cip1}$ genotype on the accumulation of AD-related pathology in the brain, the 193 subjects in the entorhinal, limbic and neocortical stage of AD were genotyped for the $p21^{cip1}$ SNPs; and temporal, frontal and occipital lobe protein extracted for quantification of AD-related pathology proteins (beta-amyloid, AT8, APP-C, DC11, GAP-43, synaptophysin, NeuN and $p21^{cip1}$: see Table 17 for description of markers). As the accumulation of AD-related pathology is dependent on brain region, data from the temporal, frontal and occipital lobes were analysed separately.

3.2.6.1. The effect of the severity of AD on beta-amyloid expression

Subjects in later stages of AD had significantly greater beta-amyloid accumulation in the temporal (Figure 22) and frontal lobe (Figure 23) than subjects in earlier stages of the disease (p=0.007 and 0.045 respectively). This was not true of the occipital lobe, with subjects in different stages of AD showing no difference in beta-amyloid expression in this region (data not shown).

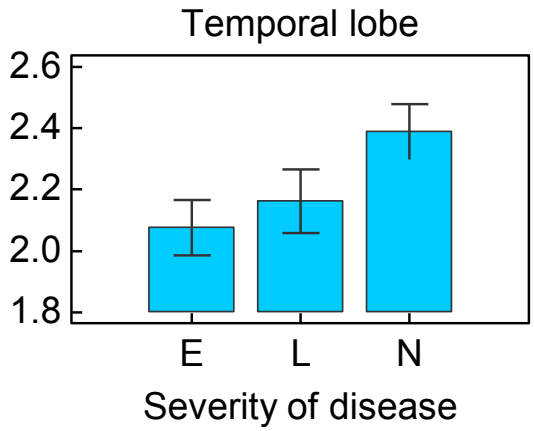

Figure 22 **The effect of the severity of AD on beta-amyloid expression in the temporal lobe (x-axis =severity of AD based on Braak staging, E= entorhinal, L= limbic, N= neocortical; y-axis= amount of beta-amyloid in the temporal lobe as determined by ELISA; top of bars represent mean; error bars represent standard error of the mean) (one-way ANOVA).**

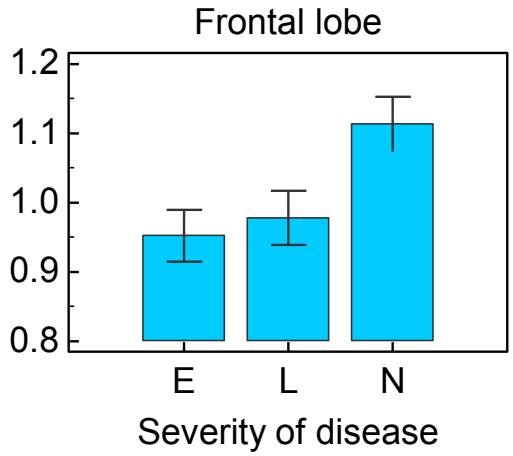

Figure 23 **The effect of the severity of AD on beta-amyloid expression in the frontal lobe (x-axis =severity of AD based on Braak staging, E= entorhinal, L= limbic, N= neocortical; y-axis= amount of beta-amyloid in the frontal lobe as determined by ELISA; top of bars represent mean; error bars represent standard error of the mean) (one-way ANOVA).**

3.2.6.2. The effect of the p21^{cip1} genotype on beta-amyloid expression

MANOVA was carried out to investigate the effect of the p21^{cip1} genotype on beta-amyloid expression in the temporal, frontal and occipital lobe. The p21^{cip1} genotype had no effect on beta-amyloid expression, irrespective of severity of AD, or brain region examined (data not shown). However, there was a trend (not statistically significant) for greater beta-amyloid accumulation in the occipital lobe in the earlier stages of AD (see Figure 24).

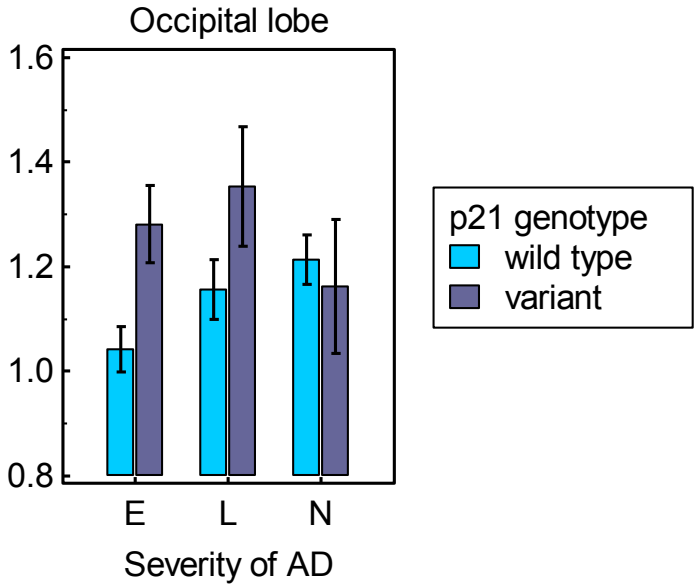

Figure 24 **The effect of the p21^{cip1} genotype on beta-amyloid expression in the occipital lobe (x-axis = severity of AD as defined by Braak staging: E = entorhinal stage, L = limbic stage, N = neocortical stage; y-axis = amount of beta-amyloid in the occipital lobe as determined by ELISA; top of bars represent mean; error bars represent standard error of the mean) (MANOVA).**

3.2.6.3. The effect of the $p21^{cip1}$ genotype on APP-C expression

MANOVA was carried out to investigate the effect of the $p21^{cip1}$ genotype on APP-C expression in the temporal, frontal and occipital lobe, independent of AD severity. APP-C expression was not altered by the severity of AD (data not shown). However, the 21^{cip1} genotype had a weak effect, with variant $p21^{cip1}$ carriers in the early stages of AD (entorhinal and limbic stage) expressing a significantly greater amount of APP-C in the frontal lobe than non carriers ($p=0.028$) (see Figure 25). The amount of APP-C expressed in the temporal and occipital lobe was independent of disease severity and $p21^{cip1}$ genotype (data not shown).

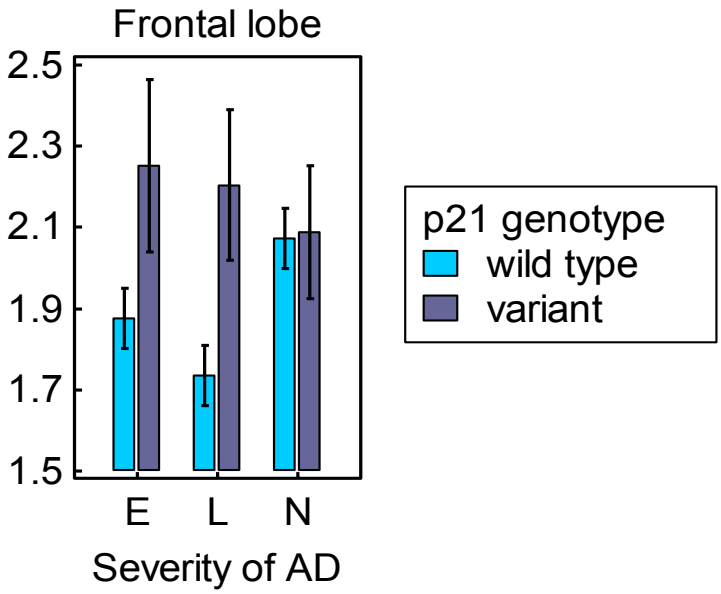

Figure 25 **The effect of the p21^{cip1} genotype on APP-C expression in the frontal lobe (x-axis = severity of AD as defined by Braak: E = entorhinal stage, L = limbic stage, N = neocortical stage; y-axis = amount of APP-C in the frontal lobe; top of bars represent mean; error bars represent standard error of the mean) (MANOVA).**

3.2.6.4. The effect of the p21^{cip1} genotype on beta-amyloid relative to APP-C expression

The p21^{cip1} genotype had no effect on the relative expression of beta-amyloid to APP-C in the temporal, frontal or occipital lobe, irrespective of AD severity (data not shown).

3.2.6.5. The effect of the $p21^{cip1}$ genotype on the accumulation of phospho-tau

AT8 is a marker of a pathologically hyperphosphorylated version of tau that is found in NFT. It detects hyperphosphorylated tau both prior to incorporation into tangles and within tangles[93].

There was a significant increase in the amount of phospho-tau (AT8) expressed in the temporal, frontal and occipital lobe as AD progressed from an early to more advanced stage ($p>0.001$) (Figure 26 to 28). Furthermore, there was a trend for greater phospho-tau (AT8) expression in the frontal and occipital lobes of subjects with variant $p21^{cip1}$ compared to wild type $p21^{cip1}$, which reached significance in the occipital lobe of limbic and neocortical stage patients only ($p = 0.0156$ and $p=0.0446$ respectively) (Figure 27 and 28). The $p21^{cip1}$ genotype had no effect on phospho-tau (AT8) accumulation in the temporal lobe, irrespective of AD severity (Figure 26).

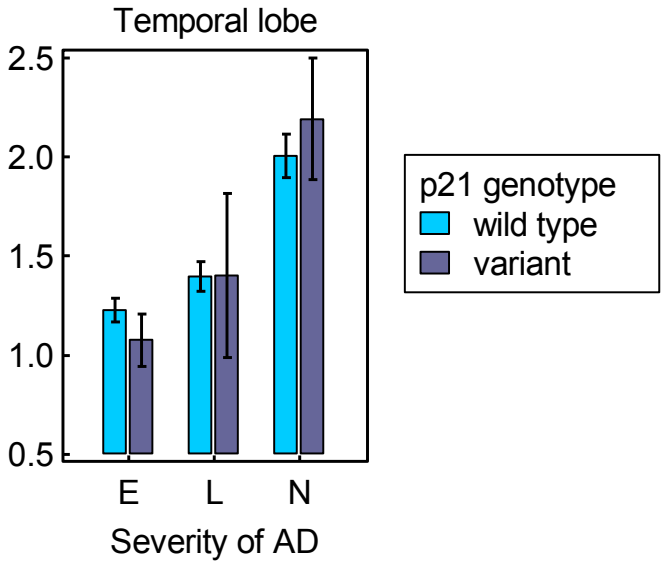

Figure 26 **The effect of the p21^{cip1} genotype on phospho-tau (AT8) deposition in the temporal lobe (x-axis = severity of AD as defined by Braak staging: E = entorhinal stage, L = limbic stage, N = neocortical stage; y-axis = amount of AT8 in the temporal lobe; top of bars represent mean; error bars represent standard error of the mean) (Kruskal Wallis).**

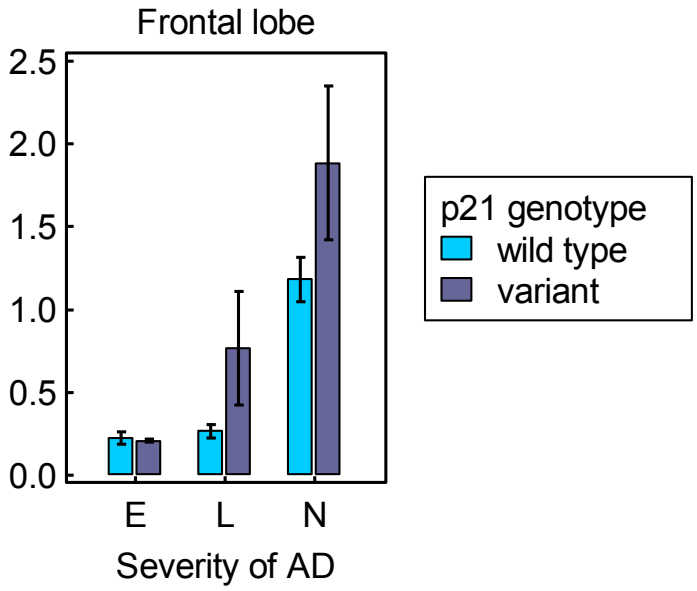

Figure 27 **The effect of the p21^{cip1} genotype on phospho-tau (AT8) deposition in the frontal lobe (x-axis = severity of AD as defined by Braak staging: E = entorhinal stage, L = limbic stage, N = neocortical stage; y-axis = amount of AT8 in the frontal lobe; top of bars represent mean; error bars represent standard error of the mean) (Kruskal Wallis).**

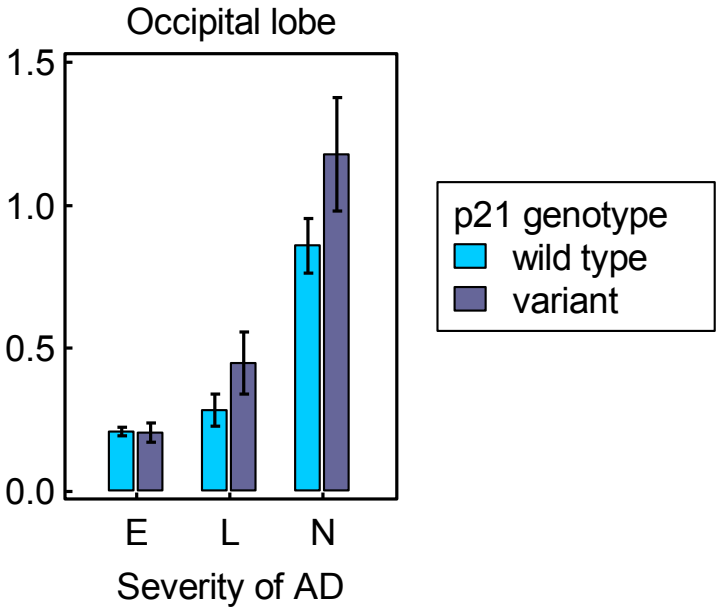

Figure 28 **The effect of the p21^{cip1} genotype on phospho-tau (AT8) deposition in the occipital lobe (x-axis = severity of AD as defined by Braak staging, E= entorhinal, L= limbic, N= neocortical; y-axis= amount of AT8 in the occipital lobe; top of bars represent mean; error bars represent standard error of the means) (Kruskal Wallis).**

The need to take the severity of AD into account when analysing the effect of the p21^{cip1} genotype lead to very low subject numbers in the p21^{cip1} variant sub-groups defined by the severity of AD. This may have contributed to the lack of statistically significant results despite visible trends. Phospho-tau (AT8) z-scores were calculated for each subject taking into account the Braak stage of the individual (a measure of AD severity) (refer to 2.10).

The results showed that ~60% of individuals with variant p21^{cip1} had greater phospho-tau (AT8) deposition in the frontal lobe than the group mean; whereas only ~33% of individuals with wild type p21^{cip1} had greater phospho-tau (AT8) deposition in the frontal lobe than the

group mean (Figure 29). This difference was statistically significant (p = 0.0419), indicating that a significantly greater percentage of individuals with variant $p21^{cip1}$ had "high" frontal lobe phospho-tau deposition than individuals with wild type $p21^{cip1}$, irrespective of severity of AD ("high" defined as above the group mean). One-way ANOVA showed that individuals with variant $p21^{cip1}$ expressed significantly more phospho-tau (AT8) in the frontal lobe than individuals with wild type $p21^{cip1}$, irrespective of AD severity (p=0.007) (Figure 30).

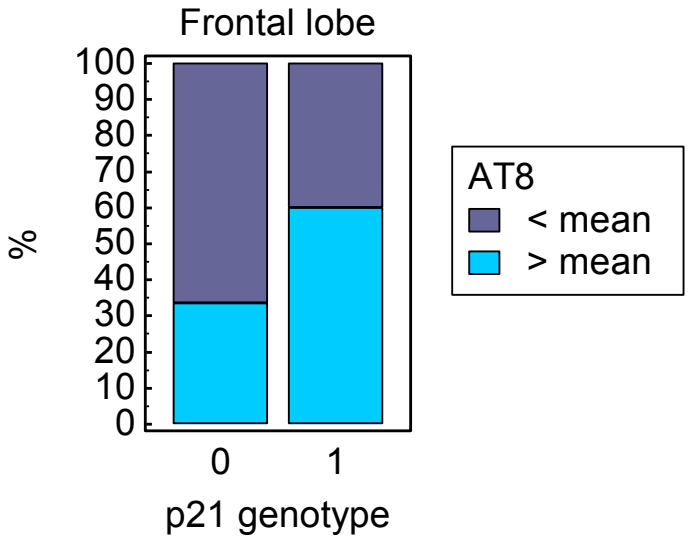

Figure 29 **The effect of the $p21^{cip1}$ genotype on phospho-tau (AT8) deposition in the frontal lobe: independent of disease severity (x-axis = $p21^{cip1}$ genotype: 0 = wild type, 1 = variant; y-axis: blue = percentage of subjects that expressed more AT8 in the frontal lobe than the group mean, purple = percentage of subjects that expressed less AT8 in the frontal lobe than the group mean; groups defined by Braak stage) (chi-square test).**

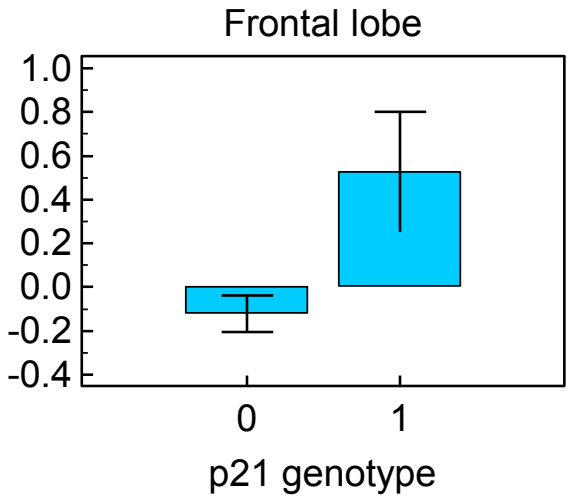

Figure 30 **The effect of the p21^{cip1} genotype on phospho-tau (AT8) deposition in the frontal lobe: independent of disease severity (x-axis = p21^{cip1} genotype: 0= wild type, 1= variant; y-axis = z-scores: deviation of each frontal lobe AT8 score from the group mean; error bars represent standard error of the means) (ANOVA).**

Furthermore, ~55% of subjects with variant p21^{cip1} had greater phospho-tau (AT8) deposition in the occipital lobe than the group mean; whereas only ~26% of subjects with wild type p21^{cip1} had greater phospho-tau (AT8) deposition in the occipital lobe than the group mean (Figure 31). This difference was statistically significant (p=0.0352), indicating that a significantly greater percentage of individuals with variant p21^{cip1} had "high" phospho-tau (AT8) expression in the occipital lobe than individuals with wild type p21^{cip1}, irrespective of AD severity (high" is defined as above the group mean).

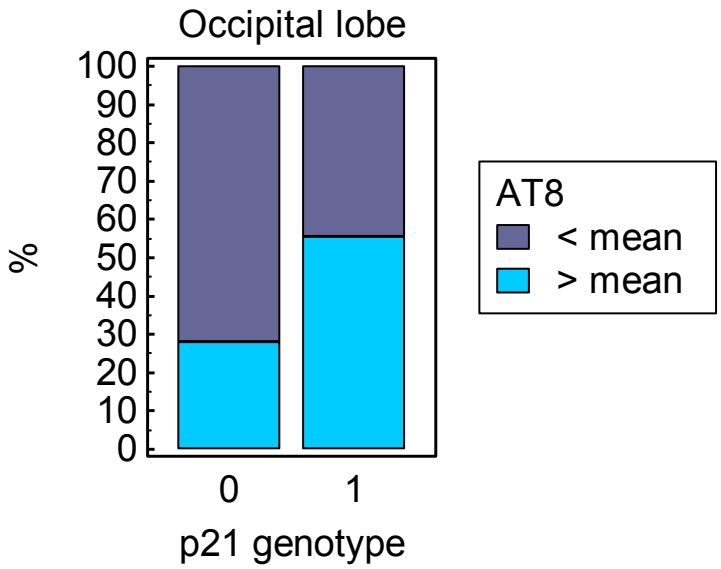

Figure 31 **The effect of the p21^{cip1} genotype on phospho-tau (AT8) deposition in the occipital lobe: independent of disease severity (x-axis = p21^{cip1} genotype: 0 = wild type, 1 = variant; y-axis: blue = percentage of subjects that express more AT8 in the occipital lobe than the group mean, purple = percentage of subjects that express less AT8 in the occipital lobe than the group mean; groups are defined by Braak stage) (chi-square test).**

Additionally, one-way ANOVA showed that subjects with variant $p21^{cip1}$ had a significantly greater amount of phospho-tau (AT8) in the occipital lobe than subjects with wild type $p21^{cip1}$, irrespective of disease severity (p=0.025) (Figure 32).

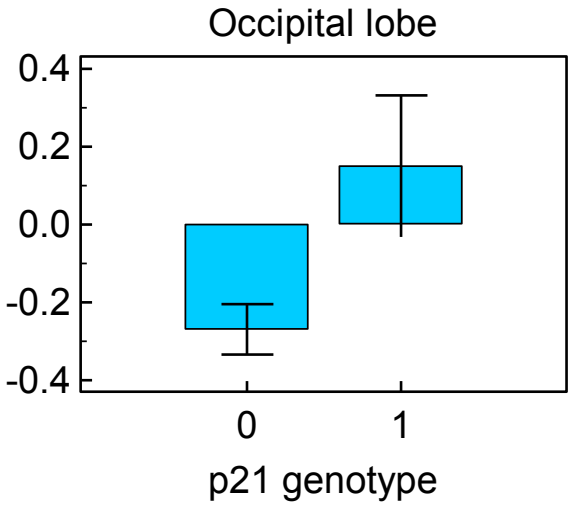

Figure 32 **The effect of the $p21^{cip1}$ genotype on phospho-tau (AT8) deposition in the occipital lobe: independent of disease severity (x-axis = $p21^{cip1}$ genotype: 0= wild type, 1= variant; y-axis = z-scores: deviation of each occipital lobe AT8 score from the group mean; error bars represent standard error of the means) (ANOVA).**

The $p21^{cip1}$ genotype had no effect on phospho-tau (AT8) deposition in the temporal lobe, irrespective of severity of AD (data not shown).

3.2.6.6. The effect of the $p21^{cip1}$ genotype on neurofibrillary tangle deposition

DC11 is a marker of neurofibrillary tangles (NFT), one of the hallmarks of AD[94]. Kruskal Wallis analysis showed that tangle (DC11) deposition was strongly dependent on disease severity ($p<0.001$) in all brain regions examined (temporal, frontal and occipital lobe). The $p21^{cip1}$ genotype had no effect on tangle deposition in the temporal lobe (data not shown). However, there was a trend for increase in tangle deposition in the frontal and occipital lobes of individuals with variant $p21^{cip1}$ compared to wild type $p21^{cip1}$ (Figure 33 and 34). The trend reached statistical significance in the occipital lobe of limbic stage patients only ($p=0.0328$).

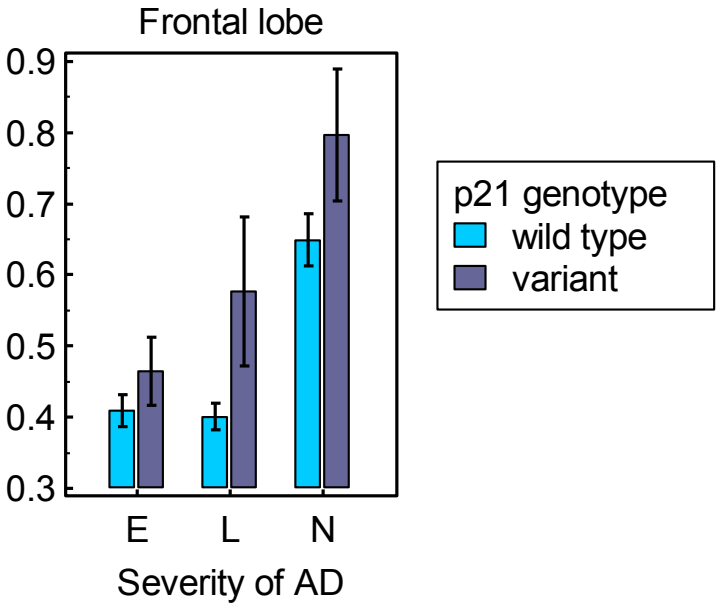

Figure 33 **The effect of the p21^{cip1} genotype on tangle (DC11) deposition in the frontal lobe (x-axis = AD severity as defined by Braak staging: E = entorhinal stage, L = limbic stage, N = neocortical stage; y-axis = amount of DC11 in the frontal lobe; top of bars represent mean; error bars represent standard error of the mean) (Kruskal Wallis).**

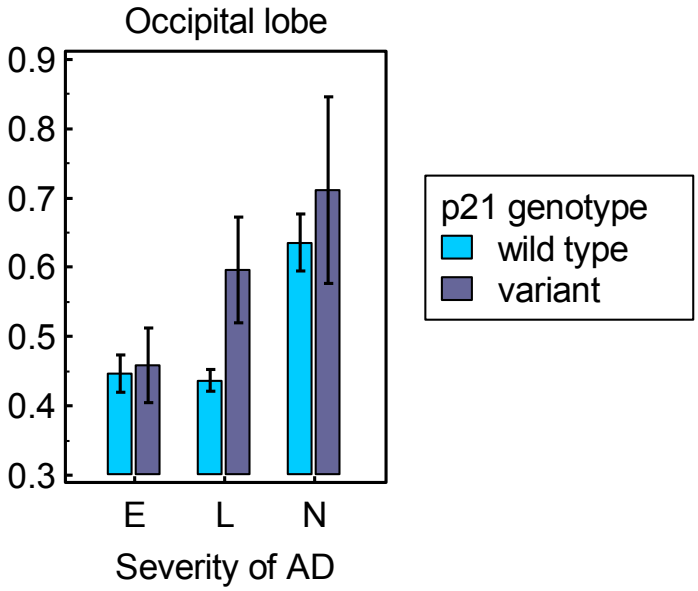

Figure 34 **The effect of the p21^{cip1} genotype on tangle deposition (DC11) in the occipital lobe (x-axis = AD severity as defined by Braak staging: E = entorhinal stage, L = limbic stage, N = neocortical stage; y-axis = amount of DC11 in the occipital lobe; top of bars represent mean; error bars represent standard error of the mean) (Kruskal Wallis).**

The need to take the severity of AD into account when analysing the effect of the p21^{cip1} genotype on NFT (DC11) deposition lead to very low subject numbers in the p21^{cip1} variant groups defined by the severity of AD. As this may have contributed to the lack of statistically significant results, DC11 z-scores were calculated for each subject taking into account disease severity (refer to 2.10).

The p21^{cip1} genotype had no effect on tangle (DC11) deposition in the temporal lobe, irrespective of disease severity (data not shown). However, the p21^{cip1} genotype had a significant effect on tangle (DC11) deposition in the frontal and occipital lobe.

Approximately 65% of individuals with variant $p21^{cip1}$ had greater tangle deposition (DC11) in the frontal lobe than the group mean; whereas only ~37% of individuals with wild type $p21^{cip1}$ had greater tangle deposition (DC11) in the frontal lobe than the group mean (Figure 35). This difference was statistically significant (p=0.0395), indicating that a significantly greater percentage of subjects with variant $p21^{cip1}$ had "high" tangle deposition in the frontal lobe than subjects with wild type $p21^{cip1}$, irrespective of AD severity ("high" defined as above the group mean).

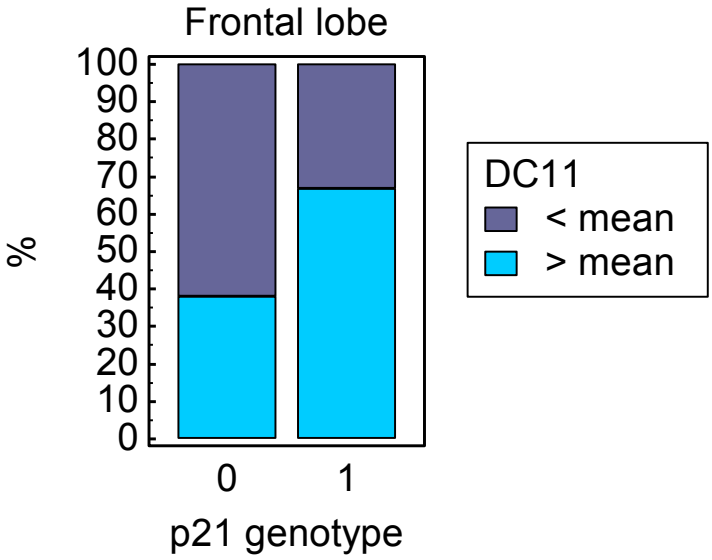

Figure 35 **The effect of the $p21^{cip1}$ genotype on tangle deposition (DC11) in the frontal lobe: independent of AD severity (x-axis = $p21^{cip1}$ genotype: 0 = wild type, 1 = variant; y-axis: blue = percentage of subjects that express more DC11 in the frontal lobe than the group mean, purple = percentage of subjects that express less DC11 in the frontal lobe than the group mean; groups are defined by Braak stage).**

Furthermore, one-way ANOVA showed that individuals with variant $p21^{cip1}$ had significantly greater tangle deposition (DC11) in the frontal lobe than individuals with wild type $p21^{cip1}$, irrespective of severity of AD (p=0.002) (Figure 36).

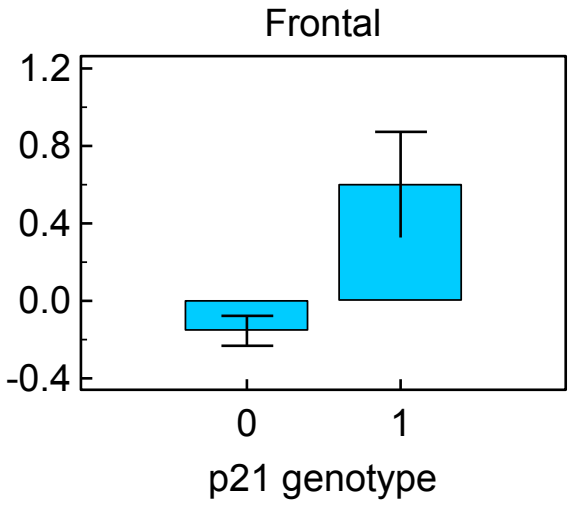

Figure 36 **The effect of the $p21^{cip1}$ genotype on tangle deposition (DC11) in the frontal lobe: independent of disease severity (x-axis = $p21^{cip1}$ genotype: 0= wild type, 1= variant; y-axis = z-scores: deviation of each frontal lobe DC11 value from the group mean; error bars represent standard error of the means) (ANOVA).**

There was no significant difference between the $p21^{cip1}$ wild type group and $p21^{cip1}$ variant group in terms of percentage of subjects with occipital lobe tangle deposition (DC11) above the group mean, irrespective of AD severity (data not shown). However, one-way ANOVA showed that individuals with variant $p21^{cip1}$ had significantly greater tangle deposition (DC11) in the occipital lobe than wild type $p21^{cip1}$ subjects (p=0.029) (Figure 37).

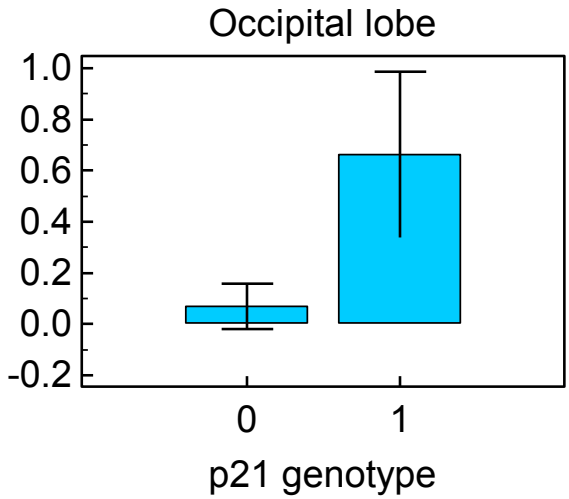

Figure 37 **The effect of the p21^{cip1} genotype on tangle deposition (DC11) in the occipital lobe: independent of disease severity (x-axis = p21^{cip1} genotype: 0= wild type, 1= variant; y-axis = z-scores: deviation of each frontal lobe DC11 value from the group mean; error bars represent standard error of the means) (ANOVA).**

3.2.6.7. The effect of the p21^{cip1} genotype on the spread of hyperphosphorylated tau from the temporal to the frontal lobe

In AD, tau pathology characteristically accumulates in the temporal lobe, with some accumulation in the frontal lobe in later stages of the disease. The occipital lobe is relatively spared even in advanced AD[15]. The extent and rate of spread of phospho-tau (AT8) from the temporal to the frontal lobe was calculated by dividing the relative amount of phospho-tau (AT8) expressed in the frontal lobe by the relative amount of phospho-tau expressed in the temporal lobe.

We demonstrate that there was significantly greater phospho-tau spread from the temporal to the frontal lobe in advanced AD patients (neocortical stage) compared to preclinical and mild AD sufferers (limbic and entorhinal stage) ($p<0.001$) (Figure 38). There was a trend for greater phospho-tau (AT8) spread from the temporal to the frontal lobe in variant p21^{cip1} carriers compared to non-carriers, which reached significance in subjects with mild AD only (limbic stage) ($p=0.0455$) (Figure 39).

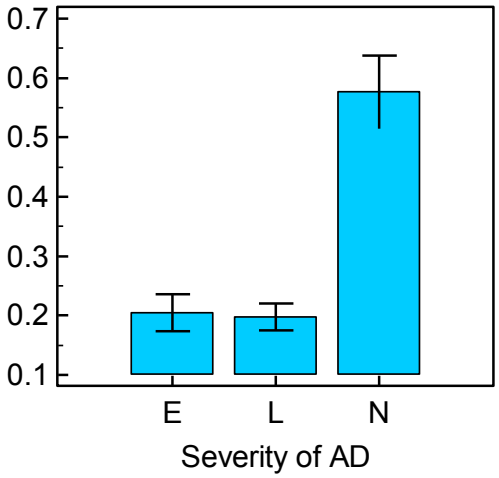

Figure 38 **The effect of the severity of AD on the rate of spread of tau pathology (AT8) from the temporal to the frontal lobe (x-axis= severity of AD, as defined by Braak staging, E= entorhinal, L= limbic, N= neocortical; y-axis= spread of AT8 pathology from the temporal to the frontal lobe; top of bars represent mean; error bars represent standard error of the means) (Kruskal Wallis).**

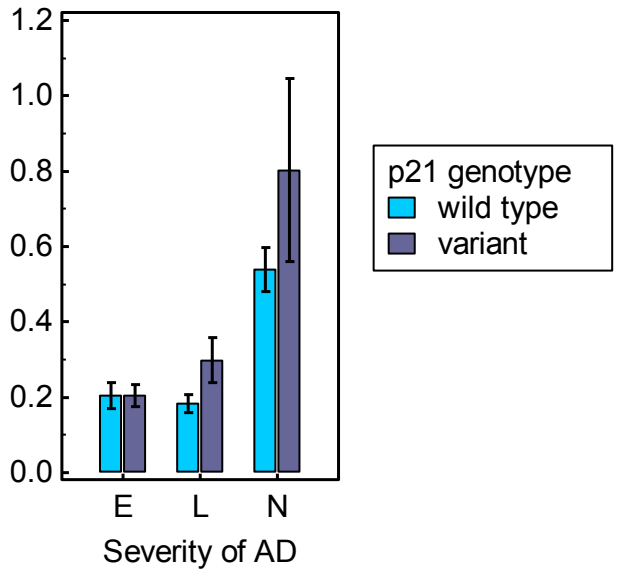

Figure 39 **The effect of the p21^{cip1} genotype on the rate of phospho-tau (AT8) spread from the temporal to the frontal lobe (x-axis = severity of AD, as defined by Braak: E= entorhinal stage, L = limbic stage, N = neocortical stage; y-axis = spread of AT8 pathology from the temporal lobe to the frontal lobe; top of bars represent mean; error bars represent standard error of the mean) (Kruskal Wallis).**

3.2.6.8. The effect of the $p21^{cip1}$ genotype on the spread of hyperphosphorylated tau from the temporal to the occipital lobe

The extent of phospho-tau (AT8) spread from the temporal to the occipital lobe was calculated by dividing the relative amount of phospho-tau expressed in the occipital lobe by the relative amount expressed in the temporal lobe. We found significantly greater phospho-tau spread from the temporal to the occipital lobe in advanced AD patients (neocortical stage) compared to preclinical and mild AD suffers (entorhinal and limbic stage) ($p<0.001$) (Figure 40). The $p21^{cip1}$ genotype had no effect on phospho-tau spread from the temporal to the occipital lobe, irrespective of disease severity. However, there was a trend (not statistically significant) for greater phospho-tau spread in variant $p21^{cip1}$ carriers compared to non-carriers (data not shown).

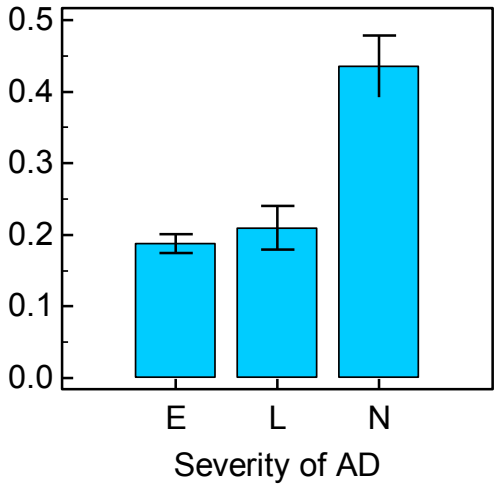

Figure 40 **The effect of the severity of AD on the rate of spread of phospho-tau (AT8) from the temporal to the occipital lobe (x-axis= severity of AD, as defined by Braak staging, E= entorhinal, L= limbic, N= neocortical; y-axis= spread of AT8 pathology from the temporal to the occipital lobe; top of bars represent mean; error bars represent standard error of the means).**

3.2.6.9. The effect of the $p21^{cip1}$ genotype on the spread of NFT from the temporal to the frontal lobe

As previously discussed, tangle pathology accumulates predominately in the temporal lobe in AD, with some accumulation in the frontal lobe in later stages. The occipital lobe is relatively spared even in advanced AD[15]. The extent and rate of spread of NFT from the temporal to the frontal lobe was calculated by dividing relative frontal lobe NFT (DC11) content by relative temporal lobe NFT (DC11) content. We found that the rate of spread of

NFTs from the temporal to the frontal lobe was independent of disease severity (data not shown). The $p21^{cip1}$ genotype had no effect on the rate of spread from the temporal to the frontal lobe in preclinical or advanced AD sufferers. However, in mild AD sufferers, the rate of spread of NFTs was significantly greater in variant $p21^{cip1}$ carriers compared to non-carriers (p=0.0431) (Figure 41).

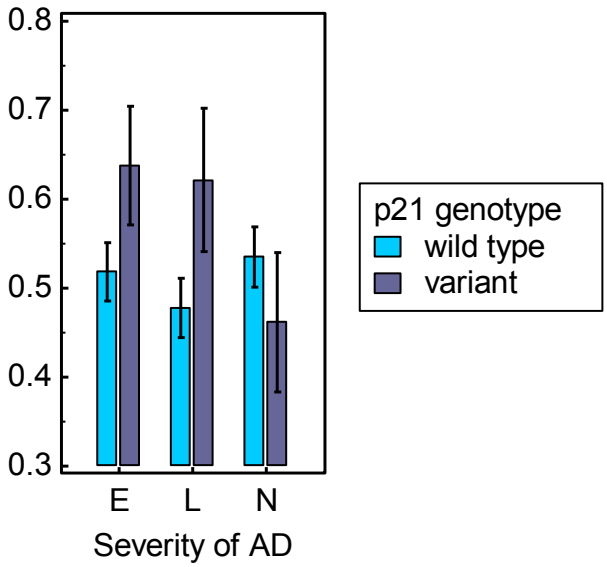

Figure 41 **The effect of the $p21^{cip1}$ genotype on the rate of spread of NFT (DC11) from the temporal to the frontal lobe (x-axis = severity of AD, as defined by Braak: E= entorhinal stage, L = limbic stage, N = neocortical stage; y-axis = rate of spread of DC11 pathology from the temporal lobe to the frontal lobe; top of bars represent mean; error bars represent standard error of the mean) (Kruskal Wallis).**

3.2.6.10. The effect of $p21^{cip1}$ genotype on the spread of NFT from the temporal to the occipital lobe

The rate of spread of NFTs from the temporal to the occipital lobe was calculated by dividing occipital lobe NFT (DC11) content by temporal lobe NFT (DC11) content. The rate of spread of NFTs was not altered by the severity of AD (data not shown). Whilst the $p21^{cip1}$ genotype had no effect on the rate of spread of NFTs from the temporal to the occipital lobe in subjects in a preclinical or advanced stage of AD: rate of spread of NFTs was significantly greater in mild AD patients (limbic stage) that were carriers of the variant $p21^{cip1}$ than non-carriers (p=0.0335) (Figure 42).

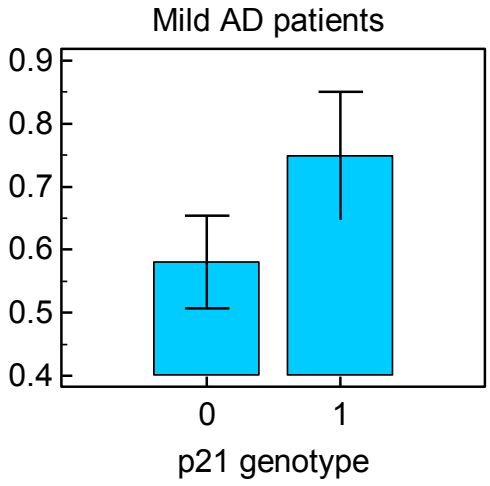

Figure 42 **The effect of the $p21^{cip1}$ genotype on the rate of spread of NFTs (DC11) from the temporal to the occipital lobe in sufferers of mild AD only (x-axis = $p21^{cip1}$ genotype: 0 = wild type, 1 = variant; y-axis = rate of spread of DC11 from the temporal to the occipital lobe; top of bars represent**

mean; error bars represent standard error of the means) (Kruskal Wallis).

3.2.6.11. The effect of the p21^{cip1} genotype on synaptic density

Synaptophysin is a glycoprotein located on neuronal synapses that can be used as a marker of synaptic density[95]. We found a trend for a decrease in the synaptic density of the temporal, frontal and occipital lobe as AD progressed from an early to more advanced stage. The trend reached statistical significance in the occipital lobe only (p=0.0012) (Figure 43). The p21^{cip1} genotype had no effect on the synaptic density of any brain region, irrespective of severity of AD (data not shown).

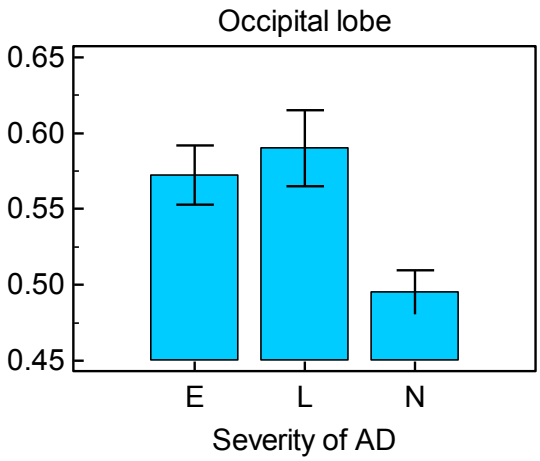

Figure 43 **The effect of the p21^{cip1} genotype on synaptic density in the occipital lobe (x-axis = AD severity as defined by Braak: E = entorhinal stage, L = limbic stage, N = neocortical stage; y-axis = synaptophysin expression in the occipital lobe; top of bars represent mean; error bars represent standard error of the mean) (Kruskal Wallis).**

3.2.6.12. The effect of the $p21^{cip1}$ genotype on neuronal density

Neuronal nuclei (NeuN) is a neuron specific protein that can be used as a marker of neuronal density[97]. We found a trend for decrease in the neuronal density of the temporal, frontal and occipital lobe as AD progressed from an early to advanced stage, which reached statistical significance in the frontal lobe only ($p<0.001$) (Figure 44). The $p21^{cip1}$ genotype had no effect on neuronal density, irrespective of brain region or severity of AD.

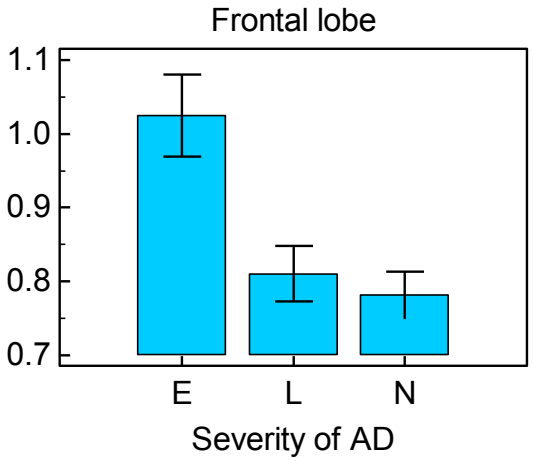

Figure 44 **The effect of the severity of AD on the neuronal density in the frontal lobe (x-axis = AD severity as defined by Braak: E = entorhinal stage, L = limbic stage, N = neocortical stage; y-axis = NeuN expression in the frontal lobe; top of bars represent mean; error bars represent standard error of the mean) (Kruskal Wallis).**

3.2.6.13. The effect of the $p21^{cip1}$ genotype on synaptic remodelling activity

Growth associated protein-43 (GAP-43) is expressed on axonal growth cones during synaptic remodelling, and can be used as a marker of synaptic remodelling activity[96]. The synaptic remodelling activity of neurons in the temporal and frontal lobe was independent of AD severity and $p21^{cip1}$ genotype. In the occipital lobe, the synaptic remodelling activity significantly decreased as AD progressed from an early to more advanced stage ($p<0.001$) (Figure 45). The $p21^{cip1}$ genotype had no effect on the synaptic remodelling activity in the occipital lobe, although there was a trend for advanced AD patients (neocortical stage) who were carriers of the variant $p21^{cip1}$ to have lower remodelling activity than those who were wild type for $p21^{cip1}$ (Figure 46).

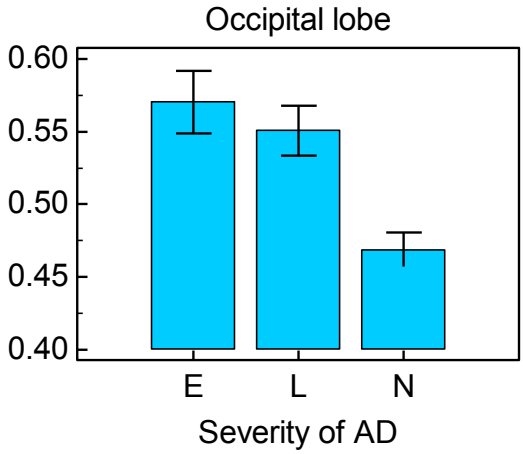

Figure 45 **The effect of the severity of AD on the synaptic remodelling activity of neurons in the occipital lobe (x-axis = severity of AD as defined by Braak: E = entorhinal stage, L = limbic stage, N = neocortical stage; y-axis = synaptic remodelling activity of neurons (GAP-43) in the occipital lobe; top of bars represent mean; error bars represent standard error of the mean) (one-way ANOVA).**

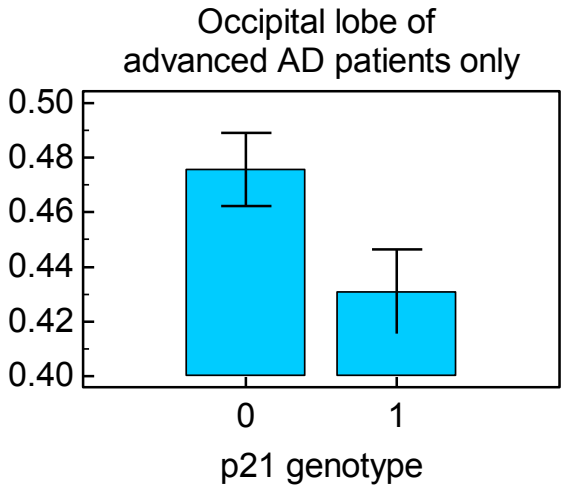

Figure 46 **The effect of the p21^{cip1} genotype on the synaptic remodelling activity of neurons in the occipital lobe of sufferers of advanced AD only (x-axis = p21^{cip1} genotype: 0 = wild type, 1 = variant; y-axis = GAP-43 expression in the occipital lobe of sufferers of advanced AD only; top of bars represent mean; error bars represent standard error of the mean) (one-way ANOVA).**

3.2.7 The effect of the p21^{cip1} genotype on cognitive performance

The available cognitive performance scores (CAMCOG) were the results of the last cognitive assessment carried out at most 6 months prior to death. As expected, the CAMCOG scores were highly dependent on severity of AD, with advanced AD patients showing significantly lower CAMCOG scores than patients in earlier stages of AD ($p<0.001$) (Figure 47). The cognitive performance was independent of the p21^{cip1} genotype, irrespective of disease severity.

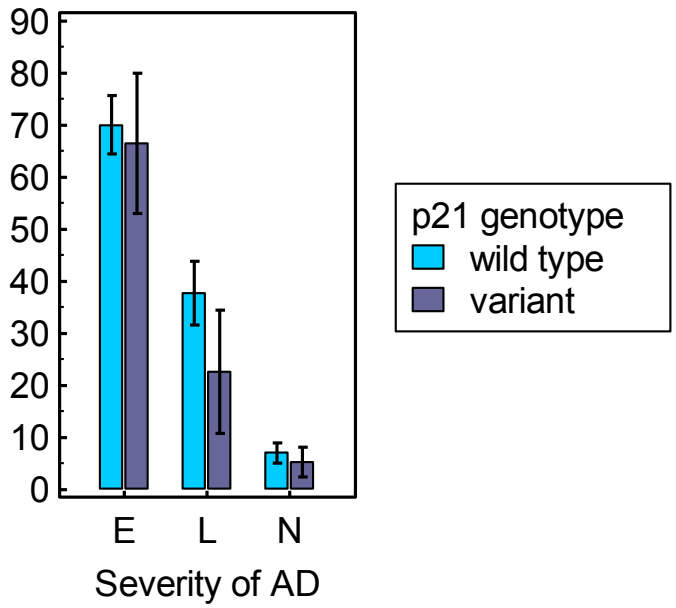

Figure 47 **The effect of the p21^{cip1} genotype on cognitive performance (x-axis = severity of AD as defined by Braak stage: E = entorhinal stage, L = limbic stage, N = neocortical stage; y-axis = cognitive performance, at most 6 months prior to death; top of bars represent mean; error bars represent standard error of the mean) (Kruskal Wallis).**

3.2.8 The effect of the p21^{cip1} genotype on the stability of p21^{cip1} mRNA and protein

The frontal lobe p21^{cip1} mRNA content was measured by Q-PCR with normalisation to beta-actin content. We found that the p21^{cip1} mRNA content was independent of the severity of AD (data not shown). The p21^{cip1} mRNA content of the frontal lobe was also independent of p21^{cip1} genotype in individuals with preclinical (entorhinal stage) and mild (limbic stage) AD. However, advanced AD (neocortical stage) patients with variant p21^{cip1} had significantly lower p21^{cip1} mRNA content in the frontal lobe than wild type patients (p= 0.0195) (Figure 48).

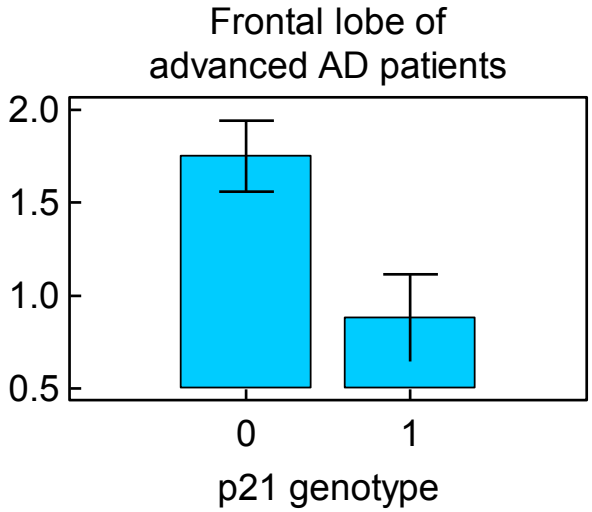

Figure 48 **The effect of the p21^{cip1} genotype on the stability of p21^{cip1} mRNA in the frontal lobe of advanced AD patients only (x-axis = p21^{cip1} genotype: 0 = wild type; 1 = variant; top of bars represent mean; error bars represent standard error of the mean) (Kruskal Wallis).**

The $p21^{cip1}$ protein content of the temporal, frontal and occipital lobe of each subject was measured by ELISA, with normalisation to overall protein content. We found that $p21^{cip1}$ protein content was significantly greater in the temporal and frontal lobe of advanced AD patients compared to control (p= 0.0087 and 0.046 respectively) (Figure 49 and Figure 50). The $p21^{cip1}$ protein content of the occipital lobe was independent of disease severity (data not shown). There was a trend for patients with advanced AD to express more $p21^{cip1}$ protein per mRNA in the frontal lobe than control, although results failed to reach statistical significance (Figure 51).

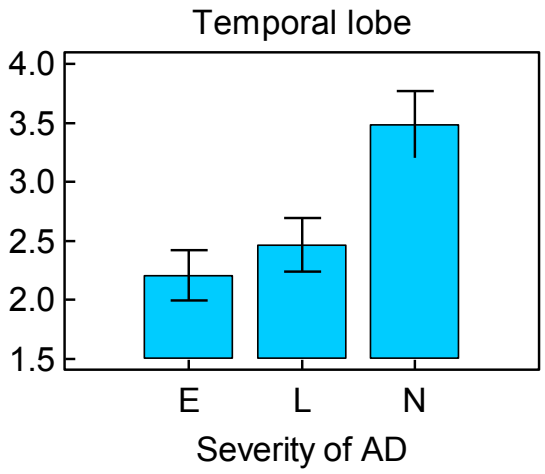

Figure 49 **The effect of the severity of AD on $p21^{cip1}$ protein expression in the temporal lobe (x-axis = severity of AD as defined by Braak stage: E = entorhinal stage, L = limbic stage, N = neocortical stage; y-axis = $p21^{cip1}$ protein content of the temporal lobe; top of bars represent mean; error bars represent standard error of the mean) (Kruskal Wallis).**

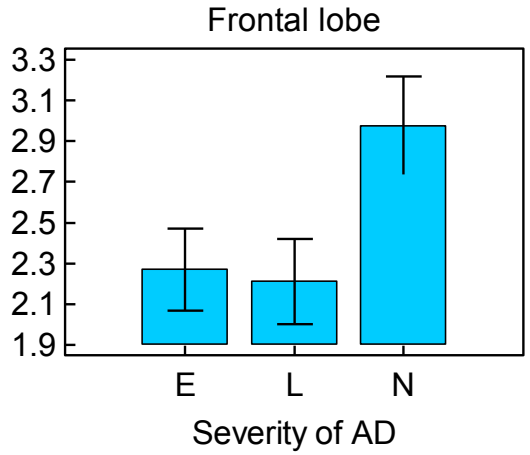

Figure 50 **The effect of the severity of AD on p21^{cip1} protein expression in the frontal lobe (x-axis = severity of AD as defined by Braak stage: E = entorhinal stage, L = limbic stage, N = neocortical stage; y-axis = p21^{cip1} protein content of the frontal lobe; top of bars represent mean; error bars represent standard error of the mean) (Kruskal Wallis).**

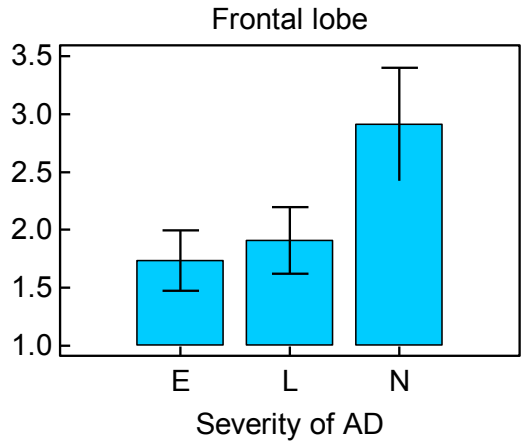

Figure 51 The effect of the severity of AD on $p21^{cip1}$ protein expression per mRNA in the frontal lobe (x-axis = severity of AD as defined by Braak stage: E = entorhinal stage, L = limbic stage, N = neocortical stage; y-axis = $p21^{cip1}$ protein expression per mRNA in the frontal lobe; top of bars represent mean; error bars represent standard error of the mean) (Kruskal Wallis).

The $p21^{cip1}$ genotype had no effect on $p21^{cip1}$ protein expression in any brain region examined, or on amount of $p21^{cip1}$ protein expressed per mRNA in the frontal lobe (data not available for the temporal or occipital lobe). Furthermore, we found no correlation between $p21^{cip1}$ mRNA content and $p21^{cip1}$ protein content in the frontal lobe, irrespective of AD severity or $p21^{cip1}$ genotype (data not shown). Multiple regression analysis showed that frontal lobe $p21^{cip1}$ protein content was dependent on frontal lobe NFT content (DC11) (R^2= 0.1, p = 0.003), and independent of $p21^{cip1}$ mRNA content and disease severity.

3.2.9 Relative expression at mRNA level of wild type to variant $p21^{cip1}$ heterozygous subjects

SNP A and B on $p21^{cip1}$ tend to be inherited together[77]. In our cohort, a small number of subjects had SNP A, but not SNP B. These subjects were excluded from this analysis.

The 26 subjects that were heterozygous for both SNP A and B on $p21^{cip1}$ were analysed by SNP dependent Q-PCR, to determine the relative expression of mRNA corresponding to wild type $p21^{cip1}$ and variant $p21^{cip1}$ in the brain of these subjects (Table 40). We would expect heterozygous subjects to express equal amounts of wild type and variant $p21^{cip1}$ mRNA, unless the rate of transcription, or stability of $p21^{cip1}$ mRNA, was altered by the $p21^{cip1}$ SNPs. Note that the brain region examined varied from subject to subject.

Table 40 Relative $p21^{cip1}$ wild type to variant mRNA expression heterozygous subjects

Effective genotype	**Number of cases**	**Percentage of all cases (26)**
Equal amount of wild type and variant $p21^{cip1}$	13	50%
More variant $p21^{cip1}$	12	46%
More wild type $p21^{cip1}$	1	4%

Of the 26 subjects that were heterozygous for both $p21^{cip1}$ SNPs: half expressed equal amounts of mRNA corresponding to the wild type and variant $p21^{cip1}$ (50%); 46% of

subjects expressed significantly more mRNA corresponding to variant $p21^{cip1}$ than wild type $p21^{cip1}$; whereas only 1 subject (4%) expressed significantly more mRNA corresponding to wild type $p21^{cip1}$ than variant $p21^{cip1}$. The ratio of wild type to variant $p21^{cip1}$ mRNA was not altered by AD, irrespective of disease severity (data not shown).

3.2.10 The effect of the $p21^{cip1}$ genotype on the function and expression of $p21^{cip1}$

In order to elucidate the effects of the $p21^{cip1}$ SNPs on the function of the protein in vitro, human embryonic kidney cells (Flp-In-T-Rex-293, Invitrogen) were transiently transfected with a vector designed to express either wild type $p21^{cip1}$, variant $p21^{cip1}$ (with SNP A and B); or no $p21^{cip1}$ (mock transfection: negative control). The Flp-In-T-Rex-293 cells were rapidly dividing and intrinsically wild type for $p21^{cip1}$.

To investigate the success of transfection, the relative expression of $p21^{cip1}$ mRNA and protein were determined by Q-PCR and Acumen Cytometry respectively in the transfected cells. Both $p21^{cip1}$ mRNA and protein content were normalised to beta-actin content (Table 41 and 42). The ratio of $p21^{cip1}$ protein to mRNA for each transfected cell population is shown in Table 43.

Table 41 P21^{cip1} mRNA expression in the transfected cells (p21^{cip1} mRNA content determined by Q-PCR with normalisation to beta-actin content)

Transfected population	RNA (p21^{cip1} / beta-actin)	Value relative to mock (expressed as a multiple)
Wild type p21^{cip1}	1524	298
Variant p21^{cip1}	1405	275
Control	5	

Table 42 P21^{cip1} protein expression in the transfected cells (p21^{cip1} protein content determined by Acumen Cytometry with normalisation to beta-actin content)

Transfected population	PROTEIN (p21^{cip1}/ beta-actin)	Value relative to mock (expressed as a multiple)
Wild type p21^{cip1}	2,609	7.2
Variant p21^{cip1}	2,932	8.1
Control	362	

Table 43 Ratio of p21^{cip1} protein to mRNA content of the transfected cells (p21^{cip1} protein and mRNA normalised to beta-actin content).

Transfected population	p21^{cip1} PROTEIN/mRNA	Relative to wild type p21^{cip1} (expressed as percentage)
Wild type p21^{cip1}	1.71	
Variant p21^{cip1}	2.09	122

The $p21^{cip1}$ transfected cells had significantly greater $p21^{cip1}$ mRNA and protein content than the control cells, irrespective of $p21^{cip1}$ genotype (Table 41 and 42). To elaborate, the cells transfected with wild type $p21^{cip1}$ had 298 times more $p21^{cip1}$ mRNA than the control; whereas the cells transfected with variant $p21^{cip1}$ had 275 times more $p21^{cip1}$ mRNA than the control. Furthermore, the cells transfected with wild type $p21^{cip1}$ expressed 7.2 times more $p21^{cip1}$ protein than the control; whereas the cells transfected with variant $p21^{cip1}$ expressed 8.1 times more $p21^{cip1}$ protein than the control. This indicates that transfection was successful and that the mRNA was successfully translated to protein.

We compared $p21^{cip1}$ protein expression per mRNA in the wild type and variant transfected populations, and found that cells transfected with variant $p21^{cip1}$ expressed 22% more $p21^{cip1}$ protein per mRNA than the cells transfected with wild type $p21^{cip1}$ (Table 43). This implies that the SNPs either increase the stability of the $p21^{cip1}$ protein, or decrease the stability of the $p21^{cip1}$ mRNA, hence altering protein to mRNA ratio.

3.2.10.1. The effect of the $p21^{cip1}$ genotype on the nuclear translocation efficiency of $p21^{cip1}$

The expression of $p21^{cip1}$ protein, in the cells transfected with wild type or variant $p21^{cip1}$, was investigated 2 days post-transfection with the Acumen Cytometer after immunostaining with a $p21^{cip1}$ antibody. Within each well, cells that were positive and negative for $p21^{cip1}$ protein were analysed separately, to avoid misinterpretation of data as a result of unequal transfection efficiency or seeding density. The $p21^{cip1}$ expression per cell was calculated by

dividing the total amount of $p21^{cip1}$ protein expressed in the transfected population by the total number of $p21^{cip1}$ positive cells in the sample. To allow comparison of the cells transfected with wild type or variant $p21^{cip1}$, $p21^{cip1}$ expression in each transfected population was normalised to that of the wild type transfected population. All results concerning $p21^{cip1}$ expression in the wild type population are therefore displayed as 100%.

There was no significant difference in $p21^{cip1}$ protein expression per cell in cells transfected with wild type or variant $p21^{cip1}$ (Figure 52). Furthermore, there was no significant difference in the $p21^{cip1}$ protein density per nucleus (Figure 53), or in the percentage of $p21^{cip1}$ nuclear positive cells (Figure 54), in cells transfected with wild type or variant $p21^{cip1}$. Taken together, the results indicate that the nuclear translocation efficiency of $p21^{cip1}$ was not altered by the SNPs.

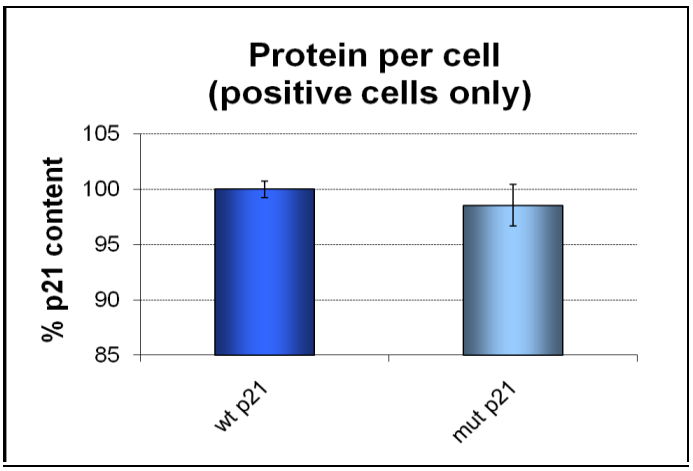

Figure 52 **Mean cellular $p21^{cip1}$ protein content of cells that were positive for $p21^{cip1}$ (x-axis: dark blue = cells transfected with wild type $p21^{cip1}$, light blue = cells transfected with variant $p21^{cip1}$; y-axis: $p21^{cip1}$ protein expression per cell expressed as a percentage of that in the wild type population).**

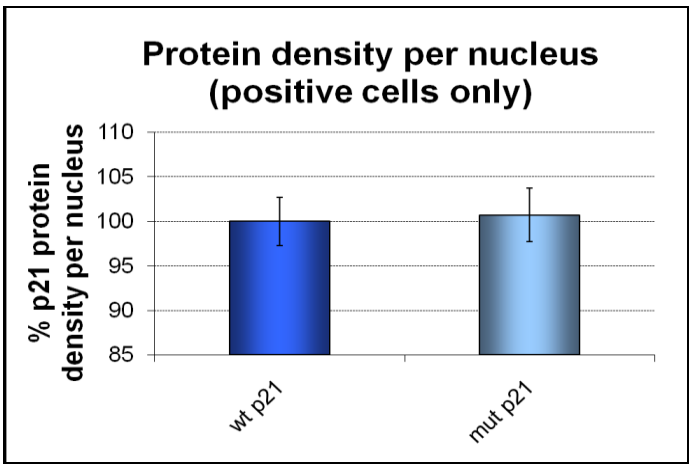

Figure 53 **Mean p21^{cip1} density per nucleus of cells that were positive for p21^{cip1} (x-axis: dark blue = cells transfected with wild type p21^{cip1}, light blue = cells transfected with variant p21^{cip1}; y-axis: p21^{cip1} protein density per nucleus expressed as a percentage of that of the wild type population).**

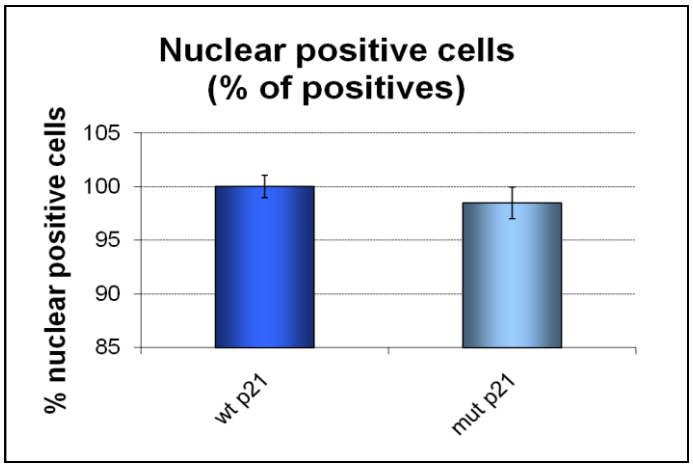

Figure 54 **Percentage of cells that were nuclear positive for p21^{cip1} (x-axis: dark blue = cells transfected with wild type p21^{cip1}, light blue = cells transfected with variant p21^{cip1}; y-axis: percentage of all p21^{cip1} positive cells that were nuclear positive for p21^{cip1}, normalised to the wild type transfected population).**

3.2.10.2. The effect of the $p21^{cip1}$ genotype on cell cycle kinetics

The cell cycle activity of the cells transfected with wild type or variant $p21^{cip1}$ was determined 2 days post-transfection with the Acumen Cytometer after propidium iodide staining. The percentage of cells in G1, S and G2/M phase of the cell cycle was calculated for each cell population. The results are displayed as a percentage change relative to the non-transfected cells within the same well (cells that were identified as negative for $p21^{cip1}$ within the cell population). Therefore, 100% represents cell cycle kinetics identical to that of the non-transfected population.

We show that the effect of $p21^{cip1}$ on cell cycle kinetics is dependent on $p21^{cip1}$ genotype, despite comparable expression and nuclear translocation efficiency of wild type and variant $p21^{cip1}$. Whilst wild type $p21^{cip1}$ induced a 41% increase in cells in the G2 phase compared to non-transfected cells, variant $p21^{cip1}$ only induced a 20% increase in G2 cells: both at the expense of cells in the G1 and S phase (Figure 55). This indicates that $p21^{cip1}$, expressed independently of p53, is a G2/M checkpoint inhibitor, and that wild type $p21^{cip1}$ is more effectively so than variant $p21^{cip1}$.

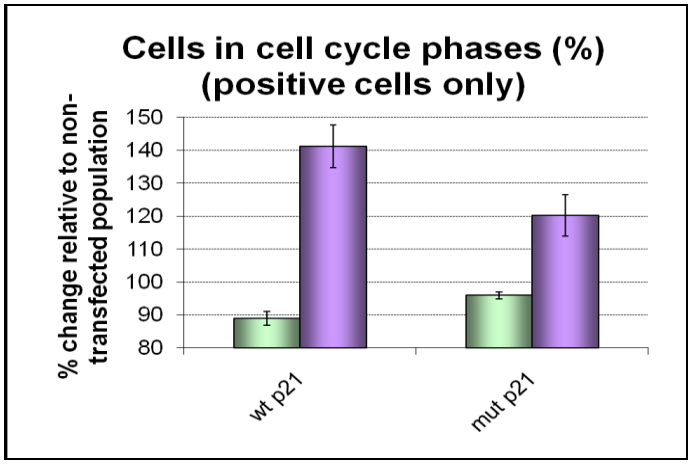

Figure 55 **Percentage of p21^{cip1} positive cells in G1 (green) and G2 (purple) phase of the cell cycle (x-axis: wt p21 = cells transfected with wild type p21^{cip1}, mut p21 = cells transfected with variant p21^{cip1}; y-axis: percentage of p21^{cip1} positive cells in G1 (green) and G2 (purple) phase of the cell cycle, expressed as a percentage change relative to cells that were not transfected with p21^{cip1}).**

3.2.10.3. The effect of the $p21^{cip1}$ genotype on apoptotic activity

The effect of $p21^{cip1}$ on the apoptotic activity of the transfected cells was determined with the Acumen Cytometer after propidium iodide staining. The results are displayed as a percentage change relative to the non-transfected cells within the same well (100% represents apoptotic activity equal to that of the non-transfected population). We show that the effect of $p21^{cip1}$ on the rate of apoptosis is dependent on $p21^{cip1}$ genotype. Wild type $p21^{cip1}$ reduced the rate of apoptosis to 42% of that of non-transfected cells, whereas variant $p21^{cip1}$ only reduced the rate of apoptosis to 49% of that of non-transfected cells (Figure 56). This indicates that $p21^{cip1}$ is an anti-apoptotic agent, and that wild type $p21^{cip1}$ is more effectively so than variant $p21^{cip1}$.

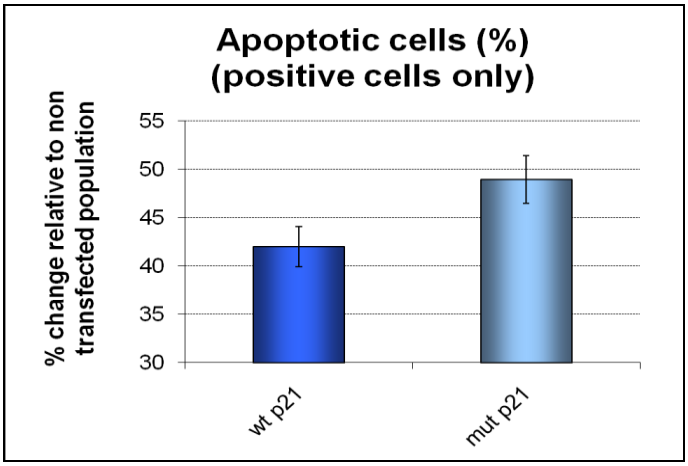

Figure 56 **Percentage of $p21^{cip1}$ positive cells undergoing apoptosis (x-axis: wt p21 = cells transfected with wild type $p21^{cip1}$, mut p21 = cells transfected with variant $p21^{cip1}$; y-axis: percentage of $p21^{cip1}$ positive cells undergoing apoptosis, expressed as a percentage change relative to the cells that were not transfected with $p21^{cip1}$).**

3.2.10.4. The effect of the $p21^{cip1}$ genotype on cellular beta-actin expression

The expression of beta-actin in the transfected cells was determined with the Acumen Cytometer by immunostaining with a beta-actin specific antibody. The amount of beta-actin expressed per cell was calculated by dividing the total amount of beta-actin expressed in the population by the total number of cells in the sample. We did not double stain with $p21^{cip1}$ antibody; and so were unable to differentiate the $p21^{cip1}$ positive population (transfected cells) from the $p21^{cip1}$ negative population (non-transfected cells). Therefore, the results are normalised to the results of the cells that were transfected with an empty vector (the negative control) (Figure 57).

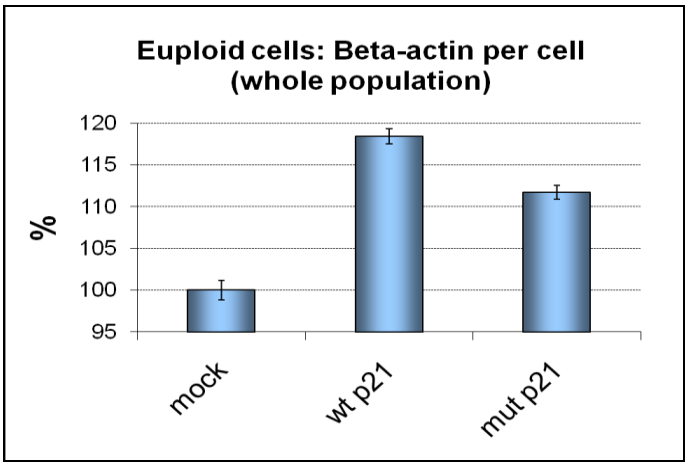

Figure 57 **Mean beta-actin expression per cell (x-axis: mock = negative control, wt p21 = cells transfected with wild type $p21^{cip1}$, mut p21 = cells transfected with variant $p21^{cip1}$; y-axis: beta-actin expression per cell, expressed as a percentage change relative to the cells that were transfected with an empty vector).**

We show that the cells transfected with $p21^{cip1}$ expressed a significantly greater amount of beta-actin per cell than the control, irrespective of $p21^{cip1}$ genotype (Figure 57). However, $p21^{cip1}$ wild type transfected cells expressed a significantly greater amount of beta-actin per cell than the $p21^{cip1}$ variant transfected cells (approximately 18% and 11% more than the control respectively).

3.3. ELUCIDATING THE IMPRINTING STATUS OF P57^{KIP2} IN THE HUMAN BRAIN; AND THE EFFECTS OF A SNP OF P57^{KIP2} ON PROTEIN EXPRESSION, AND ITS ASSOCIATION WITH AD

p57^{kip2} is involved in regulating cell cycle activity, cell survival and cytoskeleton dynamics; and has an important role in development[33]. It is an established CDKI that directly inhibits the activity of several cyclin/CDK complexes: including complexes required for progression from G1 to S phase. Aberrant neuronal progression from the G1 to S phase is hypothesised to be a cause of neurodegeneration in AD (reviewed in[29, 30]), suggesting that genetic variants of p57^{kip2} that are less effective G1/S checkpoint inhibitors, or have reduced expression, may contribute to pathogenesis. Notably, Nagy[74] found that a genetic variant of p57^{kip2} may be associated with an earlier age of onset of AD (although the result failed to reach statistical significance due to small sample size). The genetic variant had a single nucleotide substitution at a polymorphic site that triggered an amino acid substitution (alanine to valine) within the central domain of the p57^{kip2} protein (residue 159). Despite a strong association between reduced p57^{kip2} expression and cancer[31], there are no known cancer associated SNPs of p57^{kip2}. The investigated SNP was located within a proline/ alanine rich domain (PAPA domain), whose function is not fully understood, although it may be involved in the interaction of p57^{kip2} with the proteins required for its role in regulating apoptosis and cytoskeleton dynamics[33].

The elucidation of the effect of the p57^{kip2} SNP on AD pathogenesis is complicated by the finding that p57^{kip2} is paternally imprinted to some extent: with the maternal allele

preferentially expressed[33]. The expression and extent of imprinting of $p57^{kip2}$ are tissue-dependent in humans, although it has not been fully investigated in most tissues. Whilst it is known to be expressed in the adult brain[33]; there is no literature on its imprinting status in this tissue: although Matsuoka and co-workers[85] found that there was two-fold expression of the maternal allele over the paternal allele in foetal brain, in contrast to an approximately twenty-fold expression of the maternal allele over the paternal allele in the other foetal organs investigated. Therefore, an aim of the project was to determine the imprinting status of $p57^{kip2}$ in the aging brain. A second aim was to investigate the relationship between severity of AD and $p57^{kip2}$ imprinting status. It is known that abnormal imprinting of $p57^{kip2}$ can lead to altered expression and ultimately disease (for example, Beckwith-Wiederman syndrome)[31]. We will investigate the association between $p57^{kip2}$ imprinting and AD. We will also investigate the association of the $p57^{kip2}$ SNP with AD and AD-related pathology.

3.3.1 The $p57^{kip2}$ imprinting status in the aging human brain

DNA from the frontal lobe, and cDNA from the frontal and occipital lobes, of individuals in different stages of AD were genotyped for the $p57^{kip2}$ SNP. Individuals that were heterozygous for the SNP (as determined by genotyping from DNA) were informative in terms of imprinting status, as genotyping from cDNA allowed the analysis of proportion of expression of the wild type allele to the variant allele. Of the 69 individuals that were heterozygous for the $p57^{kip2}$ SNP: in the frontal lobe, 13% expressed only one of the alleles (complete imprinting); 54% showed preferential expression of one of the alleles (partial imprinting); whereas 33% had approximately equal expression of the two alleles (no

imprinting) (Table 44). In the occipital lobe: 2.9% expressed only one of the alleles (complete imprinting); 55.1% showed preferential expression of one of the alleles (partial imprinting); whereas 42% had equal expression of the two alleles (no imprinting) (Table 45). The $p57^{kip2}$ imprinting status in the frontal lobes was identical to that in the occipital lobe in 45.7% of cases (Table 46).

Table 44 $p57^{kip2}$ imprinting status in the frontal lobe

$p57^{kip2}$ imprinting status	**Number of patients**	**Percentage of total (%)**
Fully imprinted	9	13
Partially imprinted	37	54
Not imprinted	23	33
TOTAL	**69**	

Table 45 $p57^{kip2}$ imprinting status in the occipital lobe

$p57^{kip2}$ imprinting status	**Number of patients**	**Percentage of total (%)**
Fully imprinted	2	2.9
Partially imprinted	38	55.1
Not imprinted	29	42.0
TOTAL	**69**	

Table 46 Comparison of $p57^{kip2}$ imprinting status in the frontal and occipital lobe

Comparison of $p57^{kip2}$ imprinting status in frontal and occipital lobe	**Number of patients**	**Percentage of total (%)**
same	27	45.7
different	32	54.2

3.3.2 The effect of AD on $p57^{kip2}$ imprinting status

There was no significant difference in the $p57^{kip2}$ imprinting status of the occipital lobe of subjects with AD compared to control (Figure 58), or in subjects in different stages of AD (Figure 59). In the majority of subjects, $p57^{kip2}$ was either not imprinted (~42%), or partially imprinted (~58%) in this brain region, irrespective of disease severity.

In the frontal lobe, there was a trend (not statistically significant) for loss of $p57^{kip2}$ imprinting in AD subjects compared to control (Figure 60). Whilst $p57^{kip2}$ was fully imprinted (~15%), or not imprinted (15%), in the frontal lobe of some control subjects, in the majority of these cases (70%) $p57^{kip2}$ was partially imprinted. In contrast, 40% of AD sufferers had no $p57^{kip2}$ imprinting in the frontal lobe, whereas full imprinting of $p57^{kip2}$ in these subjects was reduced to only ~12% of cases. The trend for loss of imprinting with AD was also visible when subjects were analysed by disease severity (not statistically significant) (Figure 61).

The imprinting status of $p57^{kip2}$ in the frontal lobe was compared to the imprinting status of $p57^{kip2}$ in the occipital lobe in individuals in different stages of AD. There was a trend (not statistically significant) for the imprinting status of $p57^{kip2}$ to become more similar in the frontal and occipital lobe in later stages of AD (Figure 62). Our results suggest that $p57^{kip2}$ is differentially imprinted in the frontal and occipital lobe of elderly brain: with greater imprinting in the frontal lobe compared to the occipital lobe. There is a tendency for loss of imprinting in the frontal lobe as AD becomes increasingly severe.

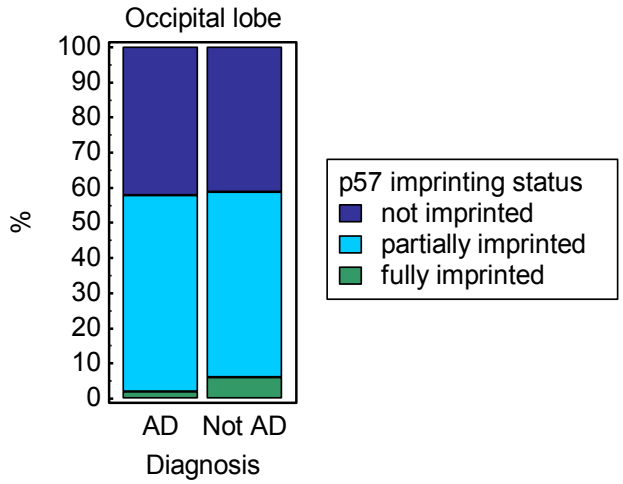

Figure 58 **Occipital lobe $p57^{kip2}$ imprinting status (x-axis = diagnosis: AD = subjects with AD, not AD = subjects without AD; y-axis = percentage of total; dark blue = no imprinting, light blue = partial imprinting, green = full imprinting).**

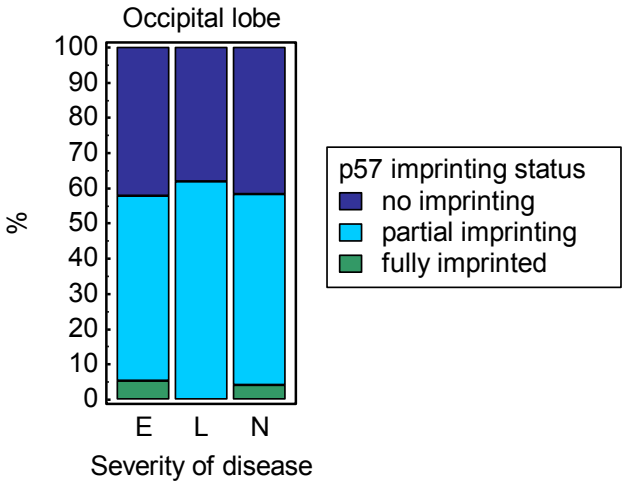

Figure 59 **Occipital lobe $p57^{kip2}$ imprinting status (x-axis = diagnosis: E = entorhinal stage, L = limbic stage, N = neocortical stage; y-axis = percentage of total; dark blue = no imprinting, light blue = partial imprinting, green = full imprinting).**

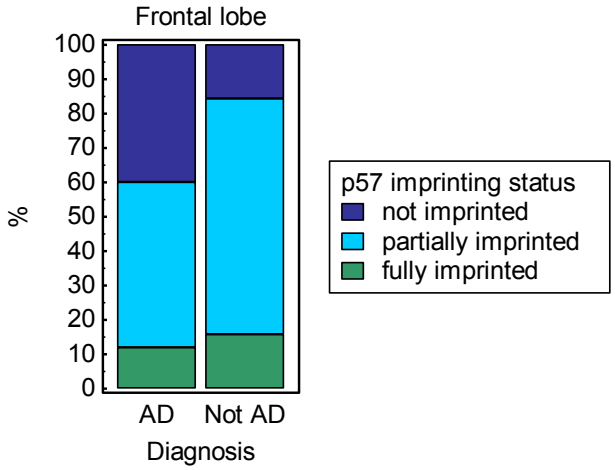

Figure 60 **Frontal lobe $p57^{kip2}$ imprinting status (x-axis = diagnosis: AD = subjects with AD, not AD = subjects without AD; y-axis = percentage of total; dark blue = no imprinting, light blue = partial imprinting, green = full imprinting).**

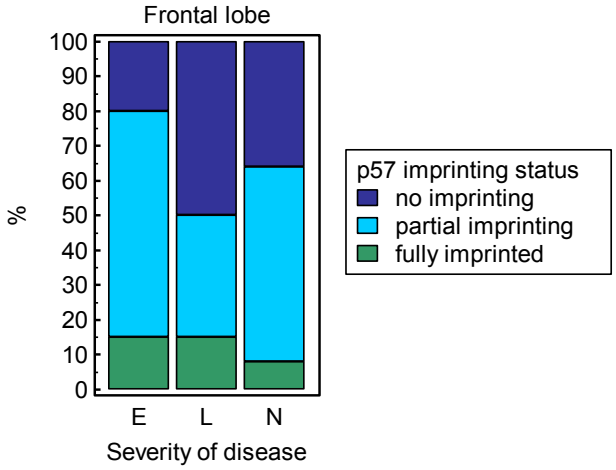

Figure 61 **Frontal lobe $p57^{kip2}$ imprinting status (x-axis = diagnosis: E = entorhinal stage, L = limbic stage, N = neocortical stage; y-axis = percentage of total; dark blue = no imprinting, light blue = partial imprinting, green = full imprinting).**

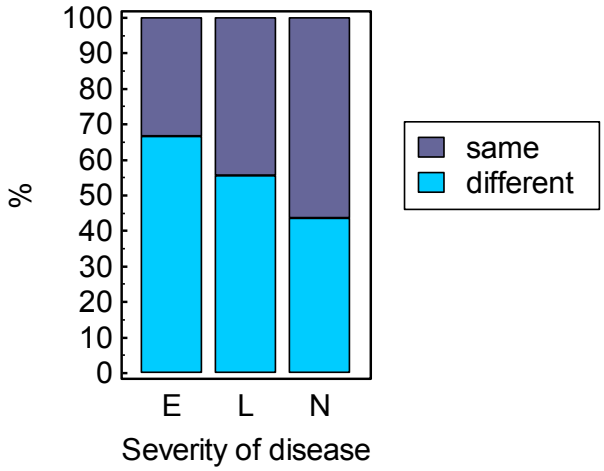

Figure 62 **Comparison of frontal and occipital lobe $p57^{kip2}$ imprinting status (x-axis = severity of AD: E = entorhinal stage, L = limbic stage, N = neocortical stage, y-axis = percentage of total; purple = identical imprinting status in the frontal and occipital lobe; light blue = different imprinting status in the frontal and occipital lobe).**

3.3.3 Frequency of the $p57^{kip2}$ variant

Of the 209 subjects available for the study, the Braak stage and $p57^{kip2}$ genotype were available for 178. Of these 178 subjects, 91 were wild type (51%), 71 heterozygous (40%), and 16 homozygous (9%) for the $p57^{kip2}$ SNP of interest (Table 47). This is consistent with the Hardy-Weinberg equilibrium. The frequency of the $p57^{kip2}$ variant allele was not significantly different in individuals in different stages of AD (Table 48). However, there was a trend (not statistically significant) for a greater percentage of advanced AD sufferers to be homozygous for the $p57^{kip2}$ variant compared to preclinical and mild AD sufferers (odds ratio = 1.7) (Table 49 and Figure 63).

Table 47 Frequency of the $p57^{kip2}$ SNP

$P57^{kip2}$ genotype	**Number of patients**	**Relative frequency %**
Wild type	91	51
Heterozygous	71	40
Homozygous	16	9
TOTAL	**178**	

Table 48 Frequency of the $p57^{kip2}$ allele in subjects in different stages of AD

DIAGNOSIS	**$P57^{kip2}$ wild type allele**	**$P57^{kip2}$ variant allele**	**Relative frequency of $p57^{kip2}$ variant allele (%)**
Control	72	28	28
Limbic stage	75	29	28
Neocortical stage	106	46	30

Table 49 Frequency of subjects homozygous for the $p57^{kip2}$ SNP

DIAGNOSIS	$P57^{kip2}$ (total no. of cases)	$P57^{kip2}$ (homozygous)	Relative frequency of homozygotes (%)	Odds ratio (homozygotes)
Control	50	3	6.0	
Limbic stage	52	3	5.7	0
Neocortical stage	76	10	13	1.7

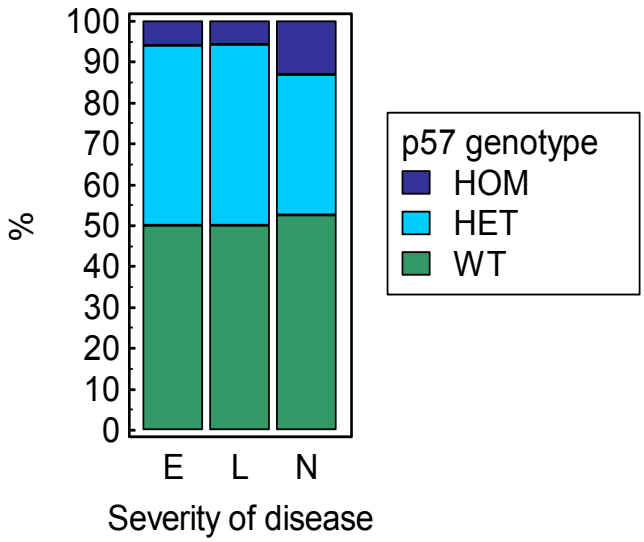

Figure 63 Distribution of $p57^{kip2}$ SNP in subjects in different stages of AD (x-axis = entorhinal stage, L = limbic stage, N = neocortical stage; y-axis = percentage of total; HOM = homozygous, HET = heterozygous, WT = wild type).

3.3.4 Frequency of additional pathology, the ApoE ε4 allele and variant $p21^{cip1}$ in subjects wild type, heterozygous and homozygous for the $p57^{kip2}$ SNP

The ApoE genotype, $p21^{cip1}$ genotype and any additional pathology are potential confounding factors in the analysis of the effect of the $p57^{kip2}$ genotype on the risk and age of onset of AD, and the accumulation of AD-related pathology. The distribution of additional pathology and ApoE genotypes by severity of AD are described previously (Figure 12, 14 and 16). The distribution of additional pathology (Figure 64), ApoE genotypes (Figure 65), the ApoE ε4 allele (Figure 66), and variant $p21^{cip1}$ (Figure 68) were investigated by $p57^{kip2}$ genotype, irrespective of disease severity.

There was a trend (not statistically significant) for individuals that were homozygous for the $p57^{kip2}$ SNP to have less additional pathology than individuals that were wild type or heterozygous for the $p57^{kip2}$ SNP, irrespective of AD severity (Figure 64). There was no significant difference in the distribution of additional pathology in individuals that were wild type or heterozygous for the $p57^{kip2}$ SNP, irrespective of disease severity.

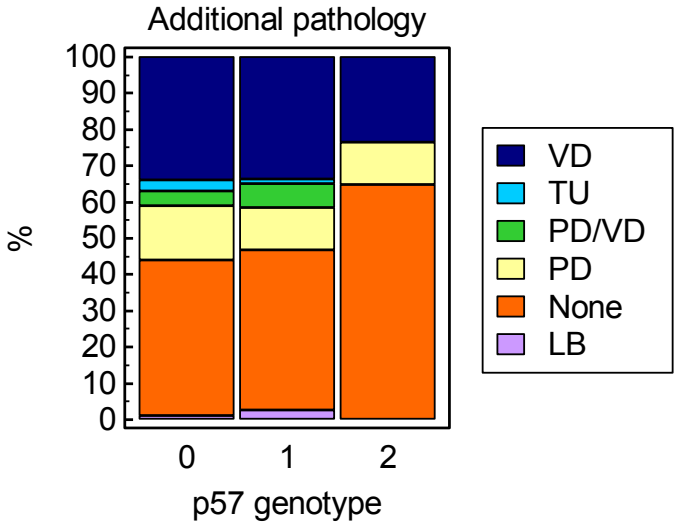

Figure 64 **Frequency of additional pathology in subjects grouped according to $p57^{kip2}$ genotype (x-axis: $p57^{kip2}$ genotype, 0 = wild type, 1 = heterozygous, 2 = homozygous; y-axis = percentage of subjects; key: VD= Vascular dementia, TU= tumours, PD= Parkinson's disease, LB= Lewy bodies, None = no additional pathology).**

There was a significant difference in the distribution of ApoE genotypes in subjects that were wild type, heterozygous and homozygous for the $p57^{kip2}$ SNP (p = 0.028) (Figure 65).

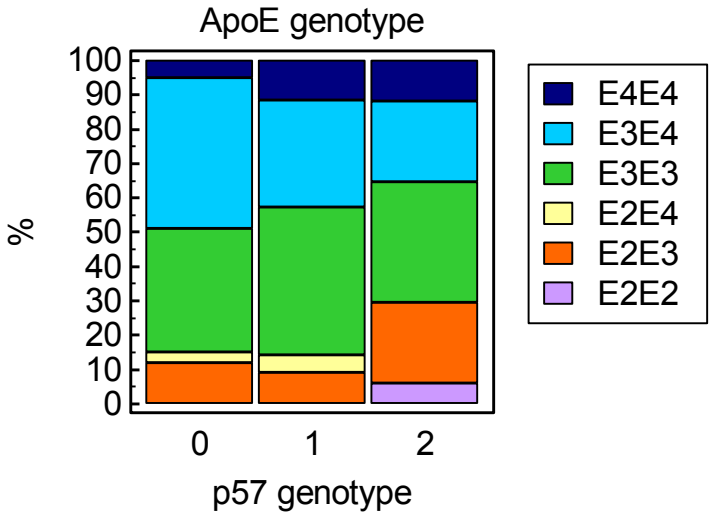

Figure 65 **Distribution of ApoE genotypes by $p57^{kip2}$ genotype (x-axis = $p57^{kip2}$ genotype, 0 = wild type, 1 = heterozygous, 2 = homozygous; y-axis = percentage of subjects; key outlined ApoE genotypes).**

However, this did not translate to a significant difference in the distribution of the ApoE ε4 allele in the different groups, irrespective of AD severity, although there was a trend for a smaller percentage of $p57^{kip2}$ homozygous subjects to be ApoE ε4 carriers than wild type or heterozygous subjects (not statistically significant) (Figure 66). . This was particularly true of subjects with advanced AD at the time of death (Figure 67), with results close to statistical significance.

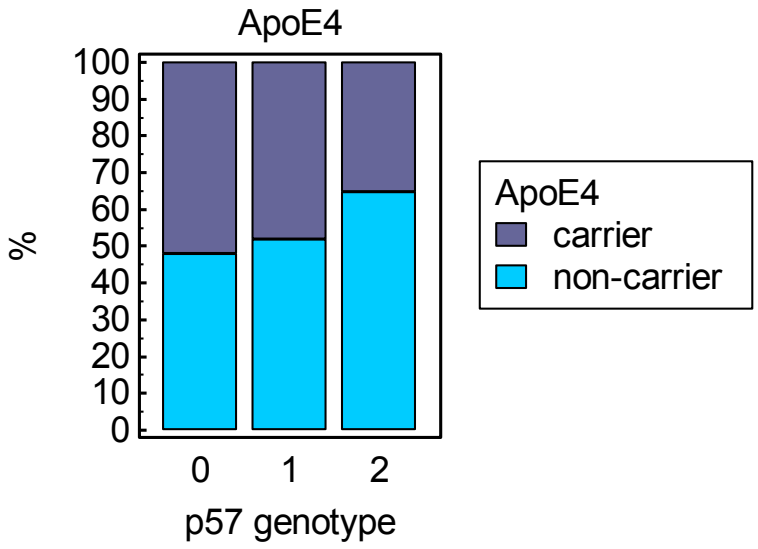

Figure 66 **Distribution of the ApoE ε4 allele by $p57^{kip2}$ genotype (x-axis = $p57^{kip2}$ genotype, 0 = wild type, 1 = heterozygous, 2 = homozygous; y-axis = percentage of subjects; key: purple = carriers of the ApoE ε4 allele, blue = non-carriers of the ApoE ε4 allele).**

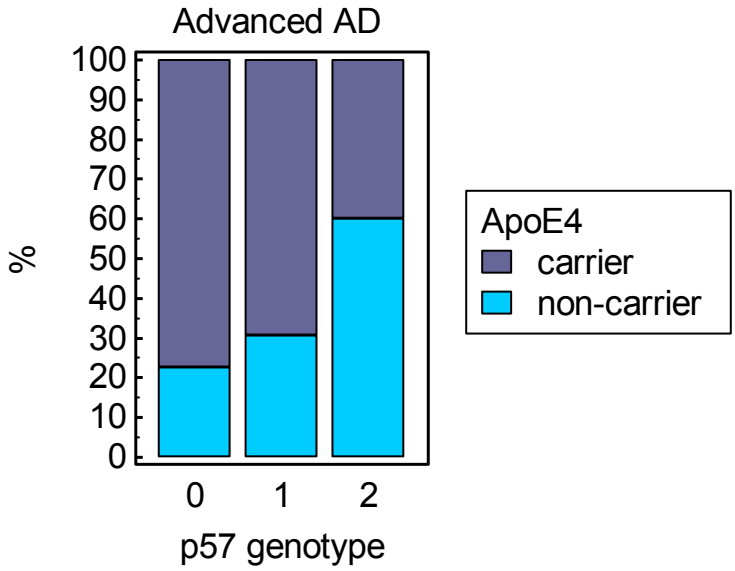

Figure 67 **Distribution of the ApoE ε4 allele by $p57^{kip2}$ genotype in subjects with advanced AD (x-axis = $p57^{kip2}$ genotype, 0 = wild type, 1 = heterozygous, 2 = homozygous; y-axis = percentage of subjects; key: purple = carriers of the ApoE ε4 allele, blue = non-carriers of the ApoE ε4 allele).**

Similarly, there was a trend (not statistically significant) for a greater percentage of subjects that were homozygous for the $p57^{kip2}$ SNP to be non-carriers of the $p21^{cip1}$ variant compared to subjects that were wild type or heterozygous for $p57^{kip2}$.

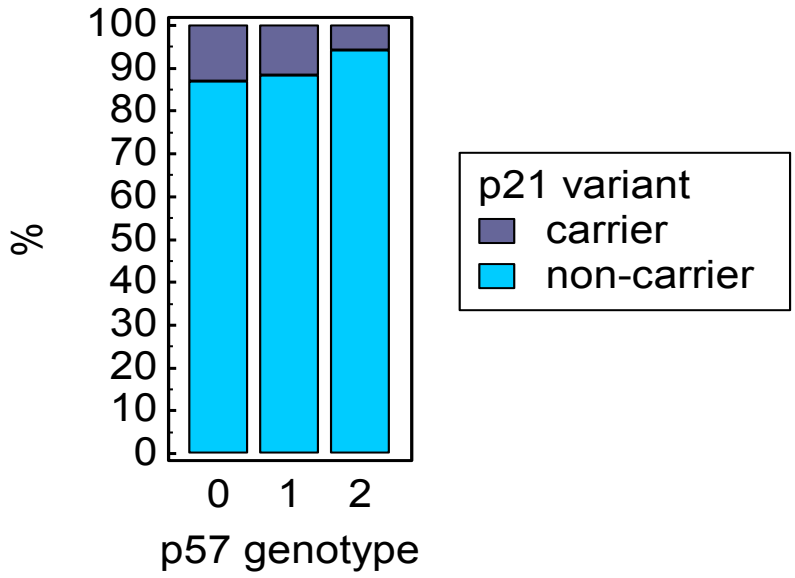

Figure 68 **Distribution of variant $p21^{cip1}$ by $p57^{kip2}$ genotype (x-axis = $p57^{kip2}$ genotype, 0 = wild type, 1 = heterozygous, 2 = homozygous; y-axis = percentage of subjects; key: purple = carriers of variant $p21^{cip1}$, blue = non-carriers of variant $p21^{cip1}$).**

3.3.5 The effect of the $p57^{kip2}$ genotype on the age at onset, age at death, the duration of AD, and the cognitive performance

In subjects with advanced AD, the age of onset of AD was independent of the $p57^{kip2}$ genotype (data not shown). However, in subjects with mild AD, there was a trend (not statistically significant) for carriers of variant $p57^{kip2}$ (heterozygous or homozygous for the p57kip2 SNP) to have an earlier age of onset than non-carriers (Table 50 and Figure 69).

Table 50 Mean age of onset of AD of mild AD sufferers that were carriers or non-carriers of the $p57^{kip2}$ SNP

$P57^{kip2}$ genotype	**Number of patients**	**Mean age of onset of AD**
Wild type for $p57^{kip2}$	19	79.7
Heterozygous or homozygous for $p57^{kip2}$ SNP	16	74.5

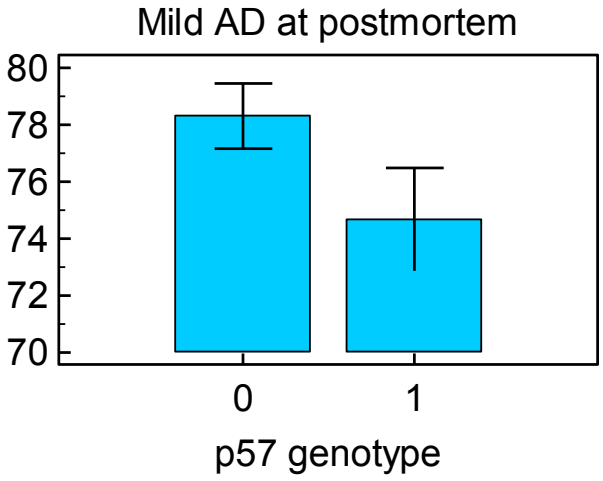

Figure 69 **Mean age of onset of AD of mild AD sufferers that were carriers or non-carriers of the $p57^{kip2}$ SNP (x-axis = $p57^{kip2}$ genotype: 0 = wild type for $p57^{kip2}$ SNP, 1 = heterozygous or homozygous for $p57^{kip2}$ SNP; y-axis = age of onset of AD; top of bars represent mean; error bars represent standard error of the mean) (one-way ANOVA).**

The $p57^{kip2}$ genotype had no effect on the mean age at death or the duration of AD, irrespective of disease severity (data not shown). Furthermore, the $p57^{kip2}$ genotype had no effect on the cognitive performance of the patients (camcog score recorded at most 6 months prior to death), irrespective of disease severity (data not shown).

3.3.6 The effect of the $p57^{kip2}$ genotype on the accumulation of AD-related pathology

To elucidate the effect of the $p57^{kip2}$ genotype on the accumulation of AD-related pathology in the frontal and occipital lobe, we first determined the effective $p57^{kip2}$ genotype in the frontal and occipital lobe, taking into account the imprinting status of $p57^{kip2}$. The effective genotype is a measure of the ratio of expression of the wild type $p57^{kip2}$ mRNA to the variant $p57^{kip2}$ mRNA, and was calculated as a value between zero and one: 0 representing 100% expression of the wild type $p57^{kip2}$; 1 representing 100% expression of the variant $p57^{kip2}$. Protein extracted from the frontal and occipital lobe was used to quantify various markers of AD-related pathology (beta-amyloid, AT8, APP-C, DC11, GAP-43, synaptophysin, and NeuN: see Table 17 for description of markers).

Multiple regression analysis was used to identify the independent variables that most accurately predict the expression of the markers of AD-related pathology in the frontal and occipital lobe. The independent variables included in the model were: effective $p57^{kip2}$ genotype; $p21^{cip1}$ genotype; ApoE genotype; and disease severity. The effective $p57^{kip2}$ genotype was not a significant predictor of the accumulation of any of the markers of AD-related pathology in the frontal or occipital lobe (data not shown).

The effect of the dose of the $p57^{kip2}$ variant allele on AD-related pathology in the frontal and occipital lobe was determined by appropriate statistical analysis (MANOVA or Kruskal Wallis depending on the distribution of the data). Note that individuals with some

expression of both the wild type and variant $p57^{kip2}$ were marked as heterozygous for the purpose of this analysis.

The $p57^{kip2}$ variant allele had no effect on the accumulation of beta-amyloid, hyperphosphorylated tau (AT8), tangles (DC11), synaptic density (synaptophysin) or synaptic remodelling activity (GAP-43) in the frontal lobe, irrespective of disease severity (data not shown). However, the $p57^{kip2}$ variant allele was significantly associated with reduced synaptic density (synaptophysin) in the frontal lobe of individuals with advanced AD ($p= 0.026$) (Figure 70). The $p57^{kip2}$ variant allele had no effect on the accumulation of tau pathology (AT8 and DC11), synaptic density (synaptophysin), synaptic regeneration activity (GAP-43) or neuronal number in the occipital lobe, irrespective of disease severity (data not shown). However, the $p57^{kip2}$ variant allele was significantly associated with increased accumulation of beta-amyloid in the occipital lobe of advanced AD patients ($p= 0.031$) (Figure 71). Furthermore, mild AD patients with the variant $p57^{kip2}$ had significantly fewer tangles relative to the amount of hyperphosphorylated tau in the frontal lobe ($p= 0.0105$) (Figure 72).

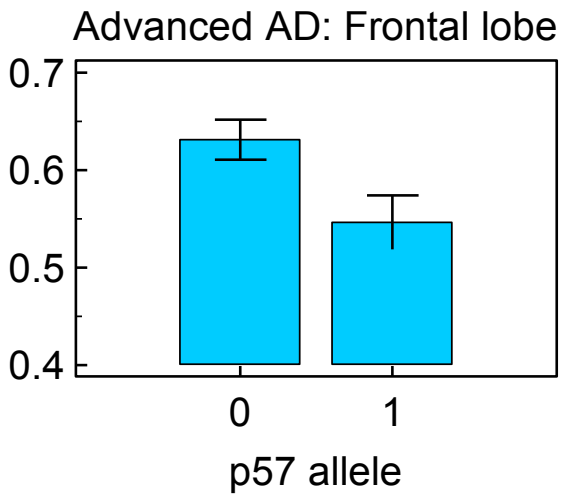

Figure 70 **The effect of the expressed version of $p57^{kip2}$ on the synaptic density of the frontal lobe of advanced AD patients (x-axis = patients grouped according to expression of the variant $p57^{kip2}$ allele: 0 = no $p57^{kip2}$ variant allele expression, 1 = some $p57^{kip2}$ variant allele expression; y-axis = synaptic density of the frontal lobe; top of bars represent mean; error bars represent standard error of the mean) (one-way ANOVA).**

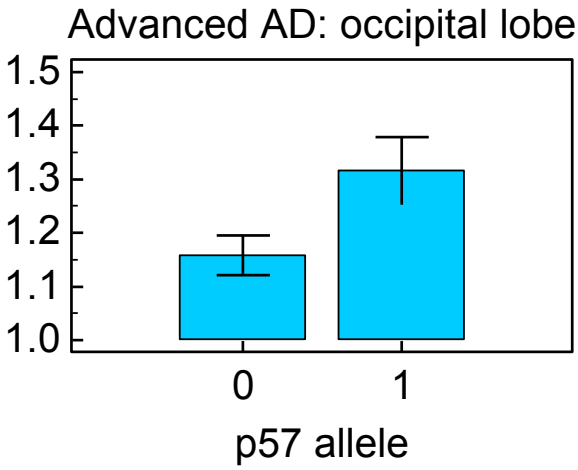

Figure 71 **The effect of the expressed version of $p57^{kip2}$ on beta-amyloid expression in the frontal lobe of advanced AD patients (x-axis = patients grouped according to expression of $p57^{kip2}$ variant allele: 0 = no $p57^{kip2}$ variant allele expression, 1 = some $p57^{kip2}$ variant allele expression; y-axis = beta-amyloid content of the frontal lobe; top of bars represent mean; error bars represent standard error of the mean) (one-way ANOVA).**

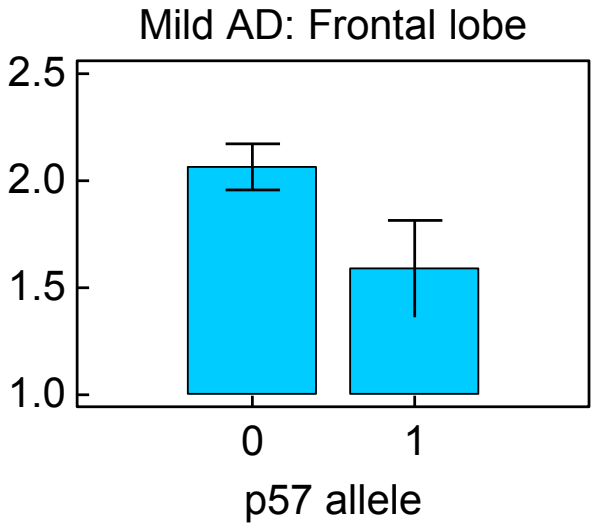

Figure 72 **The effect of the expressed version of $p57^{kip2}$ on the ratio of tau tangles to hyperphosphorylated tau in the frontal lobe of mild AD patients (x-axis = patients grouped according to expression of $p57^{kip2}$ variant allele: 0 = no $p57^{kip2}$ variant allele expression, 1 = some $p57^{kip2}$ variant allele expression; y-axis = ratio of tau tangle to hyperphosphorylated tau content of the frontal lobe; top of bars represent mean; error bars represent standard error of the mean) (one-way ANOVA).**

3.3.7 The effect of the $p57^{kip2}$ genotype on the stability and expression of $p57^{kip2}$ mRNA and protein

Q-PCR was used to measure the amount of $p57^{kip2}$ mRNA expressed in the frontal lobe of the subjects in our cohort (results normalised to beta-actin); whereas ELISA was used to measure the amount of 57^{kip2} protein expressed in the frontal lobe (results normalised to beta-actin to allow comparison).

Regression analysis showed a weak but significant positive correlation between $p57^{kip2}$ mRNA expression and $p57^{kip2}$ protein expression in the frontal lobe of subjects that expressed only wild type $p57^{kip2}$ in this region (R^2= 0.1338, p= 0.006). There was no correlation between the expression of $p57^{kip2}$ mRNA and $p57^{kip2}$ protein in the frontal lobe of subjects that expressed variant $p57^{kip2}$ to some extent (Figure 73). The result suggests that the $p57^{kip2}$ SNP alters $p57^{kip2}$ expression at the mRNA or protein level.

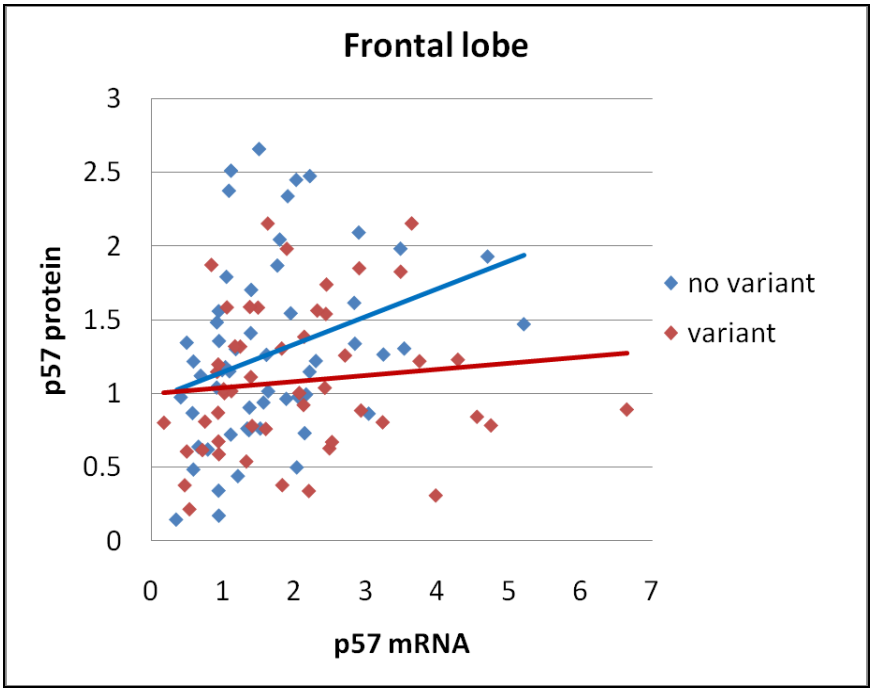

Figure 73 **Correlation between $p57^{kip2}$ mRNA and protein expression in the frontal lobe (x-axis = $p57^{kip2}$ mRNA expression in the frontal lobe; y-axis = $p57^{kip2}$ protein expression in the frontal lobe; blue represents subjects who did not express variant $p57^{kip2}$; red represents subjects who expressed variant $p57^{kip2}$).**

Multiple regression analysis was carried out to identify the independent variables that most accurately predict the frontal lobe expression of $p57^{kip2}$ at the protein level. The independent variables included in the model were: $p57^{kip2}$ mRNA content; frontal lobe effective $p57^{kip2}$ genotype; frontal lobe beta-amyloid content; frontal lobe NFT content (AT8 and DC11); and disease severity. $P57^{kip2}$ expression was most accurately predicted by the $p57^{kip2}$ mRNA content, $p57^{kip2}$ genotype and NFT content ($R^2 = 0.25$, $p < 0.001$) (Table 51). $P57^{kip2}$ protein expression in the frontal lobe positively correlated with $p57^{kip2}$ mRNA and NFT content, and negatively correlated with effective genotype. Note that for the effective genotype: 0 = 100% wild type $p57^{kip2}$ expression and 1 = 100% variant $p57^{kip2}$ expression, indicating that variant $p57^{kip2}$ was associated with reduced expression at the protein level.

Table 51 Multiple regression: Predictors of $p57^{kip2}$ protein expression

Independent variable	**Co-efficient**	**p-value**
$p57^{kip2}$ mRNA content	0.617	<0.001
$p57^{kip2}$ effective genotype	-0.224	0.004
NFT content	0.727	0.003

The effect of the $p57^{kip2}$ genotype on $p57^{kip2}$ expression in the frontal lobe, at the mRNA and protein level, was investigated in subjects in different stages of AD (MANOVA). There was a trend (not statistically significant) for an increase in the $p57^{kip2}$ mRNA content of the frontal lobe of mild and advanced AD patients that expressed only variant $p57^{kip2}$, compared to patients that expressed only wild type, or both wild type and variant, $p57^{kip2}$ (data not shown). There was also a trend (not statistically significant) for lower frontal lobe $p57^{kip2}$ protein content of subjects that expressed only variant $p57^{kip2}$, or wild type and variant $p57^{kip2}$, compared to subjects that expressed only wild type $p57^{kip2}$, irrespective of severity of

AD (data not shown). This translated to a significantly lower amount of $p57^{kip2}$ protein expressed per mRNA in the frontal lobe of subjects that expressed only variant $p57^{kip2}$ compared to subjects that expressed only wild type, or both wild type and variant, $p57^{kip2}$ (p= 0.001) (Figure 74).

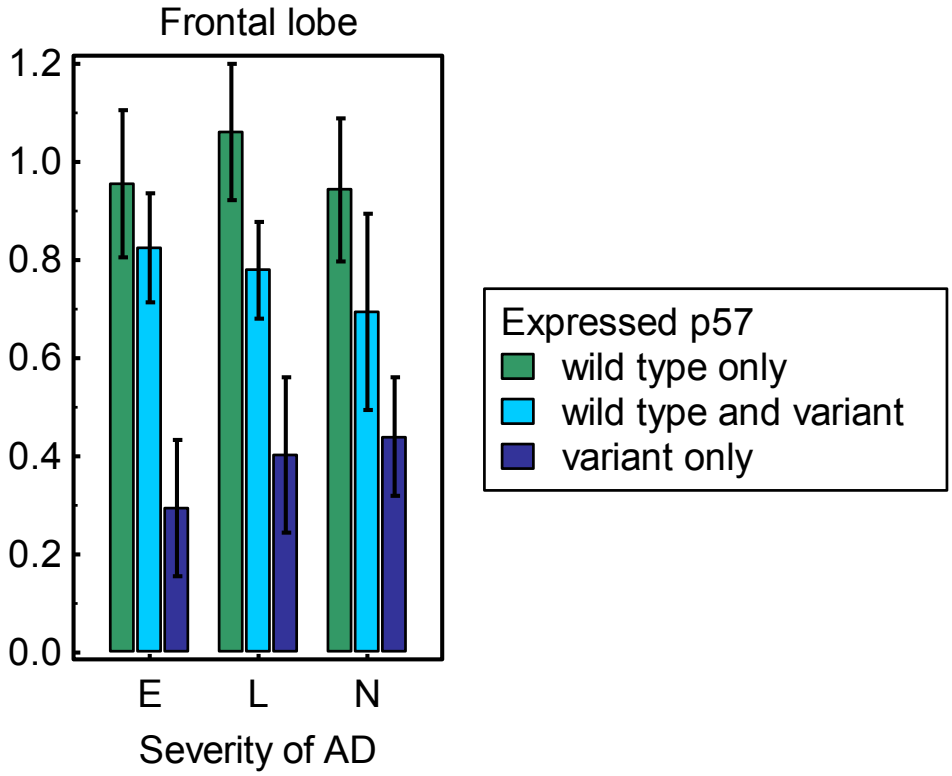

Figure 74 The effect of the severity of AD, and the expressed version of $p57^{kip2}$, on the ratio of $p57^{kip2}$ protein to mRNA in the frontal lobe (x-axis = AD severity, E = entorhinal stage, L = limbic stage, N = neocortical stage; y-axis = ratio of p57 protein to mRNA in the frontal lobe; top of bars represent mean; error bars represent standard error of the means; legend: green = subjects who expressed only wild type p57, light blue = subjects who expressed both wild type and variant p57, dark blue = subjects that expressed only variant p57).

4. DISCUSSION

4.1. ALTERED RAPAMYCIN RESPONSE ELEMENTS IN THE BRAIN OF ALZHEIMER'S DISEASE PATIENTS

Two previous studies[71, 72] have shown that lymphocytes from AD patients have a reduced response to a cell cycle inhibitor compared to lymphocytes from controls. In both studies, the cell cycle inhibitor was rapamycin: an upstream inhibitor of the cell cycle promoting mTOR pathway. The results suggest that lymphocytes from AD patients have a deficiency downstream of mTOR that leads to loss of cell cycle control. The cell cycle theory of AD postulates that neurons inappropriately re-enter and progress through the cell cycle, and that this activity is the cause of the neurodegeneration that defines AD[29, 30]. We hypothesise that the mTOR pathway components that are defective in AD lymphocytes are also responsible for the loss of cell cycle control in neurons in AD. An aim of the study was to identify the rapamycin-regulated genes that are differentially expressed in AD brain compared to control, as they may serve as novel therapeutic targets or biomarkers of AD.

The custom-made gene expression microarray was designed to include rapamycin-regulated genes, as well as other genes-of-interest (see method 2.3.2). However, only rapamycin-regulated genes were included in the analysis, so all conclusions are based on differential expression of mTOR genes in AD brain compared to control.

SAM analysis identified mTOR genes that were differentially expressed in brain affected by mild AD (limbic stage) compared to control (18 genes), and in brain affected by advanced AD (neocortical stage) compared to control (104 genes). For the purpose of the discussion, the mTOR genes altered as a result of advanced AD were taken as the overlap between the altered mTOR genes in brain affected by advanced AD from patients with the ApoE ε3/ε3 genotype and the altered mTOR genes in brain affected by advanced AD from patients with the ApoE ε3/ε4 genotype (section 3.1.3). This decision was based on the fact that the number of subjects in each group (advanced AD with ApoE ε3/ε3 genotype; advanced AD with ApoE ε3/ε4; and control with ApoE ε3/ε3) was limited. The overlap is likely to exclude false positives attributable to the low patient numbers, or to the 10% false discovery rate (FDR) that was accepted in our study (genes with less than 10% FDR were accepted as differentially expressed).

4.1.1 Altered rapamycin response elements in mild and advanced AD

Almost all of the differentially expressed mTOR genes identified early in the disease process (limbic stage) were also differentially expressed later in the disease (neocortical stage) (15 out of 18: 83%). At a simplistic level, this overlap could be expected, as genes involved early in the disease process could also be expected to be involved in advanced AD. However, the altered expression refers to a brain region (frontal lobe) that is largely unaffected by pathology in mild AD, but greatly affected in advanced AD[15]. We hypothesised that inappropriate mTOR pathway activity may be responsible for the loss of

cell cycle control in neurons in AD, so we expected altered expression of mTOR genes to be mainly an early event in the pathogenic process.

The fact that 18 of the 1172 rapamycin-regulated genes were altered in mild AD, and that 15 of these 18 genes were also differentially expressed in advanced AD, suggests that parts of the mTOR pathway are altered from an early stage, and continue to be altered as the disease progresses. mTOR pathway involvement in AD is reinforced by the large number of mTOR genes that are altered in advanced AD (104/1172: 12.5 %).

4.1.1.1. Functional clusters

The frontal lobe of both mild and advanced AD patients showed up-regulation of mTOR genes involved in transcriptional regulation, nucleic acid metabolism, post-translational modification of proteins, cell motility, tumour suppression, and inflammation. In addition, advanced AD patients showed altered expression of mTOR genes coding for various receptors, channels, growth factors and cell signalling molecules. As the number of differentially expressed genes in advanced AD was much greater than in mild AD, the number of genes in each functional category was greater for advanced AD (true for all functional categories).

A number of published studies investigate differential expression of genes in AD brain compared to control brain: albeit with differences in choice of Braak staging of patients, brain region of choice, and microarray platform[90, 91, 103-105]. In contrast to our study, the

papers discussed all used the whole human genome microarray, which identifies differentially expressed genes in the whole human genome. Avramopolous and co-workers[103] investigated altered expression in the temporal lobe of advanced AD patients compared to control. They showed up-regulation of genes involved in transcriptional regulation and nucleic acid metabolism; and down-regulation of genes involved in neuronal activities, such as synaptic transmission and ion channels. They also showed enrichment of genes involved in the inflammatory response[103]. It is long established that AD is associated with inflammation, gliosis and the loss of neurons and synapses[5], so their finding was not surprising.

Similarly, Blalock and co-workers[104] investigated differential expression in the hippocampus of a mix of mild and advanced AD patients compared to control, whereas Xu and colleagues[90, 91] investigated differential expression in the hippocampus of advanced AD patients only. Both showed up-regulated of genes involved in transcription, cell motility, cell proliferation, tumour suppression, and inflammation. Furthermore, they showed down-regulation of genes involved in energy metabolism, neuronal activities and cell signalling. Whilst the exact genes reported as differentially expressed vary from study to study, the discussed papers summarise the functional clusters that are differentially regulated in AD brain. As they all looked at brain regions that are severely affected in AD, at an advanced stage of the disease, the gene associations can be attributed to the pathological processes that define AD (for example: brain atrophy, inflammation and gliosis, and the accumulation of the hallmarks of AD)[5].

A limitation of these studies is that they do not inform on the early events in AD. One of the difficulties in interpretation of expression data lies in unravelling the causal changes from changes in response to pathology. Our analysis of a brain region that is affected later in the disease process (frontal lobe) in an early stage of the disease (limbic stage) provides vital clues to the early pathological processes involved. Our results show that the main early events that involve the mTOR pathway are up-regulation of transcriptional regulators, cell motility genes, tumour suppressors, and inflammatory genes. Our findings concerning the late events in AD are in agreement with the published literature, with the enrichment of genes in similar functional clusters. However, in contrast to the discussed studies, our expression data included only rapamycin-regulated genes. This indicates that the mTOR pathway is involved in the regulation of many of the physiological and cellular processes that are altered in AD.

The inclusion of only rapamycin-regulated genes in our analysis allowed a focused search of a pathway that is affected early in AD. On the downside, it will have lead to a concentration of genes in certain functional categories, and exclusion of others.

4.1.1.2. Pathways and networks

The only pathways significantly altered in mild AD (limbic stage) were part of the inflammatory response; whereas several pathways were additionally affected in advanced AD (neocortical stage). These included the corticotrophin releasing hormone (CRH) pathway, insulin-receptor pathway and transforming growth factor-beta (TGF-beta) pathway.

Reduced activity of the neuroprotective CRH signalling pathway[106, 107], and alterations in the insulin receptor signalling pathway[108], are known phenomena in AD. The association of AD with neuro-inflammation is also long established[109, 110], with our results indicating that inflammatory mediators are involved both early and late in the AD process. The TGF-beta signalling pathway is involved in regulating cell cycle activity and apoptosis, and can both promote and inhibit cell cycle activity in the brain depending on context[111]. Various studies have shown that TGF-beta signalling is reduced in neurons in AD[111-113], although the downstream consequences are not fully understood.

We have identified known genes of the mTOR signalling pathway that are differentially expressed in AD brain relative to control brain. We can therefore conclude that parts of the mTOR signalling pathway are differentially regulated in AD brain. This supports the hypothesis that defective components of the mTOR pathway may be responsible for the loss of cell cycle control in neurons in AD. Our study has identified both established and unknown genes of the mTOR pathway for further investigation: with a large number of these genes identified as possible therapeutic targets or biomarkers of AD (see appendix 7 and 10). Furthermore, brain from both mild and advanced AD patients showed enrichment of genes involved in cellular development, cellular growth and proliferation, and cellular movement, suggesting that alterations in cell cycle control are involved early and throughout the disease process.

4.1.2 Altered rapamycin response elements in advanced AD as a result of the ApoE ε4 allele

64 rapamycin-regulated genes were differentially expressed in the brain of advanced AD patients with the ApoE ε3/ε4 genotype but not differentially expressed in advanced AD patients with the ApoE ε3/ε3 genotype. They are presumably differentially expressed as a result of the ApoE ε4 allele only. As there were relatively few patients in each group, some of the altered genes may be false positives as a result of non-AD related patient-to-patient differences. However, the number of false positives in the analysis should be minimal as the FDR cut-off point was set at 10%.

4.1.2.1. Functional clusters

The mTOR-related genes altered in response to the ApoE ε4 allele included genes involved in apoptosis, energy metabolism (mitochondrial activity), fatty acid metabolism, synaptic activity, cell motility (e.g. adhesion, cytoskeleton structure, axonal guidance), transcriptional regulation, and cell signalling (receptors, channels and signalling molecules). The genes were significantly enriched for involvement in cell death, cellular development, cellular growth and proliferation, drug metabolism and lipid metabolism. The results should be interpreted in light of inclusion of only rapamycin-regulated genes. The ApoE ε4 allele may alter the expression of genes that were not included in the analysis, which may have prevented enrichment of genes in relevant functional clusters.

Xu and co-workers[90] carried out a similar study, investigating genes that were differentially expressed in brain of AD patients with ApoE ε4/ε4 genotype relative to control (ApoEε3/ε3 genotype) but not in brain of AD patients with ApoEε3/ε3 genotype relative to control (ApoE ε3/ε3 genotype)[90, 91]. In contrast to our study, they analysed the expression of all genes in the human genome. In agreement with our result, they demonstrate that the ApoE ε4/ε4 genotype is associated with cell cycle arrest and apoptosis; and alterations in cell signalling, mitochondrial activity, cell motility, and synaptic activity. Additionally, they showed up-regulation of genes involved in cell protection and detoxification, and genes involved in myelinogenesis.

It is well established that the ApoE ε4 allele is associated with increased risk of AD[114] and an earlier age of onset[22, 115]; although the reasons for this remain unclear[22, 116]. One of the functions of ApoE is involvement in lipid metabolism and transport in the body[116], so it was not surprising that the ApoE ε4 allele was associated with changes in lipid metabolism in AD. ApoE has also been implicated in synaptic plasticity and dendritic spine formation[117, 118]; with Tannenberg and colleagues[119] demonstrating that the ApoE ε4 allele is associated with faster rate of synaptic loss in AD. Studies have also shown that the ApoE ε4 allele is associated with defective mitochondrial metabolism[116, 120]. Our findings indicate that the ApoE ε4 allele alters mTOR pathways that affect lipid metabolism, mitochondrial activity, cell motility and synaptic plasticity. Furthermore, it demonstrates that ApoE ε4 affects numerous signalling pathways involved in regulating cell death, cell growth and cell proliferation. The results suggest that ApoE ε4 interacts with alterations in the mTOR

pathway to contribute to a more severe outcome in terms of pathology. This interaction could account for its association with greater risk and earlier age of onset of AD.

4.1.3 Validation

To validate our results, the mTOR-related genes that were differentially expressed in AD were compared to known AD associated genes, identified on the IPA Ingenuity database. The comparison showed that approximately 12% of the rapamycin-regulated genes that were differentially regulated in AD were already known to be associated with AD. Our analysis included only rapamycin-regulated genes, whereas the 954 genes identified by IPA included all genes that are established to have an association with AD. This difference in inclusion criteria accounts for the discordance in number of genes in each list. As the IPA Ingenuity database includes only verified gene/disease associations, based on publications in high quality peer-reviewed journals, the list does not include all genes that have altered expression in AD brain. Furthermore, our study was limited to mTOR-regulated genes, so did not include a large number of the genes that are known to be associated with AD. Whilst 12% overlap does not seem like a lot for validation, this must be interpreted in light of the different inclusion criteria of the two gene lists.

Our microarray results were experimentally validated by comparing the direction of altered expression of 6 genes in advanced AD brain relative to control as determined by microarray to that as determined by real time PCR (Q-PCR). Both the microarray and Q-PCR results showed down-regulation of EIF4E, MAPK1, GABBR2, and DZIP3, and up-regulation of

SEMA4C and SERPINE1 in advanced AD relative to control. The altered expression was statistically significant for all the selected genes as determined by microarray. However, despite the Q-PCR direction of expression matching that of the microarray for all genes tested, the results failed to reach statistical significance in Q-PCR. This may have been due to platform differences. The microarray results were normalised to a large number of housekeeping genes and internal controls as suggested by Agilent; whereas the Q-PCR results were only normalised to the beta-actin content of the samples. Poor choice of normalising gene for the Q-PCR may also have contributed. The literature indicates that beta-actin is down-regulated in AD brain compared to control: so it not a reliable normalising gene for diseased brain[121]. The literature indicates that the gene coding for 60S ribosomal protein L13 (RPL13) and ribosomal RNA (18S)[122] are stability expressed in brain, irrespective of disease, and so would have been more appropriate choices for normalising gene.

4.1.4 Conclusions and limitations

This study identified genes that are differentially expressed in the frontal lobe of AD patients compared to control, and are involved in pathways that may play a causal role in the pathogenesis of AD. A major drawback of microarray analysis is that it does not differentiate between the primary causal alterations and secondary alterations in response to pathology. The use of a custom-made microarray allowed a more focused search, of a pathway-of-interest, which would not have been possible with a whole human genome microarray. However, it may have excluded relevant genes. It is also important to note that

the differential expression applies to the frontal lobe: a region that contains many different cell types (predominately neurons and glial cells). Therefore, no conclusions can be drawn on expression changes in neurons alone, unless gene expression is neuron-specific.

In order to investigate altered expression of mTOR genes in neurons only, laser capture microdissection could be used: a technique that allows isolation of cells-of-interest from other cell types[105]. Another possible confounding factor was inclusion of mTOR-related genes that were polymorphic or had several splice variants on the custom-microarray. The differential expression of some of the genes may be attributable to polymorphisms or alternative splice variants that are associated with AD. It would be of interest to investigate whether published genome wide association studies have identified any of the differentially regulated mTOR genes as associated with AD.

We would expect a small proportion of the differentially expressed genes in our study to be false positives. Each group-of-interest had relatively few subjects (see 2.3.2.4), so a small proportion of the identified genes may have been differentially expressed based on non-AD related patient-to-patient differences. Furthermore, the FDR cut-off point: the estimate of the percentage of genes that are incorrectly identified as differentially expressed in an analysis, was set at 10%. However, the vast majority of the differentially expressed genes were assigned an FDR well below this value (many were around the 0% mark), keeping false positives to a minimum. Overall, the inclusion of some false positives should not have impacted significantly on the conclusions as a large number of mTOR-regulated genes were shown to be involved both early and late in the AD process.

Another possible limitation was partial degradation of the human brain RNA (RIN value ~ 2.5) secondary to unavoidable post-mortem time prior to freezing. This may have lead to loss of true-positives or inclusion of false-positives. However, RNA is thought to degrade at a steady rate, predominately in a 5' to 3' direction, with the Agilent microarrays designed to bind the 3'end where possible[86]; implying that the output is unlikely to be skewed by degradation. Notably, Lee and colleagues demonstrate that good quality expression outputs can be obtained from highly degraded RNA, with minimum loss of true positives[123].

To conclude, this study demonstrates that components of the mTOR pathway are differentially regulated in AD brain compared to control. Whilst this supports the hypothesis that defective components of the mTOR pathway may be responsible for loss of cell cycle control in AD neurons: expression data does not allow conclusions on causation. However, the early involvement of the mTOR-regulated genes in a brain region that is not yet affected by AD pathology (frontal lobe in early AD) may suggest that the inappropriate regulation of this pathway precedes pathology, and may actually be a causal factor. The identified rapamycin-regulated genes that are differentially expressed in AD brain may serve as novel therapeutic targets for AD or biomarkers of disease for further investigation.

4.2. THE EFFECT OF THE P21^{CIP1} GENOTYPE ON P21^{CIP1} EXPRESSION AND FUNCTION, AND ASSOCIATION WITH AD

The CDK inhibitor: p21^{cip1} is capable of inducing cell cycle arrest at the G1/S and G2/M checkpoints[31]. It is up-regulated on a transcriptional level in response to p53 (a DNA-damage induced transcription factor), and inhibits CDK2/cyclin A and CDK2/ cyclin E, thereby acting as a G1/S checkpoint inhibitor. In addition, a number of studies indicate that p21^{cip1}, expressed independently of p53, induces cell cycle arrest at the G2/M checkpoint[124-127]. Furthermore, p21^{cip1} has a number of additional cellular functions (reviewed in[31]). It inhibits proliferating cell nuclear antigen (PCNA), a protein required for DNA replication[128]. It also has an anti-apoptotic role: inhibiting the activity of stress activated protein kinases (SAPKs), which are involved in stress signalling and the promotion of apoptosis[129]. The location of p21^{cip1} within the cell may dictate its function: with a nuclear location required for its cell cycle regulatory role, and a cytoplasmic location required for its anti-apoptotic role[130, 131].

With its cell cycle regulatory role in mind, it is possible that polymorphisms that reduce the function or expression of p21^{cip1}, may contribute to the loss of cell cycle control and inappropriate progression beyond G1 phase, which is postulated to be a cause of neurodegeneration in AD[29, 30]. Notably, a previous study[74] found that a genetic variant of p21^{cip1}, that is known to be associated with cancer[76, 77], is also associated with an increased risk and earlier age of onset of AD. Furthermore, four genetic linkage studies have identified genetic variants of the locus on which the p21^{cip1} gene is located, as associated

with an increased risk of AD[80, 82, 83, 101]. The $p21^{cip1}$ variant has a cytosine to adenine change that induces an amino acid substitution on codon 31 of the protein that will be referred to as SNP A; and a cytosine to thymine change on the 3-prime untranslated region that will be referred to as SNP B.

An aim of the study was to elucidate the effect of the $p21^{cip1}$ SNPs on the expression and function of the $p21^{cip1}$ protein; and the association of the SNPs with AD. The literature suggests that SNPs A and B are only associated with cancer and AD when found together[74, 76, 77]. Therefore, for the purpose of this study, subjects that are heterozygous or homozygous for SNP A and B are referred to as having the variant $p21^{cipl}$; whereas individuals that are wild type for SNP A and B, or have only one of the SNPs, are referred to as having wild type $p21^{cip1}$. The cohort discussed consists of 209 subjects with a range of severities of AD (preclinical, mild and severe AD at the time of death).

4.2.1 Frequency of the $p21^{cip1}$ variant

Overall, we found that 12% of the cohort (patients with preclinical, mild and severe AD at the time of death) had the $p21^{cip1}$ variant. This is slightly above the 10% frequency found by Nagy[74] in an AD cohort of similar size; and the 10.7% frequency found by Mousses and co-workers[77] in a healthy population. The frequency of variant $p21^{cip1}$ is highest in advanced AD (neocortical stage) patients at 15.7%, but is also greater in patients with mild AD (10.7%) compared to subjects with few symptoms of AD at the time of death (entorhinal stage) (9.3%). Despite the trend suggesting that the $p21^{cip1}$ variant occurs more frequently in

individuals with advanced AD compared to control (odds ratio = 1.82), results failed to reach statistical significance. The $p21^{cip1}$ variant is relatively rare in the population, which lead to a small number of subjects with the $p21^{cip1}$ variant in the subgroups defined by severity of AD. This may have contributed to the lack of statistically significant results. The increased frequency of the $p21^{cip1}$ variant in patients with advanced and mild AD relative to control, suggests that the $p21^{cip1}$ variant is associated with increased AD risk. Nagy[74] found a similar association, despite reporting a lower frequency of variant $p21^{cip1}$ in both the AD and control group (10% and 6% frequency of variant $p21^{cip1}$ in the AD and control group respectively[74]).

The distribution of the variant $p21^{cip1}$ in the population followed the Hardy-Weinberg equilibrium. The Hardy-Weinberg equilibrium models the distribution of alleles in a population based on the assumption that the alleles are passed on randomly from generation to generation undisturbed by evolutionary forces (for example, natural selection)[102]. This implies that the $p21^{cip1}$ SNPs are not subject to negative selection.

4.2.2 Distribution of additional pathology and the ApoE ε4 allele

The cohort included some individuals with additional pathology: limited to Parkinson's disease, vascular disease, Lewy bodies and tumours. The removal of these cases from the analysis was not possible as doing so would have reduced the number of $p21^{cip1}$ variant cases in each subgroup defined by disease severity, to an extent where meaningful statistical analysis would not be possible. We found that a significantly greater percentage of the individuals in the preclinical stages of AD had additional pathology compared to individuals

in later stages of AD ($p<0.001$). This may alter the effect of the severity of AD on the outcomes analysed in our study. However, there was no significant difference in the distribution of additional pathologies in the $p21^{cip1}$ variant group compared to $p21^{cip1}$ wild type group, irrespective of disease severity.

Similarly, and for the same reason, it was not possible to remove ApoE ε4 carriers from the analysis, despite the association of the ApoE ε4 allele with increased risk and earlier age of onset of AD[25]. As expected, we found that the ApoE ε4 allele was more common in patients with advanced AD compared to individuals in earlier stages of the disease ($p<0.001$). However, there was no significant difference in the distribution of ApoE genotypes, or in the frequency of ApoE ε4 carriers, in the $p21^{cip1}$ variant group compared to $p21^{cip1}$ wild type group, irrespective of disease severity. Overall, this implies that neither additional pathologies, nor the ApoE genotype, are likely to influence the outcome of our analysis concerning the effect of the $p21^{cip1}$ genotype.

4.2.3 The effect of the $p21^{cip1}$ genotype on the age of onset and age at death

We found that patients with mild AD (limbic stage) had a significantly greater age of onset (77 years) than patients with advanced AD (neocortical stage) (69 years) ($p<0.001$). Furthermore, patients with advanced AD on average had a disease duration that was significantly longer (7.7 years) than that of patients with mild AD (6 years) ($p=0.012$). This was in agreement with the expectation: AD is a disease of long duration that occurs in the elderly, so patients that die early in the disease process (in the entorhinal or limbic stage)

would be expected to develop AD at a more advanced age, and die of conditions unrelated to AD. Individuals with entorhinal stage AD were in a pre-clinical stage at the time of death, and so did not have an age of onset.

The mean age of death of patients with advanced AD (age 77) was significantly lower ($p<0.001$) than the mean age of death of patients with mild AD (age 84). Whilst AD sufferers can expect a relatively normal lifespan, advanced AD may increase the risk of certain life threatening conditions[132, 133] that contribute to the earlier age of death of patients in this group. Interestingly, the mean age of death of patients in a preclinical stage of AD (age 80) was significantly lower than the mean age of death of patients with mild AD (84) ($p<0.001$). This may be explained by the higher prevalence of additional pathologies (discussed in section 4.2.2) in preclinical subjects compared to mild AD patients, which may have contributed to the earlier age at death of these patients. We were unable to remove cases with common additional pathologies from the analysis, as doing so would have reduced the number of cases to an extent where meaningful statistical analysis would not be possible.

In agreement with the results of a previous dataset[74], we demonstrate that the $p21^{cip1}$ variant is associated with an earlier age of onset of AD in patients with advanced AD at the time of death ($p= 0.016$). This suggests that the $p21^{cip1}$ variant may contribute to AD pathogenesis. The association was not apparent in patients with mild AD. Furthermore, the $p21^{cip1}$ genotype had no effect on the age at death or disease duration, irrespective of disease severity.

4.2.4 The effect of the severity of AD on AD-related pathology

ELISA was used to measure markers of neuronal number (NeuN), synaptic density (synaptophysin), synaptic regeneration potential (growth associated protein-43: GAP-43), beta-amyloid accumulation (beta-amyloid and APP-C) and NFT accumulation (AT8 and DC11) in the temporal, frontal and occipital lobes of 193 patients in different stages of AD (refer to Table 17 for more detailed description of markers). The accumulation of AD-related brain pathology is dependent on the severity of AD and brain region examined, and is well documented in the literature[5]. To ensure that our cohort was representative of the AD population, the effect of severity of AD on the accumulation of the selected markers in the temporal, frontal and occipital lobe was analysed, and is described below.

We found that subjects with advanced AD had significantly greater deposition of phospho-tau and tangle pathology in the temporal, frontal and occipital lobes than subjects in earlier stages of AD ($p<0.001$ for all brain regions). In addition, the rate of spread of phospho-tau from the temporal lobe to the frontal and occipital lobes was significantly greater in patients with advanced AD patients compared to control ($p<0.001$). Tau pathology was measured with the AT8 antibody that specifically detects a pathologically hyperphosphorylated version of tau, both prior to incorporation into tangles and within tangles[93]; and with the DC11 antibody that specifically detects AD tangles[94]. The spread of NFT pathology in the brain is known to correlate well with disease severity, and is the basis of the Braak staging system that was used to define severity of AD[15]. Subjects with NFT deposition in the entorhinal cortex are classed as pre-clinical (entorhinal stage); subjects with deposition in the entorhinal and limbic regions are classed as mild (limbic stage); whereas subjects with additional

widespread deposition throughout the neocortex are classed as advanced (neocortical stage). The association of severity of AD with NFT accumulation was consistent with the expectation for all three brain regions examined ($p<0.001$). Notably, we also found that the severity of AD correlated well with cognitive decline ($p< 0.001$)[12, 13].

Secondly, and consistent with the literature[5], we found that the accumulation of beta-amyloid in the temporal and frontal lobes significantly increased as AD progressed from an early to advanced stage, whereas beta-amyloid accumulation in the occipital lobe did not alter in different stages of AD. The occipital lobe is relatively spared of pathology even in advanced stages[15, 134], so this finding was expected. Neither the expression of the precursor of beta-amyloid (APP) nor the ratio of beta-amyloid to precursor APP was altered in the temporal, frontal or occipital lobes, irrespective of disease severity.

Despite extensive brain atrophy in AD[135, 136], and AD association with loss of neurons[137, 138] and synapses[139-142], we only found a trend for decrease in the number of neurons (NeuN) and synapses (synaptophysin) in the temporal, frontal and occipital lobes as AD progressed from an early to advanced stage. It is possible that the outcome was skewed by the uneven distribution of additional pathologies by severity of AD. A significantly greater percentage of preclinical subjects had additional pathology than subjects with advanced AD (see section 4.2.2). It is possible that the additional pathologies negatively influenced neuronal number and synaptic density (for example, Parkinson's disease), hence reducing the effect of disease severity on these outcomes.

The synaptic remodelling activity of neurons was investigated by measuring a neuron-specific protein that is expressed on axonal growth cones during synaptic remodelling (GAP-43). We found that the synaptic remodelling activity of neurons is significantly reduced in the occipital lobe of advanced AD patients compared to patients in earlier stages of AD ($p<0.001$). The synaptic remodelling activity of neurons in the frontal and temporal lobe did not alter in different stages of AD. There is typically a strong correlation between synaptic density and cognitive decline[5, 143], so we would have expected the synaptic remodelling activity of neurons to decrease in the brain regions primarily involved in cognition (for example, the temporal and frontal lobe). However, overall, the effect of disease severity on the accumulation of the various markers of AD-related pathology was consistent with that of published datasets; indicating that our cohort is representative of the overall AD population.

4.2.5 The effect of the $p21^{cip1}$ genotype on AD-related pathology

In order to elucidate the effect of the $p21^{cip1}$ genotype on the accumulation of AD-related pathology, data from each brain region was analysed separately in subgroups defined by disease severity. We found that AD patients with the $p21^{cip1}$ variant had significantly greater accumulation of phospho-tau and tangle pathology in the frontal and occipital lobe compared to individuals that were wild type for $p21^{cip1}$ (irrespective of disease severity) ($p < 0.05$ for all). The $p21^{cip1}$ genotype had no effect on the accumulation of tau pathology in the temporal lobe. Furthermore, we found a trend for greater rate of spread of phospho-tau and tangle pathology from the temporal lobe to the frontal and occipital lobes in patients with the $p21^{cip1}$ variant compared to patients that were wild type for $p21^{cip1}$: with results reaching

statistical significance for phospho-tau spread from the temporal lobe to the frontal lobe in patient with mild AD only ($p = 0.046$), and statistical significance for tangle pathology spread from the temporal lobe to the frontal and occipital lobes in patients with mild AD only ($p < 0.05$).

The association of the $p21^{cip1}$ variant with tangle pathology was most apparent in the early stages of the disease (e.g. limbic stage), and in parts of the brain that are affected later in the disease process (e.g. frontal and occipital lobes). When interpreted in light of the cell cycle theory of AD, this is compatible with our hypothesis. $p21^{cip1}$ is one of the G1/S checkpoint inhibitors that inhibits the cyclin/CDK complexes that are required for progression from G1 to S phase. We hypothesised that the $p21^{cip1}$ SNPs may reduce the ability of the $p21^{cip1}$ protein to inhibit cyclin/CDK2, or may reduce its expression, based on the finding that the $p21^{cip1}$ variant is associated with cancer[76, 77]. In effect, we hypothesised that the G1/S checkpoint is less tightly regulated in individuals with the $p21^{cip1}$ variant compared to individuals with wild type $p21^{cip1}$. We further hypothesised that the $p21^{cip1}$ variant may contribute to the loss of cell cycle control that is postulated to be a cause of neurodegeneration in AD[30].

There is considerable evidence to indicate that neurons in AD re-enter the cell cycle and inappropriately progress beyond the G1/S checkpoint[44, 45, 47, 48, 50, 52, 53]. However, the reasons for the loss of cell cycle control in neurons are not understood. Studies indicate that the heritability of late-onset AD is in the range 60-80%[2, 3], suggesting that there is a strong genetic component to the disease, despite few genes established to be associated. This suggests that the reasons for the loss of cell cycle control are complex, and may differ

considerably from individual to individual. Our results suggest that the $p21^{cip1}$ variant may contribute to the loss of cell cycle control, which is postulated to be a cause of neurodegeneration in AD[30], in some individuals who develop AD.

The cell cycle theory[29, 30] goes a long way to explain the accumulation of tau pathology in AD. During a normal cell cycle, the microtubule structure of the cell is extensively re-organised to allow DNA replication and ultimately cell division[10]. Tau is a microtubule associated protein involved in the re-organisation of the microtubule structure, and is itself regulated by phosphorylation[10]. Under normal circumstances, the cell cycle is driven by the activity of various kinases[31]. The failure to prevent progression at the G1/S checkpoint, which is postulated to occur in neurons in AD, may result in inappropriate kinase activity: potentially resulting in the hyperphosphorylation of tau that drives formation of insoluble NFT[10].

The fact that the association of the $p21^{cip1}$ variant with tau pathology was most apparent early in the disease process, and in brain regions that are relatively unaffected by AD, suggests that the $p21^{cip1}$ gene is involved early in the disease process. The $p21^{cip1}$ genotype did not alter the accumulation of tau pathology in the severely affected temporal lobe. It is plausible that other factors may mask the effect of the $p21^{cip1}$ variant when a lot of pathology has already accumulated. For example, the hallmarks of AD (tau and beta-amyloid) are themselves neurotoxic[21], and accumulate primarily in the temporal lobe from an early stage, potentially masking the effect of the $p21^{cip1}$ variant in this region.

The $p21^{cip1}$ genotype had no significant effect on the accumulation of beta-amyloid, or ratio of beta-amyloid to APP-C, irrespective of brain region or severity of AD. Furthermore, the $p21^{cip1}$ genotype had no significant effect on the neuronal number, synaptic density or synaptic remodelling activity of neurons in the temporal, frontal or occipital lobe, irrespective of disease severity. However, there was a trend (not statistically significant) for greater beta-amyloid accumulation in the occipital lobe of subjects with the $p21^{cip1}$ variant in a preclinical or mild stage of AD. APP levels were also significantly raised in the frontal lobe of mild AD patients with the $p21^{cip1}$ variant ($p= 0.028$) compared to control. Furthermore, there was a trend (not statistically significant) for reduced remodelling activity of neurons in the occipital lobe of advanced AD patients with the $p21^{cip1}$ variant compared to control. The fact that the association of AD with reduced synaptic density and neuronal number was non-significant in our analysis, despite a strong established association[137-139], suggests that the ELISA was not sensitive enough to pick up substantial changes in some cases.

To summarise, the association of a genetic variant of $p21^{cip1}$ (a G1/S checkpoint inhibitor) with increased accumulation of tau pathology is compatible with the cell cycle theory of AD, and suggests that the SNPs reduce the efficiency of the G1/S checkpoint. Whilst the $p21^{cip1}$ SNPs did not appear to alter the expression of the other markers of AD-related pathology, all trends that failed to reach statistical significance were in a direction to suggest variant $p21^{cip1}$ association with more severe disease.

4.2.6 The effect of the $p21^{cip1}$ genotype on $p21^{cip1}$ expression

We show that $p21^{cip1}$ expression in the temporal and frontal lobe (regions affected by AD) significantly increases as AD progresses from an early to more advanced stage. The occipital lobe, which is relatively unaffected by AD, did not show altered $p21^{cip1}$ expression. Similarly, Engidawork and co-workers[131] found a significant increase in $p21^{cip1}$ expression in the frontal lobe of AD patients, but no alteration in its expression in the cerebellum (a region largely unaffected by AD). They speculate that $p21^{cip1}$ may be up-regulated for its anti-apoptotic role in AD. However, the multi-faceted role of $p21^{cip1}$ within the cell, the lack of information regarding its cellular location, and the fact that protein was extracted from a brain region containing different cell types, prevents conclusions on the consequences or reasons for up-regulation.

Whilst it is evident that $p21^{cip1}$ levels are raised in brain regions affected by AD, it is possible that this is an artefact of inappropriate accumulation of $p21^{cip1}$, and not an active up-regulation. This is supported by the finding that $p21^{cip1}$ mRNA levels in the frontal lobe remain stable in different stages of AD. Interestingly, multiple regression analysis showed that the accumulation of $p21^{cip1}$ protein is most strongly dependent on the accumulation of tangle pathology in the brain, and not on the severity of AD itself. It is possible that $p21^{cip1}$ non-specifically binds to tangles within the cells[10], accumulating inappropriately; or that the mechanisms required for $p21^{cip1}$ protein degradation are faulty in diseased neurons[84].

We demonstrate that the $p21^{cip1}$ variant has no effect on $p21^{cip1}$ expression at the protein level in the temporal, frontal or occipital lobe, irrespective of disease severity. This may

suggest that the detrimental effects of variant $p21^{cip1}$ are not attributable to altered expression. However, we also demonstrate that advanced AD patients with the $p21^{cip1}$ variant have significantly less $p21^{cip1}$ mRNA in the frontal lobe than patients with wild type $p21^{cip1}$. As discussed above, the raised levels of $p21^{cip1}$ protein in AD may be a consequence of inappropriate accumulation as opposed to up-regulation. If this is the case, a proportion of the $p21^{cip1}$ protein in AD brain may be inappropriately located or non-functioning. Our Q-PCR results may indicate that the $p21^{cip1}$ SNPs reduce the stability of $p21^{cip1}$ mRNA, potentially altering the expression of $p21^{cip1}$ at the protein level.

We have also shown that half of the individuals that are heterozygous for SNP A and B on $p21^{cip1}$ express equal amounts of the wild type and variant $p21^{cip1}$ mRNA; whereas approximately the other half express significantly more variant $p21^{cip1}$ mRNA than wild type mRNA (although both are expressed to some extent). As the $p21^{cip1}$ gene is not imprinted, this was unexpected. It suggests that the $p21^{cip1}$ SNPs alter the stability of $p21^{cip1}$ mRNA. The reason for the differential expression in only half of the subjects is unclear, and does not relate to AD, irrespective of disease severity. Initially, we thought that the two SNPs may alter the stability of the $p21^{cip1}$ mRNA only when they are located *in cis* (on the same strand). However, the two $p21^{cip1}$ SNPs tend to be inherited together[76, 77], suggesting that the SNPs are located *in cis* in the majority of cases. This could be investigated further by sequencing.

4.2.7 The effect of the p21^{cip1} genotype on the function and expression of the protein in vitro

The fact that the p21^{cip1} variant is associated with cancer[76, 77], suggests that the p21^{cip1} variant is either a less effective G1/S checkpoint inhibitor than the wild type version, or that the SNPs alter p21^{cip1} expression. We have also found that the p21^{cip1} variant is associated with increased risk of AD, earlier age of onset, and increased accumulation of tau pathology[74].

The literature indicates that SNP A and B on p21^{cip1} are only associated with cancer and AD when found together[74, 76, 77]: the reasons for this are unclear. SNP A triggers an amino acid change in the CDK2 binding region of p21^{cip1}[74], potentially altering the ability of p21^{cip1} to inhibit cyclin/CDK2. It is also possible that SNP A alters the stability or rate of degradation of the p21^{cip1} protein, as the amino acid substitution alters the tertiary structure of the protein: potentially altering its interaction with the proteins that regulate its stability and degradation[84]. The functional consequences of SNP B are less clear, although we hypothesise that it alters the stability of the p21^{cip1} mRNA. SNP B is located on the 3'-untranslated region (UTR) of p21^{cip1}, which is involved in regulating the stability of the p21^{cip1} mRNA by its interaction with various non-coding RNAs and proteins[84].

In order to elucidate the effect of the p21^{cip1} SNPs on the function and expression of the protein in vitro, the rapidly dividing Flp-In-T-Rex-293 cell line (Invitrogen) was transiently transfected with a vector designed to express either: wild type p21^{cip1}; variant p21^{cip1} (with SNP A and B); or no p21^{cip1} (negative control). The Flp-In-T-Rex-293 cells were found to be intrinsically wild type for SNP A and B on p21^{cip1}.

We found that the cells transfected with $p21^{cip1}$ contained a significantly greater amount of $p21^{cip1}$ mRNA (as determined by Q-PCR) and $p21^{cip1}$ protein (as determined by Acumen cytometry) than the control, irrespective of $p21^{cip1}$ genotype. Acumen cytometry also demonstrated that a significantly greater proportion of the $p21^{cip1}$ wild type and variant transfected cells were positive and nuclear positive for $p21^{cip1}$ protein than the control. This indicates that the $p21^{cip1}$ vector was successfully transfected into the cells, and that $p21^{cip1}$ was successfully translated. The cells transfected with wild type $p21^{cip1}$ contained 298 times more $p21^{cip1}$ mRNA than the control; whereas the cells transfected with variant $p21^{cip1}$ contained 275 times more $p21^{cip1}$ mRNA than the control. This could suggest that transfection was more efficient for wild type $p21^{cip1}$ than variant $p21^{cip1}$. However, we have also shown that the expression of beta-actin per cell differed significantly between the control, wild type and variant transfected cell populations. The $p21^{cip1}$ mRNA content was determined by Q-PCR, and normalised to beta-actin content: on the assumption that beta-actin expression is constant. The differential expression of beta-actin in the three cell populations implies that the results regarding transfection efficiency are skewed.

4.2.8 The effect of the $p21^{cip1}$ genotype on the stability of $p21^{cip1}$ mRNA and protein

$p21^{cip1}$ expression is tightly controlled by the regulation of various steps in its production and degradation (reviewed in[84]), namely: rate of transcription; mRNA stability; rate of translation; protein stability; and rate of protein degradation. The rate of transcription is

dependent on the binding of various transcription factors to a response element in the gene: the main transcription factor being the p53 protein that binds in response to DNA damage. The stability of the $p21^{cip1}$ mRNA is extensively regulated by the binding of various non-coding RNAs[144] and proteins[84] to its 5' and 3' -UTRs. Similarly, the rate of translation can be altered by binding of various proteins to its 5' -UTR (for example, CUG-binding protein 1 and calreticulin[84]). The stability and rate of degradation of $p21^{cip1}$ protein is dependent on its interaction with various kinases and phosphotases, and the machinery that targets it for degradation[84]. It appears that the $p21^{cip1}$ protein can be degraded in an ubiquitin-dependent and independent manner[145].

In order to elucidate the effect of the SNPs on the stability of the $p21^{cip1}$ mRNA and/or protein, we calculated the $p21^{cip1}$ protein to mRNA ratio in the wild type and variant transfected cell populations. To eliminate the problem of beta-actin normalisation, we normalised both the $p21^{cip1}$ mRNA and protein results to beta-actin, to allow relative comparison of ratios in the wild type and variant transfected cells. We found that the cells transfected with $p21^{cip1}$ variant expressed 50.7% more $p21^{cip1}$ protein per mRNA than the cells transfected with wild type $p21^{cip1}$. This could indicate that the SNPs increase the stability of the $p21^{cip1}$ protein and/or that they decrease the stability of the $p21^{cip1}$ mRNA.

SNP A induces a serine to arginine substitution on codon 31: the CDK2 binding region of $p21^{cip1}$. Serine is a polar uncharged amino acid; whereas arginine is positively charged[146]: which may alter the tertiary structure of the protein and its interaction with other proteins (for example: the kinases and phosphatases that regulate its stability; or the ubiquitin ligases that target it for degradation). Therefore, it is possible that SNP A alters the stability of the

$p21^{cip1}$ protein, or its rate of degradation. SNP B is located within the 3'-UTR of $p21^{cip1}$, so it is plausible that it alters the binding of the non-coding RNAs and proteins to the $p21^{cip1}$ mRNA that regulate its stability. Two stabilising proteins that bind to the 3'-UTR are HuD and RNA-binding motif protein 38 (RBM38)[147, 148]. Whilst we cannot conclude on the individual effects of SNP A and B from these results, they suggest that SNP A alters the stability or rate of degradation of the $p21^{cip1}$ protein, and/or SNP B decreases the stability of $p21^{cip1}$ mRNA. The individual effects of the $p21^{cip1}$ SNPs could be determined by a similar transfection method, albeit replacing the variant $p21^{cip1}$ mRNA with a version contains only one of the SNPs.

4.2.9 The effect of the $p21^{cip1}$ genotype on the inhibitory function of $p21^{cip1}$

Cells transfected with wild type or variant $p21^{cip1}$ expressed a significantly greater amount of $p21^{cip1}$ protein per cell than the mock transfected cells (negative control). Furthermore, there was no significant difference in the amount of $p21^{cip1}$ protein expressed per cell, in the $p21^{cip1}$ nuclear density, or in the percentage of cells that were positive for $p21^{cip1}$ protein, in cells transfected with wild type or variant $p21^{cip1}$. This indicates that the nuclear translocation efficiency of $p21^{cip1}$ protein was not altered by the $p21^{cip1}$ SNPs.

We found that a significantly greater percentage of $p21^{cip1}$ transfected cells were in G2 phase compared to non-transfected cells, mainly at the expense of G1 cells, irrespective of $p21^{cip1}$ genotype. Whilst $p21^{cip1}$ may inhibit cell cycle progression at the G1/S and G2/M checkpoints[31], the literature indicates that $p21^{cip1}$ protein, expressed independently of p53,

induces a G2 cell cycle arrest in human embryonic kidney cells[124-127]. Therefore, the accumulation of cells in the G2 phase was expected. Interestingly, we found that the cell cycle arrest was more effective for wild type $p21^{cip1}$ than variant $p21^{cip1}$: with wild type $p21^{cip1}$ inducing a 41% increase in cells in the G2 phase, compared to only a 20% increase for variant $p21^{cip1}$. This suggests that wild type $p21^{cip1}$ is a more effective G2/M checkpoint inhibitor than variant $p21^{cip1}$. Furthermore, we show that wild type $p21^{cip1}$ is a more effective anti-apoptotic agent than variant $p21^{cip1}$. Wild type $p21^{cip1}$ reducing the rate of apoptosis to 49% of that of non-transfected cells, whereas variant $p21^{cip1}$ only reduced the rate of apoptosis by 42%.

Additionally, we have shown that cells transfected with wild type $p21^{cip1}$ expressed a significantly greater amount of beta-actin per cell than cells transfected with variant $p21^{cip1}$, although both expressed more than the control. Beta-actin is a cytoskeleton protein that is part of the internal structure of the cell, and a mediator of internal movement[149]. The cytoskeleton is extensively re-organised during the cell cycle[150]. The up-regulation of beta-actin in the $p21^{cip1}$ transfected cells suggests that both wild type and variant transfected cells are tending towards differentiation compared to control, with the effect strongest for wild type $p21^{cip1}$.

4.2.10 Conclusion and limitations

Our results indicate that variant $p21^{cip1}$ is associated with an increased risk of AD, an earlier age of onset, and an increase in the accumulation and spread of tau pathology in AD. Despite a relatively large cohort (193 subjects) the low prevalence of the $p21^{cip1}$ variant in the population (approximately 12%) lead to very few patients in the $p21^{cip1}$ variant subgroups defined by disease severity. This may have contributed to the lack of statistically significant results despite visible trends in some cases. Furthermore, there may be unknown confounding factors that were not accounted for in our analysis. The two identified potential confounding factors (ApoE genotype and additional pathology) were found to be balanced across the $p21^{cip1}$ wild type and variant groups, irrespective of disease severity, implying that they are unlikely to have altered the outcome of the effect of the $p21^{cip1}$ genotype on AD.

Our cell culture results indicate that variant $p21^{cip1}$ is a less effective G2/M checkpoint inhibitor, and anti-apoptotic agent, than wild type $p21^{cip1}$. We also demonstrate that the SNPs either decrease the stability of the $p21^{cip1}$ mRNA and/or increase the stability of the $p21^{cip1}$ protein; potentially altering $p21^{cip1}$ expression at the protein level.

We cannot conclude on the individual effects of the $p21^{cip1}$ SNPs, as the variant version of $p21^{cip1}$ contained both SNPs. However, as SNP A induces an amino acid change in the CDK2 binding region of $p21^{cip1}$, it is plausible that this SNP alters the ability of $p21^{cip1}$ to bind and inhibit CDK2. This could be investigated further by separating complexes of cyclin/CDK2/$p21^{cip1}$ from cells transfected with wild type or variant $p21^{cip1}$ (for example by immunoprecipitation), and capturing the complexes on G protein beads. The strength of the

binding of $p21^{cip1}$ to cyclin/CDK2 could be investigated by the use of a salt gradient. It is also possible that SNP A increases $p21^{cip1}$ protein levels within the cell, by altering the tertiary structure of the $p21^{cip1}$ protein and its interaction with the proteins that targets it for degradation[84]. Similarly, SNP B may alter the interaction of the $p21^{cip1}$ mRNA with the non-coding RNAs and proteins that regulate its stability[84]. The fact that the $p21^{cip1}$ SNPs are only associated with cancer and AD when found together, suggests that the individual effects of the $p21^{cip1}$ SNPs are required for a significant loss of G1/S checkpoint control.

As discussed, our findings are compatible with the cell cycle theory of AD. They suggest that variant $p21^{cip1}$ may contribute to the loss of cell cycle control that is postulated to be the cause of neurodegeneration in AD, in some individuals that develop AD. Previous studies have shown that lymphocytes from AD patients have a reduced response to rapamycin induced inhibition of the mTOR signalling pathway compared to lymphocytes from controls[71, 72]. We hypothesised that the downstream inhibitory components of the mTOR pathway that are defective in AD lymphocytes are also responsible for the loss of cell cycle control in neurons in AD. The $p21^{cip1}$ protein is one of the inhibitory proteins that functions downstream of mTOR[31], so it is plausible that variant $p21^{cip1}$ may contribute to the loss of cell cycle control that has been detected in lymphocytes from AD patients.

4.3. ELUCIDATING THE IMPRINTING STATUS OF P57^{KIP2} IN THE HUMAN BRAIN, AND THE EFFECT OF A SNP OF P57^{KIP2} ON PROTEIN EXPRESSION, AND ITS ASSOCIATION WITH AD

p57^{kip2} is a member of the cip/kip family of CDKIs that regulate cell cycle progression. In addition, it is involved in regulating cell survival, apoptosis and cytoskeleton dynamics. The p57^{kip2} protein is essential for development: with p57^{kip2} knockout mice suffering severe developmental abnormalities and early death[33]. The loss of p57^{kip2} expression has also been implicated in Beckwith-Wiedermann syndrome: an overgrowth syndrome associated with cancer (for review, see[33]).

Unlike the other cip/kip family members, the p57^{kip2} gene is paternally imprinted to some extent in humans: with the maternal allele preferentially expressed[85]. Genomic imprinting refers to the highly complex epigenetic mechanisms that lead to preferential expression of an allele of one parent-of-origin over the other[151]. The epigenetic mechanisms can include parent-of-origin specific methylation, chromatin organisation and histone modification; and are heritable. Imprinting is made more complex by the finding that imprinted genes are often imprinted in clusters via an imprinting control region (ICR) located at a distance from the genes; and that imprinted genes can help regulate the imprinting of other genes. Whilst it is established that p57^{kip2} is expressed in the human brain[33], its imprinting status in this region is not known. The literature indicates that p57^{kip2} expression and extent of imprinting are tissue dependent, with imprinting established to be partial in some human tissues[85].

The regulation of $p57^{kip2}$ imprinting in human tissues is highly complex. The $p57^{kip2}$ gene is located within a cluster of imprinted genes on chromosome 11p15.5 that share involvement in the regulation of development and cell survival[151]. $p57^{kip2}$ imprinting is controlled by an ICR located within KvDMR1: another gene member of the 11p15.5 cluster. It appears that the ICR controls imprinting by two mechanisms[152, 153]: namely, by regulating chromatin structure in a methylation-dependent manner; and by coding for an RNA transcript that inhibits $p57^{kip2}$ expression *in cis*. The transcriptional repressor: CTCF binds the ICR in a methylation-dependent manner: altering the chromatin structure to suppress gene expression. The methylation status of the ICR is heritable and established in the germline: with the maternal ICR methylated, preventing CTCF binding and promoting expression of the maternal $p57^{kip2}$ allele; and the paternal ICR unmethylated, promoting CTCF binding and preventing expression of the paternal $p57^{kip2}$ allele[154]. Secondly, the KvDMR1 ICR is itself paternally expressed; and codes for the promoter of a non-coding RNA (termed LIT1) that prevents expression of $p57^{kip2}$ *in cis*. As only the paternal LIT1 is expressed, only the paternal $p57^{kip2}$ allele is suppressed[33, 153].

Shin and co-workers[153] found that the involvement of the two mechanisms is tissue dependent, although it has not been investigated in the human brain. In addition, an imprinted gene (ZAC) located on chromosome 6q24 can bind the ICR of interest in a methylation-dependent manner, altering expression of the non-coding LIT1 transcript[155] and hence altering $p57^{kip2}$ imprinting. This highlights the complexity of $p57^{kip2}$ imprinting, and suggests that other unknown mechanisms may yet be discovered. It is established that abnormal $p57^{kip2}$ imprinting can be associated with disease[33]. However, the lack of

information about the correct imprinting of $p57^{kip2}$ in the human brain prevents research concerning disease and $p57^{kip2}$ imprinting in this region from being possible.

4.3.1 The imprinting status of $p57^{kip2}$ in the aging brain

We found that $p57^{kip2}$ imprinting status ranged from full to none in the frontal and occipital lobe of aging control brain and brain affected by AD. The imprinting status in the frontal lobe differing from that in the occipital lobe in just above half of the cases examined. Despite this, partial imprinting was the most common status in both the frontal and occipital lobe of control subjects: with $p57^{kip2}$ partially imprinted in approximately half of informative cases. Of the remaining half, imprinting status was split equally between full and none in the frontal lobe, whereas imprinting was largely absent in the occipital lobe. This suggests that $p57^{kip2}$ imprinting is brain-region specific, and that $p57^{kip2}$ is more tightly imprinted in the frontal than occipital lobe.

It could also suggest that different cell types in the brain imprint $p57^{kip2}$ to a different extent. The cDNA used for determination of $p57^{kip2}$ imprinting status was extracted from a tissue block that contained different cell types (neurons and glial cells etc). Assuming $p57^{kip2}$ imprinting status is cell-specific, the results are an average of the $p57^{kip2}$ imprinting status of the individual cells in the sample. The large variation in extent of imprinting in the elderly brain (ranging from full to none) could be a result of different proportion of cell types in the brain samples obtained from different patients and brain regions. This could be investigated further by measuring cell type-specific markers by ELISA to allow calculation of the

proportion of different cell types in a sample (for example: NeuN for neuronal density and glial fibrillary acidic protein for astrocyte density). It is also possible that $p57^{kip2}$ imprinting status is altered by aging or disease. All the brains in our cohort were from elderly individuals with or without AD, so we cannot conclude on $p57^{kip2}$ imprinting status in the brain of subjects at an earlier stage of life.

As of yet, the imprinting status of $p57^{kip2}$ in the human brain has not been investigated. Matsuoka and co-workers[85] found that there was approximately two fold preferential expression of the maternal allele in the foetal brain, in contrast to approximately twenty fold preferential expression of the maternal allele in the other foetal organs tested. Furthermore, they found approximately nine fold preferential expression of the maternal allele in the healthy human kidney. This forms the background to all literature regarding $p57^{kip2}$ imprinting: with $p57^{kip2}$ imprinting generally accepted as partial in human tissues. Interestingly, Muller and colleagues[156] found that TSSC3, another paternally imprinted member of the 11p15.5 imprinted cluster, was not imprinted in the human brain[156]. TSSC3 imprinting is under the control of the same ICR as $p57^{kip2}$, implying that it should have similar imprinting to $p57^{kip2}$, unless other unknown mechanisms, independent of the ICR, are involved in regulation. We have shown that $p57^{kip2}$ imprinting status may range from full to none in the human brain, and that imprinting status is brain region and/or cell type-specific, suggesting that the control of $p57^{kip2}$ imprinting may be more complex than generally thought.

It is known that abnormal imprinting of $p57^{kip2}$ and other imprinted genes may lead to disease. For example, Beckwith-Wiederman syndrome is associated with loss of $p57^{kip2}$

imprinting[33]; whereas some brain tumours are associated with gain-of-imprinting of TSSC3[156]. In light of this, we investigated the association of AD with $p57^{kip2}$ imprinting status in the frontal and occipital lobe. We found that $p57^{kip2}$ imprinting was not altered in the occipital lobe of AD patients compared to controls, irrespective of disease severity. However, there was a trend (not statistically significant) for loss of $p57^{kip2}$ imprinting in the frontal lobe of AD patients compared to control. Approximately 85% of control subjects had 57^{kip2} imprinting (full or partial) in the frontal lobe, whereas only ~ 60% of AD patients had $p57^{kip2}$ imprinting (full or partial) in this region. There was also a trend (not statistically significant) for the extent of imprinting to become more similar in the frontal and occipital lobe as AD progressed from a preclinical to advanced stage. It is well established that the frontal lobe is affected by AD-related pathology in AD, whereas the occipital lobe is relatively spared, even at an advanced stage[5]. The loss of $p57^{kip2}$ imprinting in the frontal lobe, but not in the occipital lobe, may be indicative of an association between AD and loss of $p57^{kip2}$ imprinting. It would be of interest to investigate the $p57^{kip2}$ imprinting status in the temporal lobe of controls and AD subjects, as this region is most severely affected in AD.

The cell cycle theory of AD states that neurodegeneration is secondary to inappropriate neuronal cell cycle activity and progression beyond the G1/S checkpoint. Nagy[74] proposed that the inappropriate progression may be a consequence of inefficient G1/S checkpoint control by the members of the cip/kip family of CDKIs, namely: $p21^{cip1}$, $p27^{kip1}$ and $p57^{kip2}$. The regulation of the imprinting of $p57^{kip2}$ contributes to the regulation of its expression[33], so it is plausible that inappropriate imprinting may lead to inappropriate expression, and inefficient G1/S checkpoint control in some cases. Alternatively, the $p57^{kip2}$ imprinting status may be altered as a consequence of disease. It is important to note that we cannot

conclude on whether imprinting is maternal or paternal, as we did not have access to parental DNA.

4.3.2 The association of a SNP of $p57^{kip2}$ with AD

As mentioned above, it has been hypothesised that inefficient G1/S checkpoint control by the cip/kip family members of CDKIs may contribute to loss of cell cycle control in neurons in AD. We have demonstrated that a genetic variant of $p21^{cip1}$ is associated with an increased risk of AD, an earlier age of onset, and an increase in the accumulation of AD-related pathology in AD. Nagy[74] identified a genetic variant of $p57^{kip2}$ that may be associated with AD. The genetic variant contained a SNP in an exonic region that induced an amino acid substitution within the central PAPA domain of $p57^{kip2}$ (residue 159). The effect of the SNP on the function and expression of $p57^{kip2}$ is unknown. The SNP has not been reported to be associated with cancer.

The $p57^{kip2}$ gene has three domains: the N-terminal domain responsible for its CDKI role; the central PAPA (proline/ alanine rich) domain of unknown function; and a C-terminal domain containing its nuclear localisation signal, which is involved in its anti-apoptotic role[33]. The central domain is postulated to be involved in the interaction of $p57^{kip2}$ with the proteins required for its additional functions. It is possible that the $p57^{kip2}$ SNP alters the expression of $p57^{kip2}$ by altering its stability or interaction with the protein degradation machinery. We investigate the effect of the $p57^{kip2}$ SNP on $p57^{kip2}$ expression and association with AD.

In our cohort, 51% of subjects were wild type, 40% heterozygous, and 9% homozygous for the $p57^{kip2}$ SNP. This is consistent with the Hardy-Weinberg equilibrium[102], indicating that the frequency of the $p57^{kip2}$ variant remains constant in the population from one generation to the next. There was no significant difference in the distribution of the $p57^{kip2}$ variant allele in individuals in different stages of AD. However, there was a trend (not statistically significant) for a greater percentage of patients with advanced AD to be homozygous for the $p57^{kip2}$ SNP compared to individuals in earlier stages of AD, suggesting that the SNP's association with AD follows a recessive model, and is independent of dose.

In agreement with the Nagy study[74], our results suggest that the $p57^{kip2}$ SNP may be associated with an increased risk of AD. It may also be associated with a reduced age of onset of AD, although results failed to reach statistical significance. Variant $p57^{kip2}$ was associated with more severe pathology for some aspects of pathology investigated. Namely, synaptic density in the frontal lobe ($p = 0.026$), and beta-amyloid accumulation in the occipital lobe ($p = 0.011$) of advanced AD patients only (the $p57^{kip2}$ imprinting status was taken into account when analysing the data). Variant $p57^{kip2}$ was also associated with greater accumulation of phospho-tau relative to tangles in the frontal lobe of mild AD patients ($p = 0.011$), although overall accumulation of phospho-tau and tangles was independent of $p57^{kip2}$ genotype, irrespective of AD severity. This suggests that the $p57^{kip2}$ SNP alters tau processing; and may interact with its role in regulating cytoskeleton dynamics[33]. Variant $p57^{kip2}$ was not associated with the other aspects of AD-related pathology (neuronal density or synaptic regeneration potential), irrespective of severity of AD.

We investigated the distribution of various confounding factors by $p57^{kip2}$ genotype to ensure that the association of variant $p57^{kip2}$ with AD was not altered by these factors. There was a trend for a smaller percentage of $p57^{kip2}$ homozygous subjects to have additional pathology, and to be ApoE ε4 and variant $p21^{cip1}$ carriers, than subjects wild type or heterozygous for the $p57^{kip2}$ SNP (irrespective of severity of AD). However, none of the trends reached statistical significance. The confounding factors were balanced across the wild type and heterozygous groups. This implies that the mentioned factors do not confound the association of the $p57^{kip2}$ variant with AD, although it is possible that there are other unknown factors. A larger cohort would be required to further disentangle the association.

4.3.3 The effect of the $p57^{kip2}$ SNP on $p57^{kip2}$ expression

The reason for the association of the $p57^{kip2}$ SNP with AD is unclear. Presumably the SNP reduces the expression or function of the $p57^{kip2}$ protein; contributing to the loss of G1/S checkpoint control that is postulated to be a cause of neurodegeneration in AD[30]. The SNP is located, not within the CDKI domain of the $p57^{kip2}$ protein, but within the central PAPA domain of unknown function. Therefore, it is unlikely that the $p57^{kip2}$ SNP reduces the CDKI function of the $p57^{kip2}$ protein; although it may interfere with the proteins' other functions (for example, role in regulating apoptosis or cytoskeleton dynamics). It is possible that the loss of the other functions may contribute to the development of AD. Alternatively, the SNP may reduce $p57^{kip2}$ expression by altering the stability or rate of degradation of the $p57^{kip2}$ protein. Our results suggest that this is the case.

We found a weak but significant positive correlation between the amount of $p57^{kip2}$ mRNA and protein in the frontal lobe of subjects that were wild type for the $p57^{kip2}$ SNP ($R^2 = 0.13$, $p = 0.006$). The association was not present in subjects that expressed only the $p57^{kip2}$ variant, or expressed the variant to some extent, suggesting that the SNP alters $p57^{kip2}$ expression at the mRNA and/or protein level. Furthermore, multiple regression analysis showed that $p57^{kip2}$ protein content was most accurately predicted by the $p57^{kip2}$ mRNA content, $p57^{kip2}$ genotype, and NFT content in the frontal lobe ($R^2 = 0.25$, $p < 0.001$). The $p57^{kip2}$ protein content negatively correlated with the expression of variant $p57^{kip2}$ ($p = 0.004$), indicating that the SNP is associated with reduced expression. The positive association between $p57^{kip2}$ protein content and NFT content may suggest that $p57^{kip2}$ protein non-specifically binds to tau tangles, as was hypothesised to be the case for $p21^{cip1}$ (see 4.2.6). Interestingly, we found that $p57^{kip2}$ homozygous subjects had a trend for increased $p57^{kip2}$ mRNA expression and reduced $p57^{kip2}$ protein expression in the frontal lobe compared to wild type and heterozygous subjects. The trends translated to a significantly reduced amount of $p57^{kip2}$ protein per mRNA in subjects that were homozygous for the $p57^{kip2}$ SNP compared to wild type and homozygous subjects.

Overall, our results indicate that the $p57^{kip2}$ SNP may decrease the half-life of the protein. The expression of $p57^{kip2}$ is subject to extensive regulation; and can be rapidly altered as a consequence of rapid turn-over (for review, see[33]). It is degraded by the proteosome in an ubiquitin-dependent manner: its rate of ubiquitination dependent on its phosphorylation status. Therefore, its stability is dependent on its interaction with various kinases and phosphotases, ubiquitin ligases, and the proteosome. It is plausible that the alanine to valine amino acid substitution induced by the $p57^{kip2}$ SNP may trigger a structural change, or alter a

phosphorylation site, that leads to more rapid degradation of the protein. However, as of yet, the altered amino acid residue (codon 159) has not been identified as involved in its degradation.

4.3.4 Conclusions and limitations

We found that $p57^{kip2}$ imprinting status ranged from full to none in the elderly brain: with $p57^{kip2}$ more tightly imprinted in the frontal lobe than occipital lobe. This could suggest that $p57^{kip2}$ imprinting status is brain-region or cell-type specific, as the distribution of different cell types in the samples was not investigated. We found a weak (not statistically significant) association between loss of $p57^{kip2}$ imprinting in the frontal lobe (affected by AD), but not in the occipital lobe (not affected by AD), which may be indicative of an association between AD and loss of imprinting of $p57^{kip2}$.

Our results may suggest that the $p57^{kip2}$ SNP is associated with an increased risk of AD, an earlier age of onset, and an increased accumulation of some aspects of AD-related pathology, although few of the results reached statistical significance. We found that the $p57^{kip2}$ SNP may reduce the half-life of the $p57^{kip2}$ protein, suggesting a mechanism for the G1/S checkpoint failure in patients with the $p57^{kip2}$ SNP. It is compatible with the cell cycle theory of AD, and suggests that the $p57^{kip2}$ SNP may contribute to the loss of cell cycle control in neurons in some individuals that develop the disease. AD may also be associated with loss of imprinting of $p57^{kip2}$ in some patients, potentially leading to reduced $p57^{kip2}$ expression and reduced G1/S checkpoint control. A larger cohort would be required to further disentangle these associations.

APPENDIX 1

Table 52 Manufacturers of chemicals required for DNA, RNA and protein extraction (TRI-reagent method)

Product	**Manufacturer**
1-bromo-3 chloropropane	Sigma
acetone	Sigma
aprotinin	Sigma
EDTA	Sigma
Ethanol	Sigma
glycerol	Sigma
guanidine hydrochloride	Sigma
high-Capacity cDNA Reverse Transcription kit	Applied bioscience
isopropanol	Sigma
nuclease free water	Qiagen
phenylmethanesulfonylfluoride	Roche
sodium chloride	Sigma
sodium citrate	Sigma
sodium dodecyl sulphate	Sigma
TRI-reagent	Sigma
tris-hydrochloride	Sigma

Table 53 Manufacturers of chemicals required for gene expression microarray analysis (Agilent)

Chemical	**Manufacturer**
acetonitrile	
DNase	Promega
ethanol	Sigma
GEx Hybridisation buffer HI-RPM	Agilent Technologies
low-input quick amplification labelling kit	Agilent Technologies
RLT-mix: Rneasy mini column kit	Qiagen
RNeasy mini column	Qiagen
RPE buffer: Rneasy mini column kit	Qiagen
stabilisation and drying solution	Agilent Technologies
wash buffer 1	Agilent Technologies
wash buffer 2	Agilent Technologies

APPENDIX 2

DNase treatment of RNA

1 unit of RNase free DNase (Qiagen) was sufficient to treat 1 µg of RNA. The quantity of RNA was determined by nanodrop spectrophotometry; and the DNase treatment mixture set up as outlined in Table 3. The mixture was incubated at 37ºC for 30 minutes; and RNA re-extracted by standardTRI-reagent protocol (adjusted for volume of TRI-reagent used) to inactive DNase (see method 2.2).

Table 54 DNase treatment of RNA

Reagent	Volume
RNA in water	1-8 µl
RQ1 RNase free DNase buffer (Qiagen)	1 µl
RQ1 RNase free DNase (Qiagen)	1unit/µg RNA (1 µl contains 1 unit)
Water to final volume (Qiagen)	10µl

Purification of RNA with Qiagen RNeasy mini column

84µl of nuclease free water (Qiagen), 350µl buffer RLT (Qiagen) and 250µl of 100% ethanol (Sigma) were added per cRNA sample. The cRNA mix was transferred to an RNeasy mini column (Qiagen) and centrifuged at 4ºC for 30 seconds at 13,000 rotations per minute (rpm). The RNeasy mini column filter was subsequently washed twice with 500µl buffer RPE (Qiagen) (with ethanol added as stated in the kit protocol), with centrifugation at 13,000rpm for 60 seconds at 4^{o}C between washes. The cRNA was eluted from the filter by the addition of 30µl nuclease free water, incubation at room temperature for 1 minute, and centrifugation at 4º for 30 sec at 13,000rpm.

APPENDIX 3

Determination of $p57^{kip2}$ imprinting status

The subjects that were heterozygous for the $p57^{kip2}$ SNP were informative in terms of imprinting status. For heterozygous DNA, the ratio of intensity of the wild type band to variant band represented equal quantity of wild type and variant allele. The ratio of the wild type band to variant band for heterozygous DNA was dependent on the overall intensity of the bands, and ranged from 1.0 to 1.22. Figure 1 shows the statistically significant positive correlation between the intensity of the wild type band and the wild type to variant band ratio for heterozygous DNA ($R^2 = 0.68$, $p < 0.001$). The DNA values deviated from the "expected values" by a maximum of 7% . Note that the expected value denotes the value that would be expected if there was equal expression of wild type and variant $p57^{kip2}$ as calculated from the regression equation (represented by the black line in Figure 75). cDNA ratios that deviated from the expected value by more than 7% were interpreted as having unequal expression of wild type and variant $p57^{kip2}$ (above the line = more wild type $p57^{kip2}$ expression than variant $p57^{kip2}$ expression; below the line = more variant $p57^{kip2}$ expression than wild type expression).

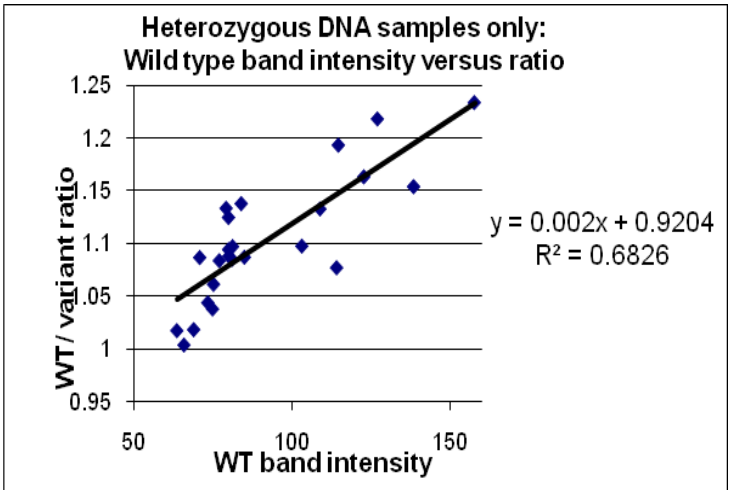

Figure 75 **Statistically significant positive correlation between the intensity of the wild type band and the ratio of the wild type to variant band intensity of heterozygous DNA (P>0.001, R^2 = 0.6826) (x axis = wild type band intensity of heterozygous DNA samples, y-axis = wild type to variant band intensity ratios for heterozygous DNA samples; regression equation shown on graph).**

APPENDIX 4

Lymphocyte cell culture and rapamycin treatment in preparation for microarray based gene expression analysis

Lymphocyte separation from blood

To identify rapamycin-regulated genes in lymphocytes, viable lymphocytes from 4 healthy subjects with maximal rapamycin response, as determined by Flow Cytometry and cell counting, were selected for microarray analysis. Buffy coat residues were provided by the NHS blood and transfusion centre. The buffy coats were enriched with 360ml of RPMI-1640 (Sigma), and diluted (15:35) with phosphate buffered saline (PBS) (Sigma). 30ml of the cell suspension was layered onto 15 ml lymphoprep (Axis Shield UK), centrifuged at 800 RCF for 30 minutes, and upper layer discarded. The middle layer was separated to a clean centrifuge tube, centrifuged at 400 RCF for 10 minutes, and supernatant discarded. The cell pellets were resuspended in 90% foetal calf serum (FCS) gold (Sigma) and 10% DMSO (Sigma), and stored at -80ºC.

Lymphocyte culture and rapamycin treatment

Frozen lymphocytes were washed in 12 times RPMI-1640 (Sigma), centrifuged at 400 RCF for 10 minutes at RT, and re-suspended in RPMI-1640 (Sigma), to give a final cell suspension of 2 million cells per ml. 75µl of cell suspension was added per well of a 96 well plate and supplemented with 75µl of lymphocyte culture medium (composed of RPMI-1640 with L-glutamine (2% final), penicillin/streptomycine (1% final), foetal calf serum heat inactivated (15% final) and PHA (PAA) (2.5% final)). After 48 hours at 37ºC, the lymphocyte cultures were treated with 150µl per well of 100ng/ml rapamycin in culture medium (composition as above). The control lymphocytes were treated with culture medium only. Cells were incubated at 37ºC for 24 hours prior to collection.

APPENDIX 5

Transient transfection of $p21^{cip1}$ into human embryonic kidney cells

Two vectors (pCMV6-XL5) were ordered from Origene: plasmids containing wild type $p21^{cip1}$ DNA; and plasmids containing variant $p21^{cip1}$ DNA (with SNP A and B). The plasmids were transiently transfected into Flp-In-T-Rex-293 cells (human embryonic kidney cell line HEK-293) (Invitrogen) by standard Lipofectamine-2000 (Invitrogen) protocol. The Flp-In-T-Rex-293 cell line was chosen as it is suitable for transfection, whilst being low maintenance and fast growing. Vector pcDNA5/FRT/TO/CAT (Invitrogen) was chosen as the negative control for the mock transfection as it does not express $p21^{cip1}$.

The Flp-In-T-Rex-293 cells were plated in $75cm^2$ flasks at a density of 40,000 cells/ml in 18.75ml of culture medium (composition: Dulbecco's modified eagle's medium (DMEM) containing 4500mg glucose/litre (Sigma); 10% fetal calf serum (FCS) gold (PAA); and 2mM L-glutamine (Gibco). The cells were grown at 37ºC until 90-95% confluence (approximately 2 days). In preparation for transfection, 30µg of plasmid DNA was diluted in 1.875ml of Opti-MEM reduced serum medium (Gibco); and 75µl of Lipofectamine 2000 (Invitrogen) diluted in 1.875ml Opti-MEM. After 5 minute incubation, the two mixtures were combined and incubated at RT for 20 minutes. The 3.75ml mixture was added to a flask of cultured cells and mixed by gentle rocking. Four flasks of Flp-In-T-Rex-293 cells were transiently transfected for each $p21^{cip1}$ vector, plus two flasks transfected with

pcDNA5/FRT/TO/CAT as the negative control. After 36 hours at 37^{o}C, the cells were dislodged by incubation with 5ml of 1mM EDTA in DMEM (Sigma) for 3 minutes.

For the majority of the flasks, the cell suspensions were transferred to 50ml falcon tubes, topped up to 50ml with DMEM (Sigma) and centrifuged at 400g for 10 minutes at RT. After supernatant removal, the cell pellets were stored at -80^{o}C in preparation for RNA and protein extraction (see section 2.2).

One flask each of wild type p21^{cip1}, variant p21^{cip1} and control transfected cells were plated into 96 well plates. A small amount of cell suspension was transferred to a 15ml tube, topped up to 3ml with culture medium (DMEM (Sigma), 10% FCS gold (PAA), and 2mM L-glutamine (Gibco)), and mixed to produce a single cell suspension. The solution was topped up with culture medium to a density of 5,000 cells/ 100µl, and incubated overnight at 37^{o}C. Following supernatant removal, cells were incubated with 100µl of Glyo-Fixx (ThermoScientific) per well for 2 hours; and 100µl of 85% ice cold ethanol (Sigma) added in preparation for p21^{cip1} and beta-actin staining for Acumen analysis.

Immunostaining and propidium iodide labelling

The transfected cells were immunolabelled for $p21^{cip1}$ and beta-actin.

Briefly, the cells were incubated with blocking solution for 30 minutes at RT (5% BSA, 0.1% Triton X in PBS), with primary antibody overnight at 4ºC, and with secondary antibody overnight at 4ºC. The primary and secondary antibodies were diluted in PBS with 0.1% Triton X, and are outlined in Table 55. Cells were subsequently stained with propidium iodide by incubation with 10µg/ml propidium iodide supplemented with 100µg/ml RNaseA and 0.1% Triton-X in PBS for 20 minutes at 37ºC. The results were read with the Acumen Explorer Cytometer.

Table 55 Antibodies selected for immunostaining

Protein	**Primary antibody**	**Secondary antibody**
$P21^{cip1}$	Rabbit polyclonal to $p21^{cip}1$ (1:500, ABcam)	Anti-rabbit IgG FITC (1:200, ABcam)
Beta-actin	Mouse monoclonal to beta-actin (1:500, ABcam)	Anti-mouse IgG FITC (1:200, ABcam)

APPENDIX 6

MICROARRAY RESULTS

Table 56 Genes that were upregulated by rapamycin in lymphocytes (upregulated in rapamycin-treated lymphocytes compared to untreated lymphocytes, FDR cut-off point of 10%) (1138 genes)

Gene	Gene description
38777	membrane-associated ring finger (C3HC4) 6
39692	septin 8
A2M	alpha-2-macroglobulin
AADACL2	arylacetamide deacetylase-like 2
AASDH	aminoadipate-semialdehyde dehydrogenase
ABCA8	ATP-binding cassette, sub-family A (ABC1), member 8"
ABCB5	ATP-binding cassette, sub-family B (MDR/TAP), member 5
ABCD2	ATP-binding cassette, sub-family D (ALD), member 2"
ABHD2	abhydrolase domain containing 2
ABI3BP	ABI family, member 3 (NESH) binding protein"
ABLIM2	actin binding LIM protein family, member 2"
ABRA	actin-binding Rho activating protein
ABTB1	ankyrin repeat and BTB (POZ) domain containing 1
ACOX2	acyl-Coenzyme A oxidase 2, branched chain"
ACPP	acid phosphatase, prostate"
ACSS1	acyl-CoA synthetase short-chain family member 1
ACTRT1	actin-related protein T1
ACVR2B	activin A receptor, type IIB"
ADAMTS13	ADAM metallopeptidase with thrombospondin type 1 motif, 13"

Gene	**Gene description**
ADAMTS15	ADAM metallopeptidase with thrombospondin type 1 motif, 15"
ADAMTS2	ADAM metallopeptidase with thrombospondin type 1 motif, 2"
ADAMTS20	ADAM metallopeptidase with thrombospondin type 1 motif, 20"
ADAMTS3	ADAM metallopeptidase with thrombospondin type 1 motif, 3"
ADAMTS9	ADAM metallopeptidase with thrombospondin type 1 motif, 9"
ADAMTSL3	ADAMTS-like 3
ADAMTSL4	ADAMTS-like 4
ADAMTSL5	ADAMTS-like 5
ADH6	alcohol dehydrogenase 6 (class V)
ADIPOQ	adiponectin, C1Q and collagen domain containing"
ADSSL1	adenylosuccinate synthase like 1
AGT	angiotensinogen (serpin peptidase inhibitor, clade A, member 8)"
AGTR1	angiotensin II receptor, type 1"
AHNAK	AHNAK nucleoprotein
AKR1D1	aldo-keto reductase family 1, member D1 (delta 4-3-ketosteroid-5-beta-reductase)"
ALDH1A3	aldehyde dehydrogenase 1 family, member A3"
AMY1C	amylase, alpha 1C (salivary)
ANGPT2	angiopoietin 2
ANGPTL2	angiopoietin-like 2
ANGPTL5	angiopoietin-like 5
ANK1	ankyrin 1, erythrocytic"
ANKRD12	ankyrin repeat domain 12
ANKRD36B	ankyrin repeat domain 36B
ANKRD36B	ankyrin repeat domain 36B
ANKRD45	ankyrin repeat domain 45
ANKRD50	ankyrin repeat domain 50
ANKRD6	ankyrin repeat domain 6
ANKS1B	ankyrin repeat and sterile alpha motif domain containing 1B
ANO3	anoctamin 3

Gene	**Gene description**
ANXA10	annexin A10
APBB1IP	amyloid beta (A4) precursor protein-binding, family B, member 1 interacting protein
APOB	apolipoprotein B (including Ag(x) antigen)
APOBEC3G	apolipoprotein B mRNA editing enzyme, catalytic polypeptide-like 3G"
APOLD1	apolipoprotein L domain containing 1
AQP12A	aquaporin 12A
AQP4	aquaporin 4
AQP7P2	aquaporin 7 pseudogene 2
ARHGEF4	Rho guanine nucleotide exchange factor (GEF) 4
ARHGEF6	Rac/Cdc42 guanine nucleotide exchange factor (GEF) 6
ARL14	ADP-ribosylation factor-like 14
ARL17	ADP-ribosylation factor-like 17
ARMC2	armadillo repeat containing 2
ARPP-21	cyclic AMP-regulated phosphoprotein, 21 kD
ARSE	arylsulfatase E (chondrodysplasia punctata 1)
ASAM	adipocyte-specific adhesion molecule
ASB11	ankyrin repeat and SOCS box-containing 11
ASPM	asp (abnormal spindle) homolog, microcephaly associated (Drosophila)"
ASXL3	additional sex combs like 3 (Drosophila)
ATF7IP	activating transcription factor 7 interacting protein
ATP13A4	ATPase type 13A4
ATP6V0D2	ATPase, H+ transporting, lysosomal 38kDa, V0 subunit d2"
ATP8B3	ATPase, class I, type 8B, member 3"
ATRNL1	attractin-like 1
AUTS2	autism susceptibility candidate 2
B2M	beta-2-microglobulin
B3GALT4	UDP-Gal:betaGlcNAc beta 1,3-galactosyltransferase, polypeptide 4"

Gene	Gene description
B4GALT6	UDP-Gal:betaGlcNAc beta 1,4- galactosyltransferase, polypeptide 6"
BAIAP2	BAI1-associated protein 2
BAIAP2L2	BAI1-associated protein 2-like 2
BARX2	BARX homeobox 2
BCL2	B-cell CLL/lymphoma 2
BEND2	BEN domain containing 2
BEND6	BEN domain containing 6
BEST3	bestrophin 3
BMP7	bone morphogenetic protein 7
BMX	BMX non-receptor tyrosine kinase
BNC1	basonuclin 1
BPESC1	blepharophimosis, epicanthus inversus and ptosis, candidate 1
BPI	bactericidal/permeability-increasing protein
BRIP1	BRCA1 interacting protein C-terminal helicase 1
BRUNOL4	bruno-like 4, RNA binding protein (Drosophila)"
BRUNOL6	bruno-like 6, RNA binding protein (Drosophila)"
BSN	bassoon (presynaptic cytomatrix protein)
BSPRY	B-box and SPRY domain containing
BTNL9	butyrophilin-like 9
BVES	blood vessel epicardial substance
C10orf10	chromosome 10 open reading frame 10
C10orf107	chromosome 10 open reading frame 107
C10orf111	chromosome 10 open reading frame 111
C10orf72	chromosome 10 open reading frame 72
C10orf79	chromosome 10 open reading frame 79
C11orf67	chromosome 11 open reading frame 67
C11orf87	chromosome 11 open reading frame 87
C11orf88	chromosome 11 open reading frame 88
C12orf42	chromosome 12 open reading frame 42
C12orf67	chromosome 12 open reading frame 67

Gene	**Gene description**
C14orf106	chromosome 14 open reading frame 106
C15orf43	chromosome 15 open reading frame 43
C15orf48	chromosome 15 open reading frame 48
C16orf65	chromosome 16 open reading frame 65
C16orf75	chromosome 16 open reading frame 75
C17orf76	chromosome 17 open reading frame 76
C17orf78	chromosome 17 open reading frame 78
C18orf26	chromosome 18 open reading frame 26
C19orf30	chromosome 19 open reading frame 30
C1orf110	chromosome 1 open reading frame 110
C1orf118	chromosome 1 open reading frame 118
C1orf127	chromosome 1 open reading frame 127
C1orf173	chromosome 1 open reading frame 173
C1orf226	chromosome 1 open reading frame 226
C1orf87	chromosome 1 open reading frame 87
C1orf92	chromosome 1 open reading frame 92
C1QTNF6	C1q and tumor necrosis factor related protein 6
C20orf114	chromosome 20 open reading frame 114
C20orf132	chromosome 20 open reading frame 132
C20orf85	chromosome 20 open reading frame 85
C21orf117	chromosome 21 open reading frame 117
C2orf16	chromosome 2 open reading frame 16
C2orf21	chromosome 2 open reading frame 21
C3orf36	chromosome 3 open reading frame 36
C3orf46	chromosome 3 open reading frame 46
C3orf70	chromosome 3 open reading frame 70
C4orf12	chromosome 4 open reading frame 12
C4orf19	chromosome 4 open reading frame 19
C4orf22	chromosome 4 open reading frame 22
C4orf36	chromosome 4 open reading frame 36

Gene	**Gene description**
C5orf39	chromosome 5 open reading frame 39
C5orf41	chromosome 5 open reading frame 41
C6orf223	chromosome 6 open reading frame 223
C6orf91	chromosome 6 open reading frame 91
C7orf41	chromosome 7 open reading frame 41
C7orf51	chromosome 7 open reading frame 51
C8orf42	chromosome 8 open reading frame 42
C9orf144B	hypothetical protein LOC259308
CA12	carbonic anhydrase XII
CA6	carbonic anhydrase VI
CADPS	Ca++-dependent secretion activator
CALD1	caldesmon 1
CARD14	caspase recruitment domain family, member 14
CATSPER2	cation channel, sperm associated 2"
CAV2	caveolin 2
CBX7	chromobox homolog 7
CBX7	chromobox homolog 7
CC2D2A	coiled-coil and C2 domain containing 2A
CCDC141	coiled-coil domain containing 141
CCDC28A	coiled-coil domain containing 28A
CCDC34	coiled-coil domain containing 34
CCDC40	coiled-coil domain containing 40
CCDC85A	coiled-coil domain containing 85A
CCL1	chemokine (C-C motif) ligand 1
CCL11	chemokine (C-C motif) ligand 11
CCL26	chemokine (C-C motif) ligand 26
CCNB2	cyclin B2
CCNG2	cyclin G2
CCR1	chemokine (C-C motif) receptor 1
CCR2	chemokine (C-C motif) receptor 2

Gene	**Gene description**
CD177	CD177 molecule
CD1A	CD1a molecule
CD1B	CD1b molecule
CD1E	CD1e molecule
CD44	CD44 molecule (Indian blood group)
CD69	CD69 molecule
CD96	CD96 molecule
CDC14B	CDC14 cell division cycle 14 homolog B (S. cerevisiae)
CDCP1	CUB domain containing protein 1
CDH1	cadherin 1, type 1, E-cadherin (epithelial)"
CDH13	cadherin 13, H-cadherin (heart)"
CDH26	cadherin-like 26
CDH7	cadherin 7, type 2
CDKN1B	cyclin-dependent kinase inhibitor 1B (p27, Kip1)"
CDKN1C	cyclin-dependent kinase inhibitor 1C (p57, Kip2)"
CDKN2C	cyclin-dependent kinase inhibitor 2C (p18, inhibits CDK4)"
CDKN2D	cyclin-dependent kinase inhibitor 2D (p19, inhibits CDK4)
CDON	Cdon homolog (mouse)
CEACAM6	carcinoembryonic antigen-related cell adhesion molecule 6 (non-specific cross reacting antigen)
CEP68	centrosomal protein 68kDa
CFHR5	complement factor H-related 5
CFTR	cystic fibrosis transmembrane conductance regulator (ATP-binding cassette sub-family C, member 7)"
CGA	glycoprotein hormones, alpha polypeptide"
CGNL1	cingulin-like 1
CHD2	chromodomain helicase DNA binding protein 2
CHP2	calcineurin B homologous protein 2
CHRDL2	chordin-like 2
CHRNA9	cholinergic receptor, nicotinic, alpha 9"

Gene	**Gene description**
CKM	creatine kinase, muscle"
CLC	Charcot-Leyden crystal protein
CLCA2	chloride channel regulator 2
CLEC7A	C-type lectin domain family 7, member A"
CLTB	clathrin, light chain (Lcb)"
CNRIP1	cannabinoid receptor interacting protein 1
CNTN3	contactin 3 (plasmacytoma associated)
COBL	cordon-bleu homolog (mouse)
COL11A1	collagen, type XI, alpha 1"
COL13A1	collagen, type XIII, alpha 1"
COL1A2	collagen, type I, alpha 2"
COL6A3	collagen, type VI, alpha 3"
COL6A6	collagen type VI alpha 6
COMMD6	COMM domain containing 6
CORIN	corin, serine peptidase
CORO2A	coronin, actin binding protein, 2A"
CPB2	carboxypeptidase B2 (plasma)
CPE	carboxypeptidase E
CPLX2	complexin 2
CPXM2	carboxypeptidase X (M14 family), member 2"
CRB1	crumbs homolog 1 (Drosophila)
CREB3L4	cAMP responsive element binding protein 3-like 4
CRIM1	cysteine rich transmembrane BMP regulator 1 (chordin-like)
CRIM2	cysteine rich BMP regulator 2 (chordin-like)
CRP	C-reactive protein, pentraxin-related"
CRTAC1	cartilage acidic protein 1
CRYBG3	beta-gamma crystallin domain containing 3
CRYGB	crystallin, gamma B"
CRYGD	crystallin, gamma D"
CSDC2	cold shock domain containing C2, RNA binding"

Gene	**Gene description**
CSF1R	colony stimulating factor 1 receptor
CSN2	casein beta
CTAG1A	cancer/testis antigen 1A
CTDSP1	CTD (carboxy-terminal domain, RNA polymerase II, polypeptide A) small phosphatase 1"
CTNNA3	catenin (cadherin-associated protein), alpha 3"
CTSF	cathepsin F
CXorf51	chromosome X open reading frame 51
CYP2C9	cytochrome P450, family 2, subfamily C, polypeptide 9"
CYP3A5	cytochrome P450, family 3, subfamily A, polypeptide 5"
CYP4F11	cytochrome P450, family 4, subfamily F, polypeptide 11"
CYP4F2	cytochrome P450, family 4, subfamily F, polypeptide 2"
CYP4F3	cytochrome P450, family 4, subfamily F, polypeptide 3"
CYP4V2	cytochrome P450, family 4, subfamily V, polypeptide 2"
CYP4X1	cytochrome P450, family 4, subfamily X, polypeptide 1"
CYP4Z1	cytochrome P450, family 4, subfamily Z, polypeptide 1"
CYR61	cysteine-rich, angiogenic inducer, 61"
CYSLTR2	cysteinyl leukotriene receptor 2
DAOA	D-amino acid oxidase activator
DAPL1	death associated protein-like 1
DCC	deleted in colorectal carcinoma
DCD	dermcidin
DCLK1	doublecortin-like kinase 1
DCN	decorin
DDI1	DDI1, DNA-damage inducible 1, homolog 1 (S. cerevisiae)"
DDX17	DEAD (Asp-Glu-Ala-Asp) box polypeptide 17
DEFA4	defensin, alpha 4, corticostatin"
DEFB119	defensin, beta 119
DHRS12	dehydrogenase/reductase (SDR family) member 12
DHRS3	dehydrogenase/reductase (SDR family) member 3

Gene	Gene description
DKFZP586K1520	DKFZP586K1520 protein
DLEU7	deleted in lymphocytic leukemia, 7
DLG2	discs, large homolog 2 (Drosophila)"
DLGAP4	discs, large (Drosophila) homolog-associated protein 4"
DLX2	distal-less homeobox 2
DMRTB1	DMRT-like family B with proline-rich C-terminal, 1"
DMRTC1	DMRT-like family C1
DMRTC2	DMRT-like family C2
DNAH1	dynein, axonemal, heavy chain 1"
DNAH6	dynein, axonemal, heavy chain 6"
DNAJB7	DnaJ (Hsp40) homolog, subfamily B, member 7"
DPY19L1P1	dpy-19-like 1 pseudogene 1 (C. elegans)
DRP2	dystrophin related protein 2
DSEL	dermatan sulfate epimerase-like
DST	dystonin
DTD1	D-tyrosyl-tRNA deacylase 1 homolog (S. cerevisiae)
DUSP13	dual specificity phosphatase 13
DUSP21	dual specificity phosphatase 21
DUSP27	dual specificity phosphatase 27 (putative)
DYNLRB1	dynein, light chain, roadblock-type 1
DZIP1L	DAZ interacting protein 1-like
DZIP3	DAZ interacting protein 3, zinc finger"
EBF2	early B-cell factor 2
EBF3	early B-cell factor 3
ECHDC2	enoyl Coenzyme A hydratase domain containing 2
ECM2	extracellular matrix protein 2, female organ and adipocyte specific
EEPD1	endonuclease/exonuclease/phosphatase family domain containing 1
EFCAB3	EF-hand calcium binding domain 3
EGF	epidermal growth factor (beta-urogastrone)
EGR1	early growth response 1

Gene	Gene description
ELAVL3	ELAV (embryonic lethal, abnormal vision, Drosophila)-like 3 (Hu antigen C)"
ELAVL4	ELAV (embryonic lethal, abnormal vision, Drosophila)-like 4 (Hu antigen D)
ELOVL7	ELOVL family member 7, elongation of long chain fatty acids (yeast)"
EMCN	endomucin
EMX2OS	EMX2 opposite strand (non-protein coding)
ENPEP	glutamyl aminopeptidase (aminopeptidase A)
ENPP6	ectonucleotide pyrophosphatase/phosphodiesterase 6
EPB41L4B	erythrocyte membrane protein band 4.1 like 4B
EPHA5	EPH receptor A5
EPO	erythropoietin
ERBB3	v-erb-b2 erythroblastic leukemia viral oncogene homolog 3 (avian)
ERBB4	v-erb-a erythroblastic leukemia viral oncogene homolog 4 (avian)
ESR1	estrogen receptor 1
EVI1	ecotropic viral integration site 1
EYA1	eyes absent homolog 1 (Drosophila)
F11	coagulation factor XI
F2	coagulation factor II (thrombin)
F2RL2	coagulation factor II (thrombin) receptor-like 2
F9	coagulation factor IX
FAM100B	family with sequence similarity 100, member B"
FAM119A	family with sequence similarity 119, member A"
FAM12A	family with sequence similarity 12, member A
FAM12B	family with sequence similarity 12, member B (epididymal)"
FAM135B	family with sequence similarity 135, member B
FAM13C1	family with sequence similarity 13, member C1
FAM149B1	family with sequence similarity 149, member B1"
FAM153A	family with sequence similarity 153, member A"

Gene	**Gene description**
FAM155A	family with sequence similarity 155, member A"
FAM162B	family with sequence similarity 162, member B"
FAM171B	family with sequence similarity 171, member B"
FAM172A	family with sequence similarity 172, member A"
FAM181B	family with sequence similarity 181, member B"
FAM19A1	family with sequence similarity 19 (chemokine (C-C motif)-like), member A1"
FAM24A	family with sequence similarity 24, member A"
FAM26D	family with sequence similarity 26, member D
FAM43B	family with sequence similarity 43, member B"
FAM5C	family with sequence similarity 5, member C
FAM62C	family with sequence similarity 62 (C2 domain containing), member C"
FAM64A	family with sequence similarity 64, member A"
FAM71D	family with sequence similarity 71, member D"
FAM74A3	family with sequence similarity 74, member A3"
FAM84A	family with sequence similarity 84, member A"
FAM92B	family with sequence similarity 92, member B
FAT3	FAT tumor suppressor homolog 3 (Drosophila)
FBLN1	fibulin 1
FBN2	fibrillin 2
FBP2	fructose-1,6-bisphosphatase 2"
FBXL16	F-box and leucine-rich repeat protein 16
FCGBP	Fc fragment of IgG binding protein
FGB	fibrinogen beta chain
FGF11	fibroblast growth factor 11
FGF23	fibroblast growth factor 23
FGF7	fibroblast growth factor 7 (keratinocyte growth factor)
FGFR1	fibroblast growth factor receptor 1
FGG	fibrinogen gamma chain

Gene	**Gene description**
FGGY	FGGY carbohydrate kinase domain containing
FGR	Gardner-Rasheed feline sarcoma viral (v-fgr) oncogene homolog
FIGN	fidgetin
FILIP1	filamin A interacting protein 1
FKSG2	apoptosis inhibitor
FLJ10357	hypothetical protein FLJ10357
FLJ12993	hypothetical LOC441027
FLJ13310	hypothetical protein FLJ13310
FLJ13769	hypothetical protein FLJ13769
FLJ21272	hypothetical protein FLJ21272
FLJ23834	hypothetical protein FLJ23834
FLJ30719	hypothetical protein FLJ30719
FLJ32679	golgin-like hypothetical protein LOC440321
FLJ32742	hypothetical locus FLJ32742
FLJ36000	hypothetical protein FLJ36000
FLJ37035	FLJ37035 protein
FLJ37060	similar to FUN14 domain containing 2
FLJ37644	hypothetical gene supported by AK094963
FLJ39609	hypothetical protein FLJ39609
FLJ40330	hypothetical LOC645784
FLJ42875	hypothetical LOC440556
FLJ45244	hypothetical locus FLJ45244
FMO3	flavin containing monooxygenase 3
FN1	fibronectin 1
FN3K	fructosamine 3 kinase
FNBP1	formin binding protein 1
FNDC5	fibronectin type III domain containing 5
FRAT2	frequently rearranged in advanced T-cell lymphomas 2
FREM3	FRAS1 related extracellular matrix 3
FRMD4A	FERM domain containing 4A

Gene	**Gene description**
FRMD6	FERM domain containing 6
FRMD7	FERM domain containing 7
FSTL5	follistatin-like 5
FUT9	fucosyltransferase 9 (alpha (1,3) fucosyltransferase)
GAB1	GRB2-associated binding protein 1
GABRA5	gamma-aminobutyric acid (GABA) A receptor, alpha 5"
GABRG1	gamma-aminobutyric acid (GABA) A receptor, gamma 1
GABRR2	gamma-aminobutyric acid (GABA) receptor, rho 2"
GAGE1	G antigen 1
GALNT10	UDP-N-acetyl-alpha-D-galactosamine:polypeptide N-acetylgalactosaminyltransferase 10 (GalNAc-T10)
GALNT5	UDP-N-acetyl-alpha-D-galactosamine:polypeptide N-acetylgalactosaminyltransferase 5 (GalNAc-T5)
GBP3	guanylate binding protein 3
GCM2	glial cells missing homolog 2 (Drosophila)
GDA	guanine deaminase
GFAP	glial fibrillary acidic protein
GFRA1	GDNF family receptor alpha 1
GFRA2	GDNF family receptor alpha 2
GHRLOS	ghrelin opposite strand (non-protein coding)
GIGYF1	GRB10 interacting GYF protein 1
GIPR	gastric inhibitory polypeptide receptor
GLI2	GLI-Kruppel family member GLI2
GLP1R	glucagon-like peptide 1 receptor
GLRA1	glycine receptor, alpha 1"
GNAL	guanine nucleotide binding protein (G protein), alpha activating activity polypeptide, olfactory type"
GNG8	guanine nucleotide binding protein (G protein), gamma 8"
GPC3	glypican 3
GPR109B	G protein-coupled receptor 109B

Gene	**Gene description**
GPR110	G protein-coupled receptor 110
GPR116	G protein-coupled receptor 116
GPR176	G protein-coupled receptor 176
GPR177	G protein-coupled receptor 177
GPR37	G protein-coupled receptor 37 (endothelin receptor type B-like)
GPR4	G protein-coupled receptor 4
GPX6	glutathione peroxidase 6 (olfactory)
GPX8	glutathione peroxidase 8 (putative)
GRIA2	glutamate receptor, ionotropic, AMPA 2"
GRIA3	glutamate receptor, ionotrophic, AMPA 3"
GRIK2	glutamate receptor, ionotropic, kainate 2"
GRIK3	glutamate receptor, ionotropic, kainate 3"
GRINL1A	glutamate receptor, ionotropic, N-methyl D-aspartate-like 1A
GRM1	glutamate receptor, metabotropic 1"
GRPR	gastrin-releasing peptide receptor
GSG1L	GSG1-like
GSN	gelsolin (amyloidosis, Finnish type)"
GSTA1	glutathione S-transferase alpha 1
GSTA5	glutathione S-transferase alpha 5
GUCY1A3	guanylate cyclase 1, soluble, alpha 3"
GUCY2F	guanylate cyclase 2F, retinal
GVIN1	GTPase, very large interferon inducible 1"
HAND1	heart and neural crest derivatives expressed 1
HAND2	heart and neural crest derivatives expressed 2
HAPLN1	hyaluronan and proteoglycan link protein 1
hCG_1655019	hCG1655019
hCG_1814486	hCG1814486
hCG_1820661	hypothetical LOC400752
HDAC5	histone deacetylase 5
HDAC9	histone deacetylase 9

Gene	**Gene description**
HESX1	HESX homeobox 1
HGF	hepatocyte growth factor (hepapoietin A; scatter factor)
HGF	hepatocyte growth factor (hepapoietin A; scatter factor)
HHIP	hedgehog interacting protein
HHIPL1	HHIP-like 1
HIST1H2BN	histone cluster 1, H2bn
HIST1H4E	histone cluster 1, H4e"
HIVEP2	human immunodeficiency virus type I enhancer binding protein 2
HMGCS2	3-hydroxy-3-methylglutaryl-Coenzyme A synthase 2 (mitochondrial)
HNF4G	hepatocyte nuclear factor 4, gamma"
HOXA2	homeobox A2
HOXA9	homeobox A9
HOXC8	homeobox C8
HOXD10	homeobox D10
HRASLS5	HRAS-like suppressor family, member 5
HSD17B13	hydroxysteroid (17-beta) dehydrogenase 13
HTN3	histatin 3
HTR2C	5-hydroxytryptamine (serotonin) receptor 2C
HTR3C	5-hydroxytryptamine (serotonin) receptor 3, family member C
HYDIN	hydrocephalus inducing homolog (mouse)
IFFO1	intermediate filament family orphan 1
IFIT2	interferon-induced protein with tetratricopeptide repeats 2
IFNA16	interferon, alpha 16"
IGBP1	immunoglobulin (CD79A) binding protein 1
IGF2	insulin-like growth factor 2 (somatomedin A)
IKZF4	IKAROS family zinc finger 4 (Eos)
IL17B	interleukin 17B
IL18	interleukin 18 (interferon-gamma-inducing factor)
IL1B	interleukin 1, beta"
IL1RAPL1	interleukin 1 receptor accessory protein-like 1

Gene	**Gene description**
IL1RN	interleukin 1 receptor antagonist
IMPG1	interphotoreceptor matrix proteoglycan 1
INSL5	insulin-like 5
IQCF1	IQ motif containing F1
IRS2	insulin receptor substrate 2
IRX4	iroquois homeobox 4
ISX	intestine-specific homeobox
ITGB3	integrin, beta 3 (platelet glycoprotein IIIa, antigen CD61)"
ITGBL1	integrin, beta-like 1 (with EGF-like repeat domains)"
JAK1	Janus kinase 1 (a protein tyrosine kinase)
JAKMIP3	janus kinase and microtubule interacting protein 3
JARID2	jumonji, AT rich interactive domain 2"
JUN	jun oncogene
KANK2	KN motif and ankyrin repeat domains 2
KCNA4	potassium voltage-gated channel, shaker-related subfamily, member 4"
KCNA7	potassium voltage-gated channel, shaker-related subfamily, member 7
KCNAB1	potassium voltage-gated channel, shaker-related subfamily, beta member 1"
KCNB2	potassium voltage-gated channel, Shab-related subfamily, member 2
KCNC1	potassium voltage-gated channel, Shaw-related subfamily, member 1"
KCNC2	potassium voltage-gated channel, Shaw-related subfamily, member 2"
KCND3	potassium voltage-gated channel, Shal-related subfamily, member 3"
KCNG4	potassium voltage-gated channel, subfamily G, member 4
KCNH7	potassium voltage-gated channel, subfamily H (eag-related), member 7"
KCNIP2	Kv channel interacting protein 2

Gene	Gene description
KCNJ5	potassium inwardly-rectifying channel, subfamily J, member 5"
KCNK10	potassium channel, subfamily K, member 10"
KCNK17	potassium channel, subfamily K, member 17"
KCNQ1	potassium voltage-gated channel, KQT-like subfamily, member 1"
KCNQ1DN	KCNQ1 downstream neighbor
KCTD19	potassium channel tetramerisation domain containing 19
KCTD4	potassium channel tetramerisation domain containing 4
KIAA0355	KIAA0355
KIAA0894	KIAA0894 protein
KIAA1045	KIAA1045
KIAA1109	KIAA1109
KIAA1239	KIAA1239
KIAA1407	KIAA1407
KIAA1462	KIAA1462
KIAA1522	KIAA1522
KIAA1545	HBV X-transactivated gene 9 protein
KIAA1652	KIAA1652 protein
KIAA1683	KIAA1683
KIF6	kinesin family member 6
KIRREL3	kin of IRRE like 3 (Drosophila)
KLF12	Kruppel-like factor 12
KLF2	Kruppel-like factor 2 (lung)
KLHDC9	kelch domain containing 9
KLHL24	kelch-like 24 (Drosophila)
KLHL4	kelch-like 4 (Drosophila)
KLRB1	killer cell lectin-like receptor subfamily B, member 1
KRT2	keratin 2
KRT72	keratin 72
KRT75	keratin 75
KRT82	keratin 82

Gene	**Gene description**
KRTAP1-1	keratin associated protein 1-1
KRTAP1-3	keratin associated protein 1-3
KRTAP15-1	keratin associated protein 15-1
KRTAP4-7	keratin associated protein 4-7
KRTAP9-2	keratin associated protein 9-2
LAIR2	leukocyte-associated immunoglobulin-like receptor 2
LAMA1	laminin, alpha 1"
LAYN	layilin
LCE1E	late cornified envelope 1E
LECT1	leukocyte cell derived chemotaxin 1
LEF1	lymphoid enhancer-binding factor 1
LEFTY1	left-right determination factor 1
LEMD1	LEM domain containing 1
LEP	leptin
LGALS13	lectin, galactoside-binding, soluble, 13"
LGALS2	lectin, galactoside-binding, soluble, 2"
LGR5	leucine-rich repeat-containing G protein-coupled receptor 5
LIFR	leukemia inhibitory factor receptor alpha
LILRB2	leukocyte immunoglobulin-like receptor, subfamily B (with TM and ITIM domains), member 2"
LIPF	lipase, gastric"
LL22NC03-75B3.6	KIAA1644 protein
LOC100127998	hypothetical protein LOC100127998
LOC100128098	hypothetical protein LOC100128098
LOC100128108	hypothetical protein LOC100128108
LOC100128175	similar to PRO2591
LOC100128178	similar to hCG2041313
LOC100129198	PRO2866
LOC100129406	hypothetical protein LOC100129406

Gene	**Gene description**
LOC100129476	hypothetical protein LOC100129476
LOC100129754	hypothetical protein LOC100129754
LOC100129775	hypothetical protein LOC100129775
LOC100130278	hypothetical protein LOC100130278
LOC100130360	hypothetical protein LOC100130360
LOC100130776	similar to hCG2014417
LOC100130797	PRO0566
LOC100130815	hypothetical LOC100130815
LOC100131176	similar to hCG1991662
LOC100131707	hypothetical LOC100131707
LOC100131720	hypothetical protein LOC100131720
LOC100131938	hypothetical LOC100131938
LOC100132116	hypothetical LOC100132116
LOC100132363	hypothetical protein LOC100132363
LOC100132853	hypothetical LOC100132853
LOC100133746	hypothetical protein LOC100133746
LOC100170939	glucuronidase, beta pseudogene"
LOC100190938	hypothetical LOC100190938
LOC100190986	hypothetical LOC100190986
LOC114227	hypothetical protein LOC114227
LOC120376	Uncharacterized protein LOC120376
LOC124220	similar to common salivary protein 1
LOC150759	hypothetical protein LOC150759
LOC200383	similar to Dynein heavy chain at 16F
LOC201229	hypothetical protein LOC201229
LOC255177	hypothetical protein LOC255177
LOC282992	hypothetical protein LOC282992
LOC283174	hypothetical LOC283174
LOC283663	hypothetical LOC283663
LOC283665	hypothetical protein LOC283665

Gene	**Gene description**
LOC283861	hypothetical locus LOC283861
LOC284033	hypothetical LOC284033
LOC284260	hypothetical gene supported by BC011527; BC021928; BC011527; BC021928
LOC284861	hypothetical gene supported by BC039313
LOC286071	hypothetical protein LOC286071
LOC286382	hypothetical protein LOC286382
LOC339260	hypothetical protein LOC339260
LOC339483	hypothetical LOC339483
LOC389023	hypothetical gene supported by BC032913; BC048425
LOC389043	hypothetical gene supported by AK125982; BC042817
LOC390595	similar to ubiquitin-associated protein 1 (predicted)
LOC390705	similar to protein phosphatase 2A 48 kDa regulatory subunit isoform 1; serine/threonine protein phosphatase 2A, 48kDa regulatory subunit; PP2A, subunit B, PR48 isoform; PP2A B subunit PR48; NY-REN-8 antigen
LOC400620	hypothetical LOC400620
LOC400655	hypothetical gene supported by BC013370; BC034583
LOC401097	Similar to LOC166075
LOC401317	hypothetical LOC401317
LOC440311	similar to P60
LOC441601	septin 7 pseudogene
LOC474358	hypothetical BC042079 locus
LOC54492	neuralized-2
LOC644192	hypothetical LOC644192
LOC644246	hypothetical protein LOC644246
LOC646471	hypothetical LOC646471
LOC646548	hypothetical LOC646548
LOC646627	phospholipase inhibitor
LOC646891	similar to serologically defined colon cancer antigen 3

Gene	**Gene description**
LOC647107	hypothetical protein LOC647107
LOC648795	hypothetical protein LOC648795
LOC653773	similar to mCG49427
LOC728323	hypothetical LOC728323
LOC728344	similar to hCG1978918
LOC728460	similar to FLJ32921 protein
LOC728516	hypothetical LOC728516
LOC728543	hypothetical protein LOC728543
LOC729082	hypothetical protein LOC729082
LOC729121	hypothetical protein LOC729121
LOC729915	hypothetical LOC729915
LOC729970	hypothetical LOC729970
LOC730834	similar to hCG1821160
LOC780529	hypothetical LOC780529
LOX	lysyl oxidase
LOXL4	lysyl oxidase-like 4
LPIN2	lipin 2
LRCH2	leucine-rich repeats and calponin homology (CH) domain containing 2
LRP1	low density lipoprotein-related protein 1 (alpha-2-macroglobulin receptor)
LRP1B	low density lipoprotein-related protein 1B (deleted in tumors)
LRRC27	leucine rich repeat containing 27
LRRC37A4	leucine rich repeat containing 37, member A4 (pseudogene)
LRRC48	leucine rich repeat containing 48
LRRCC1	leucine rich repeat and coiled-coil domain containing 1
LTBP1	latent transforming growth factor beta binding protein 1
LUM	lumican
LYPD2	LY6/PLAUR domain containing 2
LYPD6	LY6/PLAUR domain containing 6

Gene	**Gene description**
MACF1	microtubule-actin crosslinking factor 1
MAEL	maelstrom homolog (Drosophila)
MAL	mal, T-cell differentiation protein"
MAPK4	mitogen-activated protein kinase 4
MAPT	microtubule-associated protein tau
MARK1	MAP/microtubule affinity-regulating kinase 1
MARVELD3	MARVEL domain containing 3
MAS1	MAS1 oncogene
MBD3L2	methyl-CpG binding domain protein 3-like 2
MBP	myelin basic protein
MCHR2	melanin-concentrating hormone receptor 2
MCTP1	multiple C2 domains, transmembrane 1"
MDS1	myelodysplasia syndrome 1
MEG3	maternally expressed 3 (non-protein coding)
METTL7A	methyltransferase like 7A
MFAP5	microfibrillar associated protein 5
MGC16075	hypothetical protein MGC16075
MGC24103	hypothetical protein MGC24103
MGC39545	hypothetical protein LOC403312
MGC70870	C-terminal binding protein 2 pseudogene
MGEA5	meningioma expressed antigen 5 (hyaluronidase)
MIA2	melanoma inhibitory activity 2
MIER1	mesoderm induction early response 1 homolog (Xenopus laevis)
MLL	myeloid/lymphoid or mixed-lineage leukemia (trithorax homolog, Drosophila)"
MLLT4	myeloid/lymphoid or mixed-lineage leukemia (trithorax homolog, Drosophila); translocated to, 4"
MME	membrane metallo-endopeptidase
MMP12	matrix metallopeptidase 12 (macrophage elastase)
MMP16	matrix metallopeptidase 16 (membrane-inserted)

Gene	Gene description
MMP2	matrix metallopeptidase 2 (gelatinase A, 72kDa gelatinase, 72kDa type IV collagenase)"
MMP8	matrix metallopeptidase 8 (neutrophil collagenase)
MMP9	matrix metallopeptidase 9 (gelatinase B, 92kDa gelatinase, 92kDa type IV collagenase)"
MNT	MAX binding protein
MORN5	MORN repeat containing 5
MPP4	membrane protein, palmitoylated 4 (MAGUK p55 subfamily member 4)"
MPPED2	metallophosphoesterase domain containing 2
MRO	maestro
MSMB	microseminoprotein, beta-
MTHFR	5,10-methylenetetrahydrofolate reductase (NADPH)"
MTL5	metallothionein-like 5, testis-specific (tesmin)"
MTMR7	myotubularin related protein 7
MUC17	mucin 17, cell surface associated"
MXI1	MAX interactor 1
MYF6	myogenic factor 6 (herculin)
MYO16	myosin XVI
MYO3B	myosin IIIB
MYOM1	myomesin 1, 185kDa"
MYPN	myopalladin
N4BP2L1	NEDD4 binding protein 2-like 1
NAG20	NAG20
NAV2	neuron navigator 2
NBR1	neighbor of BRCA1 gene 1
NDRG2	NDRG family member 2
NECAB2	N-terminal EF-hand calcium binding protein 2
NEGR1	neuronal growth regulator 1
NEUROD4	neurogenic differentiation 4

Gene	**Gene description**
NFIB	nuclear factor I/B
NHEDC1	Na+/H+ exchanger domain containing 1
NIPBL	Nipped-B homolog (Drosophila)
NKX3-2	NK3 homeobox 2
NLRP13	NLR family, pyrin domain containing 13
NMNAT2	nicotinamide nucleotide adenylyltransferase 2
NMU	neuromedin U
NOTCH2NL	Notch homolog 2 (Drosophila) N-terminal like
NOX1	NADPH oxidase 1
NPTX1	neuronal pentraxin I
NR2F2	nuclear receptor subfamily 2, group F, member 2"
NR4A1	nuclear receptor subfamily 4, group A, member 1"
NR4A2	nuclear receptor subfamily 4, group A, member 2"
NRG2	neuregulin 2
NRIP2	nuclear receptor interacting protein 2
NRXN3	neurexin 3
NSUN7	NOL1/NOP2/Sun domain family, member 7"
NTN4	netrin 4
NTSR1	neurotensin receptor 1 (high affinity)
NUDT9P1	nudix (nucleoside diphosphate linked moiety X)-type motif 9 pseudogene 1
OCA2	oculocutaneous albinism II
OGN	osteoglycin
OIT3	oncoprotein induced transcript 3
OLFML2A	olfactomedin-like 2A
OLIG2	oligodendrocyte lineage transcription factor 2
OPRM1	opioid receptor, mu 1"
OR10T2	olfactory receptor, family 10, subfamily T, member 2
OR1E1	olfactory receptor, family 1, subfamily E, member 1
OR2C3	olfactory receptor, family 2, subfamily C, member 3"

Gene	**Gene description**
OR2L13	olfactory receptor, family 2, subfamily L, member 13
OR2S2	olfactory receptor, family 2, subfamily S, member 2"
OR2V2	olfactory receptor, family 2, subfamily V, member 2
OR4N4	olfactory receptor, family 4, subfamily N, member 4"
OR51E1	olfactory receptor, family 51, subfamily E, member 1"
OR51E2	olfactory receptor, family 51, subfamily E, member 2"
OR51Q1	olfactory receptor, family 51, subfamily Q, member 1"
OR52B2	olfactory receptor, family 52, subfamily B, member 2"
OR52K3P	olfactory receptor, family 52, subfamily K, member 3 pseudogene
OR5AK2	olfactory receptor, family 5, subfamily AK, member 2"
OSBPL2	oxysterol binding protein-like 2
OSTalpha	organic solute transporter alpha
OTX1	orthodenticle homeobox 1
OVOL1	ovo-like 1(Drosophila)
P2RY13	purinergic receptor P2Y, G-protein coupled, 13"
P2RY14	purinergic receptor P2Y, G-protein coupled, 14"
PABPC5	poly(A) binding protein, cytoplasmic 5"
PAOX	polyamine oxidase (exo-N4-amino)
PARVA	parvin, alpha"
PASD1	PAS domain containing 1
PAX3	paired box 3
PCDH11Y	protocadherin 11 Y-linked
PCDH18	protocadherin 18
PCDH21	protocadherin 21
PCDH7	protocadherin 7
PCDHB10	protocadherin beta 10
PCDHB5	protocadherin beta 5
PCDHGA9	protocadherin gamma subfamily A, 9
PCDHGB8P	protocadherin gamma subfamily B, 8 pseudogene"
PCMTD2	protein-L-isoaspartate (D-aspartate) O-methyltransferase domain

Gene	**Gene description**
	containing 2
PCNXL2	pecanex-like 2 (Drosophila)
PCSK2	proprotein convertase subtilisin/kexin type 2
PDC	phosducin
PDCD4	programmed cell death 4 (neoplastic transformation inhibitor)
PDCD4	programmed cell death 4 (neoplastic transformation inhibitor)
PDE1A	phosphodiesterase 1A, calmodulin-dependent
PDE4C	phosphodiesterase 4C, cAMP-specific (phosphodiesterase E1 dunce homolog, Drosophila)"
PDE4DIP	phosphodiesterase 4D interacting protein
PDE6A	phosphodiesterase 6A, cGMP-specific, rod, alpha
PDK4	pyruvate dehydrogenase kinase, isozyme 4"
PDLIM3	PDZ and LIM domain 3
PDZRN4	PDZ domain containing ring finger 4
PEX5L	peroxisomal biogenesis factor 5-like
PHACTR1	phosphatase and actin regulator 1
PHF12	PHD finger protein 12
PHLDB2	pleckstrin homology-like domain, family B, member 2"
PHYHD1	phytanoyl-CoA dioxygenase domain containing 1
PIM1	pim-1 oncogene
PIP	prolactin-induced protein
PITPNM2	phosphatidylinositol transfer protein, membrane-associated 2"
PKD1L1	polycystic kidney disease 1 like 1
PKHD1	polycystic kidney and hepatic disease 1 (autosomal recessive)
PKP1	plakophilin 1 (ectodermal dysplasia/skin fragility syndrome)
PLA2R1	phospholipase A2 receptor 1, 180kDa"
PLAT	plasminogen activator, tissue"
PLB1	phospholipase B1
PLCD4	phospholipase C, delta 4"
PLCH1	phospholipase C, eta 1"

Gene	**Gene description**
PLCZ1	phospholipase C, zeta 1"
PLD1	phospholipase D1, phosphatidylcholine-specific"
PLD3	phospholipase D family, member 3
PLEKHA6	pleckstrin homology domain containing, family A member 6
PLEKHH2	pleckstrin homology domain containing, family H (with MyTH4 domain) member 2"
PLGLB1	plasminogen-like B1
PLN	phospholamban
PLSCR2	phospholipid scramblase 2
PLSCR4	phospholipid scramblase 4
PM20D1	peptidase M20 domain containing 1
PMCH	pro-melanin-concentrating hormone
PMCHL1	pro-melanin-concentrating hormone-like 1
PNLIP	pancreatic lipase
PNPLA1	patatin-like phospholipase domain containing 1
PNRC1	proline-rich nuclear receptor coactivator 1
POLK	polymerase (DNA directed) kappa
PON3	paraoxonase 3
POTED	POTE ankyrin domain family, member D"
POTEE	POTE ankyrin domain family, member E"
POU4F2	POU class 4 homeobox 2
PP12708	hypothetical LOC100130609
PPAPDC1A	phosphatidic acid phosphatase type 2 domain containing 1A
PPIC	peptidylprolyl isomerase C (cyclophilin C)
PRICKLE2	prickle homolog 2 (Drosophila)
PRKAA2	protein kinase, AMP-activated, alpha 2 catalytic subunit"
PRO1596	hypothetical LOC29013
PRO2012	hypothetical protein PRO2012
PRODH2	proline dehydrogenase (oxidase) 2
PRR16	proline rich 16

Gene	**Gene description**
PRSS23	protease, serine, 23
PSORS1C1	psoriasis susceptibility 1 candidate 1
PTCH1	patched homolog 1 (Drosophila)
PTGER3	prostaglandin E receptor 3 (subtype EP3)
PTPRC	protein tyrosine phosphatase, receptor type, C"
PTPRZ1	protein tyrosine phosphatase, receptor-type, Z polypeptide 1"
PZP	pregnancy-zone protein
RAB37	RAB37, member RAS oncogene family"
RAB39	RAB39, member RAS oncogene family
RAB3C	RAB3C, member RAS oncogene family"
RAET1E	retinoic acid early transcript 1E
RAG1	recombination activating gene 1
RAMP1	receptor (G protein-coupled) activity modifying protein 1
RAVER2	ribonucleoprotein, PTB-binding 2"
RBMY1B	RNA binding motif protein, Y-linked, family 1, member B"
RBPMS2	RNA binding protein with multiple splicing 2
RERGL	RERG/RAS-like
REST	RE1-silencing transcription factor
RET	ret proto-oncogene
REXO1L1	REX1, RNA exonuclease 1 homolog (S. cerevisiae)-like 1"
RGNEF	Rho-guanine nucleotide exchange factor
RHO	rhodopsin
RHOT1	ras homolog gene family, member T1"
RIG	regulated in glioma
RIMBP3	RIMS binding protein 3
RIMS2	regulating synaptic membrane exocytosis 2
RIN2	Ras and Rab interactor 2
RIT2	Ras-like without CAAX 2
RLBP1L1	retinaldehyde binding protein 1-like 1
RND3	Rho family GTPase 3

Gene	**Gene description**
RNF125	ring finger protein 125
RNF128	ring finger protein 128
RNF133	ring finger protein 133
RNF175	ring finger protein 175
RNF8	ring finger protein 8
RORB	RAR-related orphan receptor B
RP11-218C14.6	cystatin pseudogene
RP11-327P2.4	hypothetical protein FLJ37307
RP1-21O18.1	kazrin
RP4-691N24.1	ninein-like
RP5-1022P6.2	hypothetical protein KIAA1434
RPS6KB1	ribosomal protein S6 kinase, 70kDa, polypeptide 1"
RUFY2	RUN and FYVE domain containing 2
RUNX1T1	runt-related transcription factor 1; translocated to, 1 (cyclin D-related)"
RUNX2	runt-related transcription factor 2
SALL3	sal-like 3 (Drosophila)
SCARNA17	small Cajal body-specific RNA 17
SCGN	secretagogin, EF-hand calcium binding protein"
SCN3B	sodium channel, voltage-gated, type III, beta
SCN8A	sodium channel, voltage gated, type VIII, alpha subunit
SEMA4C	sema domain, immunoglobulin domain (Ig), transmembrane domain (TM) and short cytoplasmic domain, (semaphorin) 4C"
SEMA5A	sema domain, seven thrombospondin repeats (type 1 and type 1-like), transmembrane domain (TM) and short cytoplasmic domain, (semaphorin) 5A"
SEMA6A	sema domain, transmembrane domain (TM), and cytoplasmic domain, (semaphorin) 6A"
SEMG2	semenogelin II
SERPINA10	serpin peptidase inhibitor, clade A (alpha-1 antiproteinase,

Gene	Gene description
	antitrypsin), member 10
SERPINB3	serpin peptidase inhibitor, clade B (ovalbumin), member 3"
SERPINB4	serpin peptidase inhibitor, clade B (ovalbumin), member 4
SERPIND1	serpin peptidase inhibitor, clade D (heparin cofactor), member 1
SERPINE1	serpin peptidase inhibitor, clade E (nexin, plasminogen activator inhibitor type 1), member 1"
SERTAD4	SERTA domain containing 4
SGCD	sarcoglycan, delta (35kDa dystrophin-associated glycoprotein)"
SGCZ	sarcoglycan zeta
SH3PXD2A	SH3 and PX domains 2A
SHANK3	SH3 and multiple ankyrin repeat domains 3
SHROOM2	shroom family member 2
SHROOM4	shroom family member 4
SIGLEC1	sialic acid binding Ig-like lectin 1, sialoadhesin
SIM2	single-minded homolog 2 (Drosophila)
SLC13A1	solute carrier family 13 (sodium/sulfate symporters), member 1"
SLC15A1	solute carrier family 15 (oligopeptide transporter), member 1"
SLC16A5	solute carrier family 16, member 5 (monocarboxylic acid transporter 6)
SLC18A1	solute carrier family 18 (vesicular monoamine), member 1"
SLC18A3	solute carrier family 18 (vesicular acetylcholine), member 3
SLC19A3	solute carrier family 19, member 3"
SLC22A18	solute carrier family 22, member 18"
SLC22A9	solute carrier family 22 (organic anion transporter), member 9
SLC25A27	solute carrier family 25, member 27"
SLC25A36	solute carrier family 25, member 36"
SLC35F3	solute carrier family 35, member F3
SLC38A3	solute carrier family 38, member 3"
SLC46A2	solute carrier family 46, member 2
SLC6A1	solute carrier family 6 (neurotransmitter transporter, GABA),

Gene	Gene description
	member 1"
SLC6A11	solute carrier family 6 (neurotransmitter transporter, GABA), member 11
SLC6A15	solute carrier family 6 (neutral amino acid transporter), member 15"
SLC6A19	solute carrier family 6 (neutral amino acid transporter), member 19"
SLCO1A2	solute carrier organic anion transporter family, member 1A2"
SLFN5	schlafen family member 5
SLITRK1	SLIT and NTRK-like family, member 1
SLITRK5	SLIT and NTRK-like family, member 5
SMA4	glucuronidase, beta pseudogene"
SMAD3	SMAD family member 3
SMG1	SMG1 homolog, phosphatidylinositol 3-kinase-related kinase (C. elegans)"
SMOC1	SPARC related modular calcium binding 1
SNIP	SNAP25-interacting protein
SNTB1	syntrophin, beta 1 (dystrophin-associated protein A1, 59kDa, basic component 1)"
SOCS2	suppressor of cytokine signaling 2
SORBS2	sorbin and SH3 domain containing 2
SOX11	SRY (sex determining region Y)-box 11
SOX21	SRY (sex determining region Y)-box 21
SOX7	SRY (sex determining region Y)-box 7
SOX7	SRY (sex determining region Y)-box 7
SP100	SP100 nuclear antigen
SPATA17	spermatogenesis associated 17
SPDYA	speedy homolog A (Xenopus laevis)
SPDYA	speedy homolog A (Xenopus laevis)
SPINLW1	serine peptidase inhibitor-like, with Kunitz and WAP domains 1 (eppin)"
SPOCK1	sparc/osteonectin, cwcv and kazal-like domains proteoglycan

Gene	**Gene description**
	(testican) 1"
SPP1	secreted phosphoprotein 1
SPRED2	sprouty-related, EVH1 domain containing 2"
SPRYD5	SPRY domain containing 5
SPSB3	splA/ryanodine receptor domain and SOCS box containing 3
SPTB	spectrin, beta, erythrocytic"
SSBP1	single-stranded DNA binding protein 1
SSPO	SCO-spondin homolog (Bos taurus)
SSTR1	somatostatin receptor 1
SSX4B	synovial sarcoma, X breakpoint 4B
SSX8	synovial sarcoma, X breakpoint 8"
ST3GAL6	ST3 beta-galactoside alpha-2,3-sialyltransferase 6
ST6GAL2	ST6 beta-galactosamide alpha-2,6-sialyltranferase 2"
STAG3L1	stromal antigen 3-like 1
STARD13	StAR-related lipid transfer (START) domain containing 13
STK31	serine/threonine kinase 31
STK32B	serine/threonine kinase 32B
STMN1	stathmin 1/oncoprotein 18
STMN3	stathmin-like 3
STON1-GTF2A1L	STON1-GTF2A1L readthrough transcript
STRA8	stimulated by retinoic acid gene 8 homolog (mouse)
STS	steroid sulfatase (microsomal), isozyme S"
STX1B	syntaxin 1B
SYCE2	synaptonemal complex central element protein 2
SYCP3	synaptonemal complex protein 3
SYNE2	spectrin repeat containing, nuclear envelope 2"
SYNPO2	synaptopodin 2
SYT14	synaptotagmin XIV
TACSTD2	tumor-associated calcium signal transducer 2

Gene	**Gene description**
tAKR	aldo-keto reductase, truncated"
TAOK1	TAO kinase 1
TAS2R42	taste receptor, type 2, member 42
TBX4	T-box 4
tcag7.977	hypothetical protein LOC730130
TCEA3	transcription elongation factor A (SII), 3
TCF12	transcription factor 12
TCL1B	T-cell leukemia/lymphoma 1B
TCTEX1D1	Tctex1 domain containing 1
TDH	L-threonine dehydrogenase
TEDDM1	transmembrane epididymal protein 1
TFAP2D	transcription factor AP-2 delta (activating enhancer binding protein 2 delta)
TGFB3	transforming growth factor, beta 3"
TGM4	transglutaminase 4 (prostate)
THPO	thrombopoietin
THRA	thyroid hormone receptor, alpha (erythroblastic leukemia viral (v-erb-a) oncogene homolog, avian)"
THSD7B	thrombospondin, type I, domain containing 7B"
TINAG	tubulointerstitial nephritis antigen
TLL1	tolloid-like 1
TLR4	toll-like receptor 4
TLR4	toll-like receptor 4
TLX1	T-cell leukemia homeobox 1
TM4SF18	transmembrane 4 L six family member 18
TM4SF4	transmembrane 4 L six family member 4
TMC3	transmembrane channel-like 3
TMEM146	transmembrane protein 146
TMEM37	transmembrane protein 37
TMEM45B	transmembrane protein 45B

Gene	**Gene description**
TMEM47	transmembrane protein 47
TMEM56	transmembrane protein 56
TMPRSS11A	transmembrane protease, serine 11A"
TNFAIP6	tumor necrosis factor, alpha-induced protein 6"
TNFRSF10C	tumor necrosis factor receptor superfamily, member 10c, decoy without an intracellular domain
TNFRSF19	tumor necrosis factor receptor superfamily, member 19"
TNRC4	trinucleotide repeat containing 4
TP73	tumor protein p73
TPSD1	tryptase delta 1
TRAM2	translocation associated membrane protein 2
TRIB1	tribbles homolog 1 (Drosophila)
TRIM22	tripartite motif-containing 22
TRIM34	tripartite motif-containing 34
TRIM49	tripartite motif-containing 49
TRIM6	tripartite motif-containing 6
TRIM72	tripartite motif-containing 72
TRIML1	tripartite motif family-like 1
TRIML2	tripartite motif family-like 2
TRPM1	transient receptor potential cation channel, subfamily M, member 1"
TRPV1	transient receptor potential cation channel, subfamily V, member 1"
TSPAN11	tetraspanin 11
TSPAN12	tetraspanin 12
TSPAN8	tetraspanin 8
TTC18	tetratricopeptide repeat domain 18
TTC23L	tetratricopeptide repeat domain 23-like
TTLL10	tubulin tyrosine ligase-like family, member 10"
TTN	titin
TTPA	tocopherol (alpha) transfer protein
TTTY2	testis-specific transcript, Y-linked 2 (non-protein coding)"

Gene	**Gene description**
TTTY8	testis-specific transcript, Y-linked 8"
TUSC5	tumor suppressor candidate 5
UACA	uveal autoantigen with coiled-coil domains and ankyrin repeats
UBE2R2	ubiquitin-conjugating enzyme E2R 2
UBN2	ubinuclein 2
UCA1	urothelial cancer associated 1
UGT3A1	UDP glycosyltransferase 3 family, polypeptide A1
ULK2	unc-51-like kinase 2 (C. elegans)
UNQ3028	TSSP3028
UNQ6484	ISPF6484
USP11	ubiquitin specific peptidase 11
UTS2	urotensin 2
UTS2D	urotensin 2 domain containing
VEZF1	vascular endothelial zinc finger 1
VISA	virus-induced signaling adapter
VN1R3	vomeronasal 1 receptor 3
VN1R4	vomeronasal 1 receptor 4
VSNL1	visinin-like 1
VWA1	von Willebrand factor A domain containing 1
VWA3B	von Willebrand factor A domain containing 3B
WASF2	WAS protein family, member 2"
WDR17	WD repeat domain 17
WDR40B	WD repeat domain 40B
WDR45	WD repeat domain 45
WDR49	WD repeat domain 49
WDR65	WD repeat domain 65
WDR72	WD repeat domain 72
WFDC11	WAP four-disulfide core domain 11
WFDC5	WAP four-disulfide core domain 5
WFDC6	WAP four-disulfide core domain 6

Gene	**Gene description**
WFDC9	WAP four-disulfide core domain 9
WNT8B	wingless-type MMTV integration site family, member 8B
WWP2	WW domain containing E3 ubiquitin protein ligase 2
XIRP2	xin actin-binding repeat containing 2
XRN1	5'-3' exoribonuclease 1
XYLB	xylulokinase homolog (H. influenzae)
YPEL1	yippee-like 1 (Drosophila)
YPEL2	yippee-like 2 (Drosophila)
YPEL5	yippee-like 5 (Drosophila)
ZADH2	zinc binding alcohol dehydrogenase domain containing 2
ZBTB10	zinc finger and BTB domain containing 10
ZBTB20	zinc finger and BTB domain containing 20
ZC3H6	zinc finger CCCH-type containing 6
ZC3H6	zinc finger CCCH-type containing 6
ZDHHC15	zinc finger, DHHC-type containing 15"
ZFYVE16	zinc finger, FYVE domain containing 16"
ZIC4	Zic family member 4
ZMAT1	zinc finger, matrin type 1"
ZNF292	zinc finger protein 292
ZNF385B	zinc finger protein 385B
ZNF445	zinc finger protein 445
ZNF45	zinc finger protein 45
ZNF471	zinc finger protein 471
ZNF572	zinc finger protein 572
ZNF695	zinc finger protein 695
ZNF704	zinc finger protein 704
ZNF711	zinc finger protein 711
ZNF804A	zinc finger protein 804A
ZNF81	zinc finger protein 81

Table 57 Genes that were downregulated by rapamycin in lymphocytes (downregulated in rapamycin-treated lymphocytes compared to untreated lymphocytes, FDR cut-off point of 10%) (95 genes)

Gene symbol	Gene description
40238	membrane-associated ring finger (C3HC4) 10
ACSL6	acyl-CoA synthetase long-chain family member 6
ADAMTS16	ADAM metallopeptidase with thrombospondin type 1 motif, 16"
AGT	angiotensinogen (serpin peptidase inhibitor, clade A, member 8)"
AHNAK2	AHNAK nucleoprotein 2
ANKRD42	ankyrin repeat domain 42
AP1S1	adaptor-related protein complex 1, sigma 1 subunit"
AQP9	aquaporin 9
AR	androgen receptor
ARHGAP28	Rho GTPase activating protein 28
AS3MT	arsenic (+3 oxidation state) methyltransferase
ATAD3B	ATPase family, AAA domain containing 3B"
BCCIP	BRCA2 and CDKN1A interacting protein
BSND	Bartter syndrome, infantile, with sensorineural deafness (Barttin)"
C17orf99	chromosome 17 open reading frame 99
C4orf26	chromosome 4 open reading frame 26
C5orf36	chromosome 5 open reading frame 36
C6orf168	chromosome 6 open reading frame 168
CACNA1D	calcium channel, voltage-dependent, L type, alpha 1D subunit"
CCL2	chemokine (C-C motif) ligand 2
CCL8	chemokine (C-C motif) ligand 8
CDCP2	CUB domain containing protein 2
COL1A2	collagen, type I, alpha 2"
COL8A2	collagen, type VIII, alpha 2"
CROT	carnitine O-octanoyltransferase
DYNC2LI1	dynein, cytoplasmic 2, light intermediate chain 1"
DYNC2LI1	dynein, cytoplasmic 2, light intermediate chain 1"

Gene symbol	**Gene description**
EGLN3	egl nine homolog 3 (C. elegans)
ENTPD8	ectonucleoside triphosphate diphosphohydrolase 8
FAM177A1	family with sequence similarity 177, member A1"
FAM27E3	family with sequence similarity 27, member E3"
FGF18	fibroblast growth factor 18
FGF2	fibroblast growth factor 2 (basic)
FJX1	four jointed box 1 (Drosophila)
FLJ32575	hypothetical protein FLJ32575
FLJ35946	hypothetical protein FLJ35946
FMN2	formin 2
FUT9	fucosyltransferase 9 (alpha (1,3) fucosyltransferase)"
G0S2	G0/G1switch 2
GABBR2	gamma-aminobutyric acid (GABA) B receptor, 2"
GABRA1	gamma-aminobutyric acid (GABA) A receptor, alpha 1"
GPAM	glycerol-3-phosphate acyltransferase, mitochondrial"
GPR34	G protein-coupled receptor 34
GRIA1	glutamate receptor, ionotropic, AMPA 1"
GSTM3	glutathione S-transferase mu 3 (brain)
HABP2	hyaluronan binding protein 2
HCK	hemopoietic cell kinase
IL10	interleukin 10
IL2	interleukin 2
IL3	interleukin 3 (colony-stimulating factor, multiple)"
IL31	interleukin 31
IL6	interleukin 6 (interferon, beta 2)"
INGX	inhibitor of growth family, X-linked, pseudogene"
INPP5E	inositol polyphosphate-5-phosphatase, 72 kDa"
KCNA3	potassium voltage-gated channel, shaker-related subfamily, member 3"
KL	klotho
KRT6B	keratin 6B

Gene symbol	**Gene description**
LOC100129522	similar to hCG1817212
LOC643014	similar to MDS025
LOC647946	hypothetical protein LOC647946
LOC647954	similar to keratin 8
LOXL3	lysyl oxidase-like 3
MGC29506	hypothetical protein MGC29506
MLF1	myeloid leukemia factor 1
MOXD1	monooxygenase, DBH-like 1"
MYCL1	v-myc myelocytomatosis viral oncogene homolog 1, lung carcinoma derived (avian)
MYOZ1	myozenin 1
NAV1	neuron navigator 1
ODF1	outer dense fiber of sperm tails 1
OR10J1	olfactory receptor, family 10, subfamily J, member 1
PDE8B	phosphodiesterase 8B
PES1	pescadillo homolog 1, containing BRCT domain (zebrafish)"
PHLDA3	pleckstrin homology-like domain, family A, member 3
PHYHIPL	phytanoyl-CoA 2-hydroxylase interacting protein-like
PRKG1	protein kinase, cGMP-dependent, type I"
PTGS2	prostaglandin-endoperoxide synthase 2 (prostaglandin G/H synthase and cyclooxygenase)
PYCR1	pyrroline-5-carboxylate reductase 1
RPL32P3	ribosomal protein L32 pseudogene 3
RRAD	Ras-related associated with diabetes
SGTA	small glutamine-rich tetratricopeptide repeat (TPR)-containing, alpha"
SLC4A2	solute carrier family 4, anion exchanger, member 2 (erythrocyte membrane protein band 3-like 1)"
ST6GALNAC2	ST6 (alpha-N-acetyl-neuraminyl-2,3-beta-galactosyl-1,3)-N-acetylgalactosaminide alpha-2,6-sialyltransferase 2"
TAC1	tachykinin, precursor 1

Gene symbol	**Gene description**
TFAP2A	transcription factor AP-2 alpha (activating enhancer binding protein 2 alpha)
THBS1	thrombospondin 1
TIMM17B	translocase of inner mitochondrial membrane 17 homolog B (yeast)
TIMP2	TIMP metallopeptidase inhibitor 2
TMEM192	transmembrane protein 192
TRPM6	transient receptor potential cation channel, subfamily M, member 6"
TXNRD2	thioredoxin reductase 2
UBE2M	ubiquitin-conjugating enzyme E2M (UBC12 homolog, yeast)"
UCP1	uncoupling protein 1 (mitochondrial, proton carrier)"
USP38	ubiquitin specific peptidase 38
VPS54	vacuolar protein sorting 54 homolog (S. cerevisiae)
ZCCHC12	zinc finger, CCHC domain containing 12"

Table 58 Established rapamycin-regulated genes (based on IPA Ingenuity) that were not differentially regulated in rapamycin-treated lymphocytes compared to control (38 genes)

Gene	Gene description
CLU	clusterin
DDIT4	DNA-damage-inducible transcript 4
EIF4A1	eukaryotic translation initiation factor 4A1
EIF4B	eukaryotic translation initiation factor 4B
EIF4E	eukaryotic translation initiation factor 4E
EIF4G1	eukaryotic translation initiation factor 4 gamma, 1
FKBP1A	FK506 binding protein 1A, 12kDa
HIF1A	hypoxia inducible factor 1, alpha subunit (basic helix-loop-helix transcription factor)
INS	insulin
INSR	insulin receptor
IRS1	insulin receptor substrate 1
KIAA1303	raptor
MAPK1	mitogen-activated protein kinase 1
MAPK3	mitogen-activated protein kinase 3
PDK1	pyruvate dehydrogenase kinase, isozyme 1
PLD1	phospholipase D1, phosphatidylcholine-specific
PLD2	phospholipase D2
PLD3	phospholipase D family, member 3
PLD4	phospholipase D family, member 4
PRKAA1	protein kinase, AMP-activated, alpha 1 catalytic subunit
PRKAA2	protein kinase, AMP-activated, alpha 2 catalytic subunit
PRKCA	protein kinase C, alpha
PRKCD	protein kinase C, delta
PRKCE	protein kinase C, epsilon
PRKCG	protein kinase C, gamma

Gene	**Gene description**
PRKCH	protein kinase C, eta
PRKCI	protein kinase C, iota
PRKCQ	protein kinase C, theta
PRKCZ	protein kinase C, zeta
RAC1	ras-related C3 botulinum toxin substrate 1 (rho family, small GTP binding protein Rac1)
RHEB	Ras homolog enriched in brain
RHO	rhodopsin
RICTOR	RPTOR independent companion of MTOR, complex 2
RPS6	ribosomal protein S6
RPS6KB2	ribosomal protein S6 kinase, 70kDa, polypeptide 2
TSC1	tuberous sclerosis 1
TSC2	tuberous sclerosis 2
VEGFA	vascular endothelial growth factor A

APPENDIX 7

ALTERED RAPAMYCIN RESPONSE ELEMENTS AS A RESULT OF MILD AD

Table 59 Differentially expressed transcripts in brain from mild AD patient (limbic stage: ApoE ε3/ε3) compared to brain from control subjects (entorhinal stage: ApoE ε3/ε3)

Gene	Gene description	Location	Type	Possible drug target	Possible biomarker	Drugs
CCL2	chemokine ligand 2	Extracellular Space	cytokine		x	
IL6	interleukin 6 (interferon, beta 2)	Extracellular Space	cytokine		x	tocilizumab
ENTPD8	ectonucleoside triphosphate diphosphohydrolase 8	unknown	enzyme	x		
LOXL4	lysyl oxidase-like 4	Extracellular	enzyme	x	x	

Gene	**Gene description**	**Location**	**Type**	**Possible drug target**	**Possible biomarker**	**Drugs**
		Space				
MOXD1	monooxygenase, DBH-like 1	Cytoplasm	enzyme	x		
PLD4	phospholipase D family, member 4	unknown	enzyme	x		
PRODH2	proline dehydrogenase (oxidase) 2	Cytoplasm	enzyme	x		
TGM4	transglutaminase 4 (prostate)	Extracellular Space	enzyme	x	x	
FN3K	fructosamine 3 kinase	unknown	kinase	x		
FAM64A	family with sequence similarity 64, member A	unknown	other			
FCGBP	Fc fragment of IgG binding protein	Extracellular Space	other		x	
SEMA4C	sema domain, immunoglobulin domain (Ig), transmembrane domain (TM) and short cytoplasmic domain, (semaphorin) 4C	Plasma Membrane	other			
DQ249310	urothelial cancer associated 1 (non-	unknown	other			

Gene	**Gene description**	**Location**	**Type**	**Possible drug target**	**Possible biomarker**	**Drugs**
	protein coding)					
ADAMTS2	ADAM metallopeptidase with thrombospondin type 1 motif, 2	Extracellular Space	peptidase	x	x	
HDAC5	histone deacetylase 5	Nucleus	transcription regulator			tributyrin, belinostat, pyroxamide, vorinostat, romidepsin
POU4F2	POU class 4 homeobox 2	Nucleus	transcription regulator			
RUNX1T1	runt-related transcription factor 1; translocated to, 1 (cyclin D-related)	Nucleus	transcription regulator			
SLC22A18	solute carrier family 22, member 18	Plasma Membrane	transporter	x		

APPENDIX 8

ALTERED RAPAMYCIN RESPONSE ELEMENTS AS A RESULTS OF ADVANCED AD

To identify rapamycin-regulated genes whose transcription is altered in advanced AD, gene transcripts in the frontal lobe of neocortical stage AD patients (ApoE ε3/ε3) were compared to gene transcriptions in frontal lobe of elderly control patients (ApoE ε3/ε3). Only ApoE ε3/ε3 patients were included in the analysis to eliminate any effect of the ApoE genotype.

Out of the 1172 rapamycin-regulated genes, SAM analysis identified 203 that were differentially expressed at RNA level in frontal lobe of advanced AD patients (neocortical stage) compared to controls (see Table 60). Genes for enzymes, growth factors, ion channels, receptors and transporters were marked as possible therapeutic targets; whereas genes for cytokines and proteins located in the extracellular space were marked as possible biomarkers of disease. Of the 203 genes: 79 were identified as possible drug targets, and 27 identified as possible biomarkers of disease (see Table 60). Existing drugs that target the possible drug targets are shown in Table 61.

The differentially expressed genes (Table 60) were further analysed with IPA to identify molecular and cellular functions (Table 62), diseases and disorders (Table 63) and physiological systems (Table 64) that were significantly associated with the different expressed genes.

IPA also identified a number of networks (Table 65) and pathways (Table 66) significantly associated with the differentially expressed genes Note that the score (x) in Table 65 is based on the right-tailed Fisher's exact test and represents a $1x10^{x}$ chance of the network having been randomly identified. The altered genes were strongly associated with all of the networks shown.

The differentially expressed genes included twelve (12) of the 159 genes that are known to be part of the mTOR signalling pathway, as identified by IPA Ingenuity (Table 67).

Table 60 Differentially expressed transcripts in brain from advanced AD patient (Neocortical stage: ApoE ε3/ε3) relative to control (entorhinal stage: ApoE ε3/ε3)

Gene	Gene description	Location	Type	Possible drug target	Possible bio-marker
LOX	lysyl oxidase	Extracellular Space	enzyme	x	X
LOXL3	lysyl oxidase-like 3	Extracellular Space	enzyme	x	X
TGM4	transglutaminase 4 (prostate)	Extracellular Space	enzyme	x	X
BMP7	bone morphogenetic protein 7	Extracellular Space	growth factor	x	X
FGF11	fibroblast growth factor 11	Extracellular Space	growth factor	x	X
FGF7	fibroblast growth factor 7	Extracellular Space	growth factor	x	X
VEGFA	vascular endothelial growth factor A	Extracellular Space	growth factor	x	X
CSN2	casein beta	Extracellular Space	kinase	x	X
ADAMTS2	ADAM metallopeptidase with thrombospondin type 1 motif, 2	Extracellular Space	peptidase	x	X
CPXM2	carboxypeptidase X (M14 family), member 2	Extracellular Space	peptidase	x	X
MMP16	matrix metallopeptidase 16 (membrane-inserted)	Extracellular Space	peptidase	x	X
PLAT	plasminogen activator, tissue	Extracellular Space	peptidase	x	X

Gene	**Gene description**	**Location**	**Type**	**Possible drug target**	**Possible bio-marker**
ACPP	acid phosphatase, prostate	Extracellular Space	phosphatase	x	X
CCL11	chemokine (C-C motif) ligand 11	Extracellular Space	cytokine		X
CCL2	chemokine (C-C motif) ligand 2	Extracellular Space	cytokine		X
IL18	interleukin 18 (interferon-gamma-inducing factor)	Extracellular Space	cytokine		X
IL1B	interleukin 1, beta	Extracellular Space	cytokine		X
IL6	interleukin 6 (interferon, beta 2)	Extracellular Space	cytokine		X
SPRED2	sprouty-related, EVH1 domain containing 2	Extracellular Space	cytokine		X
CARD14	caspase recruitment domain family, member 14	Cytoplasm	other		
CCNB2	cyclin B2	Cytoplasm	other		
CEP68	centrosomal protein 68kDa	Cytoplasm	other		
DAOA	D-amino acid oxidase activator	Cytoplasm	other		
DYNC2LI1	dynein, cytoplasmic 2, light intermediate chain 1	Cytoplasm	other		
ELAVL4	ELAV (embryonic lethal, abnormal vision, Drosophila)-like 4 (Hu antigen D)	Cytoplasm	other		
GAB1	GRB2-associated binding protein 1	Cytoplasm	other		
IRS2	insulin receptor substrate 2	Cytoplasm	other		

Gene	**Gene description**	**Location**	**Type**	**Possible drug target**	**Possible bio-marker**
MACF1	microtubule-actin crosslinking factor 1	Cytoplasm	other		
PEX5L	peroxisomal biogenesis factor 5-like	Cytoplasm	other		
PLN	phospholamban	Cytoplasm	other		
RPTOR	regulatory associated protein of MTOR, complex 1	Cytoplasm	other		
SGTA	small glutamine-rich tetratricopeptide repeat (TPR)-containing, alpha	Cytoplasm	other		
STARD13	StAR-related lipid transfer (START) domain containing 13	Cytoplasm	other		
SYNPO2	synaptopodin 2	Cytoplasm	other		
TSC2	tuberous sclerosis 2	Cytoplasm	other		
ADAMTSL5	ADAMTS-like 5	Extracellular Space	other		X
CGA	glycoprotein hormones, alpha polypeptide	Extracellular Space	other		X
CLU	clusterin	Extracellular Space	other		X
CRP	C-reactive protein, pentraxin-related	Extracellular Space	other		X
DCD	dermcidin	Extracellular Space	other		X

Gene	Gene description	Location	Type	Possible drug target	Possible bio-marker
FAM12B	epididymal protein 3B	Extracellular Space	other		X
FBLN1	fibulin 1	Extracellular Space	other		X
FCGBP	Fc fragment of IgG binding protein	Extracellular Space	other		
FJX1	four jointed box 1 (Drosophila)	Extracellular Space	other		
MFAP5	microfibrillar associated protein 5	Extracellular Space	other		
SERPIND1	serpin peptidase inhibitor, clade D (heparin cofactor), member 1	Extracellular Space	other		
SERPINE1	serpin peptidase inhibitor, clade E (nexin, plasminogen activator inhibitor type 1), member 1	Extracellular Space	other		
THBS1	thrombospondin 1	Extracellular Space	other		
TIMP2	TIMP metallopeptidase inhibitor 2	Extracellular Space	other		
TNFAIP6	tumor necrosis factor, alpha-induced protein 6	Extracellular Space	other		
WFDC11	WAP four-disulfide core domain 11	Extracellular Space	other		
ATAD3B	ATPase family, AAA domain containing 3B	Nucleus	other		
BCCIP	BRCA2 and CDKN1A interacting protein	Nucleus	other		
MIER1	mesoderm induction early response 1 homolog (Xenopus	Nucleus	other		

Gene	Gene description	Location	Type	Possible drug target	Possible bio-marker
	laevis)				
NAV2	neuron navigator 2	Nucleus	other		
NIPBL	Nipped-B homolog (Drosophila)	Nucleus	other		
SORBS2	sorbin and SH3 domain containing 2	Nucleus	other		
ZNF385B	zinc finger protein 385B	Nucleus	other		
ZNF711	zinc finger protein 711	Nucleus	other		
CEACAM6	carcinoembryonic antigen-related cell adhesion molecule 6 (non-specific cross reacting antigen)	Plasma Membrane	other		
COL13A1	collagen, type XIII, alpha 1	Plasma Membrane	other		
DRP2	dystrophin related protein 2	Plasma Membrane	other		
HHIP	hedgehog interacting protein	Plasma Membrane	other		
LILRB2	leukocyte immunoglobulin-like receptor, subfamily B (with TM and ITIM domains), member 2	Plasma Membrane	other		
SEMA4C	sema domain, immunoglobulin domain (Ig), transmembrane domain (TM) and short cytoplasmic domain, (semaphorin) 4C	Plasma Membrane	other		

Gene	Gene description	Location	Type	Possible drug target	Possible bio-marker
SNTB1	syntrophin, beta 1 (dystrophin-associated protein A1, 59kDa, basic component 1)	Plasma Membrane	other		
TACSTD2	tumor-associated calcium signal transducer 2	Plasma Membrane	other		
TSPAN8	tetraspanin 8	Plasma Membrane	other		
AHNAK2	AHNAK nucleoprotein 2	unknown	other		
ANKRD36B	ankyrin repeat domain 36B	unknown	other		
ATRNL1	attractin-like 1	unknown	other		
AUTS2	autism susceptibility candidate 2	unknown	other		
BTNL9	butyrophilin-like 9	unknown	other		
C11orf67	chromosome 11 open reading frame 67	unknown	other		
C16orf75	chromosome 16 open reading frame 75	unknown	other		
C18orf26	chromosome 18 open reading frame 26	unknown	other		
C1orf127	chromosome 1 open reading frame 127	unknown	other		
C3orf70	chromosome 3 open reading frame 70	unknown	other		
C4orf22	chromosome 4 open reading frame 22	unknown	other		

Gene	Gene description	Location	Type	Possible drug target	Possible bio-marker
C4orf26	chromosome 4 open reading frame 26	unknown	other		
C7orf41	chromosome 7 open reading frame 41	unknown	other		
CC2D2A	coiled-coil and C2 domain containing 2A	unknown	other		
WDR40B	DDB1 and CUL4 associated factor 12-like 1	unknown	other		
DNAH6	dynein, axonemal, heavy chain 6	unknown	other		
FAM155A	family with sequence similarity 155, member A	unknown	other		
FAM177A1	family with sequence similarity 177, member A1	unknown	other		
FAM64A	family with sequence similarity 64, member A	unknown	other		
FAT3	FAT tumor suppressor homolog 3 (Drosophila)	unknown	other		
GSG1L	GSG1-like	unknown	other		
HHIPL1	HHIP-like 1	unknown	other		
HIST1H4E	histone cluster 1, H4e	unknown	other		
HRASLS5	HRAS-like suppressor family, member 5	unknown	other		
HYDIN	hydrocephalus inducing homolog (mouse)	unknown	other		
IFFO1	intermediate filament family orphan 1	unknown	other		
KCTD19	potassium channel tetramerisation domain containing 19	unknown	other		

Gene	Gene description	Location	Type	Possible drug target	Possible bio-marker
KLHL24	kelch-like 24 (Drosophila)	unknown	other		
KRT72	keratin 72	unknown	other		
KRTAP9-2	keratin associated protein 9-2	unknown	other		
LYPD2	LY6/PLAUR domain containing 2	unknown	other		
MBD3L2	methyl-CpG binding domain protein 3-like 2	unknown	other		
MCTP1	multiple C2 domains, transmembrane 1	unknown	other		
NBR1	neighbor of BRCA1 gene 1	unknown	other		
OLFML2A	olfactomedin-like 2A	unknown	other		
PCDHGA9	protocadherin gamma subfamily A, 9	unknown	other		
PHLDA3	pleckstrin homology-like domain, family A, member 3	unknown	other		
PSORS1C1	psoriasis susceptibility 1 candidate 1	unknown	other		
SLITRK1	SLIT and NTRK-like family, member 1	unknown	other		
SLITRK5	SLIT and NTRK-like family, member 5	unknown	other		
SPRYD5	SPRY domain containing 5	unknown	other		
SSX8	synovial sarcoma, X breakpoint 8	unknown	other		
STAG3L1	stromal antigen 3-like 1	unknown	other		

Gene	**Gene description**	**Location**	**Type**	**Possible drug target**	**Possible bio-marker**
TM4SF18	transmembrane 4 L six family member 18	unknown	other		
TMEM56	transmembrane protein 56	unknown	other		
UBN2	ubinuclein 2	unknown	other		
ZC3H6	zinc finger CCCH-type containing 6	unknown	other		
DHRS3	dehydrogenase/reductase (SDR family) member 3	Cytoplasm	enzyme	x	
DZIP3	DAZ interacting protein 3, zinc finger	Cytoplasm	enzyme	x	
EGLN3	egl nine homolog 3 (C. elegans)	Cytoplasm	enzyme	x	
FKBP1A	FK506 binding protein 1A, 12kDa	Cytoplasm	enzyme	x	
GBP3	guanylate binding protein 3	Cytoplasm	enzyme	x	
MOXD1	monooxygenase, DBH-like 1	Cytoplasm	enzyme	x	
PLCH1	phospholipase C, eta 1	Cytoplasm	enzyme	x	
PRODH2	proline dehydrogenase (oxidase) 2	Cytoplasm	enzyme	x	
RAB3C	RAB3C, member RAS oncogene family	Cytoplasm	enzyme	x	
RAC1	ras-related C3 botulinum toxin substrate 1 (rho family, small GTP binding protein Rac1)	Cytoplasm	enzyme	x	
RND3	Rho family GTPase 3	Cytoplasm	enzyme	x	

Gene	**Gene description**	**Location**	**Type**	**Possible drug target**	**Possible bio-marker**
RNF128	ring finger protein 128	Cytoplasm	enzyme	x	
STS	steroid sulfatase (microsomal), isozyme S	Cytoplasm	enzyme	x	
TXNRD2	thioredoxin reductase 2	Cytoplasm	enzyme	x	
POLK	polymerase (DNA directed) kappa	Nucleus	enzyme	x	
YPEL1	yippee-like 1 (Drosophila)	Nucleus	enzyme	x	
AASDH	aminoadipate-semialdehyde dehydrogenase	unknown	enzyme	x	
DSEL	dermatan sulfate epimerase-like	unknown	enzyme	x	
ENTPD8	ectonucleoside triphosphate diphosphohydrolase 8	unknown	enzyme	x	
PLD4	phospholipase D family, member 4	unknown	enzyme	x	
CCR1	chemokine (C-C motif) receptor 1	Plasma Membrane	G-protein coupled receptor	x	
CCR2	chemokine (C-C motif) receptor 2	Plasma Membrane	G-protein coupled receptor	x	
GABBR2	gamma-aminobutyric acid (GABA) B receptor, 2	Plasma Membrane	G-protein	x	

Gene	Gene description	Location	Type	Possible drug target	Possible bio-marker
			coupled receptor		
GLP1R	glucagon-like peptide 1 receptor	Plasma Membrane	G-protein coupled receptor	x	
GPR34	G protein-coupled receptor 34	Plasma Membrane	G-protein coupled receptor	x	
NTSR1	neurotensin receptor 1 (high affinity)	Plasma Membrane	G-protein coupled receptor	x	
OR51E2	olfactory receptor, family 51, subfamily E, member 2	Plasma Membrane	G-protein coupled receptor	x	
RHO	rhodopsin	Plasma Membrane	G-protein coupled	x	

Gene	**Gene description**	**Location**	**Type**	**Possible drug target**	**Possible bio-marker**
			receptor		
CACNA1D	calcium channel, voltage-dependent, L type, alpha 1D subunit	Plasma Membrane	ion channel	x	
CFTR	cystic fibrosis transmembrane conductance regulator (ATP-binding cassette sub-family C, member 7)	Plasma Membrane	ion channel	x	
GLRA1	glycine receptor, alpha 1	Plasma Membrane	ion channel	x	
GRIK2	glutamate receptor, ionotropic, kainate 2	Plasma Membrane	ion channel	x	
KCNAB1	potassium voltage-gated channel, shaker-related subfamily, beta member 1	Plasma Membrane	ion channel	x	
KCND2	potassium voltage-gated channel, Shal-related subfamily, member 2	Plasma Membrane	ion channel	x	
KCNG4	potassium voltage-gated channel, subfamily G, member 4	Plasma Membrane	ion channel	x	
KCNIP2	Kv channel interacting protein 2	Plasma Membrane	ion channel	x	
SCN8A	sodium channel, voltage gated, type VIII, alpha subunit	Plasma Membrane	ion channel	x	
STX1B	syntaxin 1B	Plasma Membrane	ion channel	x	
DCLK1	doublecortin-like kinase 1	Cytoplasm	kinase	x	

Gene	Gene description	Location	Type	Possible drug target	Possible bio-marker
MAPK1	mitogen-activated protein kinase 1	Cytoplasm	kinase	x	
MAPK4	mitogen-activated protein kinase 4	Cytoplasm	kinase	x	
MARK1	MAP/microtubule affinity-regulating kinase 1	Cytoplasm	kinase	x	
PIM1	pim-1 oncogene	Cytoplasm	kinase	x	
PRKCH	protein kinase C, eta	Cytoplasm	kinase	x	
RPS6KB2	ribosomal protein S6 kinase, 70kDa, polypeptide 2	Cytoplasm	kinase	x	
SMG1	SMG1 homolog, phosphatidylinositol 3-kinase-related kinase (C. elegans)	Cytoplasm	kinase	x	
TAOK1	TAO kinase 1	Cytoplasm	kinase	x	
TRIB1	tribbles homolog 1 (Drosophila)	Cytoplasm	kinase	x	
FGR	Gardner-Rasheed feline sarcoma viral (v-fgr) oncogene homolog	Nucleus	kinase	x	
DLG2	discs, large homolog 2 (Drosophila)	Plasma Membrane	kinase	x	
FGFR1	fibroblast growth factor receptor 1	Plasma Membrane	kinase	x	
FN3K	fructosamine 3 kinase	unknown	kinase	x	
FBP2	fructose-1,6-bisphosphatase 2	Cytoplasm	phosphatase	x	

Gene	**Gene description**	**Location**	**Type**	**Possible drug target**	**Possible bio-marker**
CTDSP1	CTD (carboxy-terminal domain, RNA polymerase II, polypeptide A) small phosphatase 1	Nucleus	phosphatase	x	
CD69	CD69 molecule	Plasma Membrane	transmembrane receptor	x	
CHRNA9	cholinergic receptor, nicotinic, alpha 9	Plasma Membrane	transmembrane receptor	x	
SEMA5A	sema domain, seven thrombospondin repeats (type 1 and type 1-like), transmembrane domain (TM) and short cytoplasmic domain, (semaphorin) 5A	Plasma Membrane	transmembrane receptor	x	
AP1S1	adaptor-related protein complex 1, sigma 1 subunit	Cytoplasm	transporter	x	
ATP8B3	ATPase, aminophospholipid transporter, class I, type 8B, member 3	Cytoplasm	transporter	x	
SLC25A27	solute carrier family 25, member 27	Cytoplasm	transporter	x	
ZFYVE16	zinc finger, FYVE domain containing 16	Nucleus	transporter	x	
BPI	bactericidal/permeability-increasing protein	Plasma Membrane	transporter	x	
SLC18A3	solute carrier family 18 (vesicular acetylcholine), member	Plasma Membrane	transporter	x	

Gene	Gene description	Location	Type	Possible drug target	Possible bio-marker
	3				
SLC22A18	solute carrier family 22, member 18	Plasma Membrane	transporter	x	
SLC38A3	solute carrier family 38, member 3	Plasma Membrane	transporter	x	
SLC4A2	solute carrier family 4, anion exchanger, member 2 (erythrocyte membrane protein band 3-like 1)	Plasma Membrane	transporter	x	
ATF7IP	activating transcription factor 7 interacting protein	Nucleus	transcription regulator		
BARX2	BARX homeobox 2	Nucleus	transcription regulator		
BCOR	BCL6 corepressor	Nucleus	transcription regulator		
BNC1	basonuclin 1	Nucleus	transcription regulator		
CREB3L4	cAMP responsive element binding protein 3-like 4	Nucleus	transcription regulator		
GLI2	GLI family zinc finger 2	Nucleus	transcription		

Gene	**Gene description**	**Location**	**Type**	**Possible drug target**	**Possible bio-marker**
			regulator		
HDAC5	histone deacetylase 5	Nucleus	transcription regulator		
HDAC9	histone deacetylase 9	Nucleus	transcription regulator		
HOXD10	homeobox D10	Nucleus	transcription regulator		
IRX4	iroquois homeobox 4	Nucleus	transcription regulator		
KANK2	KN motif and ankyrin repeat domains 2	Nucleus	transcription regulator		
KLF2	Kruppel-like factor 2 (lung)	Nucleus	transcription regulator		
MNT	MAX binding protein	Nucleus	transcription regulator		
MYF6	myogenic factor 6 (herculin)	Nucleus	transcription		

Gene	Gene description	Location	Type	Possible drug target	Possible bio-marker
			regulator		
NFIB	nuclear factor I/B	Nucleus	transcription regulator		
NKX3-2	NK3 homeobox 2	Nucleus	transcription regulator		
POU4F2	POU class 4 homeobox 2	Nucleus	transcription regulator		
RUNX1T1	runt-related transcription factor 1; translocated to, 1 (cyclin D-related)	Nucleus	transcription regulator		
SMAD3	SMAD family member 3	Nucleus	transcription regulator		
SOX21	SRY (sex determining region Y)-box 21	Nucleus	transcription regulator		
EIF4A1	eukaryotic translation initiation factor 4A1	Cytoplasm	translation regulator		
EIF4E	eukaryotic translation initiation factor 4E	Cytoplasm	translation		

Gene	**Gene description**	**Location**	**Type**	**Possible drug target**	**Possible bio-marker**
			regulator		

Table 61 Existing drugs that target the genes identified as possible drug targets for advanced AD (neocortical stage: ApoE ε3/ε3) relative to control (entorhinal stage: ApoE ε3/ε3)

Gene symbol	Drugs
CHRNA9	ABT-089, isoflurane, mecamylamine, succinylcholine, rocuronium, doxacurium, amobarbital, mivacurium, pipecuronium, rapacuronium, metocurine, atracurium, cisatracurium, acetylcholine, nicotine, D-tubocurarine, arecoline, enflurane, pancuronium, vecuronium
VEGFA	bevacizumab, ranibizumab, aflibercept, pegaptanib
NTSR1	contulakin-G
FKBP1A	everolimus
GLP1R	liraglutide, T-0632, GLP-1 (7-36) amide, exenatide
CACNA1D	MEM-1003, clevidipine butyrate, mibefradil, bepridil, nisoldipine, isradipine, nicardipine
FGFR1	pazopanib
SCN8A	riluzole
CFTR	SP 303
STS	STX 64

Table 62 Molecular and cellular functions significantly associated with the differentially expressed transcripts in advanced AD brain (neocortical stage: ApoE ε3/ε3 genotype) relative to control (entorhinal stage: ApoE ε3/ε3 genotype)

Molecular and cellular functions	**p-value**	**Number of Genes**
Cellular Movement	<0.05	28
Cellular Growth and Proliferation	<0.05	29
Cell Signaling	<0.05	17
Small Molecule Biochemistry	<0.05	30
Vitamin and Mineral Metabolism	<0.05	14

Table 63 Diseases and disorders significantly associated with the differentially expressed transcripts in advanced AD brain (neocortical stage: ApoE ε3/ε3 genotype) relative to control (entorhinal stage: ApoE ε3/ε3 genotype)

Diseases and disorders	**p-value**	**Number of genes**
Cardiovascular Disease	<0.05	56
Inflammatory Response	<0.05	23
Hematological Disease	<0.05	21
Infectious Disease	<0.05	26
Inflammatory Disease	<0.05	57

Table 64 Physiological systems significantly associated with the differentially expressed transcripts in advanced AD brain (neocortical stage: ApoE ε3/ε3 genotype) relative to control (entorhinal stage: ApoE ε3/ε3 genotype)

Physiological system development and function	p-value	Number of genes
Tissue development	<0.05	22
Cardiovascular system development and function	<0.05	17
Organismal development	<0.05	19
Tumour morphology	<0.05	7
Immune cell trafficking	<0.05	15

Table 65 Networks significantly associated with the differentially expressed transcripts in advanced AD brain (neocortical stage: ApoE ε3/ε3 genotype) relative to control (entorhinal stage: ApoE ε3/ε3 genotype)

Network	Number of molecules	Score	Top functions
1	18	30	Cancer, Tissue Morphology, Carbohydrate Metabolism
2	17	26	Cancer, Renal and Urological Disease, Gastrointestinal Disease
3	14	21	Gene Expression, Cellular Development, Connective Tissue Development and Function

Network	**Number of molecules**	**Score**	**Top functions**
4	15	21	Cellular Movement, Skeletal and Muscular System Development and Function, Hematological System Development and Function
5	13	19	Cell Morphology, Cellular Development, Cardiovascular System Development and Function
6	12	17	Inflammatory Response, Cellular Movement, Hematological System Development and Function
7	11	16	DNA Replication, Recombination, and Repair, Nucleic Acid Metabolism, Small Molecule Biochemistry
8	11	15	Cell Morphology, Cellular Function and Maintenance, Reproductive System Development and Function
9	12	15	Cellular Assembly and Organization, Cell Morphology, Cellular Development
10	10	14	Amino Acid Metabolism, Increased Levels of AST, Increased Levels of Alkaline Phosphatase
11	10	13	Gene Expression, Endocrine System Development and Function, Tissue Morphology
12	9	12	Cellular Development, Cellular Growth and Proliferation, Hair and Skin Development and Function

Table 66 Canonical pathways associated with the differentially expressed transcripts in advanced AD brain (neocortical stage: ApoE ε3/ε3 genotype) relative to control (entorhinal stage: ApoE ε3/ε3 genotype)

Canonical pathway	**p-value**
mTOR Signaling	<0.001
TREM1 Signaling	<0.001
FGF Signaling	<0.001
Insulin Receptor Signaling	<0.001
Role of Hypercytokinemia/ hyperchemokinemia in the Pathogenesis of Influenza	<0.001

Table 67 Differentially expressed genes that are established members of the mTOR signalling pathway as defined by IPA Ingenuity (differentially expressed in advanced AD brain (neocortical: ApoE ε3/ε3) relative to control (entorhinal: ApoE ε3/ε3)).

Symbol	Entrez Gene Name	Location	Type(s)
EIF4A1	eukaryotic translation initiation factor 4A1	Cytoplasm	translation regulator
EIF4E	eukaryotic translation initiation factor 4E	Cytoplasm	translation regulator
FKBP1A	FK506 binding protein 1A, 12kDa	Cytoplasm	enzyme
MAPK1	mitogen-activated protein kinase 1	Cytoplasm	kinase
PLD4	phospholipase D family, member 4	unknown	enzyme
PRKCH	protein kinase C, eta	Cytoplasm	kinase
RAC1	ras-related C3 botulinum toxin substrate 1 (rho family, small GTP binding protein Rac1)	Cytoplasm	enzyme
RND3	Rho family GTPase 3	Cytoplasm	enzyme
RPS6KB2	ribosomal protein S6 kinase, 70kDa, polypeptide 2	Cytoplasm	kinase
RPTOR	regulatory associated protein of MTOR, complex 1	Cytoplasm	other
TSC2	tuberous sclerosis 2	Cytoplasm	other
VEGFA	vascular endothelial growth factor A	Extracellular Space	growth factor

APPENDIX 9

ALTERED RAPAMYCIN RESPONSE ELEMENTS AS A RESULT OF ADVANCED AD AND APOE ε4

To identify rapamycin-regulated genes whose transcription is altered as a result of advanced AD (AD neocortical stage) and ApoE ε4, gene transcripts in the frontal lobe of advanced AD patients (neocortical stage: ApoE ε3/ε4) were compared to gene transcripts in the frontal lobe of control subjects (ApoE ε3/ε3).

Of the 1172 identified rapamycin-regulated genes, SAM analysis identified 168 that were differentially expressed in advanced AD (neocortical stage: ApoE ε3/ε4) compared to control (ApoE ε3/ε3) (Table 68). Genes for enzymes, growth factors, ion channels, receptors and transporters were marked as possible drug targets; whereas genes for cytokines, and proteins located in the extracellular space were marked as possible biomarkers of disease. Of the 168 differentially expressed genes, 69 were identified as possible drug targets, and 27 identified as possible biomarkers of disease (Table 68). Eleven (11) drugs target the identified possible drug targets (Table 69).

The differentially expressed genes were further analysed with IPA to identify molecular and cellular functions (Table 70), diseases and disorders (Table 71), and physiological systems (Table 72) that are significantly associated with the differentially expressed genes. A

number of networks (Table 73) and pathways (Table 74) were also significantly associated with the differentially expressed genes. Note that the score (x) in Table 73 is based on the right-tailed Fisher's exact test and represents a $1x10^{x}$ chance of the network having been randomly identified.

The differentially expressed genes included 10 of the 159 well established genes of the mTOR signalling pathway (as identified by IPA Ingenuity) (Table 75).

Table 68 Differentially expressed transcripts in frontal lobe of advanced AD patients (neocortical stage: ApoE ε3/ε4) compared to control (ApoE ε3/ε3)

Gene	Gene description	Location	Type	Possible drug target	Possible bio-marker
TGM4	transglutaminase 4 (prostate)	Extracellular Space	enzyme	x	X
LOXL4	lysyl oxidase-like 4	Extracellular Space	enzyme	x	X
VEGFA	vascular endothelial growth factor A	Extracellular Space	growth factor	x	X
FGF11	fibroblast growth factor 11	Extracellular Space	growth factor	x	X
BMP7	bone morphogenetic protein 7	Extracellular Space	growth factor	x	X
CSN2	casein beta	Extracellular Space	kinase	x	X
PCSK2	proprotein convertase subtilisin/kexin type 2	Extracellular Space	peptidase	x	X
MMP16	matrix metallopeptidase 16 (membrane-inserted)	Extracellular Space	peptidase	x	X
CPXM2	carboxypeptidase X (M14 family), member 2	Extracellular Space	peptidase	x	X
ADAMTS2	ADAM metallopeptidase with thrombospondin type 1 motif, 2	Extracellular Space	peptidase	x	X
SPRED2	sprouty-related, EVH1 domain containing 2	Extracellular Space	cytokine		X
IL6	interleukin 6 (interferon, beta 2)	Extracellular Space	cytokine		X

Gene	**Gene description**	**Location**	**Type**	**Possible drug target**	**Possible bio-marker**
CCL2	chemokine (C-C motif) ligand 2	Extracellular Space	cytokine		X
CCL1	chemokine (C-C motif) ligand 1	Extracellular Space	cytokine		X
VSNL1	visinin-like 1	Cytoplasm	other		
TSC2	tuberous sclerosis 2	Cytoplasm	other		
STARD13	StAR-related lipid transfer (START) domain containing 13	Cytoplasm	other		
SGTA	small glutamine-rich tetratricopeptide repeat (TPR)-containing, alpha	Cytoplasm	other		
SCGN	secretagogin, EF-hand calcium binding protein	Cytoplasm	other		
RIMS2	regulating synaptic membrane exocytosis 2	Cytoplasm	other		
PEX5L	peroxisomal biogenesis factor 5-like	Cytoplasm	other		
KIAA1683	KIAA1683	Cytoplasm	other		
IRS2	insulin receptor substrate 2	Cytoplasm	other		
GFAP	glial fibrillary acidic protein	Cytoplasm	other		
ELAVL4	ELAV (embryonic lethal, abnormal vision, Drosophila)-like 4 (Hu antigen D)	Cytoplasm	other		

Gene	**Gene description**	**Location**	**Type**	**Possible drug target**	**Possible bio-marker**
DYNC2LI1	dynein, cytoplasmic 2, light intermediate chain 1	Cytoplasm	other		
CPLX2	complexin 2	Cytoplasm	other		
CEP68	centrosomal protein 68kDa	Cytoplasm	other		
ABLIM2	actin binding LIM protein family, member 2	Cytoplasm	other		
WFDC6	WAP four-disulfide core domain 6	Extracellular Space	other		X
SERPINE1	serpin peptidase inhibitor, clade E (nexin, plasminogen activator inhibitor type 1), member 1	Extracellular Space	other		X
SERPIND1	serpin peptidase inhibitor, clade D (heparin cofactor), member 1	Extracellular Space	other		X
NPTX1	neuronal pentraxin I	Extracellular Space	other		X
NEGR1	neuronal growth regulator 1	Extracellular Space	other		X
LECT1	leukocyte cell derived chemotaxin 1	Extracellular Space	other		X
FJX1	four jointed box 1 (Drosophila)	Extracellular Space	other		X
DEFB119	defensin, beta 119	Extracellular Space	other		X
DCD	dermcidin	Extracellular Space	other		X
CYR61	cysteine-rich, angiogenic inducer, 61	Extracellular Space	other		X

Gene	**Gene description**	**Location**	**Type**	**Possible drug target**	**Possible bio-marker**
CRP	C-reactive protein, pentraxin-related	Extracellular Space	other		X
CLU	clusterin	Extracellular Space	other		X
ADAMTSL5	ADAMTS-like 5	Extracellular Space	other		X
ZBTB20	zinc finger and BTB domain containing 20	Nucleus	other		
SORBS2	sorbin and SH3 domain containing 2	Nucleus	other		
PNRC1	proline-rich nuclear receptor coactivator 1	Nucleus	other		
ELAVL3	ELAV (embryonic lethal, abnormal vision, Drosophila)-like 3 (Hu antigen C)	Nucleus	other		
ATAD3B	ATPase family, AAA domain containing 3B	Nucleus	other		
SEMA4C	sema domain, immunoglobulin domain (Ig), transmembrane domain (TM) and short cytoplasmic domain, (semaphorin) 4C	Plasma Membrane	other		
DRP2	dystrophin related protein 2	Plasma Membrane	other		
CEACAM6	carcinoembryonic antigen-related cell adhesion molecule 6 (non-specific cross reacting antigen)	Plasma Membrane	other		
CDH13	cadherin 13, H-cadherin (heart)	Plasma Membrane	other		

Gene	**Gene description**	**Location**	**Type**	**Possible drug target**	**Possible bio-marker**
ZCCHC12	zinc finger, CCHC domain containing 12	unknown	other		
ZC3H6	zinc finger CCCH-type containing 6	unknown	other		
YPEL5	yippee-like 5 (Drosophila)	unknown	other		
DQ249310	urothelial cancer associated 1 (non-protein coding)	unknown	other		
TMEM56	transmembrane protein 56	unknown	other		
TM4SF18	transmembrane 4 L six family member 18	unknown	other		
STAG3L1	stromal antigen 3-like 1	unknown	other		
SLITRK1	SLIT and NTRK-like family, member 1	unknown	other		
SLC35F3	solute carrier family 35, member F3	unknown	other		
PHYHD1	phytanoyl-CoA dioxygenase domain containing 1	unknown	other		
PHLDA3	pleckstrin homology-like domain, family A, member 3	unknown	other		
PCDHGA9	protocadherin gamma subfamily A, 9	unknown	other		
MEG3	maternally expressed 3 (non-protein coding)	unknown	other		
MCTP1	multiple C2 domains, transmembrane 1	unknown	other		
LYPD2	LY6/PLAUR domain containing 2	unknown	other		

Gene	**Gene description**	**Location**	**Type**	**Possible drug target**	**Possible bio-marker**
KLHL24	kelch-like 24 (Drosophila)	unknown	other		
ITGBL1	integrin, beta-like 1 (with EGF-like repeat domains)	unknown	other		
HYDIN	hydrocephalus inducing homolog (mouse)	unknown	other		
HIST1H4E	histone cluster 1, H4e	unknown	other		
HHIPL1	HHIP-like 1	unknown	other		
GIGYF1	GRB10 interacting GYF protein 1	unknown	other		
LRRC37A4	leucine rich repeat containing 37, member A4 (pseudogene)	unknown	other		
FBXL16	F-box and leucine-rich repeat protein 16	unknown	other		
FAT3	FAT tumor suppressor homolog 3 (Drosophila)	unknown	other		
FAM64A	family with sequence similarity 64, member A	unknown	other		
FAM171B	family with sequence similarity 171, member B	unknown	other		
FAM155A	family with sequence similarity 155, member A	unknown	other		
DNAH6	dynein, axonemal, heavy chain 6	unknown	other		
WDR40B	DDB1 and CUL4 associated factor 12-like 1	unknown	other		

Gene	**Gene description**	**Location**	**Type**	**Possible drug target**	**Possible bio-marker**
CCDC85A	coiled-coil domain containing 85A	unknown	other		
CCDC28A	coiled-coil domain containing 28A	unknown	other		
CC2D2A	coiled-coil and C2 domain containing 2A	unknown	other		
C1orf127	chromosome 1 open reading frame 127	unknown	other		
C18orf26	chromosome 18 open reading frame 26	unknown	other		
C17orf99	chromosome 17 open reading frame 99	unknown	other		
C16orf75	chromosome 16 open reading frame 75	unknown	other		
BTNL9	butyrophilin-like 9	unknown	other		
ATRNL1	attractin-like 1	unknown	other		
ANKRD36B	ankyrin repeat domain 36B	unknown	other		
KIAA1641	ankyrin repeat domain 36B	unknown	other		
AHNAK2	AHNAK nucleoprotein 2	unknown	other		
ACTRT1	actin-related protein T1	unknown	other		
UBE2M	ubiquitin-conjugating enzyme E2M (UBC12 homolog, yeast)	Cytoplasm	enzyme	x	
RNF128	ring finger protein 128	Cytoplasm	enzyme	x	

Gene	**Gene description**	**Location**	**Type**	**Possible drug target**	**Possible bio-marker**
RAB3C	RAB3C, member RAS oncogene family	Cytoplasm	enzyme	x	
PTGS2	prostaglandin-endoperoxide synthase 2 (prostaglandin G/H synthase and cyclooxygenase)	Cytoplasm	enzyme	x	
PRODH2	proline dehydrogenase (oxidase) 2	Cytoplasm	enzyme	x	
PAOX	polyamine oxidase (exo-N4-amino)	Cytoplasm	enzyme	x	
NMNAT2	nicotinamide nucleotide adenylyltransferase 2	Cytoplasm	enzyme	x	
MOXD1	monooxygenase, DBH-like 1	Cytoplasm	enzyme	x	
HMGCS2	3-hydroxy-3-methylglutaryl-CoA synthase 2 (mitochondrial)	Cytoplasm	enzyme	x	
GALNT10	UDP-N-acetyl-alpha-D-galactosamine:polypeptide N-acetylgalactosaminyltransferase 10 (GalNAc-T10)	Cytoplasm	enzyme	x	
FKBP1A	FK506 binding protein 1A, 12kDa	Cytoplasm	enzyme	x	
DZIP3	DAZ interacting protein 3, zinc finger	Cytoplasm	enzyme	x	
ACSL6	acyl-CoA synthetase long-chain family member 6	Cytoplasm	enzyme	x	
YPEL1	yippee-like 1 (Drosophila)	Nucleus	enzyme	x	

Gene	**Gene description**	**Location**	**Type**	**Possible drug target**	**Possible bio-marker**
GNG8	guanine nucleotide binding protein (G protein), gamma 8	Plasma Membrane	enzyme	x	
PLD4	phospholipase D family, member 4	unknown	enzyme	x	
PDE8B	phosphodiesterase 8B	unknown	enzyme	x	
ENTPD8	ectonucleoside triphosphate diphosphohydrolase 8	unknown	enzyme	x	
SSTR1	somatostatin receptor 1	Plasma Membrane	G-protein coupled receptor	x	
OR52B2	olfactory receptor, family 52, subfamily B, member 2	Plasma Membrane	G-protein coupled receptor	x	
NTSR1	neurotensin receptor 1 (high affinity)	Plasma Membrane	G-protein coupled receptor	x	
GPR176	G protein-coupled receptor 176	Plasma Membrane	G-protein coupled receptor	x	
GPR109B	G protein-coupled receptor 109B	Plasma Membrane	G-protein coupled receptor	x	
GABBR2	gamma-aminobutyric acid (GABA) B receptor, 2	Plasma Membrane	G-protein	x	

Gene	**Gene description**	**Location**	**Type**	**Possible drug target**	**Possible bio-marker**
			coupled receptor		
CCR1	chemokine (C-C motif) receptor 1	Plasma Membrane	G-protein coupled receptor	x	
KCNG4	potassium voltage-gated channel, subfamily G, member 4	Cytoplasm	ion channel	x	
TRPV1	transient receptor potential cation channel, subfamily V, member 1	Plasma Membrane	ion channel	x	
STX1B	syntaxin 1B	Plasma Membrane	ion channel	x	
SCN8A	sodium channel, voltage gated, type VIII, alpha subunit	Plasma Membrane	ion channel	x	
KCND2	potassium voltage-gated channel, Shal-related subfamily, member 2	Plasma Membrane	ion channel	x	
KCNAB1	potassium voltage-gated channel, shaker-related subfamily, beta member 1	Plasma Membrane	ion channel	x	
GRIA2	glutamate receptor, ionotropic, AMPA 2	Plasma Membrane	ion channel	x	
CACNA1D	calcium channel, voltage-dependent, L type, alpha	Plasma Membrane	ion channel	x	

Gene	**Gene description**	**Location**	**Type**	**Possible drug target**	**Possible bio-marker**
	1D subunit				
TAOK1	TAO kinase 1	Cytoplasm	kinase	x	
RPS6KB2	ribosomal protein S6 kinase, 70kDa, polypeptide 2	Cytoplasm	kinase	x	
PRKCI	protein kinase C, iota	Cytoplasm	kinase	x	
PRKCH	protein kinase C, eta	Cytoplasm	kinase	x	
PRKCA	protein kinase C, alpha	Cytoplasm	kinase	x	
PIM1	pim-1 oncogene	Cytoplasm	kinase	x	
MAPK4	mitogen-activated protein kinase 4	Cytoplasm	kinase	x	
MAPK1	mitogen-activated protein kinase 1	Cytoplasm	kinase	x	
DCLK1	doublecortin-like kinase 1	Cytoplasm	kinase	x	
DLG2	discs, large homolog 2 (Drosophila)	Plasma Membrane	kinase	x	
ACVR2B	activin A receptor, type IIB	Plasma Membrane	kinase	x	
FN3K	fructosamine 3 kinase	unknown	kinase	x	
RORB	RAR-related orphan receptor B	Nucleus	ligand-dependent nuclear receptor	x	
CTDSP1	CTD (carboxy-terminal domain, RNA polymerase	Nucleus	phosphatase	x	

Gene	**Gene description**	**Location**	**Type**	**Possible drug target**	**Possible bio-marker**
	II, polypeptide A) small phosphatase 1				
TNFRSF10C	tumor necrosis factor receptor superfamily, member 10c, decoy without an intracellular domain	Plasma Membrane	transmembrane receptor	x	
SEMA5A	sema domain, seven thrombospondin repeats (type 1 and type 1-like), transmembrane domain (TM) and short cytoplasmic domain, (semaphorin) 5A	Plasma Membrane	transmembrane receptor	x	
TIMM17B	translocase of inner mitochondrial membrane 17 homolog B (yeast)	Cytoplasm	transporter	x	
SLC25A27	solute carrier family 25, member 27	Cytoplasm	transporter	x	
AP1S1	adaptor-related protein complex 1, sigma 1 subunit	Cytoplasm	transporter	x	
SLC6A15	solute carrier family 6 (neutral amino acid transporter), member 15	Plasma Membrane	transporter	x	
SLC6A11	solute carrier family 6 (neurotransmitter transporter, GABA), member 11	Plasma Membrane	transporter	x	
SLC38A3	solute carrier family 38, member 3	Plasma Membrane	transporter	x	
SLC22A18	solute carrier family 22, member 18	Plasma Membrane	transporter	x	

Gene	**Gene description**	**Location**	**Type**	**Possible drug target**	**Possible bio-marker**
SLC18A3	solute carrier family 18 (vesicular acetylcholine), member 3	Plasma Membrane	transporter	x	
BPI	bactericidal/permeability-increasing protein	Plasma Membrane	transporter	x	
CDCP2	CUB domain containing protein 2	unknown	transporter	x	
SMAD3	SMAD family member 3	Nucleus	transcription regulator		
RUNX1T1	runt-related transcription factor 1; translocated to, 1 (cyclin D-related)	Nucleus	transcription regulator		
POU4F2	POU class 4 homeobox 2	Nucleus	transcription regulator		
MYF6	myogenic factor 6 (herculin)	Nucleus	transcription regulator		
EVI1	MDS1 and EVI1 complex locus	Nucleus	transcription regulator		
KLF2	Kruppel-like factor 2 (lung)	Nucleus	transcription regulator		

Gene	**Gene description**	**Location**	**Type**	**Possible drug target**	**Possible bio-marker**
HDAC5	histone deacetylase 5	Nucleus	transcription regulator		
GLI2	GLI family zinc finger 2	Nucleus	transcription regulator		
EGR1	early growth response 1	Nucleus	transcription regulator		
CREB3L4	cAMP responsive element binding protein 3-like 4	Nucleus	transcription regulator		
BCOR	BCL6 co-repressor	Nucleus	transcription regulator		
BARX2	BARX homeobox 2	Nucleus	transcription regulator		
ATF7IP	activating transcription factor 7 interacting protein	Nucleus	transcription regulator		
EIF4E	eukaryotic translation initiation factor 4E	Cytoplasm	translation regulator		

Gene	**Gene description**	**Location**	**Type**	**Possible drug target**	**Possible bio-marker**
ABTB1	ankyrin repeat and BTB (POZ) domain containing 1	Cytoplasm	translation regulator		
BRUNOL4	CUGBP, Elav-like family member 4	Nucleus	translation regulator		

Table 69 Existing drugs that target the genes identified as possible drug targets for advanced AD (neocortical stage: ApoE ε3/ε4) compared to control (entorhinal stage: ApoE ε3/ε3)

Gene symbol	Drugs
PTGS2	5-aminosalicylic acid, acetaminophen, aspirin, balsalazide, bromfenac, butalbital, caffeine, carisoprodol, celecoxib, chlorpheniramine, clemastine, codeine, dexbrompheniramine, diclofenac, diflunisal, dihydrocodeine, dipyridamole, dipyrone, etodolac, fenoprofen, GW406381X, hydrocodone, ibuprofen, indomethacin, ketoprofen, ketorolac, licofelone, meclofenamic acid, mefenamic acid, meloxicam, menatetrenone, meprobamate, methocarbamol, misoprostol, nabumetone, naproxen, nitroaspirin, orphenadrine, oxycodone, pentazocine, phenacetin, phenylephrine, piroxicam, pravastatin, propoxyphene, propoxyphene, pseudoephedrine, racemic flurbiprofen, rofecoxib, salicylic acid, sulfasalazine, sulindac, sumatriptan, tolmetin, tramadol, valdecoxib, zomepirac
VEGFA	bevacizumab, ranibizumab, aflibercept, pegaptanib
NTSR1	contulakin-G
FKBP1A	everolimus
PRKCA	L-threo-safingol
CACNA1D	MEM-1003, clevidipine butyrate, mibefradil, bepridil, nisoldipine, isradipine, nicardipine
SSTR1	pasireotide, octreotide

Gene symbol	**Drugs**
SCN8A	riluzole
TRPV1	SB-705498, capsaicin
GRIA2	talampanel, Org 24448, LY451395, tezampanel
SLC6A11	tiagabine

Table 70 Molecular and cellular functions significantly associated with the genes identified to be differentially expressed in advanced AD brain (neocortical stage: ApoE ε3/ε4) compared to control (ApoE ε3/ε3)

Molecular and Cellular Functions	p-value	Number of Genes
Cellular Growth and Proliferation	<0.05	40
Cellular Movement	<0.05	29
Cellular Development	<0.05	27
Cell-To-Cell Signalling and Interaction	<0.05	33
Cell Death	<0.05	33

Table 71 Diseases and disorders significantly associated with the genes identified to be differentially expressed in advanced AD brain (neocortical stage: ApoE ε3/ε4) compared to control (ApoE ε3/ε3)

Diseases and Disorders	p-value	Number of Genes
Neurological Disease	<0.05	68
Genetic Disorder	<0.05	95
Cancer	<0.05	53
Cardiovascular Disease	<0.05	45
Endocrine System Disorders	<0.05	42

Table 72 Physiological systems significantly associated with the genes identified to be differentially expressed in advanced AD brain (neocortical stage: ApoE ε3/ε4) compared to control (ApoE ε3/ε3)

Physiological system development and function	p-value	Number of Genes
Organismal development	<0.05	13
Lymphoid tissue structure and function	<0.05	7
Cardiovascular system development and function	<0.05	15
Skeletal and muscular system development and function	<0.05	12
Tissue development	<0.05	24

Table 73 Top networks associated with the genes identified to be differentially expressed in advanced AD brain (ApoE ε3/ε4) compared to control (ApoEε3/ε3)

Network	Score	Focus Molecules	Top Functions
1	27	16	Organismal Development, Tissue Development, Cell Morphology
2	25	15	Cell Signaling, Cellular Function and Maintenance, Molecular Transport
3	25	15	Renal and Urological Disease, Embryonic Development, Tissue Development
4	24	16	Cell Cycle, Hair and Skin Development and Function, Cell-To-Cell Signaling and Interaction
5	19	12	Cellular Development, Nervous System Development and Function, Inflammatory Response
6	19	12	Cell Signaling, DNA Replication, Recombination, and Repair, Nucleic Acid Metabolism
7	17	11	Auditory and Vestibular System Development and Function, Organ Development, Organ Morphology
8	15	10	Cellular Function and Maintenance, Skeletal and Muscular System Development and Function, Cell Cycle
9	11	9	Gene Expression, Cancer, Cell Cycle
10	7	6	Lipid Metabolism, Small Molecule Biochemistry, Cell Signaling

Table 74 Canonical pathways significantly associated with the genes identified to be differentially expressed in advanced AD brain (ApoE ε3/ε4) compared to control (ApoEε3/ε3)

Canonical pathway	**p-value**
mTOR Signaling	<0.001
Corticotropin Releasing Hormone Signaling	<0.001
Thrombopoietin Signaling	<0.001
Insulin Receptor Signaling	<0.001
Fcγ Receptor-mediated Phagocytosis in Macrophages and Monocytes	<0.001

Table 75 Established mTOR signalling genes that were differentially expressed in advanced AD brain (ApoE ε3/ε4) compared to control (ApoE ε3/ε3)

Symbol	Entrez Gene Name	Location	Type(s)
EIF4E	eukaryotic translation initiation factor 4E	Cytoplasm	translation regulator
FKBP1A	FK506 binding protein 1A, 12kDa	Cytoplasm	enzyme
MAPK1	mitogen-activated protein kinase 1	Cytoplasm	kinase
PLD4	phospholipase D family, member 4	unknown	enzyme
PRKCA	protein kinase C, alpha	Cytoplasm	kinase
PRKCH	protein kinase C, eta	Cytoplasm	kinase
PRKCI	protein kinase C, iota	Cytoplasm	kinase
RPS6KB2	ribosomal protein S6 kinase, 70kDa, polypeptide 2	Cytoplasm	kinase
TSC2	tuberous sclerosis 2	Cytoplasm	other
VEGFA	vascular endothelial growth factor	Extracellular Space	growth factor

Symbol	**Entrez Gene Name**	**Location**	**Type(s)**
	A		
EIF4E	eukaryotic translation initiation factor 4E	Cytoplasm	translation regulator
FKBP1A	FK506 binding protein 1A, 12kDa	Cytoplasm	enzyme

APPENDIX 10

ALTERED RAPAMYCIN RESPONSE ELEMENTS AS A RESULT OF ADVANCED AD ONLY

Table 76 Genes that were differentially expressed as a result of advanced AD only (genes that were differentially expressed in advanced AD (ApoE ε3/ε4) compared to control (ApoE ε3/ε3) AND differentially expressed in advanced AD (ApoE ε3/ε3) compared to control (ApoE ε3/ε3))

Gene ID	Full name	Location	Type	Possible drug targets	Possible bio-markers
ADAMTS2	ADAM metallopeptidase with thrombospondin type 1 motif, 2	Extracellular Space	peptidase	x	x
ADAMTSL5	ADAMTS-like 5	Extracellular Space	other		x
AHNAK2	AHNAK nucleoprotein 2	unknown	other		
	ankyrin repeat domain 36B	unknown	other		

Gene ID	**Full name**	**Location**	**Type**	**Possible drug targets**	**Possible bio-markers**
ANKRD36B					
AP1S1	adaptor-related protein complex 1, sigma 1 subunit	Cytoplasm	transporter	x	
ATAD3B	ATPase family, AAA domain containing 3B	Nucleus	other		
ATF7IP	activating transcription factor 7 interacting protein	Nucleus	transcription regulator		
ATRNL1	attractin-like 1	unknown	other		x
BARX2	BARX homeobox 2	Nucleus	transcription regulator		
BCOR	BCL6 corepressor	Nucleus	transcription regulator		
BMP7	bone morphogenetic protein 7	Extracellular Space	growth factor	x	x
BPI	bactericidal/permeability-increasing protein	Plasma Membrane	transporter	x	
BTNL9	butyrophilin-like 9	unknown	other		
C16orf75	chromosome 16 open reading frame 75	unknown	other		
C18orf26	chromosome 18 open reading frame 26	unknown	other		
C1orf127	chromosome 1 open reading frame 127	unknown	other		

Gene ID	Full name	Location	Type	Possible drug targets	Possible bio-markers
CACNA1D	calcium channel, voltage-dependent, L type, alpha 1D subunit	Plasma Membrane	ion channel	x	
CC2D2A	coiled-coil and C2 domain containing 2A	unknown	other		
CCL2	chemokine (C-C motif) ligand 2	Extracellular Space	cytokine		x
CCR1	chemokine (C-C motif) receptor 1	Plasma Membrane	G-protein coupled receptor	x	
CEACAM6	carcinoembryonic antigen-related cell adhesion molecule 6 (non-specific cross reacting antigen)	Plasma Membrane	other		
CEP68	centrosomal protein 68kDa	Cytoplasm	other		
CLU	clusterin	Extracellular Space	other		X
CPXM2	carboxypeptidase X (M14 family), member 2	Extracellular Space	peptidase	x	X
CREB3L4	cAMP responsive element binding protein 3-like 4	Nucleus	transcription regulator		
CRP	C-reactive protein, pentraxin-related	Extracellular Space	other		x
CSN2	casein beta	Extracellular Space	kinase	x	x
CTDSP1	CTD (carboxy-terminal domain, RNA polymerase II,	Nucleus	phosphatase	x	

Gene ID	Full name	Location	Type	Possible drug targets	Possible bio-markers
	polypeptide A) small phosphatase 1				
DCD	dermcidin	Extracellular Space	other		x
DCLK1	doublecortin-like kinase 1	Cytoplasm	kinase	x	
DLG2	discs, large homolog 2 (Drosophila)	Plasma Membrane	kinase	x	
DNAH6	dynein, axonemal, heavy chain 6	unknown	other		
DRP2	dystrophin related protein 2	Plasma Membrane	other		
DYNC2LI1	dynein, cytoplasmic 2, light intermediate chain 1	Cytoplasm	other		
DZIP3	DAZ interacting protein 3, zinc finger	Cytoplasm	enzyme	x	
EIF4E	eukaryotic translation initiation factor 4E	Cytoplasm	translation regulator		
ELAVL4	ELAV (embryonic lethal, abnormal vision, Drosophila)-like 4 (Hu antigen D)	Cytoplasm	other		
ENTPD8	ectonucleoside triphosphate diphosphohydrolase 8	unknown	enzyme	x	
FAM155A	family with sequence similarity 155, member A	unknown	other		
FAM64A	family with sequence similarity 64, member A	unknown	other		
FAT3	FAT tumor suppressor homolog 3 (Drosophila)	unknown	other		

Gene ID	Full name	Location	Type	Possible drug targets	Possible bio-markers
FGF11	fibroblast growth factor 11	Extracellular Space	growth factor	x	x
FJX1	four jointed box 1 (Drosophila)	Extracellular Space	other		x
FKBP1A	FK506 binding protein 1A, 12kDa	Cytoplasm	enzyme	x	
FN3K	fructosamine 3 kinase	unknown	kinase	x	
GABBR2	gamma-aminobutyric acid (GABA) B receptor, 2	Plasma Membrane	G-protein coupled receptor	x	
GLI2	GLI family zinc finger 2	Nucleus	transcription regulator		
HDAC5	histone deacetylase 5	Nucleus	transcription regulator		
HHIPL1	HHIP-like 1	unknown	other		
HIST1H4E	histone cluster 1, H4e	unknown	other		
HYDIN	hydrocephalus inducing homolog (mouse)	unknown	other		
IL6	interleukin 6 (interferon, beta 2)	Extracellular Space	cytokine		x
IRS2	insulin receptor substrate 2	Cytoplasm	other		
KCNAB1	potassium voltage-gated channel, shaker-related	Plasma Membrane	ion channel	x	

Gene ID	Full name	Location	Type	Possible drug targets	Possible bio-markers
	subfamily, beta member 1				
KCND2	potassium voltage-gated channel, Shal-related subfamily, member 2	Plasma Membrane	ion channel	x	
KCNG4	potassium voltage-gated channel, subfamily G, member 4	Plasma Membrane	ion channel	x	
KLF2	Kruppel-like factor 2 (lung)	Nucleus	transcription regulator		
KLHL24	kelch-like 24 (Drosophila)	unknown	other		
LYPD2	LY6/PLAUR domain containing 2	unknown	other		
MAPK1	mitogen-activated protein kinase 1	Cytoplasm	kinase	x	
MAPK4	mitogen-activated protein kinase 4	Cytoplasm	kinase	x	
MCTP1	multiple C2 domains, transmembrane 1	unknown	other		
MMP16	matrix metallopeptidase 16 (membrane-inserted)	Extracellular Space	peptidase	x	x
MOXD1	monooxygenase, DBH-like 1	Cytoplasm	enzyme	x	
MYF6	myogenic factor 6 (herculin)	Nucleus	transcription regulator		

Gene ID	Full name	Location	Type	Possible drug targets	Possible bio-markers
NTSR1	neurotensin receptor 1 (high affinity)	Plasma Membrane	G-protein coupled receptor	x	
PCDHGA9	protocadherin gamma subfamily A, 9	unknown	other		
PEX5L	peroxisomal biogenesis factor 5-like	Cytoplasm	other		
PHLDA3	pleckstrin homology-like domain, family A, member 3	unknown	other		
PIM1	pim-1 oncogene	Cytoplasm	kinase	x	
PLD4	phospholipase D family, member 4	unknown	enzyme	x	
POU4F2	POU class 4 homeobox 2	Nucleus	transcription regulator		
PRKCH	protein kinase C, eta	Cytoplasm	kinase	x	
PRODH2	proline dehydrogenase (oxidase) 2	Cytoplasm	enzyme	x	
RAB3C	RAB3C, member RAS oncogene family	Cytoplasm	enzyme	x	
RNF128	ring finger protein 128	Cytoplasm	enzyme	x	
RPS6KB2	ribosomal protein S6 kinase, 70kDa, polypeptide 2	Cytoplasm	kinase	x	
RUNX1T1	runt-related transcription factor 1; translocated to, 1 (cyclin D-related)	Nucleus	transcription regulator		

Gene ID	Full name	Location	Type	Possible drug targets	Possible bio-markers
SCN8A	sodium channel, voltage gated, type VIII, alpha subunit	Plasma Membrane	ion channel	x	
SEMA4C	sema domain, immunoglobulin domain (Ig), transmembrane domain (TM) and short cytoplasmic domain, (semaphorin) 4C	Plasma Membrane	other		
SEMA5A	sema domain, seven thrombospondin repeats (type 1 and type 1-like), transmembrane domain (TM) and short cytoplasmic domain, (semaphorin) 5A	Plasma Membrane	transmembrane receptor	x	
SERPIND1	serpin peptidase inhibitor, clade D (heparin cofactor), member 1	Extracellular Space	other		x
SERPINE1	serpin peptidase inhibitor, clade E (nexin, plasminogen activator inhibitor type 1), member 1	Extracellular Space	other		x
SGTA	small glutamine-rich tetratricopeptide repeat (TPR)-containing, alpha	Cytoplasm	other		
SLC18A3	solute carrier family 18 (vesicular acetylcholine), member 3	Plasma Membrane	transporter	x	
SLC22A18	solute carrier family 22, member 18	Plasma Membrane	transporter	x	

Gene ID	Full name	Location	Type	Possible drug targets	Possible bio-markers
SLC25A27	solute carrier family 25, member 27	Cytoplasm	transporter	x	
SLC38A3	solute carrier family 38, member 3	Plasma Membrane	transporter	x	
SLITRK1	SLIT and NTRK-like family, member 1	unknown	other		
SMAD3	SMAD family member 3	Nucleus	transcription regulator		
SORBS2	sorbin and SH3 domain containing 2	Nucleus	other		
SPRED2	sprouty-related, EVH1 domain containing 2	Extracellular Space	cytokine		x
STAG3L1	stromal antigen 3-like 1	unknown	other		
STARD13	StAR-related lipid transfer (START) domain containing 13	Cytoplasm	other		
STX1B	syntaxin 1B	Plasma Membrane	ion channel	x	
TAOK1	TAO kinase 1	Cytoplasm	kinase	x	
TGM4	transglutaminase 4 (prostate)	Extracellular Space	enzyme	x	x
TM4SF18	transmembrane 4 L six family member 18	unknown	other		
TMEM56	transmembrane protein 56	unknown	other		
TSC2	tuberous sclerosis 2	Cytoplasm	other		

Gene ID	Full name	Location	Type	Possible drug targets	Possible bio-markers
VEGFA	vascular endothelial growth factor A	Extracellular Space	growth factor	x	x
WDR40B	DDB1 and CUL4 associated factor 12-like 1	unknown	other		
YPEL1	yippee-like 1 (Drosophila)	Nucleus	enzyme	x	
ZC3H6	zinc finger CCCH-type containing 6	unknown	other		

Table 77 Drugs that target the genes identified as differentially expressed as a result of advanced AD only

Gene symbol	Drugs
VEGFA	bevacizumab, ranibizumab, aflibercept, pegaptanib
NTSR1	contulakin-G
FKBP1A	everolimus
CACNA1D	MEM-1003, clevidipine butyrate, mibefradil, bepridil, nisoldipine, isradipine, nicardipine
SCN8A	riluzole

APPENDIX 11

ALTERED RAPAMYCIN RESPONSE ELEMENTS AS A RESULT OF THE APOE ε4 ALLELE

Table 78 Transcripts that were differentially expressed as a result of the ApoE ε4 allele only (transcripts that were differentially expressed in advanced AD (ApoE ε3/ε4) compared to control (ApoE ε3/ε3) but NOT differentially expressed in advanced AD (ApoE ε3/ε3) compared to control (ApoE ε3/ε3))

Gene symbol	Full name	Location	Type	Possible drug targets	Possible biomarkers
LOXL4	lysyl oxidase-like 4	Extracellular Space	enzyme	x	x
PCSK2	proprotein convertase subtilisin/kexin type 2	Extracellular Space	peptidase	x	x
CCL1	chemokine (C-C motif) ligand 1	Extracellular Space	cytokine		x
VSNL1	visinin-like 1	Cytoplasm	other		x
SCGN	secretagogin, EF-hand calcium binding protein	Cytoplasm	other		x

Gene symbol	**Full name**	**Location**	**Type**	**Possible drug targets**	**Possible biomarkers**
RIMS2	regulating synaptic membrane exocytosis 2	Cytoplasm	other		x
KIAA1683	KIAA1683	Cytoplasm	other		x
GFAP	glial fibrillary acidic protein	Cytoplasm	other		x
CPLX2	complexin 2	Cytoplasm	other		x
ABLIM2	actin binding LIM protein family, member 2	Cytoplasm	other		x
WFDC6	WAP four-disulfide core domain 6	Extracellular Space	other		x
NPTX1	neuronal pentraxin I	Extracellular Space	other		x
NEGR1	neuronal growth regulator 1	Extracellular Space	other		x
LECT1	leukocyte cell derived chemotaxin 1	Extracellular Space	other		x
DEFB119	defensin, beta 119	Extracellular Space	other		x
CYR61	cysteine-rich, angiogenic inducer, 61	Extracellular Space	other		x
ZBTB20	zinc finger and BTB domain containing 20	Nucleus	other		x
PNRC1	proline-rich nuclear receptor coactivator 1	Nucleus	other		x
ELAVL3	ELAV (embryonic lethal, abnormal vision, Drosophila)-like 3 (Hu antigen C)	Nucleus	other		x

Gene symbol	**Full name**	**Location**	**Type**	**Possible drug targets**	**Possible biomarkers**
CDH13	cadherin 13, H-cadherin (heart)	Plasma Membrane	other		x
ZCCHC12	zinc finger, CCHC domain containing 12	unknown	other		x
YPEL5	yippee-like 5 (Drosophila)	unknown	other		x
DQ249310	urothelial cancer associated 1 (non-protein coding)	unknown	other		x
SLC35F3	solute carrier family 35, member F3	unknown	other		x
PHYHD1	phytanoyl-CoA dioxygenase domain containing 1	unknown	other		x
MEG3	maternally expressed 3 (non-protein coding)	unknown	other		x
ITGBL1	integrin, beta-like 1 (with EGF-like repeat domains)	unknown	other		x
GIGYF1	GRB10 interacting GYF protein 1	unknown	other		x
LRRC37A4	leucine rich repeat containing 37, member A4 (pseudogene)	unknown	other		x
FBXL16	F-box and leucine-rich repeat protein 16	unknown	other		x

Gene symbol	**Full name**	**Location**	**Type**	**Possible drug targets**	**Possible biomarkers**
FAM171B	family with sequence similarity 171, member B	unknown	other		x
CCDC85A	coiled-coil domain containing 85A	unknown	other		x
CCDC28A	coiled-coil domain containing 28A	unknown	other		x
C17orf99	chromosome 17 open reading frame 99	unknown	other		x
KIAA1641	ankyrin repeat domain 36B	unknown	other		x
ACTRT1	actin-related protein T1	unknown	other		x
UBE2M	ubiquitin-conjugating enzyme E2M (UBC12 homolog, yeast)	Cytoplasm	enzyme	x	
PTGS2	prostaglandin-endoperoxide synthase 2 (prostaglandin G/H synthase and cyclooxygenase)	Cytoplasm	enzyme	x	
PAOX	polyamine oxidase (exo-N4-amino)	Cytoplasm	enzyme	x	
NMNAT2	nicotinamide nucleotide adenylyltransferase 2	Cytoplasm	enzyme	x	

Gene symbol	**Full name**	**Location**	**Type**	**Possible drug targets**	**Possible biomarkers**
HMGCS2	3-hydroxy-3-methylglutaryl-CoA synthase 2 (mitochondrial)	Cytoplasm	enzyme	x	
GALNT10	UDP-N-acetyl-alpha-D-galactosamine:polypeptide N-acetylgalactosaminyltransferase 10 (GalNAc-T10)	Cytoplasm	enzyme	x	
ACSL6	acyl-CoA synthetase long-chain family member 6	Cytoplasm	enzyme	x	
GNG8	guanine nucleotide binding protein (G protein), gamma 8	Plasma Membrane	enzyme	x	
PDE8B	phosphodiesterase 8B	unknown	enzyme	x	
SSTR1	somatostatin receptor 1	Plasma Membrane	G-protein coupled receptor	x	
OR52B2	olfactory receptor, family 52, subfamily B, member 2	Plasma Membrane	G-protein coupled receptor	x	
GPR176	G protein-coupled receptor 176	Plasma Membrane	G-protein	x	

Gene symbol	**Full name**	**Location**	**Type**	**Possible drug targets**	**Possible biomarkers**
			coupled receptor		
GPR109B	G protein-coupled receptor 109B	Plasma Membrane	G-protein coupled receptor	x	
TRPV1	transient receptor potential cation channel, subfamily V, member 1	Plasma Membrane	ion channel	x	
GRIA2	glutamate receptor, ionotropic, AMPA 2	Plasma Membrane	ion channel	x	
PRKCI	protein kinase C, iota	Cytoplasm	kinase	x	
PRKCA	protein kinase C, alpha	Cytoplasm	kinase	x	
ACVR2B	activin A receptor, type IIB	Plasma Membrane	kinase	x	
RORB	RAR-related orphan receptor B	Nucleus	ligand-dependent nuclear receptor	x	
	tumor necrosis factor receptor superfamily, member	Plasma Membrane		x	

Gene symbol	**Full name**	**Location**	**Type**	**Possible drug targets**	**Possible biomarkers**
TNFRSF10C	10c, decoy without an intracellular domain		transmembrane receptor		
TIMM17B	translocase of inner mitochondrial membrane 17 homolog B (yeast)	Cytoplasm	transporter	x	
SLC6A15	solute carrier family 6 (neutral amino acid transporter), member 15	Plasma Membrane	transporter	x	
SLC6A11	solute carrier family 6 (neurotransmitter transporter, GABA), member 11	Plasma Membrane	transporter	x	
CDCP2	CUB domain containing protein 2	unknown	transporter	x	
EVI1	MDS1 and EVI1 complex locus	Nucleus	transcription regulator		
EGR1	early growth response 1	Nucleus	transcription regulator		
ABTB1	ankyrin repeat and BTB (POZ) domain containing 1	Cytoplasm	translation regulator		

Gene symbol	**Full name**	**Location**	**Type**	**Possible drug targets**	**Possible biomarkers**
BRUNOL 4	CUGBP, Elav-like family member 4	Nucleus	translation regulator		

APPENDIX 12

Table 79 Transcripts that were differentially expressed in brain affected by AD, irrespective of disease severity (Overlap in differentially expressed transcripts in mild AD and advanced AD).

Gene ID	Full name	Location	Type	Possible drug targets	Possible biomarkers
ADAMTS2	ADAM metallopeptidase with thrombospondin type 1 motif, 2	Extracellular Space	peptidase	X	X
CCL2	chemokine (C-C motif) ligand 2	Extracellular Space	cytokine		X
ENTPD8	ectonucleoside triphosphate diphosphohydrolase 8	unknown	enzyme	X	
FAM64A	family with sequence similarity 64, member A	unknown	other		
FN3K	fructosamine 3 kinase	unknown	kinase	X	
HDAC5	histone deacetylase 5	Nucleus	transcription regulator		
IL6	interleukin 6 (interferon, beta 2)	Extracellular Space	cytokine		X
MOXD1	monooxygenase, DBH-like 1	Cytoplasm	enzyme	X	

Gene ID	Full name	Location	Type	Possible drug targets	Possible biomarkers
PLD4	phospholipase D family, member 4	unknown	enzyme	X	
POU4F2	POU class 4 homeobox 2	Nucleus	transcription regulator		
PRODH2	proline dehydrogenase (oxidase) 2	Cytoplasm	enzyme	X	
RUNX1T1	runt-related transcription factor 1; translocated to, 1 (cyclin D-related)	Nucleus	transcription regulator		
SEMA4C	sema domain, immunoglobulin domain (Ig), transmembrane domain (TM) and short cytoplasmic domain, (semaphorin) 4C	Plasma Membrane	other		
SLC22A18	solute carrier family 22, member 18	Plasma Membrane	transporter	X	
TGM4	transglutaminase 4 (prostate)	Extracellular Space	enzyme	X	

Table 80 Transcripts that were differentially expressed in advanced AD, but not in mild AD (transcripts that were differentially expressed in advanced AD compared to control but not differentially expressed in mild AD compared to control).

Gene	Full name	Location	Type	Possible drug target	Possible biomarker
ADAMTSL5	ADAMTS-like 5	Extracellular Space	other		x
AHNAK2	AHNAK nucleoprotein 2	unknown	other		
ANKRD36B	ankyrin repeat domain 36B	unknown	other		
AP1S1	adaptor-related protein complex 1, sigma 1 subunit	Cytoplasm	transporter	x	
ATAD3B	ATPase family, AAA domain containing 3B	Nucleus	other		
ATF7IP	activating transcription factor 7 interacting protein	Nucleus	transcription regulator		
ATRNL1	attractin-like 1	unknown	other		
BARX2	BARX homeobox 2	Nucleus	transcription regulator		
BCOR	BCL6 corepressor	Nucleus	transcription regulator		
BMP7	bone morphogenetic protein 7	Extracellular Space	growth factor	x	x
BPI	bactericidal/permeability-increasing protein	Plasma Membrane	transporter	x	

Gene	Full name	Location	Type	Possible drug target	Possible biomarker
BTNL9	butyrophilin-like 9	unknown	other		
C16orf75	chromosome 16 open reading frame 75	unknown	other		
C18orf26	chromosome 18 open reading frame 26	unknown	other		
C1orf127	chromosome 1 open reading frame 127	unknown	other		
CACNA1D	calcium channel, voltage-dependent, L type, alpha 1D subunit	Plasma Membrane	ion channel	x	
CC2D2A	coiled-coil and C2 domain containing 2A	unknown	other		
CCR1	chemokine (C-C motif) receptor 1	Plasma Membrane	G-protein coupled receptor	x	
CEACAM6	carcinoembryonic antigen-related cell adhesion molecule 6 (non-specific cross reacting antigen)	Plasma Membrane	other		
CEP68	centrosomal protein 68kDa	Cytoplasm	other		
CLU	clusterin	Extracellular Space	other		x
CPXM2	carboxypeptidase X (M14 family), member 2	Extracellular Space	peptidase	x	x
CREB3L4	cAMP responsive element binding protein 3-like 4	Nucleus	transcription regulator		

Gene	Full name	Location	Type	Possible drug target	Possible biomarker
CRP	C-reactive protein, pentraxin-related	Extracellular Space	other		x
CSN2	casein beta	Extracellular Space	kinase	x	x
CTDSP1	CTD (carboxy-terminal domain, RNA polymerase II, polypeptide A) small phosphatase 1	Nucleus	phosphatase	x	
WDR40B	DDB1 and CUL4 associated factor 12-like 1	unknown	other		
DCD	dermcidin	Extracellular Space	other		x
DCLK1	doublecortin-like kinase 1	Cytoplasm	kinase	x	
DLG2	discs, large homolog 2 (Drosophila)	Plasma Membrane	kinase	x	
DNAH6	dynein, axonemal, heavy chain 6	unknown	other		
DRP2	dystrophin related protein 2	Plasma Membrane	other		
DYNC2LI1	dynein, cytoplasmic 2, light intermediate chain 1	Cytoplasm	other		
DZIP3	DAZ interacting protein 3, zinc finger	Cytoplasm	enzyme	x	
EIF4E	eukaryotic translation initiation factor 4E	Cytoplasm	translation regulator		
ELAVL4	ELAV (embryonic lethal, abnormal vision, Drosophila)-like 4 (Hu antigen D)	Cytoplasm	other		

Gene	Full name	Location	Type	Possible drug target	Possible biomarker
FAM155A	family with sequence similarity 155, member A	unknown	other		
FAT3	FAT tumor suppressor homolog 3 (Drosophila)	unknown	other		
FGF11	fibroblast growth factor 11	Extracellular Space	growth factor	x	x
FJX1	four jointed box 1 (Drosophila)	Extracellular Space	other		x
FKBP1A	FK506 binding protein 1A, 12kDa	Cytoplasm	enzyme	x	
GABBR2	gamma-aminobutyric acid (GABA) B receptor, 2	Plasma Membrane	G-protein coupled receptor	x	
GLI2	GLI family zinc finger 2	Nucleus	transcription regulator		
HHIPL1	HHIP-like 1	unknown	other		
HIST1H4E	histone cluster 1, H4e	unknown	other		
HYDIN	hydrocephalus inducing homolog (mouse)	unknown	other		
IRS2	insulin receptor substrate 2	Cytoplasm	other		
KCNAB1	potassium voltage-gated channel, shaker-related subfamily, beta member 1	Plasma Membrane	ion channel	x	
KCND2	potassium voltage-gated channel, Shal-related	Plasma Membrane	ion channel	x	

Gene	Full name	Location	Type	Possible drug target	Possible biomarker
	subfamily, member 2				
KCNG4	potassium voltage-gated channel, subfamily G, member 4	Plasma Membrane	ion channel	x	
KLF2	Kruppel-like factor 2 (lung)	Nucleus	transcription regulator		
KLHL24	kelch-like 24 (Drosophila)	unknown	other		
LYPD2	LY6/PLAUR domain containing 2	unknown	other		
MAPK1	mitogen-activated protein kinase 1	Cytoplasm	kinase	x	
MAPK4	mitogen-activated protein kinase 4	Cytoplasm	kinase	x	
MCTP1	multiple C2 domains, transmembrane 1	unknown	other		
MMP16	matrix metallopeptidase 16 (membrane-inserted)	Extracellular Space	peptidase	x	x
MYF6	myogenic factor 6 (herculin)	Nucleus	transcription regulator		
NTSR1	neurotensin receptor 1 (high affinity)	Plasma Membrane	G-protein coupled receptor	x	
PCDHGA9	protocadherin gamma subfamily A, 9	unknown	other		

Gene	Full name	Location	Type	Possible drug target	Possible biomarker
PEX5L	peroxisomal biogenesis factor 5-like	Cytoplasm	other		
PHLDA3	pleckstrin homology-like domain, family A, member 3	unknown	other		
PIM1	pim-1 oncogene	Cytoplasm	kinase	x	
PRKCH	protein kinase C, eta	Cytoplasm	kinase	x	
RAB3C	RAB3C, member RAS oncogene family	Cytoplasm	enzyme	x	
RNF128	ring finger protein 128	Cytoplasm	enzyme	x	
RPS6KB2	ribosomal protein S6 kinase, 70kDa, polypeptide 2	Cytoplasm	kinase	x	
SCN8A	sodium channel, voltage gated, type VIII, alpha subunit	Plasma Membrane	ion channel	x	
SEMA5A	sema domain, seven thrombospondin repeats (type 1 and type 1-like), transmembrane domain (TM) and short cytoplasmic domain, (semaphorin) 5A	Plasma Membrane	transmembrane receptor	x	
SERPIND1	serpin peptidase inhibitor, clade D (heparin cofactor), member 1	Extracellular Space	other		x
SERPINE1	serpin peptidase inhibitor, clade E (nexin, plasminogen activator inhibitor type 1), member 1	Extracellular Space	other		x

Gene	Full name	Location	Type	Possible drug target	Possible biomarker
SGTA	small glutamine-rich tetratricopeptide repeat (TPR)-containing, alpha	Cytoplasm	other		
SLC18A3	solute carrier family 18 (vesicular acetylcholine), member 3	Plasma Membrane	transporter	x	
SLC25A27	solute carrier family 25, member 27	Cytoplasm	transporter	x	
SLC38A3	solute carrier family 38, member 3	Plasma Membrane	transporter	x	
SLITRK1	SLIT and NTRK-like family, member 1	unknown	other		
SMAD3	SMAD family member 3	Nucleus	transcription regulator		
SORBS2	sorbin and SH3 domain containing 2	Nucleus	other		
SPRED2	sprouty-related, EVH1 domain containing 2	Extracellular Space	cytokine		x
STAG3L1	stromal antigen 3-like 1	unknown	other		
STARD13	StAR-related lipid transfer (START) domain containing 13	Cytoplasm	other		
STX1B	syntaxin 1B	Plasma Membrane	ion channel	x	
TAOK1	TAO kinase 1	Cytoplasm	kinase	x	

Gene	**Full name**	**Location**	**Type**	**Possible drug target**	**Possible biomarker**
TM4SF18	transmembrane 4 L six family member 18	unknown	other		
TMEM56	transmembrane protein 56	unknown	other		
TSC2	tuberous sclerosis 2	Cytoplasm	other		
VEGFA	vascular endothelial growth factor A	Extracellular Space	growth factor	x	x
YPEL1	yippee-like 1 (Drosophila)	Nucleus	enzyme	x	
ZC3H6	zinc finger CCCH-type containing 6	unknown	other		

REFERENCE LIST

1. Ballard,C. *et al.* Alzheimer's disease. *Lancet* **377**, 1019-1031 (2011).

2. Bertram,L. *et al.* Genome-wide association analysis reveals putative Alzheimer's disease susceptibility loci in addition to APOE. *Am. J. Hum. Genet.* **83**, 623-632 (2008).

3. Bettens,K. *et al.* Follow-Up Study of Susceptibility Loci for Alzheimer's Disease and Onset Age Identified by Genome-Wide Association. *J. Alzheimers. Dis.*(2009).

4. Smith,M.A. Alzheimer disease. *Int. Rev. Neurobiol.* **42**, 1-54 (1998).

5. Perl,D.P. Neuropathology of Alzheimer's disease. *Mt. Sinai J. Med.* **77**, 32-42 (2010).

6. Priller,C. *et al.* Synapse formation and function is modulated by the amyloid precursor protein. *J. Neurosci.* **26**, 7212-7221 (2006).

7. Turner,P.R., O'Connor,K., Tate,W.P., & Abraham,W.C. Roles of amyloid precursor protein and its fragments in regulating neural activity, plasticity and memory. *Prog. Neurobiol.* **70**, 1-32 (2003).

8. Aizenstein,H.J. *et al.* Frequent amyloid deposition without significant cognitive impairment among the elderly. *Arch. Neurol.* **65**, 1509-1517 (2008).

9. Metcalfe,M.J. & Figueiredo-Pereira,M.E. Relationship between tau pathology and neuroinflammation in Alzheimer's disease. *Mt. Sinai J. Med.* **77**, 50-58 (2010).

10. Iqbal,K. & Grundke-Iqbal,I. Alzheimer neurofibrillary degeneration: significance, etiopathogenesis, therapeutics and prevention. *J. Cell Mol. Med.* **12**, 38-55 (2008).

11. Stieler,J. *et al.* Multivariate analysis of differential lymphocyte cell cycle activity in Alzheimer's disease. *Neurobiol. Aging*(2010).

12. Huppert,F.A., Brayne,C., Gill,C., Paykel,E.S., & Beardsall,L. CAMCOG--a concise neuropsychological test to assist dementia diagnosis: socio-demographic determinants in an elderly population sample. *Br. J. Clin. Psychol.* **34 (Pt 4)**, 529-541 (1995).

13. Roth M, Huppert FA, Tym E, & Mountjoy CQ CAMDEX. In: The Cambridge examination for mental disorders. 1-72 (Cambridge University Press, Cambridge, 1988).

14. Mirra,S.S. *et al.* The Consortium to Establish a Registry for Alzheimer's Disease (CERAD). Part II. Standardization of the neuropathologic assessment of Alzheimer's disease. *Neurology* **41**, 479-486 (1991).

15. Braak,H. & Braak,E. Neuropathological stageing of Alzheimer-related changes. *Acta Neuropathol.* **82**, 239-259 (1991).

16. Arriagada,P.V., Growdon,J.H., Hedley-Whyte,E.T., & Hyman,B.T. Neurofibrillary tangles but not senile plaques parallel duration and severity of Alzheimer's disease. *Neurology* **42**, 631-639 (1992).

17. Gomez-Isla,T. *et al.* Neuronal loss correlates with but exceeds neurofibrillary tangles in Alzheimer's disease. *Ann. Neurol.* **41**, 17-24 (1997).

18. Hampel,H. *et al.* Biomarkers for Alzheimer's disease: academic, industry and regulatory perspectives. *Nat. Rev. Drug Discov.* **9**, 560-574 (2010).

19. Hardy,J.A. & Higgins,G.A. Alzheimer's disease: the amyloid cascade hypothesis. *Science* **256**, 184-185 (1992).

20. Verdile,G. *et al.* The role of beta amyloid in Alzheimer's disease: still a cause of everything or the only one who got caught? *Pharmacol. Res.* **50**, 397-409 (2004).

21. Rapoport,M., Dawson,H.N., Binder,L.I., Vitek,M.P., & Ferreira,A. Tau is essential to beta -amyloid-induced neurotoxicity. *Proc. Natl. Acad. Sci. U. S. A* **99**, 6364-6369 (2002).

22. Coon,K.D. *et al.* A high-density whole-genome association study reveals that APOE is the major susceptibility gene for sporadic late-onset Alzheimer's disease. *J. Clin. Psychiatry* **68**, 613-618 (2007).

23. Strittmatter,W.J. *et al.* Apolipoprotein E: high-avidity binding to beta-amyloid and increased frequency of type 4 allele in late-onset familial Alzheimer disease. *Proc. Natl. Acad. Sci. U. S. A* **90**, 1977-1981 (1993).

24. Gomez-Isla,T. *et al.* Clinical and pathological correlates of apolipoprotein E epsilon 4 in Alzheimer's disease. *Ann. Neurol.* **39**, 62-70 (1996).

25. Mahley,R.W., Weisgraber,K.H., & Huang,Y. Apolipoprotein E4: a causative factor and therapeutic target in neuropathology, including Alzheimer's disease. *Proc. Natl. Acad. Sci. U. S. A* **103**, 5644-5651 (2006).

26. Zhu,X. *et al.* Differential activation of neuronal ERK, JNK/SAPK and p38 in Alzheimer disease: the 'two hit' hypothesis. *Mech. Ageing Dev.* **123**, 39-46 (2001).

27. Zhu,X., Raina,A.K., Perry,G., & Smith,M.A. Alzheimer's disease: the two-hit hypothesis. *Lancet Neurol.* **3**, 219-226 (2004).

28. Zhu,X., Lee,H.G., Perry,G., & Smith,M.A. Alzheimer disease, the two-hit hypothesis: an update. *Biochim. Biophys. Acta* **1772**, 494-502 (2007).

29. Currais,A., Hortobagyi,T., & Soriano,S. The neuronal cell cycle as a mechanism of pathogenesis in Alzheimer's disease. *Aging (Albany. NY)* **1**, 363-371 (2009).

30. Nagy,Z. The last neuronal division: a unifying hypothesis for the pathogenesis of Alzheimer's disease. *J. Cell Mol. Med.* **9**, 531-541 (2005).

31. Besson,A., Dowdy,S.F., & Roberts,J.M. CDK inhibitors: cell cycle regulators and beyond. *Dev. Cell* **14**, 159-169 (2008).

32. Harper,J.W., Adami,G.R., Wei,N., Keyomarsi,K., & Elledge,S.J. The p21 Cdk-interacting protein Cip1 is a potent inhibitor of G1 cyclin-dependent kinases. *Cell* **75**, 805-816 (1993).

33. Pateras,I.S., Apostolopoulou,K., Niforou,K., Kotsinas,A., & Gorgoulis,V.G. p57KIP2: "Kip"ing the cell under control. *Mol. Cancer Res.* **7**, 1902-1919 (2009).

34. Bonda,D.J. *et al.* Pathological implications of cell cycle re-entry in Alzheimer disease. *Expert. Rev. Mol. Med.* **12**, e19 (2010).

35. Wang,W. *et al.* Neural cell cycle dysregulation and central nervous system diseases. *Prog. Neurobiol.* **89**, 1-17 (2009).

36. Arendt,T. Alzheimer's disease as a disorder of mechanisms underlying structural brain self-organization. *Neuroscience* **102**, 723-765 (2001).

37. Arendt,T. Synaptic plasticity and cell cycle activation in neurons are alternative effector pathways: the 'Dr. Jekyll and Mr. Hyde concept' of Alzheimer's disease or the yin and yang of neuroplasticity. *Prog. Neurobiol.* **71**, 83-248 (2003).

38. Arendt,T. & Bruckner,M.K. Linking cell-cycle dysfunction in Alzheimer's disease to a failure of synaptic plasticity. *Biochim. Biophys. Acta* **1772**, 413-421 (2007).

39. Connor,B. *et al.* Insulin-like growth factor-I (IGF-I) immunoreactivity in the Alzheimer's disease temporal cortex and hippocampus. *Brain Res. Mol. Brain Res.* **49**, 283-290 (1997).

40. Crutcher,K.A., Scott,S.A., Liang,S., Everson,W.V., & Weingartner,J. Detection of NGF-like activity in human brain tissue: increased levels in Alzheimer's disease. *J. Neurosci.* **13**, 2540-2550 (1993).

41. Fahnestock,M., Scott,S.A., Jette,N., Weingartner,J.A., & Crutcher,K.A. Nerve growth factor mRNA and protein levels measured in the same tissue from normal and Alzheimer's disease parietal cortex. *Brain Res. Mol. Brain Res.* **42**, 175-178 (1996).

42. Gartner,U., Holzer,M., Heumann,R., & Arendt,T. Induction of p21ras in Alzheimer pathology. *Neuroreport* **6**, 1441-1444 (1995).

43. Gartner,U., Holzer,M., & Arendt,T. Elevated expression of p21ras is an early event in Alzheimer's disease and precedes neurofibrillary degeneration. *Neuroscience* **91**, 1-5 (1999).

44. Bonda,D.J. *et al.* Evidence for the progression through S-phase in the ectopic cell cycle re-entry of neurons in Alzheimer disease. *Aging (Albany. NY)* **1**, 382-388 (2009).

45. McShea,A., Harris,P.L., Webster,K.R., Wahl,A.F., & Smith,M.A. Abnormal expression of the cell cycle regulators P16 and CDK4 in Alzheimer's disease. *Am. J. Pathol.* **150**, 1933-1939 (1997).

46. Nagy,Z., Esiri,M.M., & Smith,A.D. Expression of cell division markers in the hippocampus in Alzheimer's disease and other neurodegenerative conditions. *Acta Neuropathol.* **93**, 294-300 (1997).

47. Nagy,Z., Esiri,M.M., Cato,A.M., & Smith,A.D. Cell cycle markers in the hippocampus in Alzheimer's disease. *Acta Neuropathol.* **94**, 6-15 (1997).

48. Ogawa,O. *et al.* Ectopic localization of phosphorylated histone H3 in Alzheimer's disease: a mitotic catastrophe? *Acta Neuropathol.* **105**, 524-528 (2003).

49. Raina,A.K. *et al.* Cyclin' toward dementia: cell cycle abnormalities and abortive oncogenesis in Alzheimer disease. *J. Neurosci. Res.* **61**, 128-133 (2000).

50. Smith,M.Z., Nagy,Z., & Esiri,M.M. Cell cycle-related protein expression in vascular dementia and Alzheimer's disease. *Neurosci. Lett.* **271**, 45-48 (1999).

51. Thakur,A. *et al.* Retinoblastoma protein phosphorylation at multiple sites is associated with neurofibrillary pathology in Alzheimer disease. *Int. J. Clin. Exp. Pathol.* **1**, 134-146 (2008).

52. Vincent,I., Jicha,G., Rosado,M., & Dickson,D.W. Aberrant expression of mitotic cdc2/cyclin B1 kinase in degenerating neurons of Alzheimer's disease brain. *J. Neurosci.* **17**, 3588-3598 (1997).

53. Yang,Y., Geldmacher,D.S., & Herrup,K. DNA replication precedes neuronal cell death in Alzheimer's disease. *J. Neurosci.* **21**, 2661-2668 (2001).

54. Zhu,X. *et al.* Neuronal binucleation in Alzheimer disease hippocampus. *Neuropathol. Appl. Neurobiol.* **34**, 457-465 (2008).

55. Raina,A.K. *et al.* Apoptotic promoters and inhibitors in Alzheimer's disease: Who wins out? *Prog. Neuropsychopharmacol. Biol. Psychiatry* **27**, 251-254 (2003).

56. McDonald,D.R., Bamberger,M.E., Combs,C.K., & Landreth,G.E. beta-Amyloid fibrils activate parallel mitogen-activated protein kinase pathways in microglia and THP1 monocytes. *J. Neurosci.* **18**, 4451-4460 (1998).

57. Pyo,H., Jou,I., Jung,S., Hong,S., & Joe,E.H. Mitogen-activated protein kinases activated by lipopolysaccharide and beta-amyloid in cultured rat microglia. *Neuroreport* **9**, 871-874 (1998).

58. Emiliani,C. *et al.* Up-regulation of glycohydrolases in Alzheimer's Disease fibroblasts correlates with Ras activation. *J. Biol. Chem.* **278**, 38453-38460 (2003).

59. Hirashima,N. *et al.* Calcium responses in human fibroblasts: a diagnostic molecular profile for Alzheimer's disease. *Neurobiol. Aging* **17**, 549-555 (1996).

60. Shalit,F., Sredni,B., Brodie,C., Kott,E., & Huberman,M. T lymphocyte subpopulations and activation markers correlate with severity of Alzheimer's disease. *Clin. Immunol. Immunopathol.* **75**, 246-250 (1995).

61. Stieler,J.T. *et al.* Impairment of mitogenic activation of peripheral blood lymphocytes in Alzheimer's disease. *Neuroreport* **12**, 3969-3972 (2001).

62. Ye,W. & Blain,S.W. S phase entry causes homocysteine-induced death while ataxia telangiectasia and Rad3 related protein functions anti-apoptotically to protect neurons. *Brain*(2010).

63. Zhang,J. *et al.* Telomere dysfunction of lymphocytes in patients with Alzheimer disease. *Cogn Behav. Neurol.* **16**, 170-176 (2003).

64. Behrens,M.I., Lendon,C., & Roe,C.M. A common biological mechanism in cancer and Alzheimer's disease? *Curr. Alzheimer Res.* **6**, 196-204 (2009).

65. Roe,C.M., Behrens,M.I., Xiong,C., Miller,J.P., & Morris,J.C. Alzheimer disease and cancer. *Neurology* **64**, 895-898 (2005).

66. Roe,C.M. *et al.* Cancer linked to Alzheimer disease but not vascular dementia. *Neurology* **74**, 106-112 (2010).

67. Burke,W.J. *et al.* Occurrence of cancer in Alzheimer and elderly control patients: an epidemiologic necropsy study. *Alzheimer Dis. Assoc. Disord.* **8**, 22-28 (1994).

68. Urcelay,E., Ibarreta,D., Parrilla,R., Ayuso,M.S., & Martin-Requero,A. Enhanced proliferation of lymphoblasts from patients with Alzheimer dementia associated with calmodulin-dependent activation of the na+/H+ exchanger. *Neurobiol. Dis.* **8**, 289-298 (2001).

69. Yoon,S.C. *et al.* Altered cell viability and proliferation activity of peripheral lymphocytes in patients with Alzheimer's disease. *Psychiatry Investig.* **7**, 68-71 (2010).

70. Paccalin,M. *et al.* Activated mTOR and PKR kinases in lymphocytes correlate with memory and cognitive decline in Alzheimer's disease. *Dement. Geriatr. Cogn Disord.* **22**, 320-326 (2006).

71. Nagy,Z., Combrinck,M., Budge,M., & McShane,R. Cell cycle kinesis in lymphocytes in the diagnosis of Alzheimer's disease. *Neurosci. Lett.* **317**, 81-84 (2002).

72. Zhou,X. & Jia,J. P53-mediated G(1)/S checkpoint dysfunction in lymphocytes from Alzheimer's disease patients. *Neurosci. Lett.* **468**, 320-325 (2010).

73. Gibbons,J.J., Abraham,R.T., & Yu,K. Mammalian target of rapamycin: discovery of rapamycin reveals a signaling pathway important for normal and cancer cell growth. *Semin. Oncol.* **36 Suppl 3**, S3-S17 (2009).

74. Nagy,Z. The dysregulation of the cell cycle and the diagnosis of Alzheimer's disease. *Biochim. Biophys. Acta* **1772**, 402-408 (2007).

75. Chedid,M., Michieli,P., Lengel,C., Huppi,K., & Givol,D. A single nucleotide substitution at codon 31 (Ser/Arg) defines a polymorphism in a highly conserved region of the p53-inducible gene WAF1/CIP1. *Oncogene* **9**, 3021-3024 (1994).

76. Facher,E.A., Becich,M.J., Deka,A., & Law,J.C. Association between human cancer and two polymorphisms occurring together in the p21Waf1/Cip1 cyclin-dependent kinase inhibitor gene. *Cancer* **79**, 2424-2429 (1997).

77. Mousses,S. *et al.* Two variants of the CIP1/WAF1 gene occur together and are associated with human cancer. *Hum. Mol. Genet.* **4**, 1089-1092 (1995).

78. Sjalander,A. *et al.* Association between the p21 codon 31 A1 (arg) allele and lung cancer. *Hum. Hered.* **46**, 221-225 (1996).

79. Yoon,M.K. *et al.* Residual structure within the disordered C-terminal segment of p21(Waf1/Cip1/Sdi1) and its implications for molecular recognition. *Protein Sci.* **18**, 337-347 (2009).

80. Blacker,D. *et al.* Results of a high-resolution genome screen of 437 Alzheimer's disease families. *Hum. Mol. Genet.* **12**, 23-32 (2003).

81. Holmans,P. *et al.* Genome screen for loci influencing age at onset and rate of decline in late onset Alzheimer's disease. *Am. J. Med. Genet. B Neuropsychiatr. Genet.* **135B**, 24-32 (2005).

82. Lee,J.H. *et al.* Expanded genomewide scan implicates a novel locus at 3q28 among Caribbean hispanics with familial Alzheimer disease. *Arch. Neurol.* **63**, 1591-1598 (2006).

83. Hiltunen,M. *et al.* Genome-wide linkage disequilibrium mapping of late-onset Alzheimer's disease in Finland. *Neurology* **57**, 1663-1668 (2001).

84. Jung,Y.S., Qian,Y., & Chen,X. Examination of the expanding pathways for the regulation of p21 expression and activity. *Cell Signal.* **22**, 1003-1012 (2010).

85. Matsuoka,S. *et al.* Imprinting of the gene encoding a human cyclin-dependent kinase inhibitor, p57KIP2, on chromosome 11p15. *Proc. Natl. Acad. Sci. U. S. A* **93**, 3026-3030 (1996).

86. Opitz,L. *et al.* Impact of RNA degradation on gene expression profiling. *BMC. Med. Genomics* **3**, 36 (2010).

87. Copois,V. *et al.* Impact of RNA degradation on gene expression profiles: assessment of different methods to reliably determine RNA quality. *J. Biotechnol.* **127**, 549-559 (2007).

88. Fleige,S. & Pfaffl,M.W. RNA integrity and the effect on the real-time qRT-PCR performance. *Mol. Aspects Med.* **27**, 126-139 (2006).

89. Tan,M.G. *et al.* Genome wide profiling of altered gene expression in the neocortex of Alzheimer's disease. *J. Neurosci. Res.* **88**, 1157-1169 (2010).

90. Xu,P.T. *et al.* Differences in apolipoprotein E3/3 and E4/4 allele-specific gene expression in hippocampus in Alzheimer disease. *Neurobiol. Dis.* **21**, 256-275 (2006).

91. Xu,P.T. *et al.* A SAGE study of apolipoprotein E3/3, E3/4 and E4/4 allele-specific gene expression in hippocampus in Alzheimer disease. *Mol. Cell Neurosci.* **36**, 313-331 (2007).

92. Tusher,V.G., Tibshirani,R., & Chu,G. Significance analysis of microarrays applied to the ionizing radiation response. *Proc. Natl. Acad. Sci. U. S. A* **98**, 5116-5121 (2001).

93. Goedert,M., Jakes,R., & Vanmechelen,E. Monoclonal antibody AT8 recognises tau protein phosphorylated at both serine 202 and threonine 205. *Neurosci. Lett.* **189**, 167-169 (1995).

94. Vechterova,L. *et al.* DC11: a novel monoclonal antibody revealing Alzheimer's disease-specific tau epitope. *Neuroreport* **14**, 87-91 (2003).

95. Clare,R., King,V.G., Wirenfeldt,M., & Vinters,H.V. Synapse loss in dementias. *J. Neurosci. Res.* **88**, 2083-2090 (2010).

96. Masliah,E. *et al.* Altered expression of synaptic proteins occurs early during progression of Alzheimer's disease. *Neurology* **56**, 127-129 (2001).

97. Mullen,R.J., Buck,C.R., & Smith,A.M. NeuN, a neuronal specific nuclear protein in vertebrates. *Development* **116**, 201-211 (1992).

98. Warden,D.R. & Refsum,H. Detection of single-nucleotide polymorphisms by PCR with universal energy transfer-labeled primers: application to folate- and cobalamin-related genes. *Clin. Chem.* **51**, 1713-1716 (2005).

99. Darzynkierricz,Z., Crissman,H.A., & Robinson,J.P. *Cytometry: Methods in Cellular Biology*(Academics, San Diego, CA, 2001).

100. Stieler,J.T. *et al.* Impairment of mitogenic activation of peripheral blood lymphocytes in Alzheimer's disease. *Neuroreport* **12**, 3969-3972 (2001).

101. Holmans,P. *et al.* Genome screen for loci influencing age at onset and rate of decline in late onset Alzheimer's disease. *Am. J. Med. Genet. B Neuropsychiatr. Genet.* **135B**, 24-32 (2005).

102. Ryckman,K. & Williams,S.M. Calculation and use of the Hardy-Weinberg model in association studies. *Curr. Protoc. Hum. Genet.* **Chapter 1**, Unit (2008).

103. Avramopoulos,D., Szymanski,M., Wang,R., & Bassett,S. Gene expression reveals overlap between normal aging and Alzheimer's disease genes. *Neurobiol. Aging*(2010).

104. Blalock,E.M. *et al.* Incipient Alzheimer's disease: microarray correlation analyses reveal major transcriptional and tumor suppressor responses. *Proc. Natl. Acad. Sci. U. S. A* **101**, 2173-2178 (2004).

105. Liang,W.S. *et al.* Altered neuronal gene expression in brain regions differentially affected by Alzheimer's disease: a reference data set. *Physiol Genomics* **33**, 240-256 (2008).

106. Bayatti,N. & Behl,C. The neuroprotective actions of corticotropin releasing hormone. *Ageing Res. Rev.* **4**, 258-270 (2005).

107. Swaab,D.F., Bao,A.M., & Lucassen,P.J. The stress system in the human brain in depression and neurodegeneration. *Ageing Res. Rev.* **4**, 141-194 (2005).

108. Nelson,T.J. & Alkon,D.L. Insulin and cholesterol pathways in neuronal function, memory and neurodegeneration. *Biochem. Soc. Trans.* **33**, 1033-1036 (2005).

109. DeLegge,M.H. & Smoke,A. Neurodegeneration and inflammation. *Nutr. Clin. Pract.* **23**, 35-41 (2008).

110. Wyss-Coray,T. Inflammation in Alzheimer disease: driving force, bystander or beneficial response? *Nat. Med.* **12**, 1005-1015 (2006).

111. Wyss-Coray,T. Transforming growth factor-beta signaling pathway as a therapeutic target in neurodegeneration. *J. Mol. Neurosci.* **24**, 149-153 (2004).

112. Das,P. & Golde,T. Dysfunction of TGF-beta signaling in Alzheimer's disease. *J. Clin. Invest* **116**, 2855-2857 (2006).

113. Tesseur,I. *et al.* Deficiency in neuronal TGF-beta signaling promotes neurodegeneration and Alzheimer's pathology. *J. Clin. Invest* **116**, 3060-3069 (2006).

114. Corder,E.H. *et al.* Gene dose of apolipoprotein E type 4 allele and the risk of Alzheimer's disease in late onset families. *Science* **261**, 921-923 (1993).

115. Tang,M.X. *et al.* Relative risk of Alzheimer disease and age-at-onset distributions, based on APOE genotypes among elderly African Americans, Caucasians, and Hispanics in New York City. *Am. J. Hum. Genet.* **58**, 574-584 (1996).

116. Bekris,L.M., Yu,C.E., Bird,T.D., & Tsuang,D.W. Genetics of Alzheimer disease. *J. Geriatr. Psychiatry Neurol.* **23**, 213-227 (2010).

117. Dumanis,S.B. *et al.* ApoE Receptor 2 Regulates Synapse and Dendritic Spine Formation. *PLoS. One.* **6**, e17203 (2011).

118. Oh,J.Y. *et al.* Apolipoprotein E mRNA is transported to dendrites and may have a role in synaptic structural plasticity. *J. Neurochem.* **114**, 685-696 (2010).

119. Tannenberg,R.K., Scott,H.L., Tannenberg,A.E., & Dodd,P.R. Selective loss of synaptic proteins in Alzheimer's disease: evidence for an increased severity with APOE varepsilon4. *Neurochem. Int.* **49**, 631-639 (2006).

120. Gibson,G.E. *et al.* Mitochondrial damage in Alzheimer's disease varies with apolipoprotein E genotype. *Ann. Neurol.* **48**, 297-303 (2000).

121. Gutala,R.V. & Reddy,P.H. The use of real-time PCR analysis in a gene expression study of Alzheimer's disease post-mortem brains. *J. Neurosci. Methods* **132**, 101-107 (2004).

122. Gebhardt,F.M., Scott,H.A., & Dodd,P.R. Housekeepers for accurate transcript expression analysis in Alzheimer's disease autopsy brain tissue. *Alzheimers. Dement.* **6**, 465-474 (2010).

123. Lee,J., Hever,A., Willhite,D., Zlotnik,A., & Hevezi,P. Effects of RNA degradation on gene expression analysis of human postmortem tissues. *FASEB J.* **19**, 1356-1358 (2005).

124. Bates,S., Ryan,K.M., Phillips,A.C., & Vousden,K.H. Cell cycle arrest and DNA endoreduplication following p21Waf1/Cip1 expression. *Oncogene* **17**, 1691-1703 (1998).

125. Devlin,A.M. *et al.* HCaRG is a novel regulator of renal epithelial cell growth and differentiation causing G2M arrest. *Am. J. Physiol Renal Physiol* **284**, F753-F762 (2003).

126. Evdokiou,A., Raggatt,L.J., Atkins,G.J., & Findlay,D.M. Calcitonin receptor-mediated growth suppression of HEK-293 cells is accompanied by induction of p21WAF1/CIP1 and G2/M arrest. *Mol. Endocrinol.* **13**, 1738-1750 (1999).

127. Evdokiou,A., Raggatt,L.J., Sakai,T., & Findlay,D.M. Identification of a novel calcitonin-response element in the promoter of the human p21WAF1/CIP1 gene. *J. Mol. Endocrinol.* **25**, 195-206 (2000).

128. Chen,J., Jackson,P.K., Kirschner,M.W., & Dutta,A. Separate domains of p21 involved in the inhibition of Cdk kinase and PCNA. *Nature* **374**, 386-388 (1995).

129. Shim,J., Lee,H., Park,J., Kim,H., & Choi,E.J. A non-enzymatic p21 protein inhibitor of stress-activated protein kinases. *Nature* **381**, 804-806 (1996).

130. Asada,M. *et al.* Apoptosis inhibitory activity of cytoplasmic p21(Cip1/WAF1) in monocytic differentiation. *EMBO J.* **18**, 1223-1234 (1999).

131. Engidawork,E., Gulesserian,T., Seidl,R., Cairns,N., & Lubec,G. Expression of apoptosis related proteins in brains of patients with Alzheimer's disease. *Neurosci. Lett.* **303**, 79-82 (2001).

132. Kalia,M. Dysphagia and aspiration pneumonia in patients with Alzheimer's disease. *Metabolism* **52**, 36-38 (2003).

133. Mortel,K.F. *et al.* Factors influencing survival among patients with vascular dementia and Alzheimer's disease. *J. Stroke Cerebrovasc. Dis.* **8**, 57-65 (1999).

134. Giannakopoulos,P., Hof,P.R., Michel,J.P., Guimon,J., & Bouras,C. Cerebral cortex pathology in aging and Alzheimer's disease: a quantitative survey of

large hospital-based geriatric and psychiatric cohorts. *Brain Res. Brain Res. Rev.* **25**, 217-245 (1997).

135. Jack,C.R., Jr. *et al.* Medial temporal atrophy on MRI in normal aging and very mild Alzheimer's disease. *Neurology* **49**, 786-794 (1997).

136. Mann,D.M. The topographic distribution of brain atrophy in Alzheimer's disease. *Acta Neuropathol.* **83**, 81-86 (1991).

137. Gomez-Isla,T. *et al.* Profound loss of layer II entorhinal cortex neurons occurs in very mild Alzheimer's disease. *J. Neurosci.* **16**, 4491-4500 (1996).

138. West,M.J., Coleman,P.D., Flood,D.G., & Troncoso,J.C. Differences in the pattern of hippocampal neuronal loss in normal ageing and Alzheimer's disease. *Lancet* **344**, 769-772 (1994).

139. Masliah,E. *et al.* Synaptic and neuritic alterations during the progression of Alzheimer's disease. *Neurosci. Lett.* **174**, 67-72 (1994).

140. Scheff,S.W. & Price,D.A. Alzheimer's disease-related alterations in synaptic density: neocortex and hippocampus. *J. Alzheimers. Dis.* **9**, 101-115 (2006).

141. Terry,R.D. *et al.* Physical basis of cognitive alterations in Alzheimer's disease: synapse loss is the major correlate of cognitive impairment. *Ann. Neurol.* **30**, 572-580 (1991).

142. Scheff,S.W. & Price,D.A. Synapse loss in the temporal lobe in Alzheimer's disease. *Ann. Neurol.* **33**, 190-199 (1993).

143. Salminen,A., Suuronen,T., & Kaarniranta,K. ROCK, PAK, and Toll of synapses in Alzheimer's disease. *Biochem. Biophys. Res. Commun.* **371**, 587-590 (2008).

144. Filipowicz,W., Bhattacharyya,S.N., & Sonenberg,N. Mechanisms of post-transcriptional regulation by microRNAs: are the answers in sight? *Nat. Rev. Genet.* **9**, 102-114 (2008).

145. Touitou,R. *et al.* A degradation signal located in the C-terminus of p21WAF1/CIP1 is a binding site for the C8 alpha-subunit of the 20S proteasome. *EMBO J.* **20**, 2367-2375 (2001).

146. Alberts *et al. Molecular biology of the cell*(Garland Science, New York, 2002).

147. Joseph,B., Orlian,M., & Furneaux,H. p21(waf1) mRNA contains a conserved element in its 3'-untranslated region that is bound by the Elav-like mRNA-stabilizing proteins. *J. Biol. Chem.* **273**, 20511-20516 (1998).

148. Shu,L., Yan,W., & Chen,X. RNPC1, an RNA-binding protein and a target of the p53 family, is required for maintaining the stability of the basal and stress-induced p21 transcript. *Genes Dev.* **20**, 2961-2972 (2006).

149. Insall,R.H. & Machesky,L.M. Actin dynamics at the leading edge: from simple machinery to complex networks. *Dev. Cell* **17**, 310-322 (2009).

150. Heng,Y.W. & Koh,C.G. Actin cytoskeleton dynamics and the cell division cycle. *Int. J. Biochem. Cell Biol.* **42**, 1622-1633 (2010).

151. Smith,A.C., Choufani,S., Ferreira,J.C., & Weksberg,R. Growth regulation, imprinted genes, and chromosome 11p15.5. *Pediatr. Res.* **61**, 43R-47R (2007).

152. Fitzpatrick,G.V. *et al.* Allele-specific binding of CTCF to the multipartite imprinting control region KvDMR1. *Mol. Cell Biol.* **27**, 2636-2647 (2007).

153. Shin,J.Y., Fitzpatrick,G.V., & Higgins,M.J. Two distinct mechanisms of silencing by the KvDMR1 imprinting control region. *EMBO J.* **27**, 168-178 (2008).

154. Diaz-Meyer,N. *et al.* Silencing of CDKN1C (p57KIP2) is associated with hypomethylation at KvDMR1 in Beckwith-Wiedemann syndrome. *J. Med. Genet.* **40**, 797-801 (2003).

155. Arima,T. *et al.* ZAC, LIT1 (KCNQ1OT1) and p57KIP2 (CDKN1C) are in an imprinted gene network that may play a role in Beckwith-Wiedemann syndrome. *Nucleic Acids Res.* **33**, 2650-2660 (2005).

156. Muller,S. *et al.* Retention of imprinting of the human apoptosis-related gene TSSC3 in human brain tumors. *Hum. Mol. Genet.* **9**, 757-763 (2000).